

AD - A133748

(12)

THE DESIGN OF AN EXPERIMENTAL APPARATUS  
TO MEASURE THE MOTIONS OF A TOWED  
SUBMERSIBLE ENVIRONMENTAL SENSOR VEHICLE

by

Robert A. Granger

EW-24-83 ✓

July 1983

UNITED STATES NAVAL ACADEMY  
DIVISION OF  
ENGINEERING AND WEAPONS  
ANNAPOLIS, MARYLAND

DTIC FILE COPY

Approved for distribution

DTIC

18

83-10 17 06



Unclassified

SECURITY CLASSIFICATION OF THIS PAGE (When Data Entered)

REPORT DOCUMENTATION PAGE		READ INSTRUCTIONS BEFORE COMPLETING FORM
1. REPORT NUMBER N61331-81-WR-00142-1983-1	2. GOVT ACCESSION NO. AD-A133 744	3. RECIPIENT'S CATALOG NUMBER
4. TITLE (and Subtitle) THE DESIGN OF AN EXPERIMENTAL APPARATUS TO MEASURE THE MOTIONS OF A TOWED SUBMERSIBLE ENVIRONMENTAL SENSOR VEHICLE.		5. TYPE OF REPORT & PERIOD COVERED Final Report June 15, 1980 - June 14, 1983
7. AUTHOR(s)  Robert A. Granger		6. PERFORMING ORG. REPORT NUMBER
9. PERFORMING ORGANIZATION NAME AND ADDRESS Department of Mechanical Engineering U.S. Naval Academy Annapolis, Maryland 21402		8. CONTRACT OR GRANT NUMBER(s) N61331-80-WR-00142 N61331-81-WR-00142
11. CONTROLLING OFFICE NAME AND ADDRESS Naval Coastal Systems Center Panama City, Florida 32407		10. PROGRAM ELEMENT, PROJECT, TASK AREA & WORK UNIT NUMBERS
14. MONITORING AGENCY NAME & ADDRESS (if different from Controlling Office)		12. REPORT DATE June 1983
		13. NUMBER OF PAGES
		15. SECURITY CLASS. (of this report) Unclassified
		15a. DECLASSIFICATION/DOWNGRADING SCHEDULE
16. DISTRIBUTION STATEMENT (of this Report)  Approved for public release; distribution unlimited.		
17. DISTRIBUTION STATEMENT (of the abstract entered in Block 20, if different from Report)		
18. SUPPLEMENTARY NOTES		
19. KEY WORDS (Continue on reverse side if necessary and identify by block number)  Hydrodynamics, experimental methods, towed vehicles		
20. ABSTRACT (Continue on reverse side if necessary and identify by block number) An experimental investigation of the motions of a towed submersible sensing vehicle due to external forcing functions of surge and heave is made. Using the U.S. Naval Academy's high speed tow tank facility, experiments were conducted using a half scale model of a current NCSC towed vehicle in which was carried a motion measurement package that measured pitch, roll, yaw, longitudinal and vertical accelerations. Surge and heave displacements at various forcing frequencies and displacements up to (+) 1.0 ft were generated		

DD FORM 1473  
1 JAN 73

EDITION OF 1 NOV 65 IS OBSOLETE  
S/N U102-LF-014-6601

Unclassified  
SECURITY CLASSIFICATION OF THIS PAGE (When Data Entered)

for -



Unclassified

SECURITY CLASSIFICATION OF THIS PAGE (When Data Entered)

REPORT DOCUMENTATION PAGE		READ INSTRUCTIONS BEFORE COMPLETING FORM
1. REPORT NUMBER N61331-81-WR-00142-1983-1	2. GOVT ACCESSION NO. AD-A133 744	3. RECIPIENT'S CATALOG NUMBER
4. TITLE (and Subtitle) THE DESIGN OF AN EXPERIMENTAL APPARATUS TO MEASURE THE MOTIONS OF A TOWED SUBMERSIBLE ENVIRONMENTAL SENSOR VEHICLE.		5. TYPE OF REPORT & PERIOD COVERED Final Report June 15, 1980 - June 14, 1983
7. AUTHOR(s)  Robert A. Granger		6. PERFORMING ORG. REPORT NUMBER
9. PERFORMING ORGANIZATION NAME AND ADDRESS Department of Mechanical Engineering U.S. Naval Academy Annapolis, Maryland 21402		8. CONTRACT OR GRANT NUMBER(s) N61331-80-WR-00142 N61331-81-WR-00142
11. CONTROLLING OFFICE NAME AND ADDRESS Naval Coastal Systems Center Panama City, Florida 32407		10. PROGRAM ELEMENT, PROJECT, TASK AREA & WORK UNIT NUMBERS
14. MONITORING AGENCY NAME & ADDRESS (if different from Controlling Office)		12. REPORT DATE June 1983
		13. NUMBER OF PAGES
		15. SECURITY CLASS. (of this report) Unclassified
		15a. DECLASSIFICATION/DOWNGRADING SCHEDULE
16. DISTRIBUTION STATEMENT (of this Report)  Approved for public release; distribution unlimited.		
17. DISTRIBUTION STATEMENT (of the abstract entered in Block 20, if different from Report)		
18. SUPPLEMENTARY NOTES		
19. KEY WORDS (Continue on reverse side if necessary and identify by block number)  Hydrodynamics, experimental methods, towed vehicles		
20. ABSTRACT (Continue on reverse side if necessary and identify by block number) An experimental investigation of the motions of a towed submersible sensing vehicle due to external forcing functions of surge and heave is made. Using the U.S. Naval Academy's high speed tow tank facility, experiments were conducted using a half scale model of a current NCSC towed vehicle in which was carried a motion measurement package that measured pitch, roll, yaw, longitudinal and vertical accelerations. Surge and heave displacements at various forcing frequencies and displacements up to (+) 1.0 ft were generated		

DD FORM 1 JAN 73 1473

EDITION OF 1 NOV 65 IS OBSOLETE  
S/N U102-LF-014-6601

Unclassified

SECURITY CLASSIFICATION OF THIS PAGE (When Data Entered)

for -




Unclassified

SECURITY CLASSIFICATION OF THIS PAGE (When Data Entered)

20. ABSTRACT

Cont after developing excitation apparatus that would be compatible with the tow tank facility. Effects of tow cable geometry and towing speeds were investigated. A simple mathematical model for heaving motion was developed to lend verification to experimental measurements. An audio-colored visual tape of the experimental study was made showing the salient aspects of the investigation.



S/N 0102- LF-014-6601

SECURITY CLASSIFICATION OF THIS PAGE (When Data Entered)



### Acknowledgements

Appreciation is extended to Dr. Delbert Summey, Head of the Hydromechanics Branch, NCSC, Panama City, Fla. for overseeing the project, making it possible for the U.S. Naval Academy to conduct the experimental study. Acknowledgement is due to a great many people who aided in bringing this task to completion. Ensign Steve Burris' assistance is gratefully acknowledged. The computer program and solutions of problems associated with the electronics were due to Paco Rodriguez, Head of CADIG. The design of many of the structural elements was due to Lawrence Heisig, Director of the Technical Support Department. Assisting in the fabrication of the towing system were Robert Woody, Bernie Deichgraber, Art Goehring, Herb Woffritz, Carl Owen, Tom Price, Ray Sears, Bob Sleighter and George Staab of the Technical Support Department. Special acknowledgement is given to John Hill, Head of the Hydromechanics Lab and his excellent crew, Donald Bunker and Steve Enzinger. The television production was due to the effort of the Chief Producer, Jim Kiser. The Director of the production was Laren Leonard. Appreciation is given to William Clepson for graphics, Steve Bennet and Al Hammond (EFP Engineers) and Dave Rector and Ryan Collinson (Studio Engineers). The typing was due to Inez Johnson and Jodi Gittes of the Mechanical Engineering Department. Any errors or mistakes are of course due to the author and principal investigator, R. Granger.



Acknowledgment For	
1	<input checked="checked" type="checkbox"/>
2	<input type="checkbox"/>
3	<input type="checkbox"/>
4	<input type="checkbox"/>
5	<input type="checkbox"/>
6	<input type="checkbox"/>
7	<input type="checkbox"/>
8	<input type="checkbox"/>
9	<input type="checkbox"/>
10	<input type="checkbox"/>
11	<input type="checkbox"/>
12	<input type="checkbox"/>
13	<input type="checkbox"/>
14	<input type="checkbox"/>
15	<input type="checkbox"/>
16	<input type="checkbox"/>
17	<input type="checkbox"/>
18	<input type="checkbox"/>
19	<input type="checkbox"/>
20	<input type="checkbox"/>
21	<input type="checkbox"/>
22	<input type="checkbox"/>
23	<input type="checkbox"/>
24	<input type="checkbox"/>
25	<input type="checkbox"/>
26	<input type="checkbox"/>
27	<input type="checkbox"/>
28	<input type="checkbox"/>
29	<input type="checkbox"/>
30	<input type="checkbox"/>
31	<input type="checkbox"/>
32	<input type="checkbox"/>
33	<input type="checkbox"/>
34	<input type="checkbox"/>
35	<input type="checkbox"/>
36	<input type="checkbox"/>
37	<input type="checkbox"/>
38	<input type="checkbox"/>
39	<input type="checkbox"/>
40	<input type="checkbox"/>
41	<input type="checkbox"/>
42	<input type="checkbox"/>
43	<input type="checkbox"/>
44	<input type="checkbox"/>
45	<input type="checkbox"/>
46	<input type="checkbox"/>
47	<input type="checkbox"/>
48	<input type="checkbox"/>
49	<input type="checkbox"/>
50	<input type="checkbox"/>
51	<input type="checkbox"/>
52	<input type="checkbox"/>
53	<input type="checkbox"/>
54	<input type="checkbox"/>
55	<input type="checkbox"/>
56	<input type="checkbox"/>
57	<input type="checkbox"/>
58	<input type="checkbox"/>
59	<input type="checkbox"/>
60	<input type="checkbox"/>
61	<input type="checkbox"/>
62	<input type="checkbox"/>
63	<input type="checkbox"/>
64	<input type="checkbox"/>
65	<input type="checkbox"/>
66	<input type="checkbox"/>
67	<input type="checkbox"/>
68	<input type="checkbox"/>
69	<input type="checkbox"/>
70	<input type="checkbox"/>
71	<input type="checkbox"/>
72	<input type="checkbox"/>
73	<input type="checkbox"/>
74	<input type="checkbox"/>
75	<input type="checkbox"/>
76	<input type="checkbox"/>
77	<input type="checkbox"/>
78	<input type="checkbox"/>
79	<input type="checkbox"/>
80	<input type="checkbox"/>
81	<input type="checkbox"/>
82	<input type="checkbox"/>
83	<input type="checkbox"/>
84	<input type="checkbox"/>
85	<input type="checkbox"/>
86	<input type="checkbox"/>
87	<input type="checkbox"/>
88	<input type="checkbox"/>
89	<input type="checkbox"/>
90	<input type="checkbox"/>
91	<input type="checkbox"/>
92	<input type="checkbox"/>
93	<input type="checkbox"/>
94	<input type="checkbox"/>
95	<input type="checkbox"/>
96	<input type="checkbox"/>
97	<input type="checkbox"/>
98	<input type="checkbox"/>
99	<input type="checkbox"/>
100	<input type="checkbox"/>

A



### Summary

An experimental investigation of the motions of a towed submersible sensing vehicle due to external forcing functions of surge and heave is made. Using the U.S. Naval Academy's high speed tow tank facility, experiments were conducted using a half scale model of a current NCSC towed vehicle in which was carried a motion measurement package that measured pitch, roll, yaw, longitudinal and vertical accelerations. Surge and heave displacements at various forcing frequencies and displacements up to  $\pm 1.0$  ft were generated after developing excitation apparatus that would be compatible with the tow tank facility. Effects of tow cable geometry and towing speeds were investigated. A simple mathematical model for heaving motion was developed to lend verification to experimental measurements. An audio-colored visual tape of the experimental study was made showing the salient aspects of the investigation.



## Table of Contents

	Page No.
1. Introduction	1
2. Principle of Operation	3
3. Sensor Vehicle Design	5
3.1 Requirements	5
3.2 Vehicle	6
3.3 Towing Spar	7
3.4 Longitudinal Excitation Apparatus	9
4. Assembly Procedure	10
5. Data Acquisition and Recovery System	13
6. Problem Areas	15
7. Mathematical Model of the Vertical Excitation	17
8. Results of Analysis	21
9. Result of Experimental Program	24
9.1 Pitch	26
9.2 Roll	27
9.3 Yaw	28
9.4 Longitudinal Acceleration	30
9.5 Vertical Acceleration	31
10. Conclusion	33
Appendix A. Operation of the Transera Analog to Digital Converter	36
Appendix B. Printout of Data	44
Appendix C. Computer Solutions of Vertical Motion Laplace Transform Equation (11) for $R = 0.5$ ft, $l = 10$ ft.	48
Appendix D. Description of USNA High Speed Towing Tank	50
List of Tables	x
List of Illustrations	iii



### List of Illustrations

Figure No.	Page No.
1. Design of Overall Towed System	54
2. Vehicle Geometry	55
3. Towing Plug	56
4. Photograph of the Towed Submersible	57
5. Stainless Steel Sheet Attached to Spar and Trailing Edge	58
6. Trailing and Leading Edges of Spar Showing Rib Sections	59
7. The Box Beam Assembly	60
8. Finished Assembly	61
9. Feeder Block	62
10. Wheel for Stainless Steel Cable at Spar Tip	63
11. Vehicle Excitation Apparatus	64
12. Strain Gages Mounted at Tip of Spar	65
13. Strain Gages on Spar	66
14. Horizontal Excitation Apparatus	67
15. Electrical Hookup of Hydraulic Unit	68
16. Electrical Hookup of the Digital-Analog Converter	69
17. Bent Stainless Steel Pipe	70
18. Damaged Towing Cable	71
19. Geometry for Vehicle Vertical Motion	72
20. Vertical Response for $R = 0.5$ ft, $\ell = 10$ ft.	73
21. Analog Computer Simulation of Vertical Motion	74
22. Acceleration vs. time for $R = 5/12, 1/2, 7/12$ ft, $\ell = 10$ ft	75
23. Acceleration vs. time for $R = 2/3, 11/12, 1$ ft, $\ell = 10$ ft	76
24. Acceleration vs. time for $R = 5/12, 1/2, 7/12$ ft, $\ell = 12.5$ ft	77
25. Acceleration vs time for $R = 2/3, 11/12, 1$ ft, $\ell = 12.5$ ft	78



Figure No.	Page No.
26. Acceleration vs time for $R = 5/12, 1/2, 7/12$ ft, $l = 15$ ft	79
27. Acceleration vs time for $R = 2/3, 11/12, 1$ ft, $l = 15$ ft	80
28. Acceleration vs time for $R = 5/12, 2/3, 1$ ft, $l = 12.5$ ft	81
29. Acceleration vs time for $R = 1$ ft, $l = 15$ ft	82
30. Velocity vs time for $R = 5/12, 1/2, 7/12$ ft, $l = 10$ ft	83
31. Velocity vs time for $R = 2/3, 11/12, 1$ ft, $l = 10$ ft	84
32. Velocity vs time for $R = 5/12, 1/2, 7/12$ ft, $l = 12.5$ ft	85
33. Velocity vs time for $R = 2/3, 11/12, 1$ ft, $l = 12.5$ ft	86
34. Velocity vs time for $R = 5/12, 1/2, 7/12$ ft, $l = 15$ ft	87
35. Velocity vs time for $R = 2/3, 11/12, 1$ ft, $l = 15$ ft	88
36. Velocity vs time for $R = 5/12, 2/3, 1$ ft, $l = 12.5$ ft	89
37. Velocity vs time for $R = 1$ ft, $l = 15$ ft	90
38. Displacement vs time for $R = 5/12, 1/2, 7/12$ ft, $l = 10$ ft	91
39. Displacement vs time for $R = 2/3, 11/12, 1$ ft, $l = 10$ ft	92
40. Displacement vs time for $R = 5/12, 1/2, 7/12$ ft, $l = 12.5$ ft	93
41. Displacement vs time for $R = 2/3, 11/12, 1$ ft, $l = 12.5$ ft	94
42. Displacement vs time for $R = 5/12, 1/2, 7/12$ ft, $l = 15$ ft	95
43. Displacement vs time for $R = 2/3, 11/12, 1$ ft, $l = 15$ ft	96
44. Displacement vs time for $R = 5/12, 1/2, 7/12$ ft, $l = 15$ ft	97
45. Displacement vs time for $R = 1$ ft, $l = 15$ ft	98
46. Towed Submersible's Velocity vs Time, Case 2	99
47. Towed Submersible's Velocity vs Time, Case 3	100
48. Towed Submersible's Velocity vs Time, Case 4	101
49. Towed Submersible's Velocity vs Time, Case 5	102
50. Towed Submersible's Velocity vs Time, Case 6	103
51. Towed Submersible's Velocity vs Time, Case 7	104



Figure No.	Page No.
52. Towed Submersible's Velocity vs Time, Case 8	105
53. Towed Submersible's Velocity vs Time, Case 9	106
54. Towed Submersible's Velocity vs Time, Case 10	107
55. Towed Submersible's Velocity vs Time, Case 11	108
56. Towed Submersible's Velocity vs Time, Case 12	109
57. Towed Submersible's Velocity vs Time, Case 13	110
58. Towed Submersible's Velocity vs Time, Case 14	111
59. Towed Submersible's Velocity vs Time, Case 15	112
60. Towed Submersible's Velocity vs Time, Case 16	113
61. Towed Submersible's Velocity vs Time, Case 17	114
62. Towed Submersible's Velocity vs Time, Case 18	115
63. Towed Submersible's Velocity vs Time, Case 19	116
64. Towed Submersible's Velocity vs Time, Case 20	117
65. Towed Submersible's Velocity vs Time, Case 21	118
66. Towed Submersible's Velocity vs Time, Case 22	119
67. Towed Submersible's Velocity vs Time, Case 23	120
68. Towed Submersible's Velocity vs Time, Case 24	121
69. Towed Submersible's Pitch vs Time, Case 2	122
70. Towed Submersible's Pitch vs Time, Case 3	123
71. Towed Submersible's Pitch vs Time, Case 4	124
72. Towed Submersible's Pitch vs Time, Case 5	125
73. Towed Submersible's Pitch vs Time, Case 6	126
74. Towed Submersible's Pitch vs Time, Case 7	127
75. Towed Submersible's Pitch vs Time, Case 8	128
76. Towed Submersible's Pitch vs Time, Case 9	129
77. Towed Submersible's Pitch vs Time, Case 10	130



Figure No.	Page No.
78. Towed Submersible's Pitch vs Time, Case 11	131
79. Towed Submersible's Pitch vs Time, Case 12	132
80. Towed Submersible's Pitch vs Time, Case 13	133
81. Towed Submersible's Pitch vs Time, Case 14	134
82. Towed Submersible's Pitch vs Time, Case 15	135
93. Towed Submersible's Pitch vs Time, Case 16	136
84. Towed Submersible's Pitch vs Time, Case 17	137
85. Towed Submersible's Pitch vs Time, Case 18	138
86. Towed Submersible's Pitch vs Time, Case 19	139
87. Towed Submersible's Pitch vs Time, Case 20	140
88. Towed Submersible's Pitch vs Time, Case 21	141
89. Towed Submersible's Pitch vs Time, Case 22	142
90. Towed Submersible's Pitch vs Time, Case 23	143
91. Towed Submersible's Pitch vs Time, Case 24	144
92. Towed Submersible's Roll vs Time, Case 2	145
93. Towed Submersible's Roll vs Time, Case 3	146
94. Towed Submersible's Roll vs Time, Case 4	147
95. Towed Submersible's Roll vs Time, Case 5	148
96. Towed Submersible's Roll vs Time, Case 6	149
97. Towed Submersible's Roll vs Time, Case 7	150
98. Towed Submersible's Roll vs Time, Case 8	151
99. Towed Submersible's Roll vs Time, Case 9	152
100. Towed Submersible's Roll vs Time, Case 10	153
101. Towed Submersible's Roll vs Time, Case 11	154
102. Towed Submersible's Roll vs Time, Case 12	155
103. Towed Submersible's Roll vs Time, Case 13	156



Figure No.	Page No.
104. Towed Submersible's Roll vs Time, Case 14	157
105. Towed Submersible's Roll vs Time, Case 15	158
106. Towed Submersible's Roll vs Time, Case 16	159
107. Towed Submersible's Roll vs Time, Case 17	160
108. Towed Submersible's Roll vs Time, Case 18	161
109. Towed Submersible's Roll vs Time, Case 19	162
110. Towed Submersible's Roll vs Time, Case 20	163
111. Towed Submersible's Roll vs Time, Case 21	164
112. Towed Submersible's Roll vs Time, Case 22	165
113. Towed Submersible's Roll vs Time, Case 23	166
114. Towed Submersible's Roll vs Time, Case 24	167
115. Towed Submersible's Yaw vs Time, Case 2	168
116. Towed Submersible's Yaw vs Time, Case 3	169
117. Towed Submersible's Yaw vs Time, Case 4	170
118. Towed Submersible's Yaw vs Time, Case 5	171
119. Towed Submersible's Yaw vs Time, Case 6	172
120. Towed Submersible's Yaw vs Time, Case 8	173
121. Towed Submersible's Yaw vs Time, Case 9	174
122. Towed Submersible's Yaw vs Time, Case 10	175
123. Towed Submersible's Yaw vs Time, Case 11	176
124. Towed Submersible's Yaw vs Time, Case 12	177
125. Towed Submersible's Yaw vs Time, Case 13	178
126. Towed Submersible's Yaw vs Time, Case 14	179
127. Towed Submersible's Yaw vs Time, Case 15	180
128. Towed Submersible's Yaw vs Time, Case 16	181
129. Towed Submersible's Yaw vs Time, Case 17	182



Figure No.	Page No.
130. Towed Submersible's Yaw vs Time, Case 18	183
131. Towed Submersible's Yaw vs Time, Case 19	184
132. Towed Submersible's Yaw vs Time, Case 20	185
133. Towed Submersible's Yaw vs Time, Case 21	186
134. Towed Submersible's Yaw vs Time, Case 22	187
135. Towed Submersible's Yaw vs Time, Case 23	188
136. Towed Submersible's Yaw vs Time, Case 24	189
137. Towed Submersible's Longitudinal Acceleration vs Time, Case 2	190
138. Towed Submersible's Longitudinal Acceleration vs Time, Case 3	191
139. Towed Submersible's Longitudinal Acceleration vs Time, Case 4	192
140. Towed Submersible's Longitudinal Acceleration vs Time, Case 5	193
141. Towed Submersible's Longitudinal Acceleration vs Time, Case 6	194
142. Towed Submersible's Longitudinal Acceleration vs Time, Case 7	195
143. Towed Submersible's Longitudinal Acceleration vs Time, Case 9	196
144. Towed Submersible's Longitudinal Acceleration vs Time, Case 10	197
145. Towed Submersible's Longitudinal Acceleration vs Time, Case 11	198
146. Towed Submersible's Longitudinal Acceleration vs Time, Case 13	199
147. Towed Submersible's Longitudinal Acceleration vs Time, Case 14	200
148. Towed Submersible's Longitudinal Acceleration vs Time, Case 15	201
149. Towed Submersible's Longitudinal Acceleration vs Time, Case 16	202
150. Towed Submersible's Longitudinal Acceleration vs Time, Case 17	203
151. Towed Submersible's Longitudinal Acceleration vs Time, Case 18	204
152. Towed Submersible's Longitudinal Acceleration vs Time, Case 19	205
153. Towed Submersible's Longitudinal Acceleration vs Time, Case 20	206
154. Towed Submersible's Longitudinal Acceleration vs Time, Case 21	207
155. Towed Submersible's Longitudinal Acceleration vs Time, Case 22	208



Figure No.	Page No.
156. Towed Submersible's Longitudinal Acceleration vs Time, Case 23	209
157. Towed Submersible's Longitudinal Acceleration vs Time, Case 24	210
158. Towed Submersible's Vertical Acceleration vs Time, Case 2	211
159. Towed Submersible's Vertical Acceleration vs Time, Case 3	212
160. Towed Submersible's Vertical Acceleration vs Time, Case 4	213
161. Towed Submersible's Vertical Acceleration vs Time, Case 5	214
162. Towed Submersible's Vertical Acceleration vs Time, Case 6	215
163. Towed Submersible's Vertical Acceleration vs Time, Case 7	216
164. Towed Submersible's Vertical Acceleration vs Time, Case 9	217
165. Towed Submersible's Vertical Acceleration vs Time, Case 10	218
166. Towed Submersible's Vertical Acceleration vs Time, Case 11	219
167. Towed Submersible's Vertical Acceleration vs Time, Case 12	220
168. Towed Submersible's Vertical Acceleration vs Time, Case 13	221
169. Towed Submersible's Vertical Acceleration vs Time, Case 14	222
170. Towed Submersible's Vertical Acceleration vs Time, Case 15	223
171. Towed Submersible's Vertical Acceleration vs Time, Case 16	224
172. Towed Submersible's Vertical Acceleration vs Time, Case 17	225
173. Towed Submersible's Vertical Acceleration vs Time, Case 18	226
174. Towed Submersible's Vertical Acceleration vs Time, Case 19	227
175. Towed Submersible's Vertical Acceleration vs Time, Case 20	228
176. Towed Submersible's Vertical Acceleration vs Time, Case 21	229
177. Towed Submersible's Vertical Acceleration vs Time, Case 22	230
178. Towed Submersible's Vertical Acceleration vs Time, Case 23	231
179. Towed Submersible's Vertical Acceleration vs Time, Case 24	232



List of Tables

<u>Table No</u>		<u>Page No</u>
1	Properties of the Towed Submersible Vehicle	7
2	Results of Maximum Acceleration ( $\ddot{Z}_{\max}$ ) for Different Tows and Amplitudes	22
3	Results of Vertical Displacement Z for Different Tow Lengths and Amplitudes	23
4	Experimental Parameters	25



### Synopsis

This report describes and discusses the towed sensing submersible system which was designed, constructed and recently put into service at the United States Naval Academy. The most unique feature of the system is the method used to impart the longitudinal and heaving motions to a given submerged body. This enables the accurate determination of individual motions, whether in pure axial translation or pure vertical translation, or coupled together.

The instrumentation measuring apparatus is self contained and read-outs of the pitch, roll, yaw, axial acceleration and vertical acceleration can be measured simultaneously.

The recording system is automatic upon command and contains features which are intended to reduce data processing to a minimum. The steady state data can be obtained digitally or recorded on strip charts or recording tape. The oscillation measurements are recorded as essentially discrete values of inphase components for prescribed tow velocities, cable tow lengths, heaving and longitudinal excitation frequencies, and heaving and longitudinal excitation amplitudes.



## 1. Introduction

Simulation of underwater environmental situations for towed sensing vehicles is of increased interest to the marine engineer and to the U.S. Navy. Towed submersibles with sensing devices are used to detect underwater fixed and moving objects as well as to provide information on the properties of the sea.

The U.S. Naval Academy (USNA) conducted a hydrodynamic experimental analysis of a unique sensing vehicle designed by the Naval Coastal Systems Center (NCSC). This vehicle conformed to a specific set of requirements for stable operation through a range of fixed depth towed velocities and cable lengths. For simulation tests, the vehicle had to be redesigned to half scale. A towing apparatus had to be designed to tow the model at a fixed depth along with a means to vary the length of towing cable. Accurate simulation of prototype motions required designing devices to impose vertical and horizontal oscillatory motions of various amplitude and frequency to the towed vehicle. This would help create actual sea-state conditions found to exist for the prototype towed vehicle. The project goal was to simulate the principle variables necessary for hydrodynamic stability that exist for a vehicle being towed by a ship in the ocean.

The design, construction, assembly and operation for each component of the laboratory towing system had to be compatible with the limitations of the USNA high speed towing carriage. The tear-down operation of the entire experimental apparatus had to be simple yet highly efficient as the USNA towing carriage had numerous users. Repeatability of any test had to give consistent results. The design of the towing device required it was not to interfere hydrodynamically with the towed vehicle.

The experimental analysis discusses the effect of speed, cable tow length,



excitation frequency and response on the pitch, roll, yaw, axial and vertical accelerations of the towed vehicle.

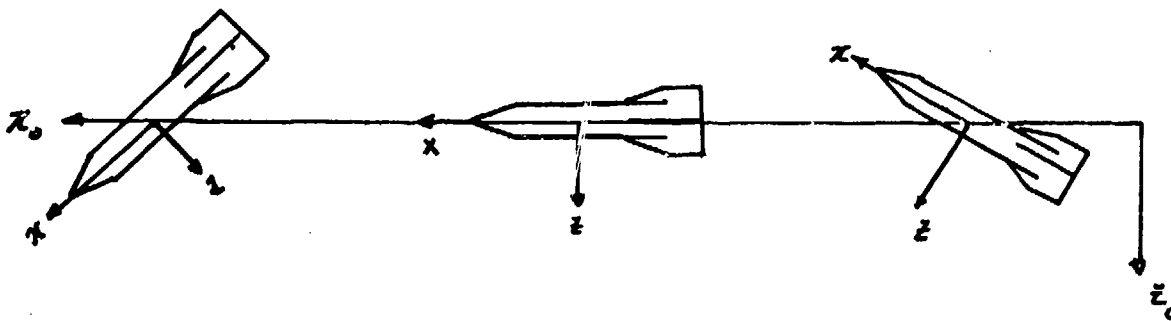
This report documents the experimental design by presenting the design requirements, defining the constraints of the towed vehicle, evaluating the effects of external parametric properties on the vehicle's motion, and developing the criteria for stable operation based upon measured results. An experimental analysis for modeling tow tank testing is also presented.



## 2. Principle of Operation

The USNA Towed Submersible System as it physically exists is described in the next section. It is desirable, however, to consider first the principles underlying the operation of the mechanism so that the design concept can be understood. The system was designed primarily for obtaining oscillatory types of motion of deeply submerged bodies in the vertical plane of motion. It can be used as well to obtain vertical-plane motions for bodies operating near or on the water surface.

The diagram below schematically represents this type of motion. The components are given with respect to a body-axis system with the origin at the center of gravity, c.g.



The system produces this motion indirectly, by using the towing carriage shown in Figures A.1 and A.2 and the excitation apparatus described in section 3.4. Sinusoidal motions are imposed to the towed submerged vehicle at the point of attachment of the towing cable located at the towing spar while the model is being towed through the water by the tow carriage. The motions are phased in such a manner as to produce the designed conditions of hydrodynamically pure heave and pure surge. It is possible to produce various combinations of heave and surge.

Since the model is subjected to both linear and angular accelerations a mixture of static, rotary and acceleration forces and moments result, which



determine the pitch, roll and yaw responses of the model in addition to the longitudinal and vertical accelerations. A pure heaving motion is obtained by the vertical excitation apparatus, keeping the horizontal excitation apparatus at zero frequency. The model c.g. moves in a sinusoidal path where the pitch angle  $\theta$  is also sinusoidal.



### 3. Sensor Vehicle Design

#### 3.1 Requirements

The design requirements of the towed system were dictated primarily by the operational requirements of the sensor vehicle. The design objectives are summarized below:

- (1) Operational depth, 10 feet below water surface.
- (2) Operational speeds, 0-18 ft/s.
- (3) Tow lengths, 5-15 ft.
- (4) Cylindrical section in model for instrumentation cannister and excess cable.
- (5) Bouyancy mechanism to control c.g/c.b location.
- (6) Longitudinal excitation at cable attachment point,  
 $0 < \omega_{\ell} < 1.0 \text{ Hz.}$
- (7) Longitudinal amplitude,  $0 < \lambda < \underline{+} 1 \text{ ft.}$
- (8) Vertical excitation at cable attachment point,  $0 < \omega_e < 1.0 \text{ Hz.}$
- (9) Vertical amplitude,  $0 < \lambda < \underline{+} 1 \text{ ft.}$
- (10) Maximum  $\underline{+} 3 \text{ ft}$  depth excursions.
- (11) Maximum  $\underline{+} 1$  degree angle-of-attack excursions.
- (12) Minimum 10 second vehicle resonant period.
- (13) Safety devices to fail safe on all moving components, and arresting gear for towed vehicle at end of run.

The conceptual design of the overall towed system is shown in Figure 1. The towed vehicle was approximately one-half scale of the prototype vehicle. The size and volume requirements were adjusted to accomodate the full scale instrumentation cannister. This required that the model be 9 in in diameter and 189.5 in long. The towing cable was fed down through the towing spar, turned and fitted into a feeder block so that a predetermined length of tow was available. The cable was led into the model's semi-spherical nose and



plugged into the instrumentation cannister that rested inside the towed vehicle. The towing spar was hoisted onto the USNA hydromechanic towing carriage and bolted onto pillow blocks that moved on specially designed tracks mounted on the towing carriage beams. The vertical excitation apparatus was built into a box beam structure which supported the loads from the spar. The horizontal excitation apparatus was built onto the towing carriage. Each of the components will be discussed in the following sections. Each component was designed to optimize the vehicle to perform to a desired level. In addition, each component had to be easily set-up, so that tear-down time would be minimal.

### 3.2 Vehicle

The prototype towed vehicle was designed by NCSC. The geometry that was chosen had to meet specific design requirements. Once the geometry was defined, then modifications were made based upon its performance, (notably its dynamic response). Figure 2 shows the geometric configuration of the model. A 9 in diameter was chosen to meet the housing of the instrumentation cannister that contained the sensor electronics and motion measurement package. Special metal rings were inserted into the body to confine the cannister in the body of the vehicle and to help achieve neutral bouyancy. The geometric description of the vehicle is presented in Figure 2 along with the location of the c.g. and c.b. The support for the fin was designed so that other fin geometries could be investigated. This report confines the discussion to a fixed geometry that is 22 in at the root chord and 16.5 in at the tip. The trailing edge is straight and is 12.5 in. There is a 2 in radius of curvature at the tip leading edge. The fin thickness is 0.75 in, tapering to 0.25 in at a distance of 3 in from the trailing edge.

The vehicle's nose is hemispherical of 4.5 in radius. A metal plug fits into the hemispherical nose to arrest the towing cable, as shown in Figure 3.



The two vertical and two horizontal fins were based on a NCSC design. Early models were constructed out of wood, but after several tows, the fins proved unsatisfactory resulting in metal fins being made. The geometry of the fins is given in Figure 2.

Table 1 presents the properties of the sensor vehicle.

Table 1

Properties of the Towed Submersible Vehicle

Vehicle length, (ft)	15.375
Vehicle dry weight, (lb)	109.5
Body wetted area, (ft <sup>2</sup> )	68.31
Mass of water inside vehicle, (slugs)	7.12
Total mass of vehicle, (including water)	10.53
Fin planform area, (ft <sup>2</sup> )	1.67
Longitudinal location of c.g., (ft) (from nose)	5.17
Longitudinal location of c.b., (ft) (from nose)	5.17
Vertical distance c.g. to c.b., (ft)	0.21

Figure 4 is a photograph of the third class of three models used in the testing program. The first class was constructed out of wood and plastic. The nose and tail assembly were constructed out of yellow pine and treated with an epoxy to keep it dry. The body was constructed out of plastic. The second towed submersible was constructed entirely of plastic. Frequent testing fatigued the plastic resulting in numerous cracks leading to structural failure. The third class was constructed out of aluminum. Though more expensive to construct, it proved to be the most satisfactory of models.

### 3.3 Towing Spar

Figure 5 is a photograph of the towing spar with its box beam assembly.



The towing spar was 12 ft long two-dimensional wing of NACA 0024 profile. Several wing sections were constructed and tested in the USNA recirculating water table for a range of free stream velocities. Only the NACA 0024 proved to provide negligible shed vortices that could effect the towed vehicle motion and maintain nominal drag. The strength member of the strut is a 16 ft length of schedule 40, 3 in stainless steel pipe of  $1/4$  in thickness. The pipe was supported by an aluminum box beam. Numerous stainless steel ribs were attached to the pipe to create the critical shape of the spar. The geometry for the ribs was derived from the NACA 0024 airfoil. The geometric information was mathematically programmed into the USNA CADIG PDP 11 Computer, and with the USNA's technological tooling devices, the information was fed to a milling machine which fabricated the ribs.

Once the ribs were attached to the pipe, sheets of stainless steel were laid over the structure (see Figure 5) and then fitted to a wooden leading edge. A wooden streamlined airfoil section was attached to the tip of the spar. The trailing edge of the strut was constructed out of several hollow stainless steel rib sections (see Figure 6). A towing cable was allowed to pass through the hollow rib sections along the length of the spar up to the box beam.

One end of the pipe passed through two aluminum thick plates that were welded to the box beam (see Figure 7). An annular stainless steel ring, seated into the pipe, was bolted to the upper box beam plate. The wooden leading edge and stainless steel sheets were then attached to the pipe, as shown in Figure 8.

Internal to the towing spar was a feeder block that was designed to move the towing cable, transmitting its motion to the towed vehicle. This mechanism, shown in Figure 9, transmitted vertical motions of various amplitudes and frequencies to the towed vehicle. It also allowed the cable length to be



adjusted by loosening a cover plate and sliding the appropriate length through a 90° curved section.

The feeder block was mounted on tracks that allowed it to be moved  $\pm 1$  ft maximum from its centerline position. Stainless steel cables attached to each end of the feeder block were led up directly through the spar. By means of a wheel mounted at the tip of the spar (see Figure 10), the steel cables passed up to an oscillating bar which controlled the vertical movement of the feeder block.

The vertical excitation apparatus is shown in Figure 11. It's principal part is a motor which drives an oscillating bar. At one end of the bar was pinned, a second bar. At one end of the bar was pinned a second bar. By moving the point of where the bar was pinned, we could change the amplitude of the motion. Figure 11 shows the second bar mounted for a 9 in maximum amplitude. At the other end of the bar was a slider block which slid along a vertical rail. The two ends of the stainless steel cable were attached to the slider block.

Before the box beam spar assembly was mounted on the carriage for dynamic tests, the structure was statically and dynamically tested in the USNA's structural dynamics laboratory. Strain gages were attached at numerous locations on the assembly. Figure 12 is a photograph of strain gages mounted both inside and outside the stainless steel pipe at the spar's tip. Figure 13 shows 4 strain gages at one spanwise location, one on a rib, two on the pipe and one on the feeder block rail. Concentrated loads were applied on the spar, and deflections measured. Then impact loads up to 100 lbs were applied, and deflections measured. The structure was proven to be extremely stiff, with no significant deflections up to 100 pound impact loads.

### 3.4 Longitudinal Excitation Apparatus

The longitudinal excitation apparatus was designed to provide surging motion of particular frequency and amplitude to the towed vehicle. Figure 14



shows some of the components of the apparatus. Two 2 in diameter ground steel shafts along with associated shaft supports were mounted on the lower machined rails of the towing carriage. Four pillow blocks attached to the box beam assembly provided support on the shafts when the box beam spar assembly was lowered into place. A yoke fitting from a bar attached to a hydraulic ram assembly pushed or pulled the box beam along the two shafts. The yoke fitting was attached to a backing plate attached to the box beam assembly to distribute the load across the box beam. In order to minimize the dynamic loading at the contact point between the support plates and the rail module, foam rubber pads were inserted. These pads increased the coefficient of friction and reduced the chances of support bolts from loosening during test runs. A set of casters were clamped to the box beam providing a roller mechanism along the lower machined surface of the rail module to correct an imbalance between the ram contact point and the box beam assembly support point. A hydraulic pump was located on the towing carriage, as shown in Figure 14. Hydraulic lines from the pump were fed to the hydraulic ram. Adjustment of pump pressure controlled the frequency, and adjustment of the ram controlled the amplitude.

#### 4. Assembly Procedure

The installation of the apparatus was reduced from three to one and one-half working days after a computer set of parts and tooling requirements were drawn using a step-by-step procedure. This included time for proper alignment of the assembly so that no initial angle-of-attack or side slip for the spar existed. The procedure used and to be used in future investigations is as follows:

1. With the vehicle resting on its mount, remove the nose and tail sections. Insert the instrument package, along with the two retainer rings, into the body. Use set screws to secure the retainer rings. Insert both air bladders. To facilitate moving the vehicle, attach a line at each end: a stopper



knot in the nose and a knot through the eye bolt at the tail.

2. Move the following to the tow tank:

- a. Entire strut with the cable run through and with all moving parts greased
- b. Vehicle with its instrument package
- c. Hydraulic unit
- d. Motor and gear reducer

3. Raise the tow tank's beach out of the water. With a guiding line attached to the end of the strut boom, hoist the strut up horizontally and move it over the beach. Lower the strut onto the beach, remove the lifting strap and hoist the hook all the way to the top.

4. Manually move the tow tank carriage until the mounting track is centered over the strut. Attach the lifting strap at the end of the strut frame. Begin lowering the beach and hoist up on the strut slowly, so that as little force as possible is on the tip of the strut boom. Use the guiding line if necessary to ease any force.

5. Lift the strut frame through the carriage mounting tracks until the bottom edge of the strut frame is even with the bottom rail of the mount.

6. With the strut hanging in this position, attach the two slide rails by screwing the pillow block bearings into the strut frame. Then twist the entire strut so that it is aligned in the proper direction. Lower the strut down on the mounting rail and clamp down all four corners. However, clamp down an aluminum shim on the forward end of the upper mounting rail to prevent the slide rails mounts from sliding into the vertical tracks of the carriage mount frame in case of a quick stop.

7. Return the hoist and pick up the motor and gear reducer unit and bring it back to the carriage. Mount this unit on top of the strut frame.

8. Return the hoist, pick up the hydraulic unit, bring it to the



carriage and set it down on the back end of the carriage deck. See Figure 14.

9. Using a plywood board as a seat between the lower count rails and by using the hoist, lower the two large aluminum plates to the lower mount rail.

10. While sitting on the seat, bolt the two plates together onto the rail. Be sure to use foam rubber between the plates and the rail.

11. Lower the hydraulic ram into position below the two plates and screw it into the bottom plate. Next, attach the piston to the two-way joint located on the strut frame. Then connect the hydraulic hoses between the pump and the ram.

12. Screw the vertical pushrod into the rotating arm coming out of the gear reducer.

13. Lubricate the vertical slide, both slide rails and the hydraulic piston.

14. Clamp the 4 caster wheels, using 3 aluminum shims for each wheel to the bottom edge of the strut frame. Leave around 1/8 inch clearance between the wheel and the bottom rail.

15. Clamp the limit switches to the lower mount rail after having determined their positions by sliding the strut to the limit of the slide rail. Clamp the mounting bracket to the strut frame and clamp down the adjustable rams when the desired amplitude is measured between the two rams and their limit switches.

16. Hook up the power panel in the tow carriage house and then hook up the two limit switches to the power panel. Using the pump's wiring diagram, hook up the hydraulic pump motor and the electric motor (from gear reducer) to the start-stop switches located on the power panel. Refer to Figure 15.

17. On the catwalk, remove the rope from the nosecone and then run the tow cable through the nosecone and hook up to the instrument package.



18. Measure the tow cable length and adjust if necessary by moving the clamp which is attached to the steel excitation cable.

19. Run the cable from the strut frame through the carriage frame and over to the high speed carriage.

20. Hook up the electrical system on the high speed carriage as shown in Figure 16.

21. Attach an eye bolt to the end of a 15 ft piece of angle aluminum and clamp the other end to the back end of the carriage deck next to the hydraulic unit. Run the monofilament braking line through the eye bolt and replace it on the tail of the vehicle,

22. Screw on nosecone and put the vehicle in the water.

23. The vehicle is ready for test.

#### 5. Data Acquisition and Recovery System

Early in the test program, the instrumentation and data acquisition system contained a common ground problem which resulted in cross-channel interference among all six data channels. This problem was resolved in the software of the data acquisition system. The vertical drive motor was found to trip itself off the line after running for periods where extreme loads existed. This was rectified by starting the motor just prior to a run and turning it off after completing a run.

Data acquisition involved the CADIG 4051 Tektronix computer data acquisition and graphic display system. The Tektronix 4050 series computers can be used as stand alone graphics and data acquisition systems as well as graphics terminals. When using the data acquisition capabilities of the Tektronix computers, it is often useful to plot the data to verify the correct operation of an experiment. Even data which has been stored on the Tektronix data cartridges may be plotted without the need for an external computer.



After utilizing the data acquisition for two test programs, three major areas of concern were noted:

1. Set up of the system itself inside the carriage housing proved to be a cumbersome and time-consuming operation.
2. Data acquisition required an operator to monitor the computer the entire time throughout a data run to input various commands. This allowed for several carriage runs to be made in which data was lost due to mistaken inputs by the operator.
3. The NCSC instrumentation package and NCSC suppressor box produced a  $\pm 20$  volt signal, while the Cadig 4051 Tektronix was equipped to handle only a  $\pm 10$  volt signal effectively. This resulted in clipped signal transmission, and eventual system overload on certain data channels.

After two sessions of testing in the tow tank with little accumulation of significant data, it was decided a more reliable and responsive system of data acquisition was required. The problem was eventually resolved by re-wiring the suppressor box ground system on the six data channels. This created  $\pm 10$  volt maximum output signal, and allowed for use of the USNA laser modulated data transmission system and the data acquisition computer.

The Transera analog to digital converter was used to read voltages up to 16 different sources with 8 or 12 bits of resolution over the input voltage range. The a/d module plugs into the ROM sockets on the back of the Tektronix 4051 computer. Twelve routines which control the converter and manipulate the data are included in the module and are directly callable from the Tektronix.

Sixteen channels of differential inputs are available. The maximum data rate depends on the resolution desired; 8 bit samples may be acquired at the rate of 32,000 samples per second while 12 bit samples may be obtained at 20,000 samples per second. A programmable gain amplifier is included in the module for measuring low level voltages. The table of gains below shows the voltage range and resolution for each setting.



TABLE OF GAINS

GAIN	VOLTAGE	12 BIT RESOLUTION	8 BIT RESOLUTION
X 1	$\pm 10$	5 mv	78 mv
X 4	$\pm 2.5$	1.25 mv	20 mv
X 32	$\pm 0.3$	0.25 mv	2.5 mv

Two modes perform automatic gain selection, another allows any channel to be programmed, while another restricts the channels which may be programmed.

Appendix A contains the operation of the Transera analog to digital converter.

Once the instrumentation of the sensing device was made compatible with the data acquisition and graphic display system, the test runs began and the data was compiled. Appendix B contains a sample of some of the data taken.

#### 6. Problem Areas

Numerous problems were encountered in the design and test of the experimental apparatus. Aside from the electronics problems mentioned in the previous sections, the problems encountered were largely in the structural dynamics field. Rather than simply itemizing them, the following narration as taken from the log is typical of the problems that arose.

"On the second day of testing the sealant failed on the wooden sections and the vehicle began absorbing water. They became so heavily ballasted that it would ride off the bottom of the tow tank at low speeds (3-6 fps). This dragging effect produced significant wear in the tow cable and damaged the tail fins." Another problem that was logged: "There are several groups of steel bolts anchored into the bottom of the tow tank that gouge the wooden nose of the vehicle as it was dragging the vehicle back to the start of the test. Eventually the vehicle snagged one of these bolts as the carriage was being backed at 3 fps, forcing the steel center pipe in the strut to bend.



(See Figure 17). The damage was severe enough to cause a shut down of all testing for the remainder of the month to consider a redesign of several systems. Later analysis revealed that the moment arm created by the loading on the bottom of the strut, and the knife-edge support at top, resulted from a snag force of 204 lbs or greater."

"The remainder of the summer was spent in repairing the damaged systems. In order to remove the bend in the strut, it was cut 8 inches above and below the bend. Then a steel sleeve was made as an insert. The sleeve was turned down from a piece of 3 in. schedule 180 steel pipe. The sleeve was butt welded to the stainless as well as mechanically fastened with 8 3/8" x 16" screw. However since the sleeve is not made of stainless, this area had to be monitored in all future runs for damage due to corrosion. In subsequent testing the repair appeared to be withstanding all loading conditions, including hoisting operations, with no inelastic bending effects."

The major point of concern was that the damage would have never occurred had the vehicle not become waterlogged and sank. Therefore, it was decided to replace all wooden parts with those made of material resistant to water absorption, and provide a secure ballasting system. A new nose piece was cast of aluminum in the USNA foundry, and then turned to final specifications on the numerical-control lathe.

The tail section was cast in the form of a cone over a three day period of 301 plastic casting material. It was then turned to size and milled for T slots to allow easily interchangeable fin designs. In order to provide increased bouyancy the tail was filled with a two-part closed cell foam known as iso-foam. To provide for quick ballasting two air bladders with fill valves on the exterior of the vehicle were installed. A portable regulator and air cylinder were provided to allow ballasting of vehicle directly alongside the tow tank carriage.



In addition to such structural failures, there were numerous problems with the NCSC suppressor box and the instrumentation package. The suppressor box had to be rewired numerous times, and the bread board of the instrumentation package had to be carefully analyzed as frequent failures of the instrumentation resulted in a suspension of the testing program for months.

Sections of the towing cable had to be spliced due to lack of armor and exterior protection. A typical damaged section is shown in Figure 18.

#### 7. Mathematical Model of the Vertical Excitation

To gain some insight into the response of the towed vehicle in one of its excitation modes a mathematical model of the behavior of the towed vehicle in the vertical direction was studied. The vertical motion was assumed to be independent of all horizontal planar motions. The tow is assumed to be of a neutrally bouyant completely submerged vehicle that has a vertical force  $F_z$  and a longitudinal force  $F_x$ . Since the analysis is restricted to solely the vertical direction, Newton's equation of motion shows that for uncoupled motion only vertical forces need be considered.

The vertical force  $F_z$  originates from the feeder block of Figure 9, which is the result of an electric motor generating a sinusoidal force through an adjustable oscillatory arm in which  $\omega$  (the rotational speed) has been reduced by a set of reduction gears and a pulley system.

Let the tow cable be assumed rigid and massless. Assume the vehicle has negligible angle-of-attack while being towed. This is partly due to the counteracting forces generated by the stabilizing fins. (High speed photography verified this assumption.) Body forces due to gravity are neglected since the vehicle is neutrally bouyant.

Figure 19 depicts the geometry for the analysis. The length of the tow cable is denoted by  $l$  and the mass of the vehicle (including inside mass of



water) is  $M$ . Let  $z_1$  be the distance from the tank floor to the feeder block, and  $z_2$  be the distance from the tank floor to the C.M. of the vehicle. One can then show from Newton's second law of motion and the geometry of Figure 19 that

$$M\ddot{z}_2 + C\dot{z}_2 + (F_z)_{\max} z_2/\ell = (F_z)_{\max} z_1/\ell \quad \dots 1)$$

since

$$M\ddot{z}_2 = (F_z)_{\max} \sin\theta \quad \dots 2)$$

and

$$\theta = (z_1 - z_2)/\ell \quad \dots 3)$$

for small angles  $\theta$ . The viscous damping force is related to the vertical velocity of the C.M. by a damping coefficient  $C$ . Since

$$z_1 = 3 + R \sin \omega t \quad \dots 4)$$

where  $R$  is the amplitude governed by the rotating motor arm of Figure 11, we consider the neutral bouyancy case where  $z_2 = z_1 = z$ .

The maximum force delivered to the cable was evaluated using data from the motor, estimating the law of power through the gears ( $\eta \approx 93\%$ ) using a reduction of 60, and the pulley system of Figure 10 reducing the angular speed  $\omega$  by a factor of 2 resulting in the expression for power  $P$

$$(F_z)_{\max} \omega R = P \quad \dots 5)$$

$$\frac{(F_z)_{\max} \left( \frac{1750 \text{ rev}}{\text{min}} \times \frac{2\pi \text{ rad}}{1 \text{ rev.}} \times \frac{1 \text{ min}}{60 \text{ s}} \right) \left( \frac{1}{60 \times 2} \right)}{\left( 33,000 \frac{\text{ft-lbf}}{\text{min}} \right) \left( \frac{1 \text{ min}}{60 \text{ s}} \right)} R = (0.93) (1 \text{ hp}) \quad \dots 6)$$

or

$$(F_z)_{\max} = \frac{334.31 \text{ lbf ft}}{R} \quad \dots 7)$$



The damping coefficient C was evaluated by measuring the force that pulled the vehicle through the water at approximately 1 ft/s. The damping coefficient was calculated to be

$$C = \frac{3.75 \text{ lbf}}{\text{ft/s}} \quad \dots 8)$$

Substituting the measured and calculated constants into the equation of vertical motion resulted in

$$10.53 \ddot{z} + 3.75 \dot{z} + \frac{334.31}{R\ell} z = \frac{334.31}{R\ell} [3 + R \sin(1.53 t)] \quad \dots 9)$$

The values of the amplitude R ranged from 0.5 ft to 1 ft, and three values of tow length were chosen: 10, 12.5, and 15 ft. For example, for R = 0.5 ft, and  $\ell = 10$  ft, Equation (9) becomes

$$10.53 \ddot{z} + 3.75 \dot{z} + 80.23 z = 80.23 [3 + 0.5 \sin(1.53 t)] \quad \dots 10)$$

Using the method of Laplace transformations, the transform yields after a bit of manipulation

$$z(s) = \frac{s^2 + 0.213 s + 2.34}{s^5 + 0.356 s^4 + 9.96 s^3 + 0.833 s^2 + 17.83 s} \quad \dots 11)$$

Rather than solve the transform through standard analytical techniques, a computer solution was investigated.

The following data statements required entry into the computer program which delineated the number of polynomials in the numerator and denominator, the order of the polynomials, and the coefficients of the polynomials.

```
100 DATA 1
110 DATA 1
120 DATA 2,1,.213,2.340
130 DATA 1
140 DATA 5,1,.356,9.96,.833,17.831,0
150 DATA YES,0,10,.1
160 DATA YES
```

Three computer solutions are included in Appendix C each using the values of R = 0.5 ft and  $\ell = 10$  ft. The first solution is for a run-time of ten seconds with 0.1 second intervals. The second solution is for a 50 second run-time at 2.5 second intervals, and the third solution is a 50 second run-time at 1 second intervals.



Figure 20 is a plot of the values of the response  $z(t)$  obtained from the computer print-out of Appendix C. The response shows an initial amplitude divergence, but this gradually dampens out, indicating a stable response. The frequency of the response is 0.44 cps, or 2.76 rad/s for a forcing frequency of 1.53 rad/s.

An analog solution of the equation of vertical motion for  $R = 0.5$  ft, and  $\ell = 10$  ft was investigated so that a comparison could be made against the digital solution (Equation 10) was normalized such that

$$\ddot{z} = -0.356 \dot{z} - 7.62 z + 3.17 \sin 1.53 t + 22.86 \quad \dots(12)$$

Let

$$\ddot{z}_n = 4 \text{ ft/s}^2 ; \dot{z}_n = 2 \text{ ft/s} ; z_n = 1 \text{ ft} \quad \dots(13)$$

such that

$$\ddot{z} \frac{z_n}{z_n} = -0.356 \dot{z} \frac{\dot{z}_n}{z_n} - 7.62 z \frac{z_n}{z_n} + 3.17 \sin 1.53 t + 22.86 \quad \dots(14)$$

Setting

$$\ddot{Z} = \ddot{z}/z_n ; \dot{Z} = \dot{z}/z_n ; Z = z/z_n \quad \dots(15)$$

we transform Equation (14) as

$$\ddot{Z} = -0.356 \dot{Z} \left( \frac{\dot{z}_n}{z_n} \right) - 7.62 Z \left( \frac{z_n}{z_n} \right) + \frac{3.17}{z_n} \sin 1.53 t + \frac{22.86}{z_n} \quad \dots(16)$$

resulting in

$$\ddot{Z} = 0.178 \dot{Z} - 1.91 Z + 0.794 \sin 1.53 t + 5.71 \quad \dots(17)$$

Figure 21 shows the flow diagram for Equation (17). The motion of the vehicle is determined over 10, 20 and 50 seconds of actual towing time. Pots ①, ⑦ and ⑧ of Figure 21 depend upon the values of  $R$  and  $\ell$ , according to the following equation:

$$\ddot{Z} = -0.178 \dot{Z} - \frac{7.94}{R\ell} + \frac{7.94}{\ell} + \frac{23.81}{R\ell} \quad \dots(18)$$

$\begin{matrix} \uparrow & \uparrow & \uparrow \\ \textcircled{7} & \textcircled{8} & \textcircled{1} \end{matrix}$



For pots (2) and (4), we use the following: for pot (2)

$$\frac{\ddot{z}_n}{\dot{z}_n} = \frac{4}{2} = 2.0 \quad \dots 19)$$

or 0.2 with 10 gain, and for pot (4),

$$\frac{\dot{z}_n}{z_n} = \frac{2}{1} = 2.0 \quad \dots 20)$$

or 0.2 with 10 gain. The values of these two pots were constant throughout the analysis. The sine generator in Figure 21 came from a slave unit and its pots and amplifier numbers are denoted by a prime. The results of the analog simulation are presented in Figures 22 to 45.

### 8. Results of Analysis

Tables 2 and 3 summarize the maximum vertical acceleration, response frequency and relative stability of the vertical motion of the towed submersible under the constraints given in the previous sections. The results are for 3 different tow lengths, and 6 different excitation amplitudes for a fixed excitation frequency of 1.53 rad/s.

In general, a lengthening of the tow cable decreased the magnitude of the vertical acceleration, particularly the third cycle. (Compare Figures 29, 37 and 45.) The greater the excitation amplitude, the greater the magnitude of the vertical acceleration.

Consider Figures 26, 34 and 42. They are for a 15 ft tow. Figure 26 is the vehicles' acceleration  $\ddot{Z}$  versus real time  $t$ . Figure 34 is the vehicle's velocity  $\dot{Z}$  versus  $t$ , and Figure 42 is the vehicle's displacement  $Z$  versus  $t$ . For all three figures, let us compare the curves for an excitation amplitude of 0.5 ft. When the displacement  $Z = 0$ , the vehicle is in the static equilibrium position directly behind the feeder block. The vehicle oscillates vertically as it is towed at a frequency of 0.245 cps and passes through the static equilibrium position at  $t = 2.6, 4.1, 6.4, 8.1$ , etc. seconds at which



Table 2

Results of Maximum Acceleration for Different Tows and Amplitudes

$\ell$ Tow Length	R (ft)	Initial Value	$\ddot{z}_{\max}$	Frequency (CPS)	Relative Stability	
10.0 ft	$\frac{5}{12}$	2.3	5.0	.230	No change	Figure 22
	$\frac{6}{12}$	2.0	5.0	.230	No change	
	$\frac{7}{12}$	1.75	5.0	.230	No change	
	$\frac{8}{12}$	1.40	5.2	.244	Decrease	Figure 23
	$\frac{11}{12}$	1.1	5.0	.227	Increase	
	1	1.0	4.9	.222	Increase	
12.5 ft	$\frac{5}{12}$	1.8	4.9	.238	No change	Figure 24
	$\frac{6}{12}$	1.6	4.9	.238	No change	
	$\frac{7}{12}$	1.2	4.85	.238	Increase	
	$\frac{8}{12}$	1.20	4.82	.238	Increase	Figure 25
	$\frac{11}{12}$	.80	4.80	.238	Increase	
	1	.78	4.70	.238	Increase	
15.0 ft	$\frac{5}{12}$	1.50	3.85	.256	Increase	Figure 26
	$\frac{6}{12}$	1.20	4.00	.244	Decrease	
	$\frac{7}{12}$	1.00	4.45	.238	Decrease	
	$\frac{8}{12}$	1.00	4.70	.237	Decrease	Figure 27
	$\frac{11}{12}$	0.75	4.40	.233	Increase	
	1	0.75	4.37	.230	Increase	



Table 3

Results of Vertical Displacement Z for Different Tows Lengths and Amplitudes

$\lambda$	R (ft)	(Z) <sub>max</sub>	Frequency (CPS)	Relative Stability	
10.0 ft	$\frac{5}{12}$	1.36	.243	No change	Figure 38
	$\frac{6}{12}$	1.36	.243	No change	
	$\frac{7}{12}$	1.36	.243	No change	
	$\frac{8}{12}$	1.35	.243	No change	Figure 39
	$\frac{11}{12}$	1.35	.243	No change	
	1	1.35	.243	No change	
12.5 ft	$\frac{5}{12}$	1.35	.243	No change	Figure 40
	$\frac{6}{12}$	1.35	.243	No change	
	$\frac{7}{12}$	1.35	.243	No change	
	$\frac{8}{12}$	1.35	.243	No change	Figure 41
	$\frac{11}{12}$	1.35	.243	No change	
	1	1.35	.243	No change	
15.0 ft	$\frac{5}{12}$	1.35	.243	No change	Figure 42
	$\frac{6}{12}$	1.35	.243	No change	
	$\frac{7}{12}$	1.35	.243	No change	
	$\frac{8}{12}$	1.35	.243	No change	Figure 43
	$\frac{11}{12}$	1.35	.243	No change	
	1.0	1.35	.243	No change	



time the velocity  $\dot{Z}$  is a maximum (see Figure 34) and the acceleration  $\ddot{Z}$  is zero (See Figure 26). Similarly, the maximum displacements (and accelerations) of the vehicle occur when the velocity is zero, i.e., at  $t = 1.75, 3.375, 5.375, 7.25$ , etc., seconds. A similar conclusion is reached for other combinations of tow length and excitation amplitude.

A comparison of the simplified mathematical model against actual experimental measurements showed similar behavior and response frequencies. For example, comparing the mathematical solution of the acceleration  $\ddot{Z}(t)$  of Figure 22 with the experimental measurement for  $\ddot{Z}(t)$  of case 7 (Figure 163) shows the response frequencies within 5% error. Hence, the mathematical model served as a first order approximation to validate the experimental measurements.

#### 9. Result of Experimental Program

Figures 46-179 present a small portion of the experimental measurements. Figures 46-68 show the variation of velocity with real time for a variety of tow lengths, excitation amplitudes and frequencies. The figures are important as they show the precise time the vehicle reaches its desired velocity as well as the interval of time at which the velocity is constant. During this interval of time we are interested in measuring the pitch, roll, yaw, x-acceleration, and z-acceleration.

Case numbers 2-4, 8, 15, and 16 are for no excitation in the horizontal and vertical modes. All other runs are for various combinations of excitation frequency and amplitude. The predetermined value of vertical excitation frequency and amplitude match the value of the horizontal excitation frequency and amplitude. (See Table 4 for identifying the parameters that were varied in the experiment.)

Figures 69-91 contain the vehicle's pitch response versus real time for Cases 2-24. Figures 92-114 contain the vehicle's roll response versus real time



TABLE 4

## EXPERIMENTAL PARAMETERS

Case	Velocity, (ft/s)	Tow Length, (ft)	Frequency, (Hz)	Amplitude, (in)
2	4.02	15	0	0
3	6.0	15	0	0
4	5.98	15	0	0
5	6.0	15	0.1	18
6	6.0	15	0.2	18
7	6.0	15	0.2	9
8	18.0	15	0	0
9	18.0	15	0.2	9
10	18.0	15	0.33	9
11	6.0	15	0.33	9
12	18.0	15	0.2	18
13	18.0	15	0.1	18
14	6.0	15	0.1	18
15	6.0	5	0	0
16	18.0	5	0	0
17	18.0	5	0.1	18
18	6.0	5	0.1	18
19	6.0	5	0.2	18
20	18.0	5	0.2	18
21	18.0	5	0.2	0
22	6.0	5	0.2	9
23	6.0	5	0.3	9
24	18.0	5	0.3	9



for runs 2-24. Figures 115-136 contain the vehicle's yaw response versus real time for runs 2-24. Figures 137-157 contain the vehicle's z-acceleration versus real time for runs 2-24. Figures 158-179 contain the vehicle's z-acceleration versus real time for runs 2-24.

### 9.1 Pitch

With no excitation, the pitch increases as the vehicle accelerates, then slowly decays to near equilibrium position. (See Figure 70.) Whenever the vehicle decelerates, the pitch may initially increase (see Figures 70 and 75) then slowly decays back to its equilibrium position, and in other cases, the pitch decays (see Figure 71).

With external excitation, the towed submersible's pitch increases suddenly during the acceleration until reaching a relatively large pitching angle. Once the vehicle reaches uniform velocity, the vehicle overshoots its equilibrium pitch position then dampens to a rather small value. (See Figures 72-76.) There was never an instability or a divergence of pitch for any combination of parameters. The largest pitch response was for a short tow, low velocity, large excitation amplitude and small excitation frequency (Case 14 or Figure 81, and Case 18 or Figure 85). The response frequency is very nearly the excitation frequency in all cases tested. (See in particular Figures 78, 85 and 86.)

Changing the tow cable length influences the pitch. Comparing Figure 73 with Figure 86 we see that the maximum pitch amplitudes are nearly identical for low velocity, moderate excitation frequency and large excitation amplitude. Yet when we increase the excitation frequency from 0.2 Hz to 0.33 Hz, the maximum pitch response of the short tow is half as large as for the long tow. (Compare Figure 78 with Figure 90.) At high speeds, the long tow has a pitch response as large as the short tow case for the moderate excitation frequency (the same conclusion for the low speed tow), as can be seen from Figures 79 and 8



we increase the excitation from 0.2 Hz to 0.33 Hz the maximum pitch response of the long tow is half as large as for the short tow. (Compare Figures 77 and 91.) This is just the opposite to what we learned for a low velocity tow.

Changing the excitation frequency influences the maximum pitch response. (See Figures 72 and 73, 79 and 80 for no influence.) Examination of Figures 85 and 86 show that as the excitation frequency is increased from 0.1 Hz to 0.2 Hz, the maximum pitch angle is halved. Note both responses are damped.

## 9.2 Roll

As the vehicle accelerates to its predetermined experimental velocity, it rolls to a significantly large angle, and in the majority of cases quickly rolls back to nearly its static condition during its constant velocity run. (See Figures 94 to 100, and 104.)

For the case of no external excitation (see Figures 92-94, 98, 105, and 106), all but for the short tow, high velocity case (Figure 106), the vehicle had a stable response. In Figure 106, we note a significant large oscillatory roll during the constant velocity run that may not die out. The time interval was too small to determine whether the response would dampen to small maximum amplitudes.

Let us consider what happens when we introduce an excitation. Comparing Figure 100 with Figure 101 shows that the response frequency for a low value of tow velocity is over twice as large as the response frequency for a large tow velocity. There is insufficient experimental data to propose an empirical equation between the roll response frequency and tow velocity except that

$$\omega_{\text{roll}} \propto \frac{1}{V} \quad \dots 21)$$

Changing the length of tow cable does not affect the roll frequency. Comparing Figures 96 with 109 shows that the roll frequency for a cable length



of 15 ft (Figure 96) is the same as the roll frequency for a cable length of 6 ft (Figure 109).

A change in the excitation frequency had no large effect on the roll frequency. (Compare Figures 95 with 96, 102 with 103, 108 with 109 and 112 with 113.) The excitation amplitude also had little effect on the roll frequency.

Parameters which influenced the roll amplitude are interesting. The greater the tow velocity the greater the roll response amplitude. (Compare Figure 100 with Figure 101 and Figure 107 with Figure 108.) The shorter the tow cable, the larger the roll response amplitude (compare Figure 96 with Figure 109). A change in excitation frequency does not significantly alter the response amplitude. (Compare Figure 108 with Figure 109.)

In Figure 109, we see the amplitude of the roll increasing during the constant velocity run, yet in Figure 104 we see the amplitude decreasing indicating that short tows are conducive to divergent behavior. We can see a marked divergent behavior in Figure 110, where there is a short tow and high velocity. The roll maximum angles have doubled in magnitude (compare Figure 109 with Figure 110) for a triple increase in tow velocity. Even halving the excitation amplitude, the divergent behavior is evident, though the maximum response amplitudes have been reduced considerably. (Compare Figure 110 with Figure 112.) However, once we exceed the excitation frequency  $\omega = 0.2$  Hz, the roll response appears stable (compare Figure 113 with Figure 112), although the response roll maximum amplitude remains unchanged. Even tripling the tow velocity will not trip the roll response into its divergent behavior providing the excitation frequency is greater than 0.2 Hz.

### 9.3 Yaw

Like pitch and roll, yaw had similar responses to changes in towing velocity, cable tow length, excitation frequency and amplitudes. As the vehicle



accelerates to its predetermined experimental velocity, it rolls to a significantly large angle, then slowly returns to its equilibrium position. (See Figures 116, 117 and 118.)

Figures 115-117, 120, 127 and 128 are the runs where no excitation was introduced. The yaw response was relatively high frequency (0.4 Hz) at low maximum amplitudes. (See Figures 117 and 127.) The vehicle was stable. Note, even the short tow (Figure 128) did not indicate any yaw divergence.

Let us consider what transpires when we introduce excitation. Comparing Figure 122 with Figure 123, we see that the response frequency for a low value of tow velocity is somewhat lower than the response frequency for large values of tow velocity. Thus, it appears that the yaw frequency is not overly dependent on the tow velocity.

Changing the length of tow cable does not affect the yaw frequency. Comparing Figure 119 with Figure 131 shows that for a cable length of 15 ft (Figure 119) the yaw frequency is the same as in the case of a cable length of 6 ft (Figure 131).

A change in the excitation frequency has a direct effect on the yaw frequency. (Compare Figures 118 and 119, 124 and 125, 130 and 131, 134, and 135.) The response frequency is exactly the forcing frequency.

Parameters which influenced the yaw response amplitude are interesting. The greater the tow velocity the smaller the maximum yaw amplitude. (Compare Figures 122 and 123, and Figures 129 and 130.) This is just the opposite to what occurred for roll. The shorter the tow cable the smaller the maximum yaw amplitude. (Compare Figure 119 with Figure 131.) This also is opposite to the roll response. A change in forcing frequency has a pronounced effect on the amplitude of the yaw response. Comparing Figure 130 with Figure 131, we see that for an excitation forcing frequency  $\omega_e = 0.1$  Hz,  $L = 5$  ft,  $V = 6$  ft/s



$\lambda_e = 18$  in (Figure 130), the amplitude is nearly half the value when  $\omega_e = 0.2$  Hz,  $\ell = 5$  ft,  $V = 6$  ft/s,  $\lambda_e = 18$  in (Figure 131). But increasing the excitation frequency to 0.3 Hz does not alter the maximum yaw amplitude. This suggests that  $\omega_e = 0.2$  Hz is the critical frequency for the towed submersible.

In each of the runs, the amplitudes of yaw remained similar, neither decaying nor growing.

In all but one case, the amplitudes of yaw remained similar, neither decaying nor growing. Only for the low velocity tow and short cable length case (Figures 130, and 131) is there a pronounced damping of the yawing motion. None of the experimental runs produced any unstable yawing motion.

#### 9.4 Longitudinal Acceleration

Figure 139 shows the longitudinal acceleration of the towed missile. Once the carriage has reached uniform velocity of 6 ft/s (at  $t = 23.1$  s), the missile decelerates to zero acceleration in 6.9 s and remains at zero acceleration for the constant velocity run. However, at high towing speeds the vehicle's longitudinal acceleration was never zero during the brief 7.5 s constant velocity run. (See Figure 149.) Hence, for high velocity tows we cannot state that the vehicle was at uniform velocity. This might possibly be due to a malfunction of the rate gyros, but it is not considered likely due to the repeatability of the data.

Figure 142 shows the longitudinal acceleration for a long tow (15 ft) and moderate excitation frequency of 0.2 Hz. The vehicle's response is easily identifiable, picking up the surging excitation and responding at 0.2 Hz.

Increasing the excitation frequency from 0.2 Hz to 0.3 Hz with no change in excitation amplitude, resulted in large changes in acceleration at a frequency 0.3 Hz that matched the excitation frequency. (Compare Figure 142 with Figure 145.) This is also verified in Figures 151 and 152, and Figures 155 and 156. In these examples, the response is stable though slightly damped.



Change of cable length influenced the longitudinal acceleration. For example Figure 141 is the case where  $V = 6$  ft/s,  $\omega_e = 0.2$  Hz,  $\lambda_e = 18$  in and  $l = 15$  ft. Figure 152 is the case where  $V = 6$  ft/s,  $\omega_e = 0.2$  Hz,  $\lambda_e = 18$  in and  $l = 5$  ft. In the former, there is no appreciable change in acceleration except an impulsive change every 10 s, whereas in the latter, there are continual changes of acceleration, yet the response is stable and slightly damped. Comparing Figure 144 with Figure 157, the long tow has the greater change in longitudinal acceleration. Yet in comparing Figure 142 with Figure 155, we see that the two responses are similar to nearly identical, such that one must exercise caution in making general statements on the longitudinal acceleration response to a change in tow cable length.

A change in tow velocity (keeping all other parameters fixed) results in a change in the maximum longitudinal acceleration response, as can be seen by comparing Figures 144 with 145. Small tow velocities give small maximum response, and large tow velocities give large maximum response. (See also Figures 146 and 147.) The responses have similar signatures with a change in tow velocity, and the responses are all stable.

The longitudinal acceleration was stable and damped for all excitation variations. This is evident by examining a few examples, such as Figures 151-157.

#### 9.5 Vertical Acceleration

Figures 159, 160, 170 and 171 show the vertical acceleration response of the towed submersible for the case of no excitation. Once the tow carriage reaches uniform velocity, the vehicle has very small vertical motion. In Figure 159, the towed vehicle was initially resting on the water surface, which is indicated by the near zero voltage line for approximately 9 seconds. When the tow carriage commenced accelerating the towed submersible dove deeply and within 5 seconds reached dynamic equilibrium.



Figures 165 and 166 show the effect of change in tow velocity on the towed submersible's vertical acceleration. At a velocity of 6 ft/s (Figure 166), the maximum vertical acceleration is almost one-half the maximum vertical acceleration for a tow velocity of 18 ft/s, (see Figure 166). This is true whether for a long tow cable length, or a short cable length. (Compare Figures 172 and 173.)

The effect of varying the tow cable length on the towed vehicle's vertical acceleration can best be seen by comparing Figure 163 with Figure 177. For a long tow (15 ft), the maximum vertical acceleration is almost identical to the short tow (5 ft). These results are for an excitation frequency of 0.2 Hz. Increasing the excitation frequency to 0.33 Hz, we find the long tow (15 ft) case (Figure 166) has a maximum vertical excitation response much less than the short tow (5 ft) case (Figure 178). But then if we increase the tow carriage velocity three-fold for the short tow, the acceleration response is reduced nearly one-third. This is substantiated if we compare Figures 174 and 175. At a reduced excitation frequency of 0.2 Hz, we see that for the short tow length, a tripling of tow speed has reduced the maximum vertical acceleration by one-third. A combination of tow cable length and tow speed are important parameters influencing the towed submersible's vertical acceleration.

A change of excitation frequency on the maximum vertical acceleration of the towed vehicle is seen by comparing Figures 167 and 168, Figures 173 and 174 and Figures 177 and 178. For long tows and high speeds, a change in excitation frequency does not have significant influence on the vertical acceleration. (Compare Figure 167 with 168.) An increase of excitation frequency does have an influence for low speed and short tows. An increase of frequency decreases the maximum vertical accelerations (see Figures 173 and 174). But then, let us see what happens when we halve the excitation amplitude. Figures 173 and 174 were for a 18 in crest-to-trough amplitude. If we compare Figures 177 and 178 (which



are for a 9 in amplitude), an increase of excitation frequency gives an increase of maximum vertical excitation. Thus a reversal of trend can be had by manipulating the excitation amplitude. There also appears to be a gradual growth of maximum acceleration in this latter case.

The only combination of parameters lending itself to a possible instability are the conditions for Figures 166 and 178; i.e., the low velocity tow, high excitation frequency and small excitation amplitude. Both the short tow and long tow have no marked effect on this trend towards divergent motion.

#### 10. Conclusions

There are a number of important conclusions obtained from this experiment. Some of them are general and appear to hold for the range of test parameters whereas others are specific and hold for unique values of test parameters.

The towed submersible proved to be stable in both the longitudinal and vertical domain providing the towed vehicle is not accelerated. Any acceleration will cause the pitch angle to grow. In most instances of deceleration there is also a very large increase of pitch.

Acceleration also causes large initial rolling of the towed submersible, whereas deceleration produces no large changes. There does not appear to be any reasonable explanation why roll angle diverges for certain combinations of parameters and not others. There is nothing consistent in its behavior. For example at high frequency of excitation (Cases 10, 11, 23, and 24) there is a damped roll response for all cases except for Case 11.

Acceleration causes large yawing motion, but during the constant velocity runs, the yaw is extremely stable. Deceleration produces large yaw angles, as would be expected.

The longitudinal acceleration showed no surprises, its response being predictable and well-behaved. The vertical acceleration was stable for all ranges of parameters, and its motion was verified by the mathematical model of section 6.



The towed submersible's response frequency matched the excitation frequency. Spurious data was obtained at times and was attributed to gyro malfunction.

The towed submersible overshoot its equilibrium position in most every instance of acceleration and deceleration, which is easily explained by examining the characteristic equations of hydrodynamic stability of towed systems, e.g., Reference 1. Anytime there are oscillatory roots of the characteristic stability equation, one can expect that the vehicle will overshoot while returning to its equilibrium position.

The faster the body was towed, the less the natural period of oscillation. For example, in the transition from 6 ft/s to 18 ft/s the period varied from 1.5 to 1.2 seconds for the vertical motion. The mathematical model verified an oscillatory motion with little tendency to dampen out. The digital solution obtained has an exponential coefficient of nearly unity ( $\sim e^0$ ). If an instability is desired it is recommended trying to force positional instability by forcing an unstable acceleration of the system using a short tow cable length (i.e., 1-3 ft). High speed films show the towed submersible oscillates vertically about its dynamic equilibrium position with nearly zero angle-of-attack.

As the towing cable length is reduced, there is a corresponding decrease in the natural vehicle motion. For low tow velocities, the maximum pitch response for a short tow is half the value for the long tow. But at high speeds, the situation is reversed. A change in cable length does not affect the roll frequency or the yaw frequency.

The effect of buoyancy and longitudinal c.g. position on the motion of the towed submersible was not significant, and so the data is not presented.

Reference 2 is an audio-colored visual tape of the present experimental project, showing the stages of development of the experimental apparatus, actual test runs, and test results.



## References

1. Sumney, D. C., "Hydrodynamic Design and Analysis of a Towed Environmental Sensor Vehicle," NCSC report (14 August 1979).
2. Granger, R. A., "Submerged Sensing Simulation," ERC Control No. 05850-822115, U. S. Naval Academy, (1983).



## APPENDIX A

### Operation of the Transera Analog to Digital Converter



CALL "8BIT"  
CALL "12BIT"

There are two routines to select the resolution of the A/D module. Executing CALL "8BIT" in Tektronix BASIC will cause the module to convert data to 8 bit data. One byte is used to store data in this format. Executing CALL "12BIT" causes the module to convert data to 12 bit format and store it in 2 bytes. The module powers on in 12 bit mode.

CALL "A/D" X,C

Call "A/D", X,C causes the channel designated by the variable C to be read 16 times, the samples averaged, and the result stored in the variable X. This routine always operates in 12 bit mode and automatically sets the gain.

EXAMPLE:

```
100 X=0
110 C=1
120 CALL "A/D",X,C
130 PRINT X
140 END
```

CALL "A/D",A1

This call reads a series of channels. Is identical to the above routine except that it requires that A1 be an array which has been dimensioned to the number of channels to read. For example,

```
100 DIM A1(4)
110 A1=0
120 CALL "A/D",a1
130 PRINT A1
140 END
```

will cause the voltages at channels 1 thru 4 to be read into the array A1. Note that the array must not be dimensioned any larger than 16 and that the array must be zeroed before it is used the first time. This routine also operates in 12 bit mode and performs automatic gain selection.



CALL "BURST",A\$,N,P,C,T,R

This routine reads samples from a single channel at a rate specified by the user.

N = number of samples to read.

A\$ = array to hold sample data.

Dimension to N for 8 bit data and to N\*2 for 12 bit data. Define the array prior to the CALL by A\$="".

P = period (in seconds) of delay between samples.

The 4051 maximum is .63 and its minimum is 3.12E-5 for 8 bit resolution and 4.8E-5 for 12 bits. The 4052/4 maximum is .41 and its minimum is 3.33E-5 in 8 bit mode and 4.94E-5 in 12 bit mode.

C = channel to read.

T = trigger mode.

0 starts converting at the call.

1 starts on a low TTL level on the trigger input.

2 starts on a high TTL level on the trigger input.

R = gain (range) select.

Valid gains are 1, 4, or 32 for any channel.

#### EXAMPLE:

```
100 N=100
110 DIM A$(N*2)
120 P=1.0E-3
130 C=1
140 T=0
150 R=1
160 REM INITIALIZE A$
170 A$=""
180 REM READ DATA
190 CALL "BURST",A$,N,P,C,T,R
200 REM TO PRINT THE DATA IT MUST BE UNPACKED.
210 REM REFER TO THE ROUTINE "UNPAK2"
220 O=2048
230 D=204.8 * R
240 B=2
250 DIM A(N)
260 A=0
270 CALL "UNPAK2",A$,A,N,B,O,D
280 PRINT A
290 END
```

This mode is where the high speed may be obtained. All others are slower.



CALL "SCAN",A\$,N,P,C\$,T,R,L,S

Scan is similar to BURST except that it allows a sequence of channels to be scanned, triggering on the level of an input signal, and allows a number of samples prior to the trigger to be saved. Its maximum rate is about 3000 samples per second.

N = number of samples after the trigger.

S = number of samples before the trigger.

A\$ = array to hold data.

Dimensioned to S+N for 8 bit data and 2\*(S+N) for 12 bit data.

P = time delay before scanning channels again.

If C = the number of channels specified in C\$, then for the 4051 the maximum time is  $P = C*368E-6$  and the maximum time is  $P = .63$  seconds. For the 4052/4,  $P(\text{min}) = C*307E-6$  and  $P(\text{max}) = .41$  seconds. Appendix E of the Transera manual elaborates on this delay.

C\$ = string containing the channel sequence.

Numbers 1-9 specify channels 1-9, letters A-G specify channels 10-16. The channel sequence may be any length and will be repeated until the number of samples specified by N are taken.

T = trigger mode.

0 starts at call.

1 starts at a low TTL level on trigger input.

2 starts at a high TTL level on trigger input.

3 starts when the input on channel C\$(1) is less than the value of L.

4 starts when the input on channel C\$(1) is greater than the value of L.

R = gain (range) select.

Valid gains for the first 8 channels are 1,4, or 32.

The next 4 channels are preset with a gain of 4 and the last 4 channels are preset to 32.

L = level trigger on.

If T=0, then L must still be defined.

S = number of samples to save prior to the trigger.

If T=0, then S must still be defined.



EXAMPLE:

```

110 S=0
120 DIM A$(2*(N+S))
130 P=1.0E-3
140 C$="123459"
150 T=0
160 R=1
170 L=C
180 REM INITIALIZE A$
190 A$=""
200 REM SCAN CHANNELS
210 CALL "SCAN",A$,N,P,C$,T,R,L,S
220 REM TO PRINT THE DATA IT MUST BE UNPACKED.
230 REM REFER TO THE ROUTINE "UNPAK2".
240 C=2048
250 D=204.8 * R
260 B=2
270 DIM A(N=S)
280 A=0
290 CALL "UNPAK2",A$,A,N,B,0,D
300 PRINT A
310 END

```

This example scans channels 1,2,3,4,5, and 9. The time between sampling consecutive channels is 368E-6 seconds for the 4051. However, 1.0E-3 second will elapse before the same channel is read the next time. L and S are not used, but must be defined and passed to the routine. Ten samples are saved from before the trigger and 100 samples are saved after the trigger. The gain is set on 8 of the inputs in scan mode. Of the 16 channels, the first 8 can be programmed with any of three gains. The next 4 channels are set to a gain of 4 and the last 4 are set for a gain of 32.



CALL "UNPAK2",A\$,A,N,B,S,D

The UNPAK2 routine is used to convert data samples read from the BURST and scan routines into floating point numbers which correspond to the actual voltages read.

N = number of samples to unpack

A\$ = array to hold unpacked data.

A = array to hold unpacked floating point data.

B = number of bytes per sample.  
1 for 8 bit data.  
2 for 12 bit data.

S = offset subtractor value.  
S = 2048 for 12 bit data.  
S = 128 for 8 bit data.

D = scaling factor.  
Set D to  $204.8 * R$  for 12 bit data.  
Set D to  $12.8 * R$  for 8 bit data. Where R is the gain factor specified in the SCAN or BURST routine.

EXAMPLE:

```
100 N=100
110 DIM A$(N*2),A(N)
120 P=1.0E-3
130 C=1
140 T=0
150 R=1
160 B=2
170 C=2048
180 D=204.8 * R
190 REM INITIALIZE A$ and A
200 A$=""
210 A=0
220 REM READ DATA
230 CALL "BURST",A$,N,P,C,T,R
240 REM NOW UNPACK THE DATA FOR PRINTING
250 CALL "UNPAK2",A$,A,N,B,0,D
260 REM PRINT THE RESULTS.
270 FOR I=1 TO N
280 PRINT "A(";I;") = ";A(I)
290 NEXT I
300 END
```

This example reads 12 bit data from channel 1 in burst mode and unpacks it into the array A as numbers corresponding to the actual voltage read. The data is then printed.



CALL "MIN\$",A\$,M1,F,B  
CALL "MAX\$",A\$,M2,F,B

These routine are used to find the minimum or maximum values of data samples taken by the BURST or SCAN routines.

A\$ = array of packed data from SCAN or BURST routine.

M1 = variable to be assigned the min value.

M2 = variable to be assigned the max value.

F = position of the min/max value within the array.

B = number of bytes per sample.

The values of the MIN and MAX can be used to set the WINDOW before a call to PLOT\$. Refer to the PLOT\$ routine on the next page for an example of the use of MIN\$ and MAX\$.



CALL "PLOT",A\$,E,B,C,I

PLOT does a continuous line plot of packed data to the screen or external plotter. The value of each sample is plotted in the Y direction and the X direction is automatically indexed to correspond to the sample being plotted. A WINDOW command must be executed in Tektronix BASIC prior to the PLOT\$ call. The window in the X direction should be set to the number of samples to be plotted. The window in the Y direction should be set to 4096 for 12 bit data or 256 for 8 bit data.

A\$ = array to hold sample data from SCAN or BURST.

E = device number to plot on.

Tektronix Screen = 32

Television Display Generator = 1

B = number of bytes per sample.

C = number of channels scanned.

A separate plot will be generated for each channel.

The value of C should equal 1 for BURST data.

I = number of samples per channel to plot.

**EXAMPLE:**

```
100 N=100
110 DIM A$(N*2)
120 P=1.0E-3
130 C=1
140 T=0
150 R=1
160 E=32
170 I=N
180 B=2
190 REM INITIALIZE A$
200 A$=""
210 REM READ DATA
220 CALL "BURST",A$,N,P,C,T,R
230 REM FIND THE MAX AND MIN VALUES OF THE DATA.
240 CALL "MIN$",A$,M1,F,B
250 CALL "MAX$",A$,M2,F,B
260 REM NOW SET THE WINDOW
270 WINDOW 0,N,M1,M2
280 REM PLOT THE DATA
290 CALL "PLOT$",A$,E,B,C,I
300 END
```

This program reads 100 samples in BURST mode from channel 1. The MAX/MIN values of the samples are found in order to set the window so that Y ranges from the bottom to the top of the plot, i.e., YMIN is at the bottom and YMAX is at the top of the screen. Plotting is done to the Tektronix screen (device #32) and all data points are plotted. The axis is not drawn or labeled, however this may be done by functions within Tektronix BASIC



**APPENDIX B**  
**Printout of Data**



Naval Academy Time-Sharing  
Line 0/0232 on at 17:31 21 Mar 82, 054 users.

ATTN USERS: THE COMPUTER WILL BE UP UNTIL 0630 MONDAY MORNING.

User number--820876,88888888  
Course number--NOC

Ready

OLD L.ES\*\*\*:INVERSE  
Ready

100 DATA 1  
110 DATA 1  
120 DATA 2,1,.213,2.340  
130 DATA 1  
140 DATA 5,1,.356,9.96,.833,17.831,0  
150 DATA YES,0,10,.1  
160 DATA YES  
RUN

INVERSE 21 Mar 82 17:33

=====

GAIN = 1

NUMERATOR TERMS  
1 0.213 2.34

NUMERATOR ROOTS  
-0.1065 J-1.52599  
-0.1065 J 1.52599

DENOMINATOR TERMS  
1 0.356 9.96 0.833 17.831 0

-----

DENOMINATOR ROOTS	MULTIPLICITY
0 J 0	1
0 J-1.52972	1
0 J 1.52972	1
-0.178005 J-2.75468	1
-0.178005 J 2.75468	1

-----

THE SOLUTION, X(T), IS

0.1312  
0.0262 \*EXP( 0 T)\*SIN( 1.52972 \*T+(-6 ))  
WN = 1.52972 Z = 0  
0.1305 \*EXP(-0.178005 T)\*SIN( 2.75468 \*T+(-101 ))  
WN = 2.76043 Z = 5.44845E-2

-----

THE RESPONSE OF X(T) IS

TIME	X(T)
0	(MIN) 1.09896E-7
0.1	1.09896E-7

45



0.6	0.104286
0.7	0.13937
0.8	0.173699
0.9	0.20486
1.	0.23073
1.1	0.248625
1.2	0.260408
1.3	(MAX.) 0.262554
1.4	0.256165
1.5	0.241946
1.6	0.22113
1.7	0.195371
1.8	0.166609
1.9	0.13692
2.	0.108358
2.1	8.28124E-2
2.2	6.18724E-2
2.3	4.67273E-2
2.4	0.038096
2.5	(min) 3.61948E-2
2.6	4.07432E-2
2.7	5.10071E-2
2.8	6.58728E-2
2.9	8.39468E-2
3.	0.103672
3.1	0.123452
3.2	0.141773
3.3	0.157313
3.4	0.169035
3.5	0.176255
3.6	(max) 0.178676
3.7	0.176396
3.8	0.169887
3.9	0.15994
4.	0.14759
4.1	0.134033
4.2	0.120521
4.3	0.108264
4.4	9.83359E-2
4.5	9.15967E-2
4.6	(min) 8.86294E-2
4.7	0.089702
4.8	9.47551E-2
4.9	0.103413
5.	0.115022
5.1	0.1287
5.2	0.143417
5.3	0.158068
5.4	0.171559
5.5	0.182993
5.6	0.191232
5.7	0.195966
5.8	(max) 0.196746
5.9	0.193504
6.	0.186454
6.1	0.176071
6.2	0.167045
6.3	0.148234
6.4	0.132596
6.5	0.117116
6.6	0.102742
6.7	9.03168E-2



7.2	(max)	8.00705E-2
7.3		8.84115E-2
7.4		9.83093E-2
7.5		0.109024
7.6		0.119812
7.7		0.129976
7.8		0.138918
7.9		0.146171
8.		0.151432
8.1		0.154569
8.2	(max)	0.155624
8.3		0.154798
8.4		0.152425
8.5		0.148938
8.6		0.14483
8.7		0.140609
8.8		0.136755
8.9		0.133685
9.		0.131715
9.1		0.131043
9.2		0.131734
9.3		0.133717
9.4		0.136798
9.5		0.140673
9.6		0.144962
9.7		0.149238
9.8		0.15306
9.9		0.156016
10.		0.15775

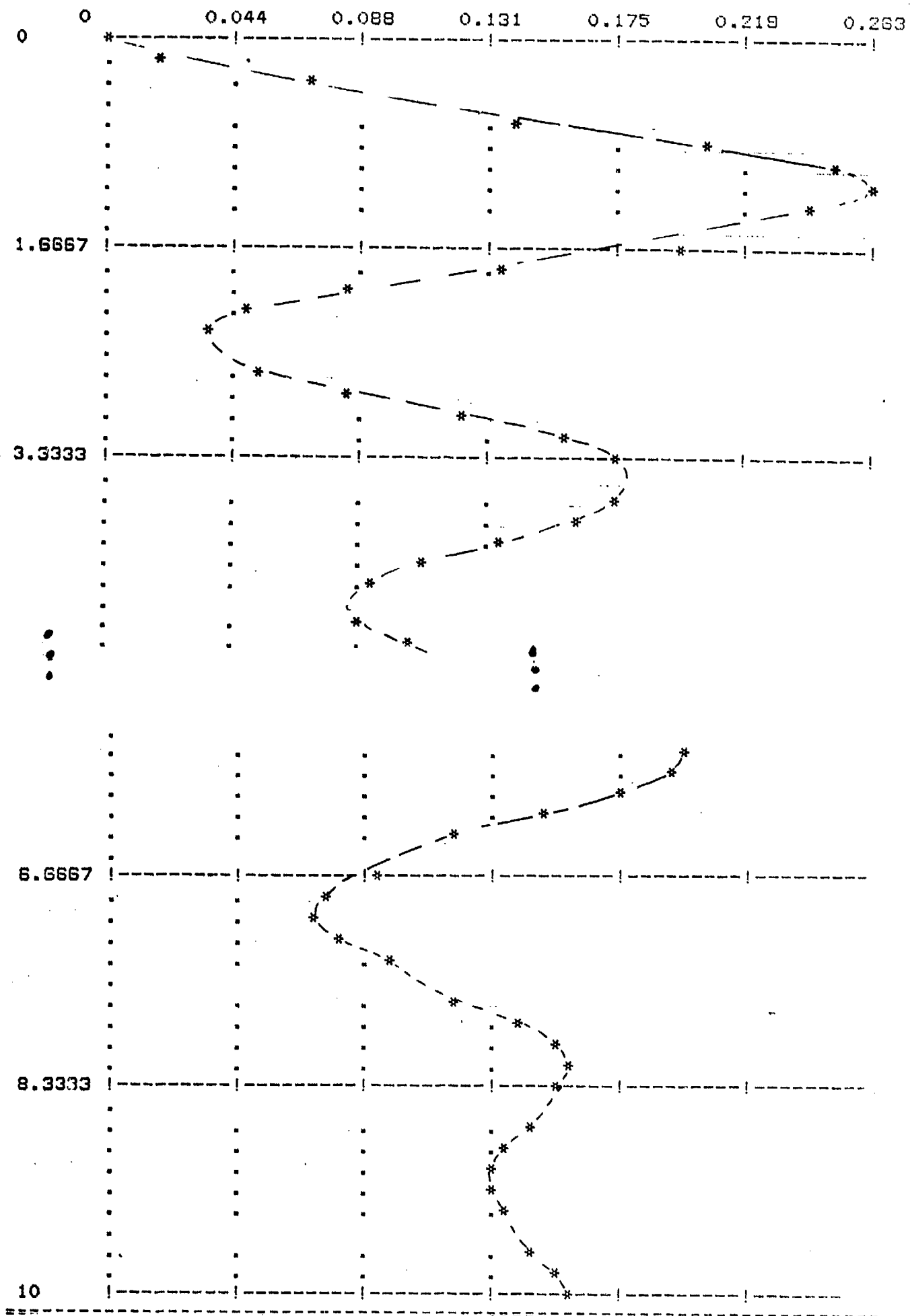
---



#### APPENDIX C

Computer Solution of Vertical Motion Laplace Transform Equation 11)  
for  $R = 0.5$  ft,  $l = 10$  ft







#### APPENDIX D

#### Description of USNA High Speed Towing Tank



Figure A.1 is a longitudinal view of the USNA's 380 ft long, 26 ft wide and 16 ft deep towing tank. The 380 ft operating length was chosen to give 5 seconds of steady-state data at 30 knots and sufficient length to accelerate, stabilize, and decelerate the 2000 lb carriage and 800 lb towing strut assembly.

The tank cross section is shown in Figure A-2. The 16 ft depth minimizes surface wave problems and ventilation for high speed submerged vehicles. The 26 ft width minimizes blockage corrections.

The rail supports are structurally isolated from the tank walls to minimize carriage generated noise transferring into the water as well as to raise or lower the water level without affecting rail alignment.

The high speed carriage is externally powered and provided the housing for the investigator and instrumentation.

Measurements made in the high speed basin at NSRDC revealed that any noise caused by the rooster tail of a towing strut, together with cavitation and ventilation near the water surface may be a serious problem at frequencies above 1 kHz. Thus only at high velocities of tow would rooster tails be a problem, and thus a bottom plate was attached to the box beam to catch the spray before it hit the surface.



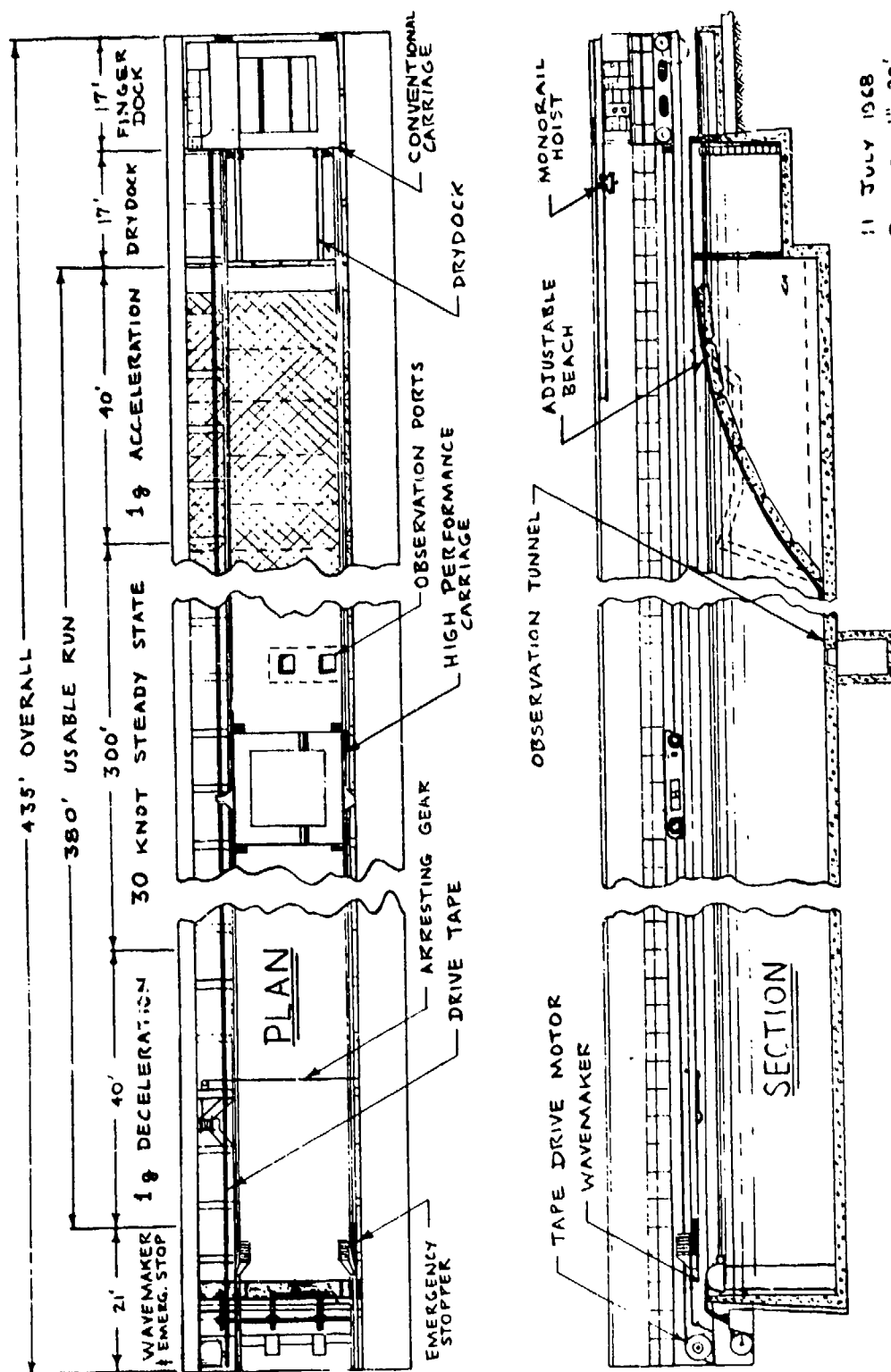
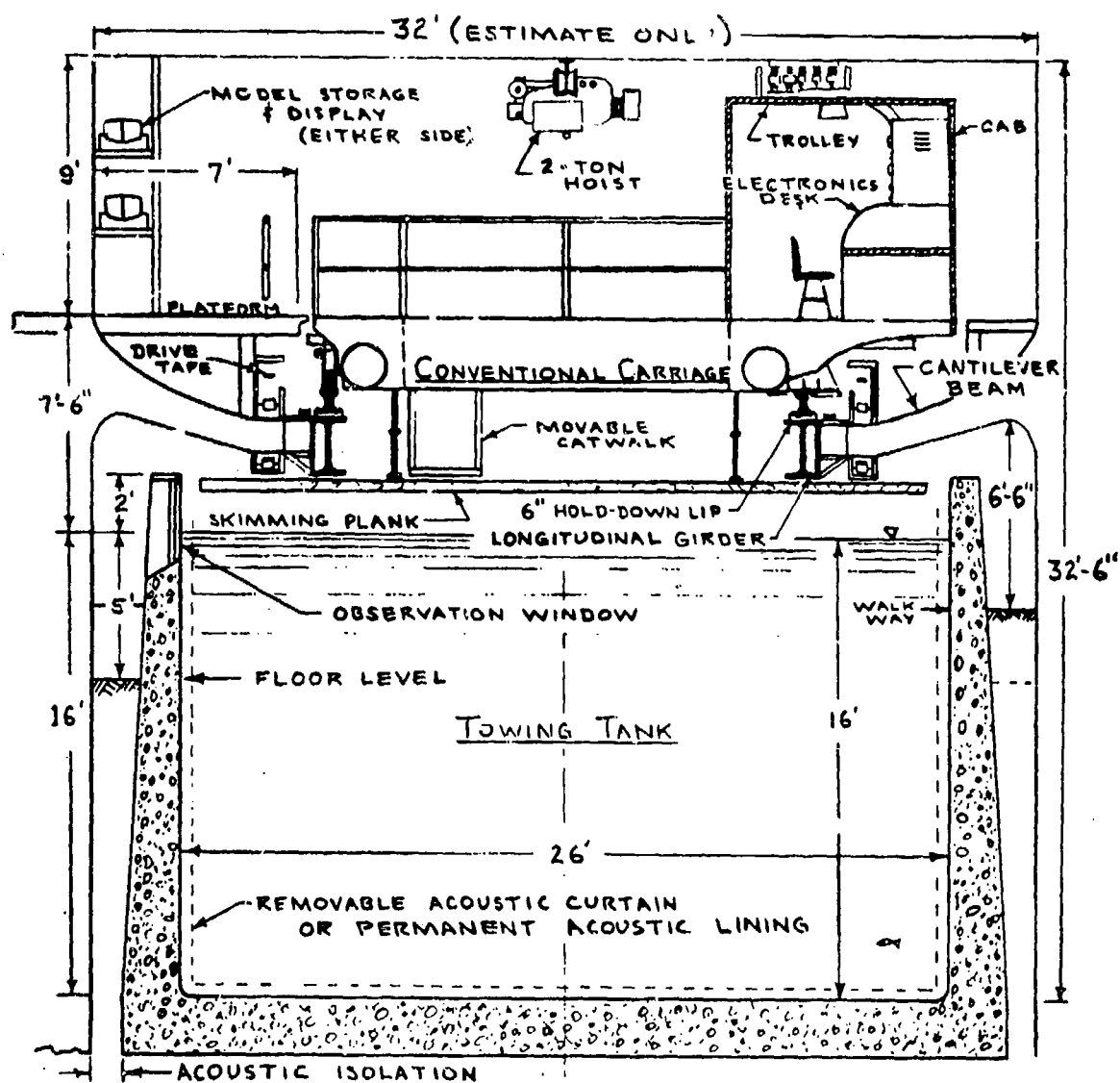


Fig. A.1 Longitudinal view of 380-ft tank





11 JULY 1968  
SCALE: 1" = 5'

Fig. A-2 Sectional view of 380-ft tank



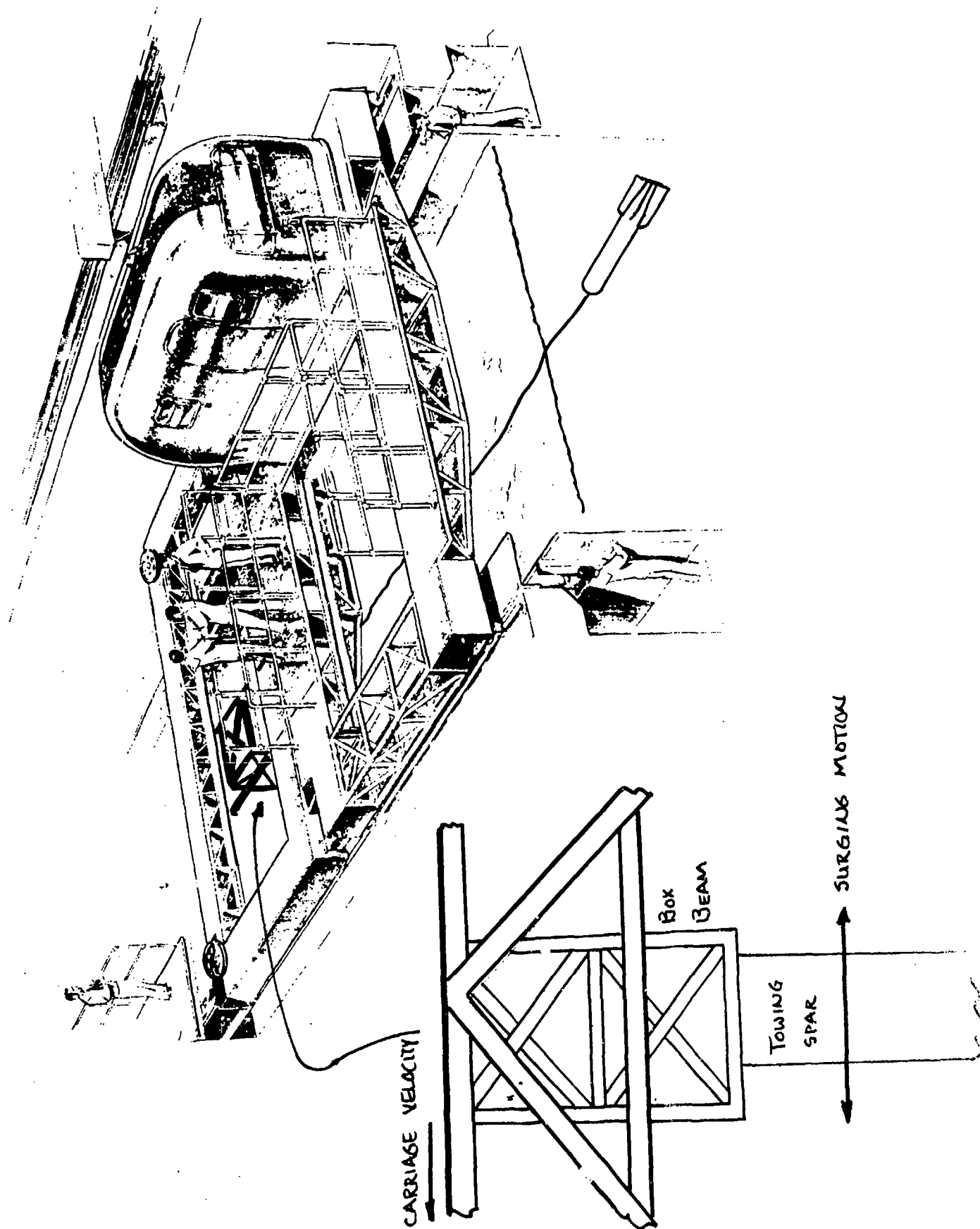


Figure No. 1. Design of Overall Towed System



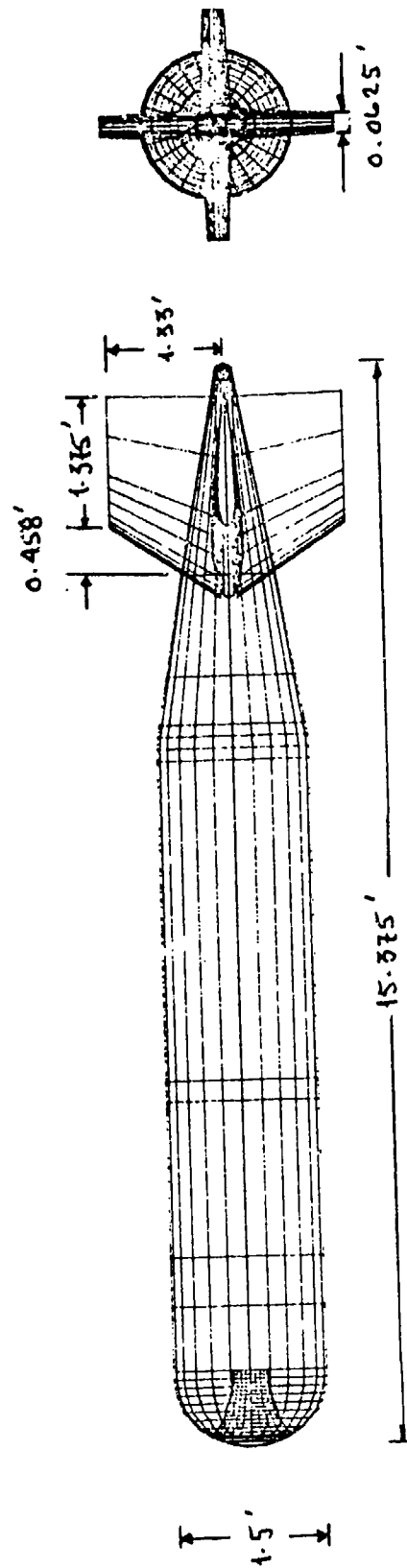


Figure No. 2. Vehicle Geometry



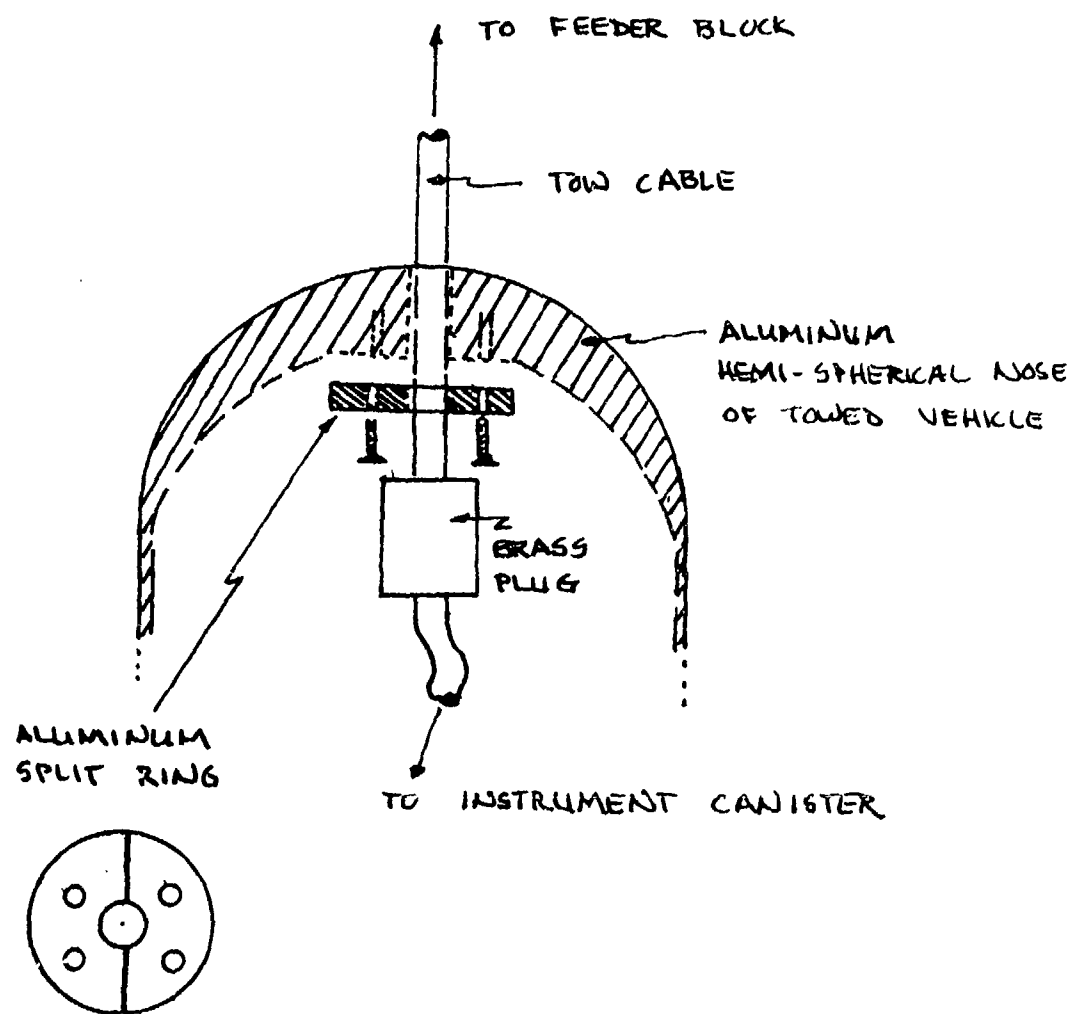


Figure No. 3. Towing Plug



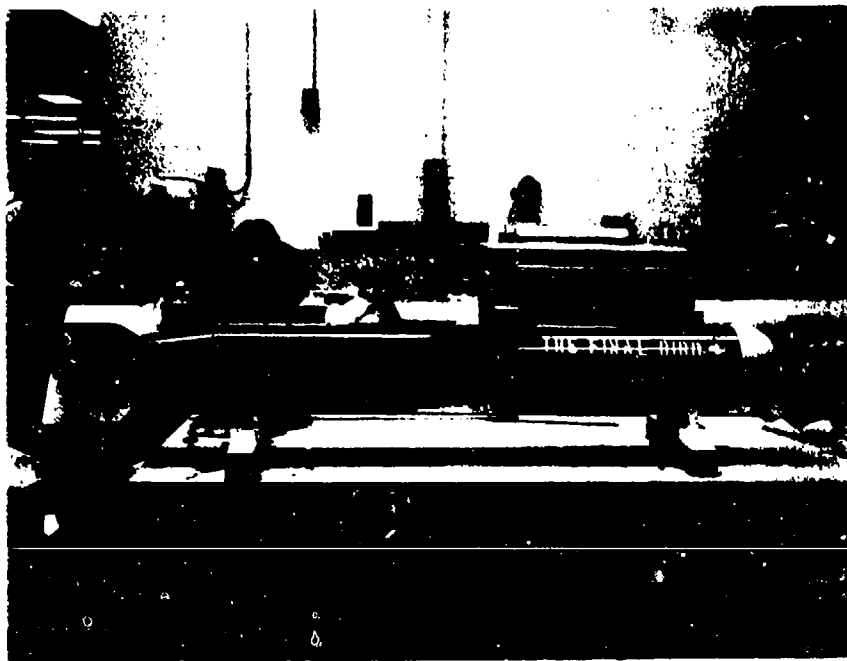


Figure No. 4. Photograph of the Towed Submersible





Figure No. 5. Stainless Steel Sheet Attached to Spar and Trailing Edge



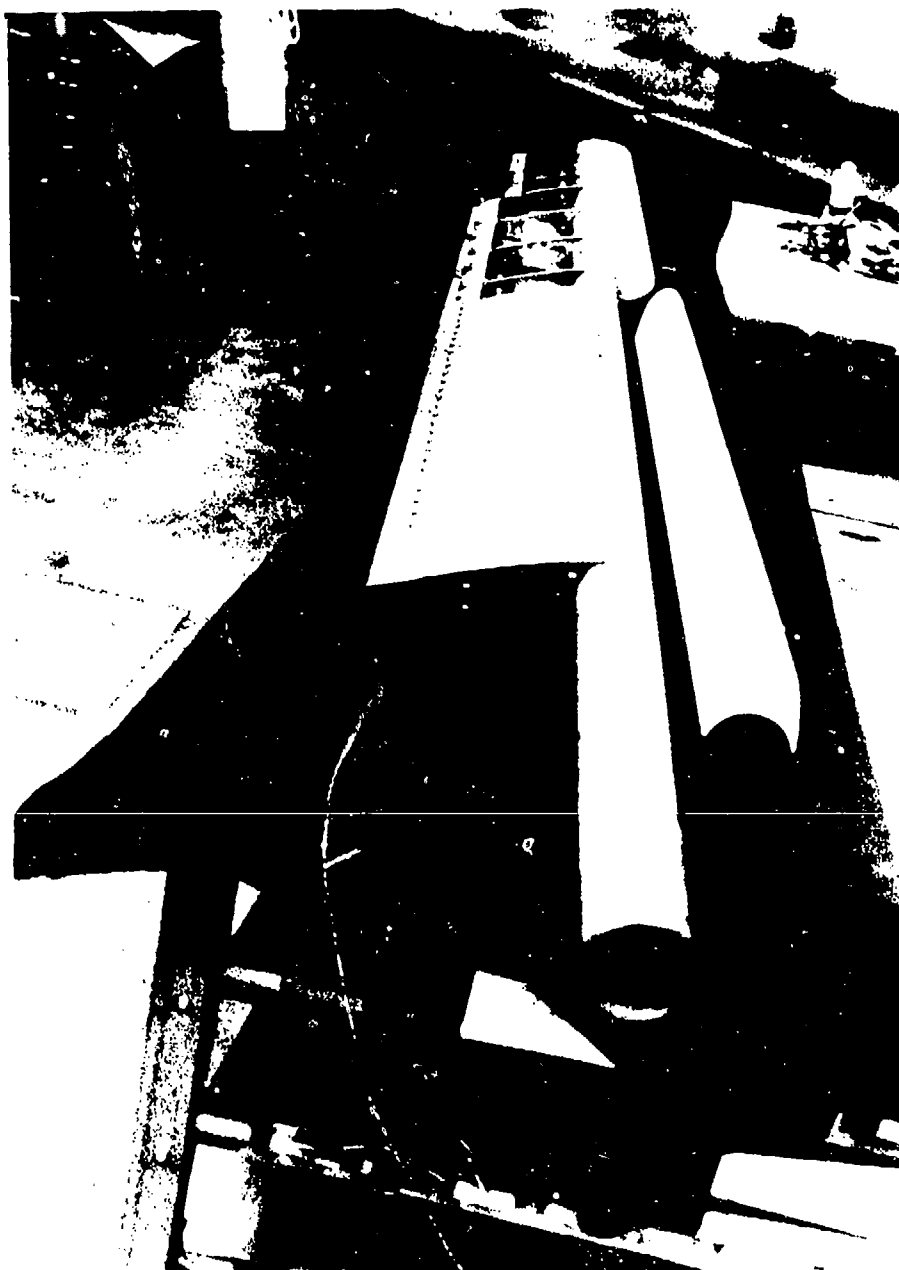


Figure No. 6. Trailing and Leading Edges of Spar Showing Rib Sections



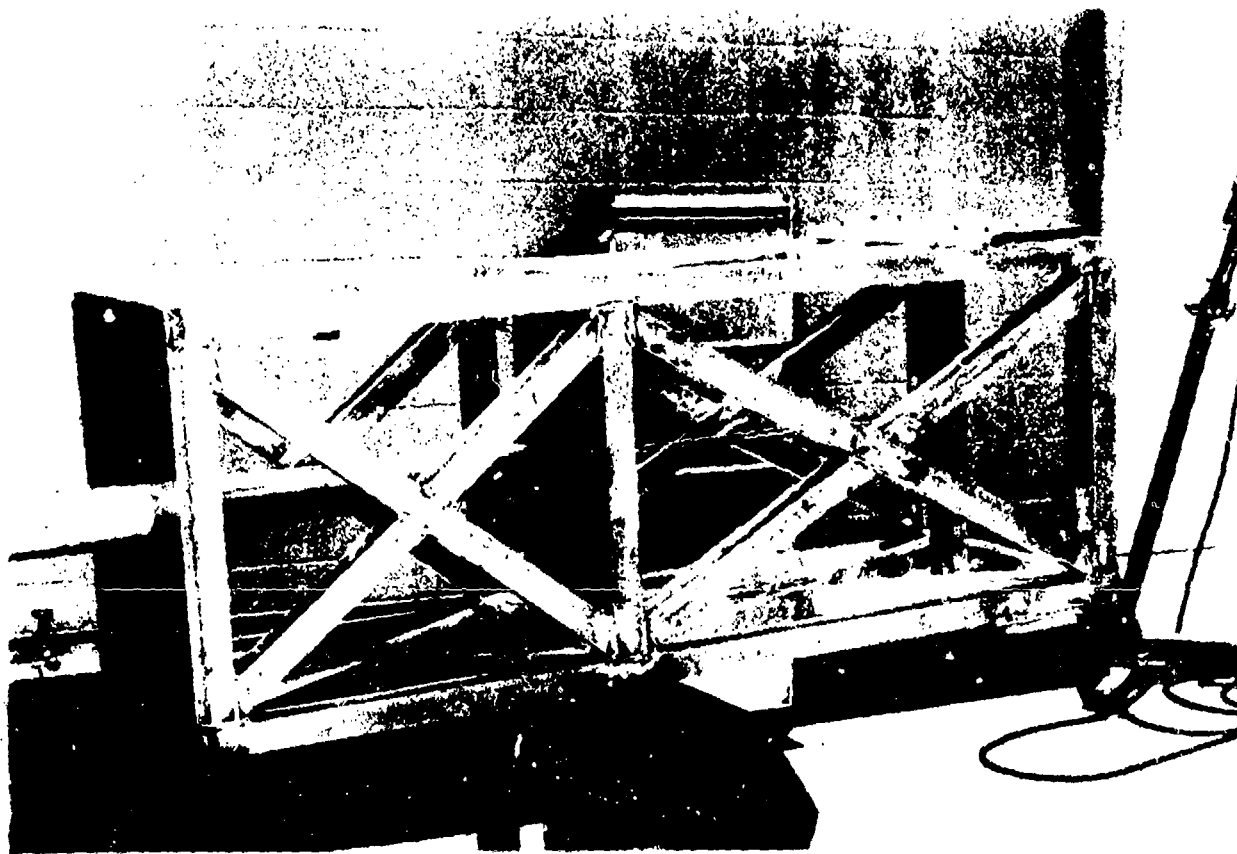


Figure No. 7. The Box Beam Assembly



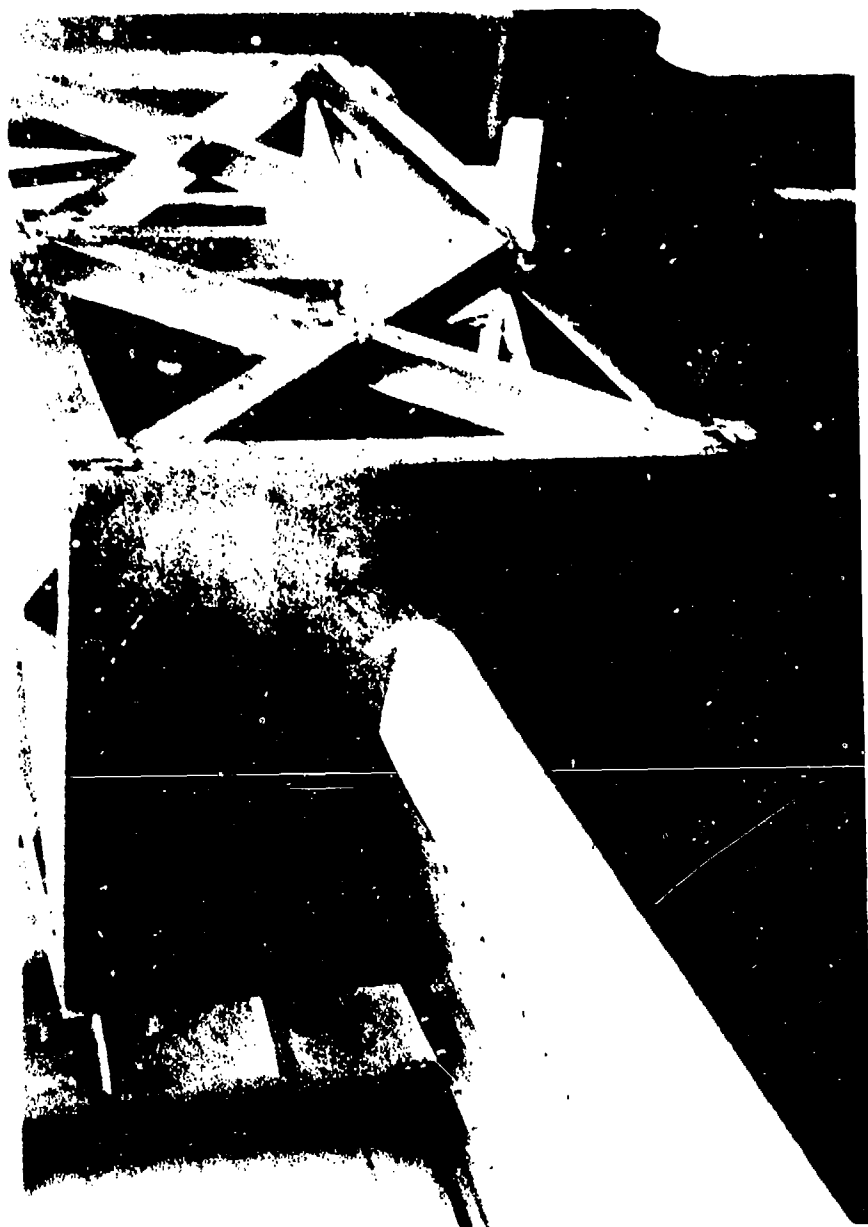


Figure No. 8. Finished Assembly



14 ft. Stainless Steel Pipe  
inside Towing Spar

Feeder Block with cover  
plate removed to show  
cable inset. Note cable  
attachments on both sides  
of block that connect cable  
from vertical excitation  
apparatus

Trailing Edge of Spar

Figure No. 9. Feeder Block





Figure No. 10. Wheel for Stainless Steel Cable at Spar Tip



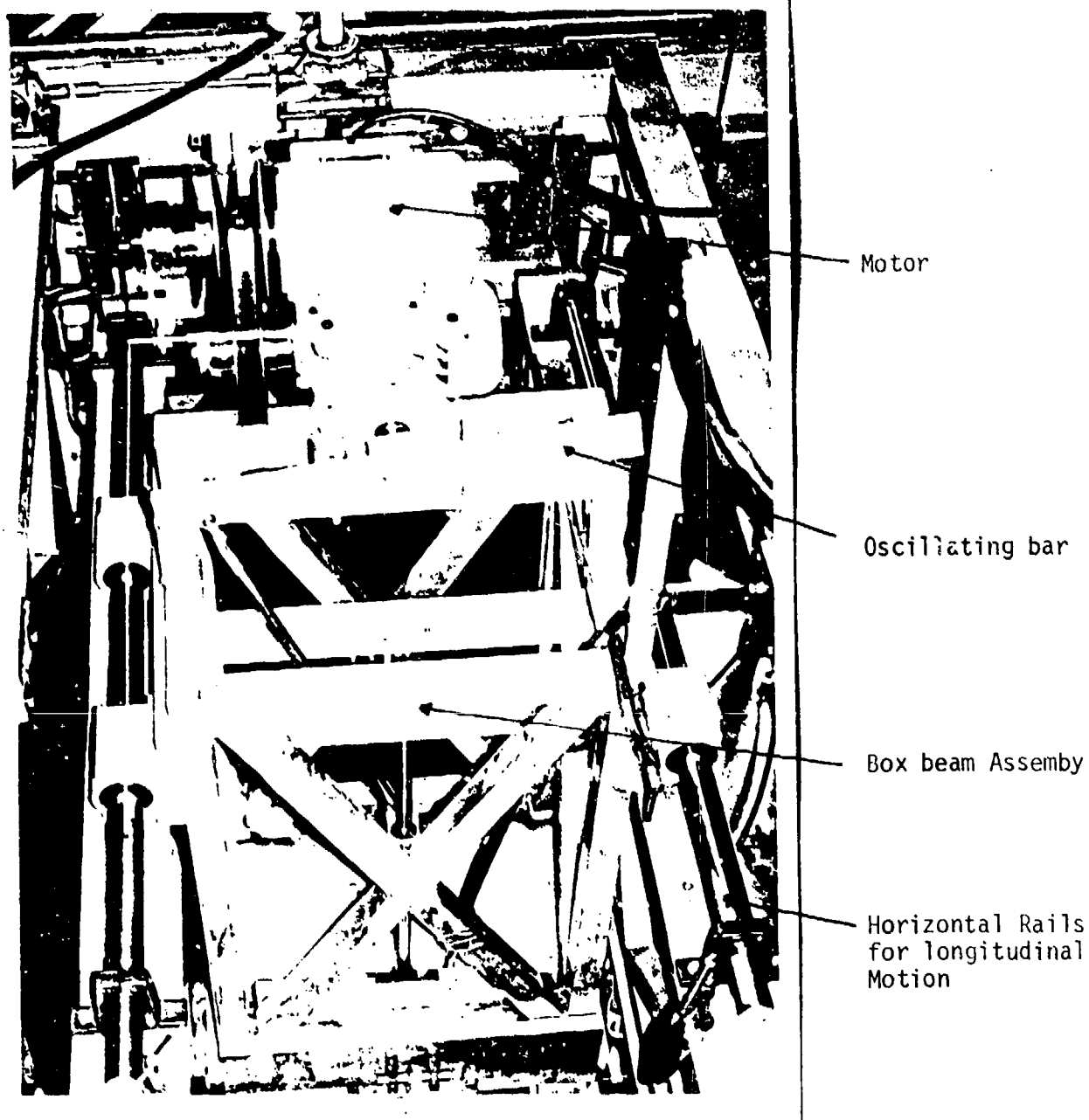


Figure No. 11. Vehicle Excitation Apparatus



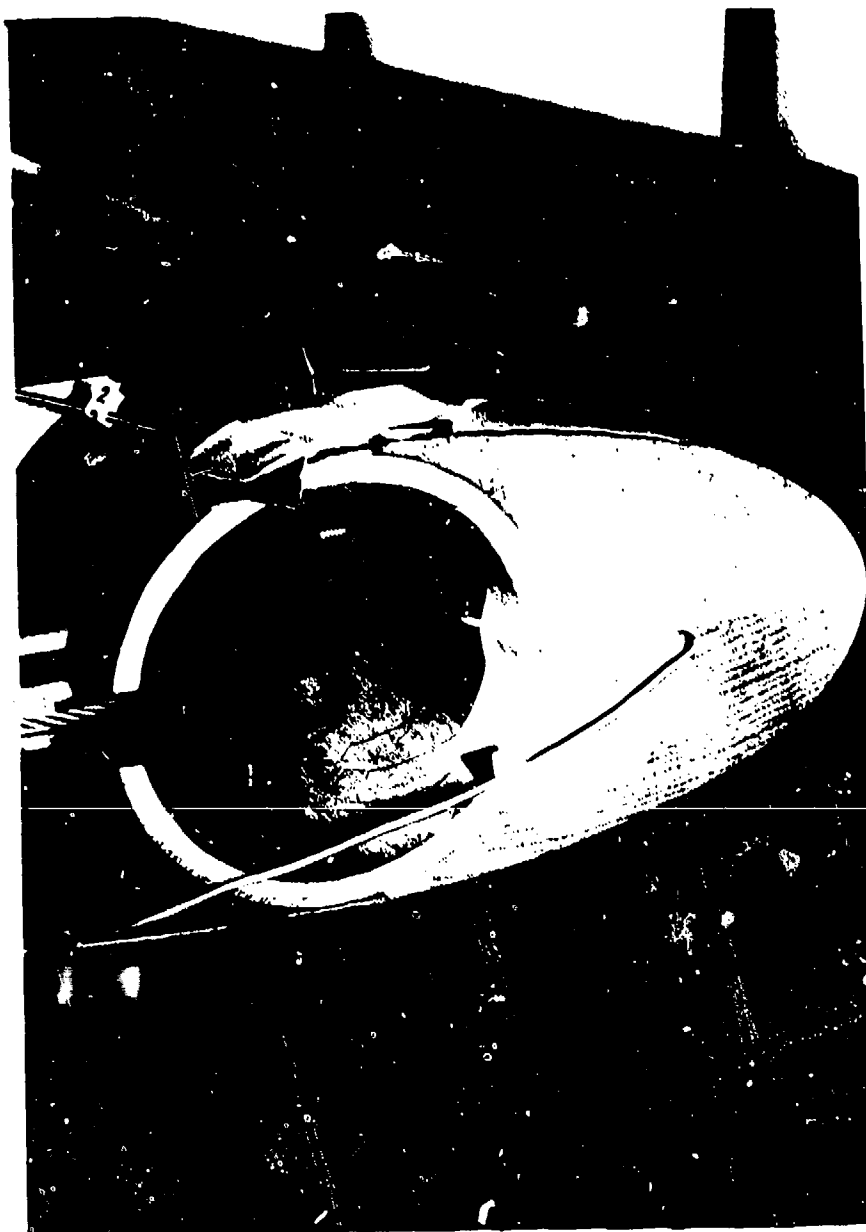


Figure No. 12. Strain Gages Mounted at Tip of Spar



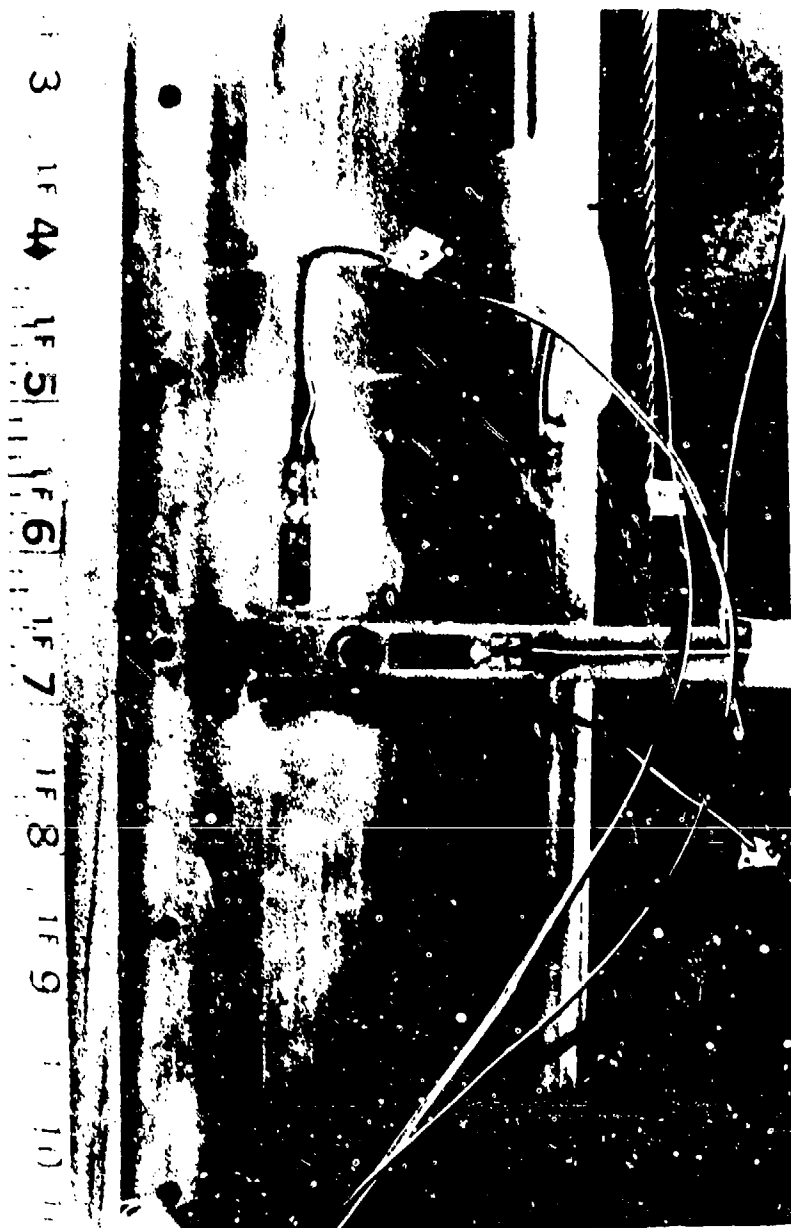
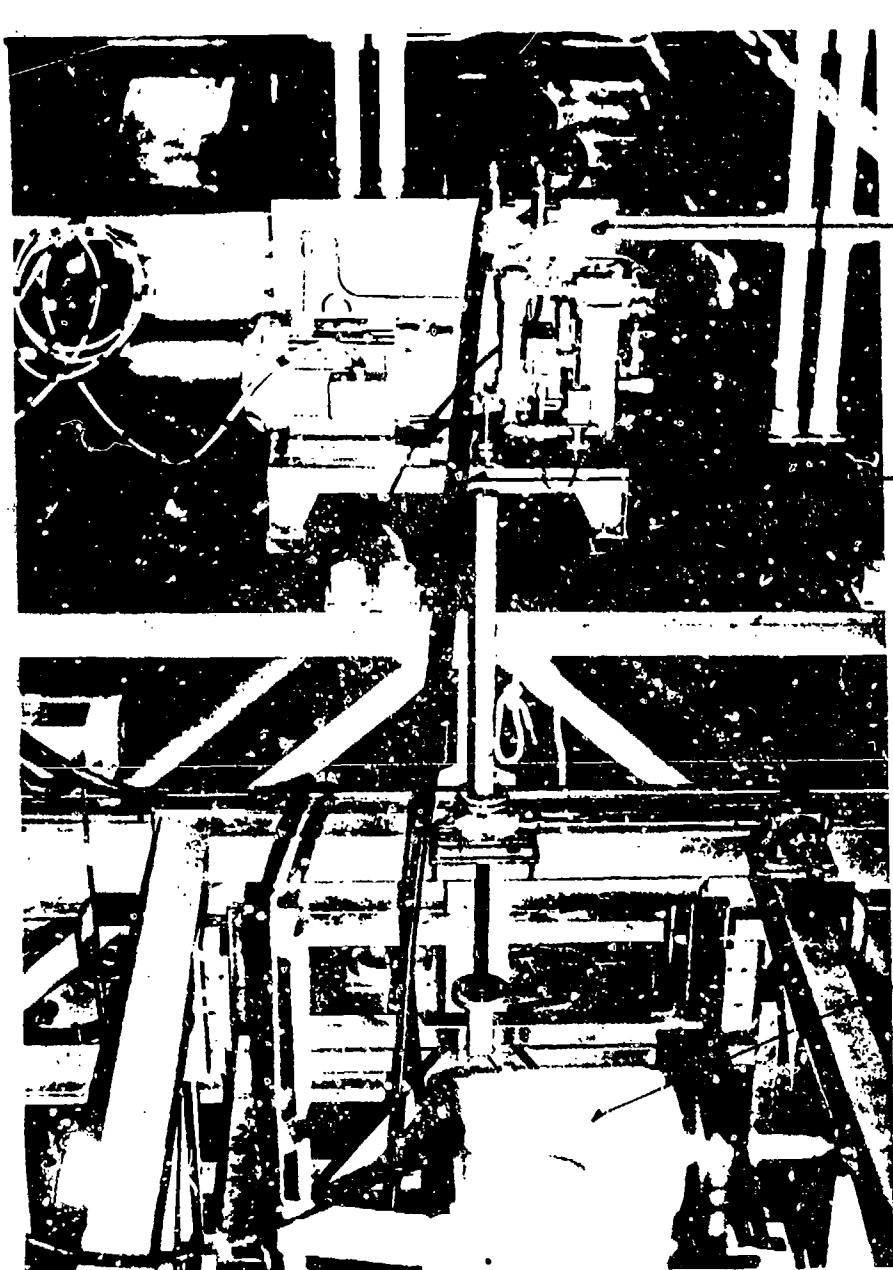


Figure No. 13. Strain Gages on Spar





Hydraulic Pump  
Mounted on tow  
carriage deck

Hydraulic Lines to  
Piston Actuator

Motor for Vertical  
Excitation

Figure No. 14. Horizontal Excitation Apparatus



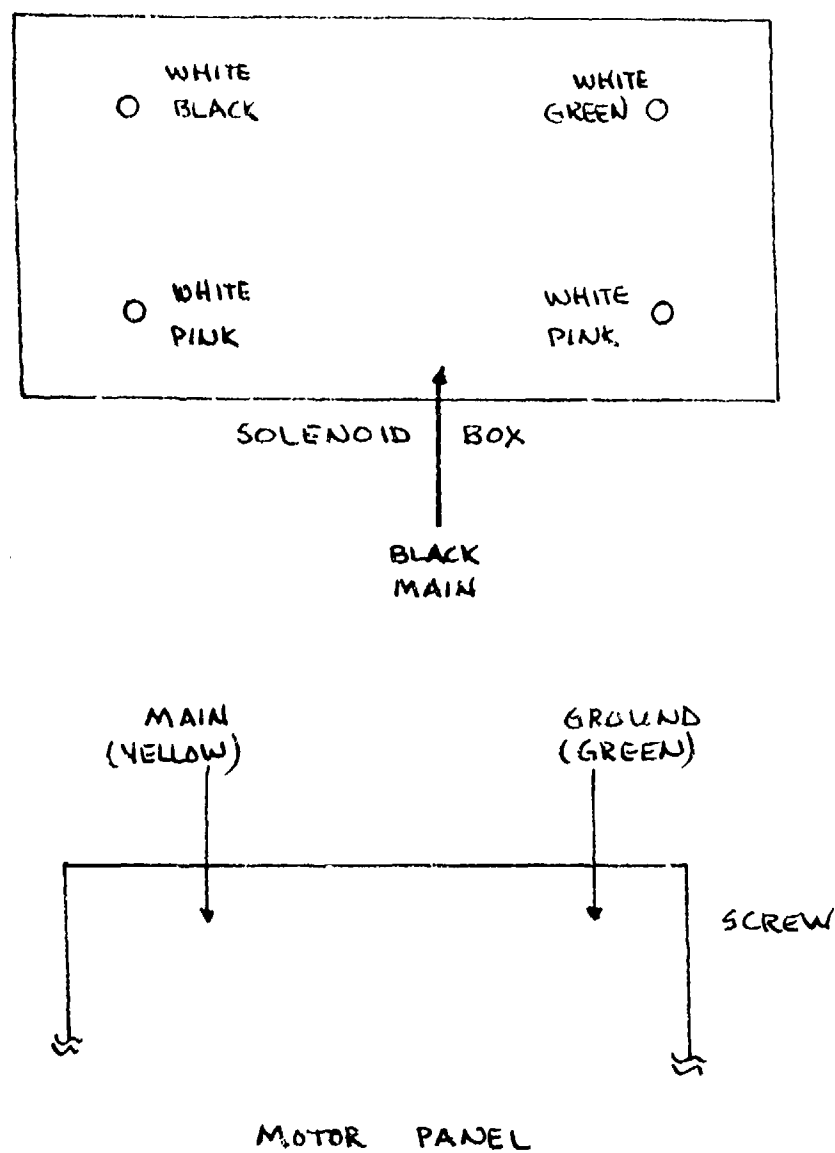


Figure No. 15. Electrical Hookup of Hydraulic Unit



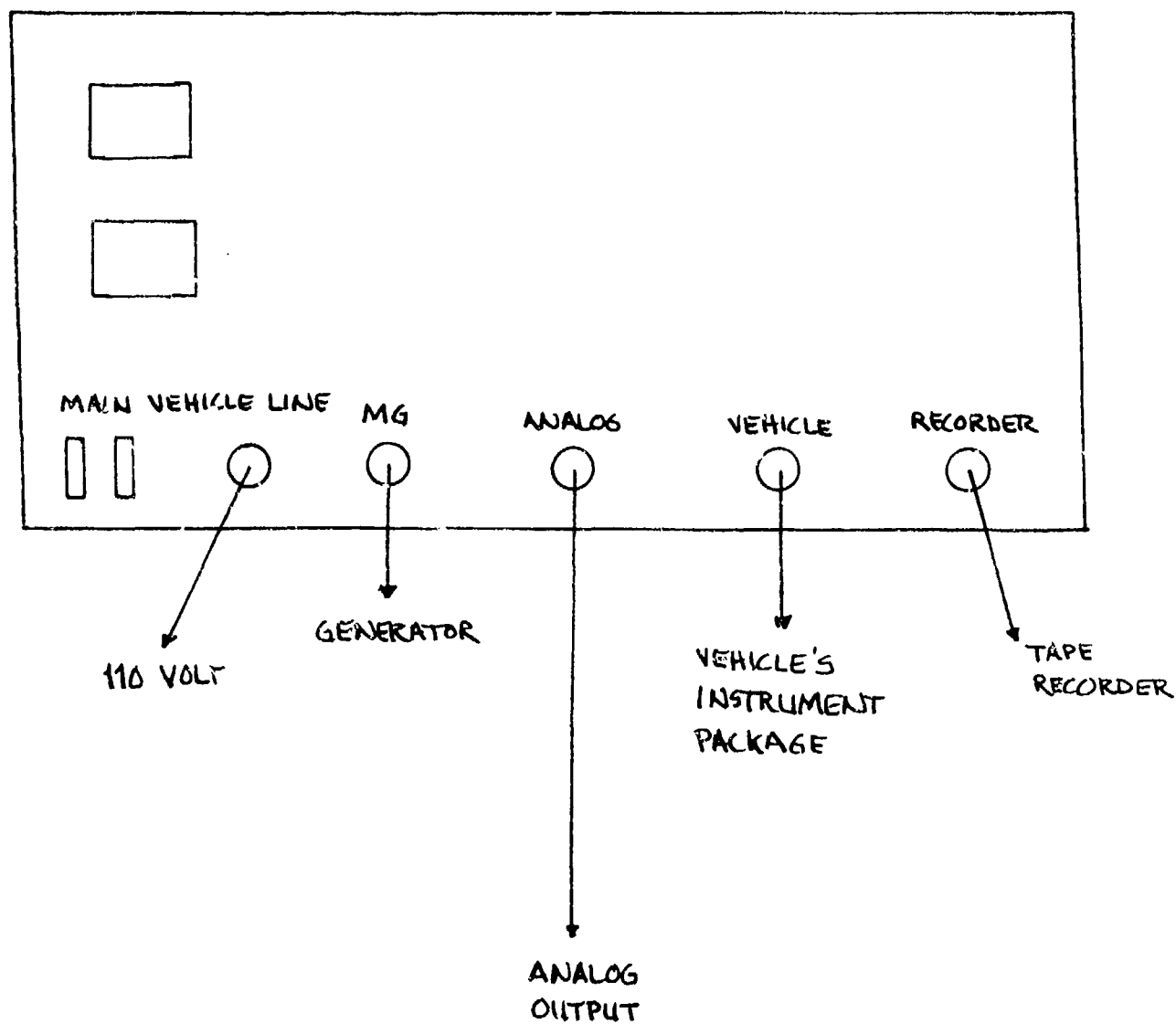


Figure No. 16. Electrical Hookup of the Digital-Analog Converter





Figure No. 17. Bent Stainless Steel Pipe



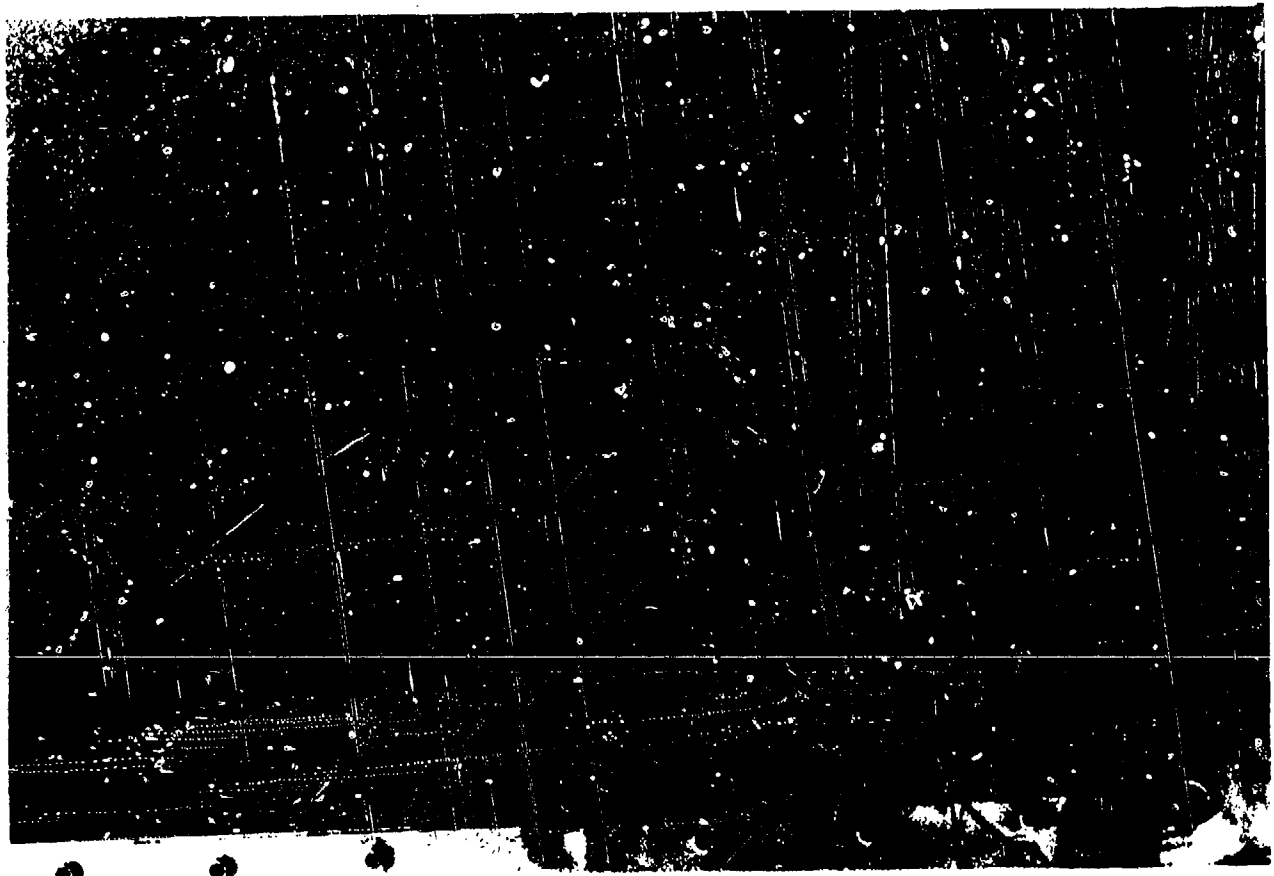


Figure No. 18. Damaged Towing Cable



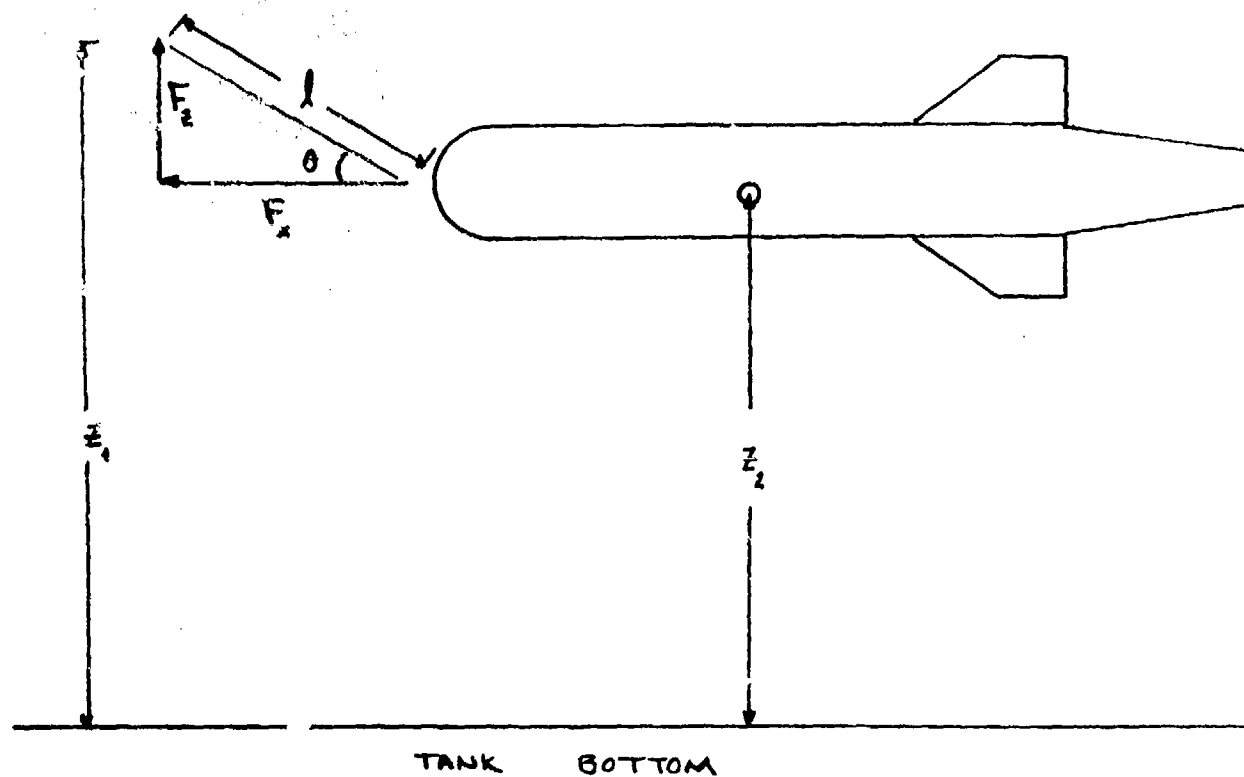


Figure No. 19. Geometry for Vehicle Vertical Motion



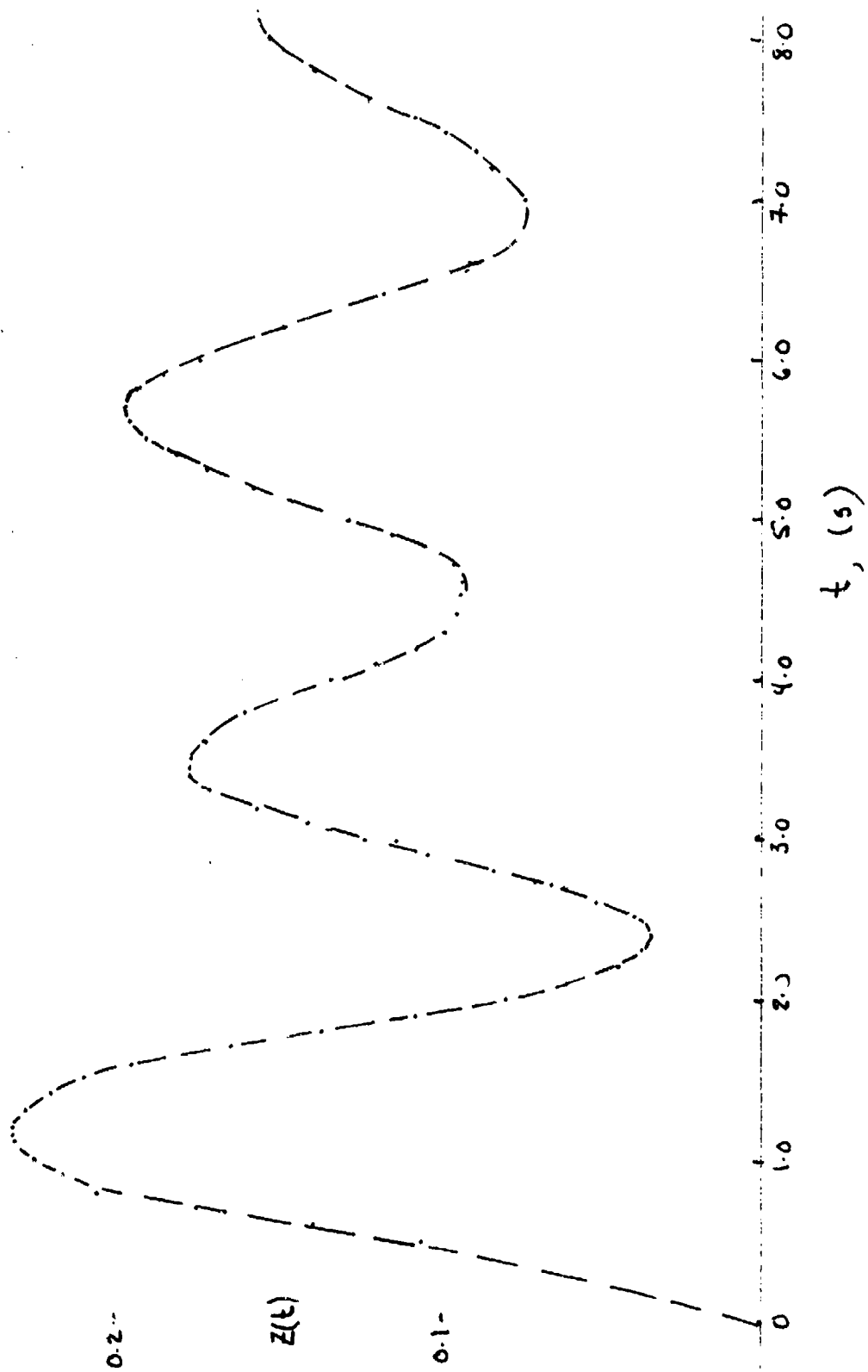
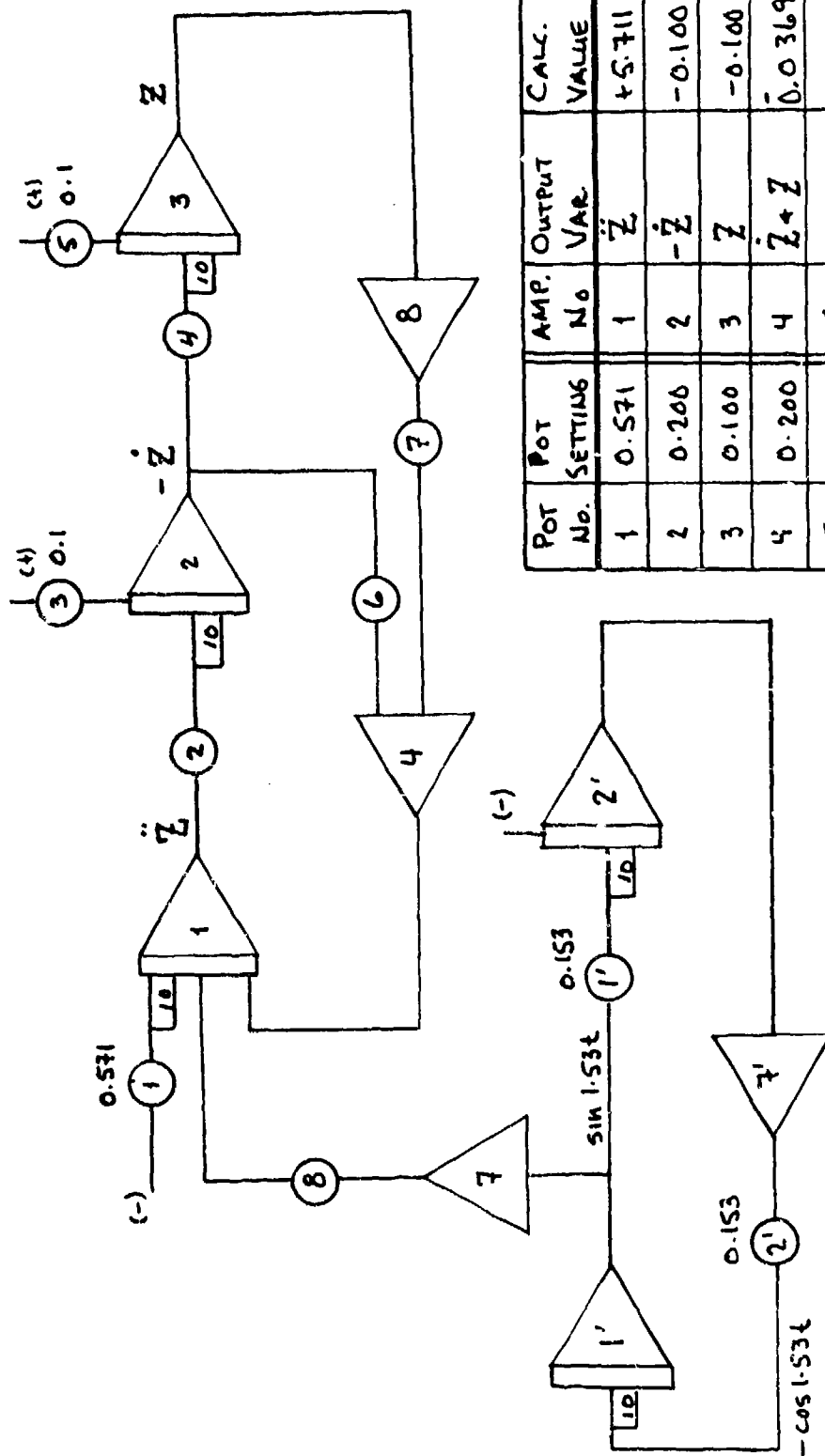


Figure No. 20. Vertical Response for  $R = 0.5$  ft,  $\lambda = 10$  ft.





POT No.	POT SETTING	AMP. No.	Output VAR.	CALC. VALUE	MEAS. VALUE
1	0.571	1	$\ddot{Z}$	+5.711	
2	0.200	2	$-\dot{Z}$	-0.100	-0.100
3	0.100	3	$Z$	-0.100	-0.100
4	0.200	4	$\dot{Z} + Z$	-0.0369	-0.0369
5	0.100	5			
6	0.178	6			
7	0.141	7	$-\sin 1.53t$	N.A.	N.A.
8	0.794	8	$-Z$	+0.100	+0.100
1'	0.153	1'	$\sin 1.53t$	N.A.	N.A.
2'	0.153	2'	$\cos 1.53t$	N.A.	N.A.
3'	0.100	3'	$\cos 1.53t$	N.A.	N.A.

$$\ddot{Z} = -0.178\dot{Z} - 1.91Z + 0.794 \sin 1.53t + 5.71$$

$$\dot{Z}(0) = 0$$

$$Z(0) = 0$$

Figure No. 21. Analog Computer Simulation of Vertical Motion



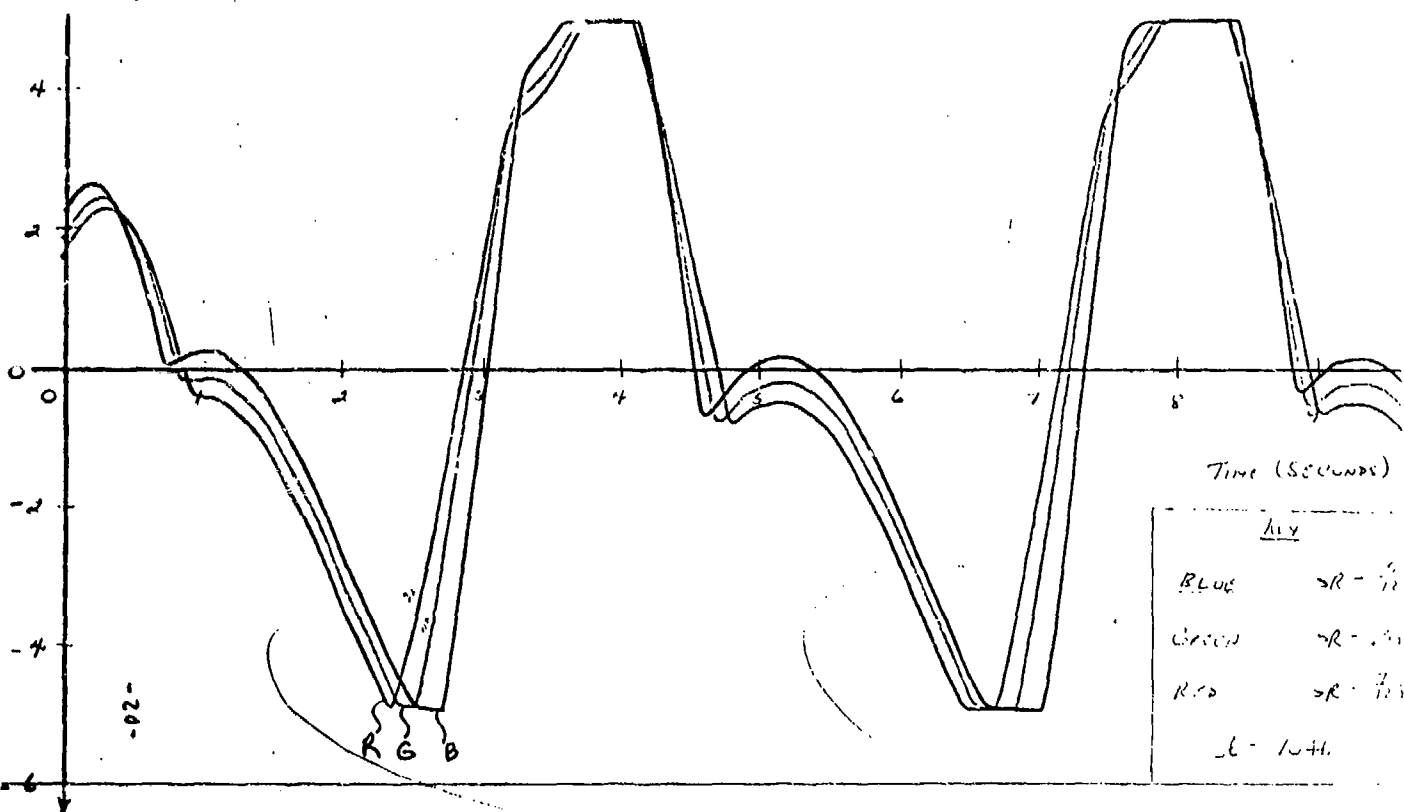


Figure No. 22. Acceleration vs. time for  $R = 5/12, 1/2, 7/12$  ft,  $L = 10$  ft



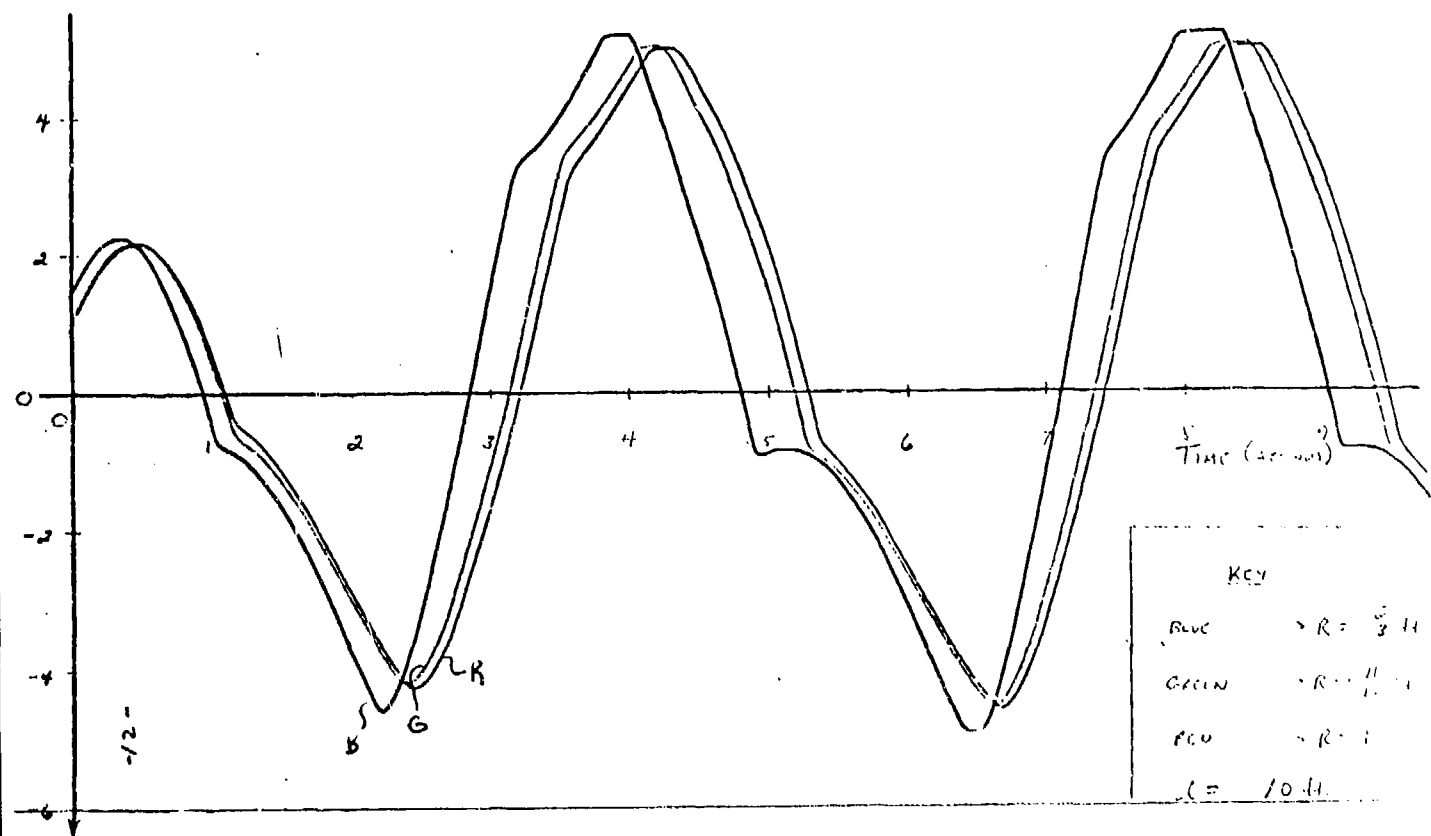


Figure No. 23. Acceleration vs. time for  $R = 2/3, 11/12, 1$  ft,  $L = 10$  ft



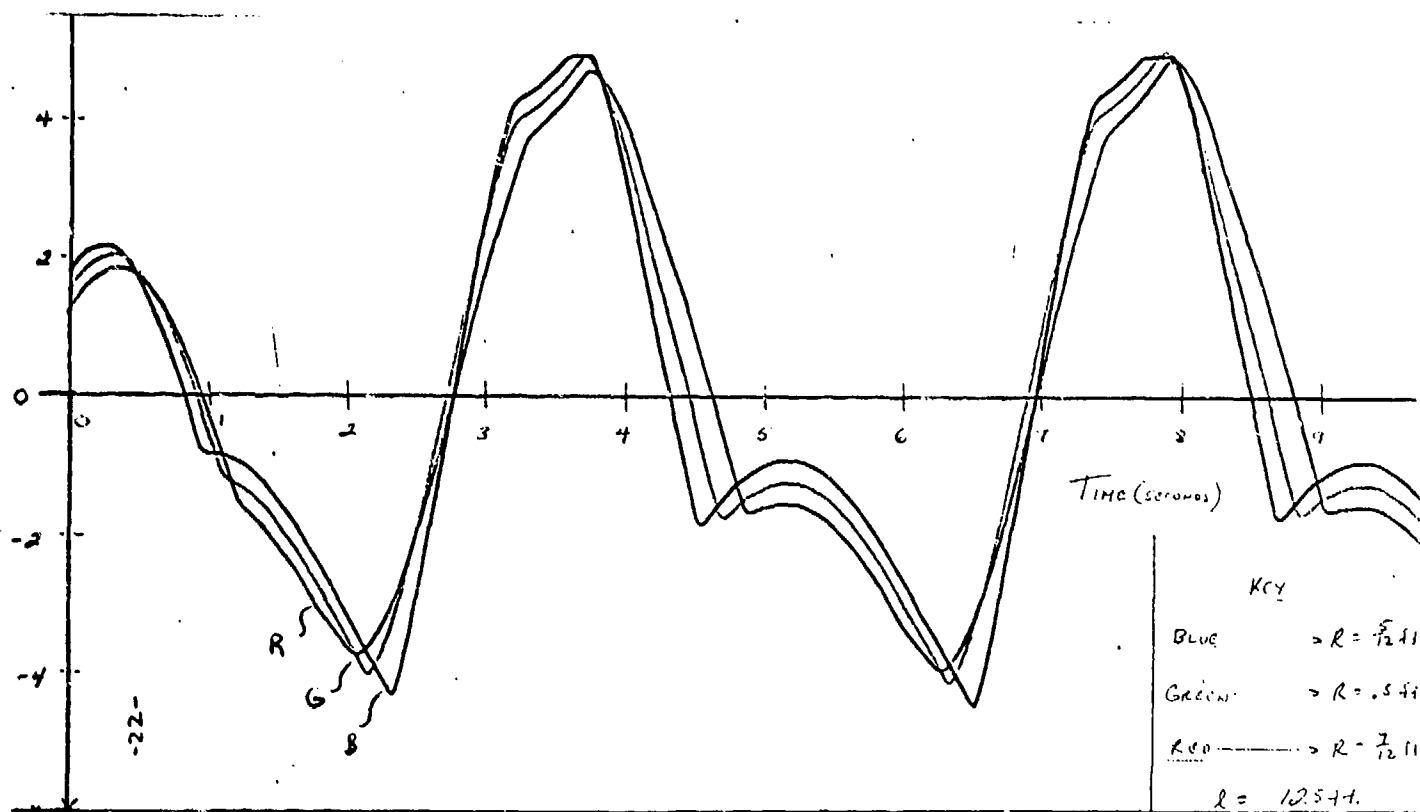


Figure No. 24. Acceleration vs. time for  $R = 5/12, 1/2, 7/12 \text{ ft}$ ,  $\ell = 12.5 \text{ ft}$



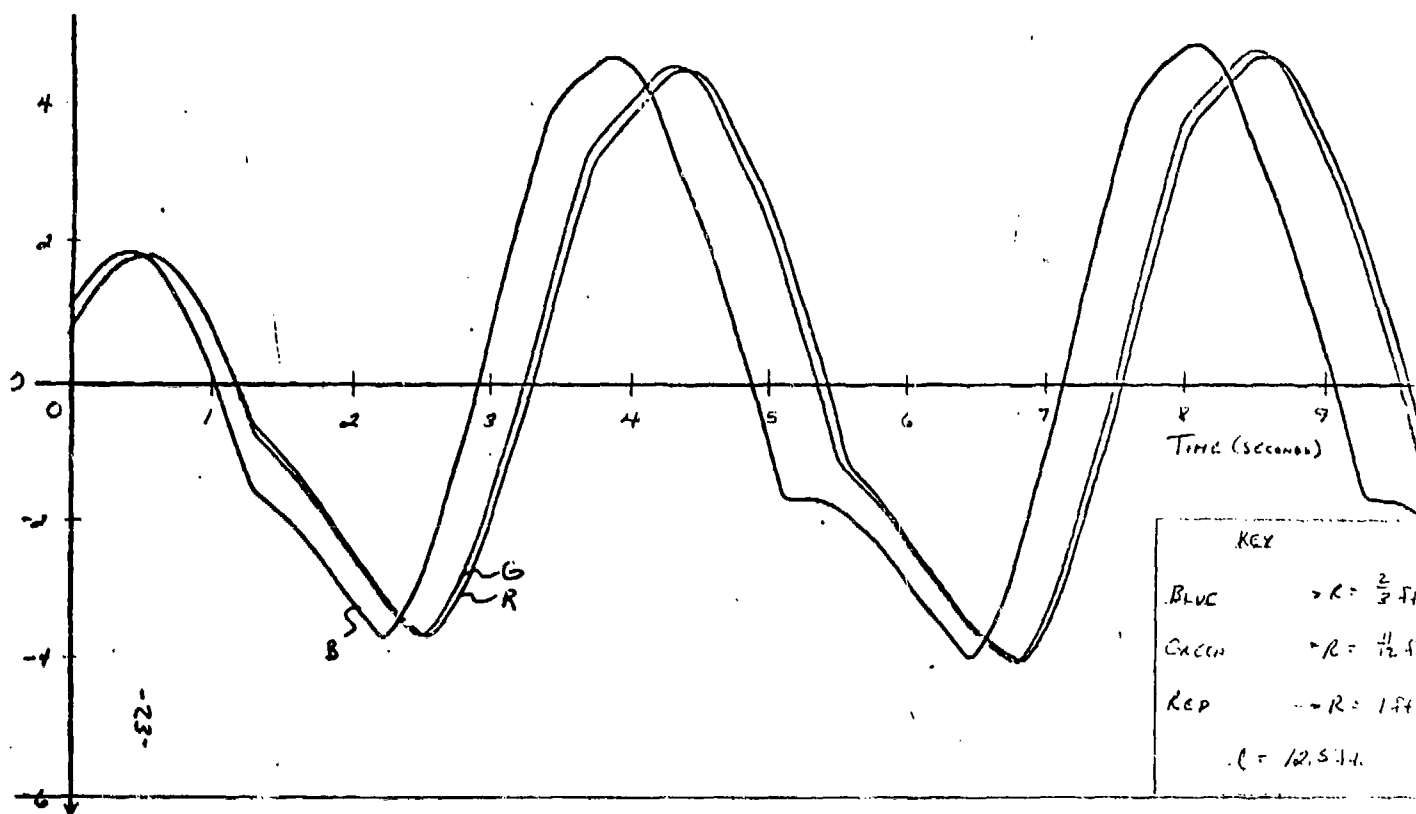


Figure No. 25. Acceleration vs. time for  $R = 2/3, 11/12, 1 \text{ ft}$ ,  $l = 12.5 \text{ ft}$



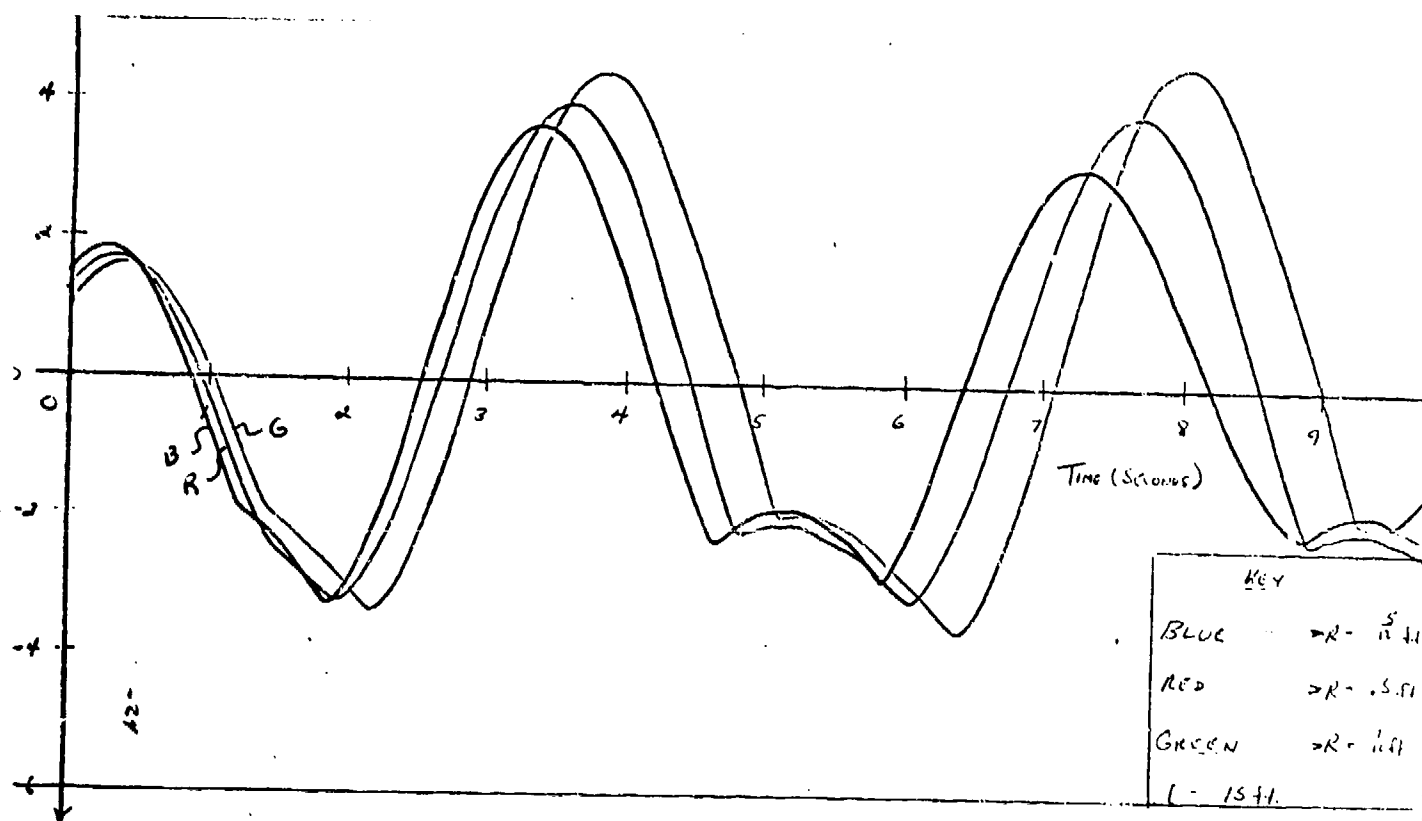


Figure No. 26. Acceleration vs time for  $R = 5/12, 1/2, 7/12$  ft,  $l = 15$  ft



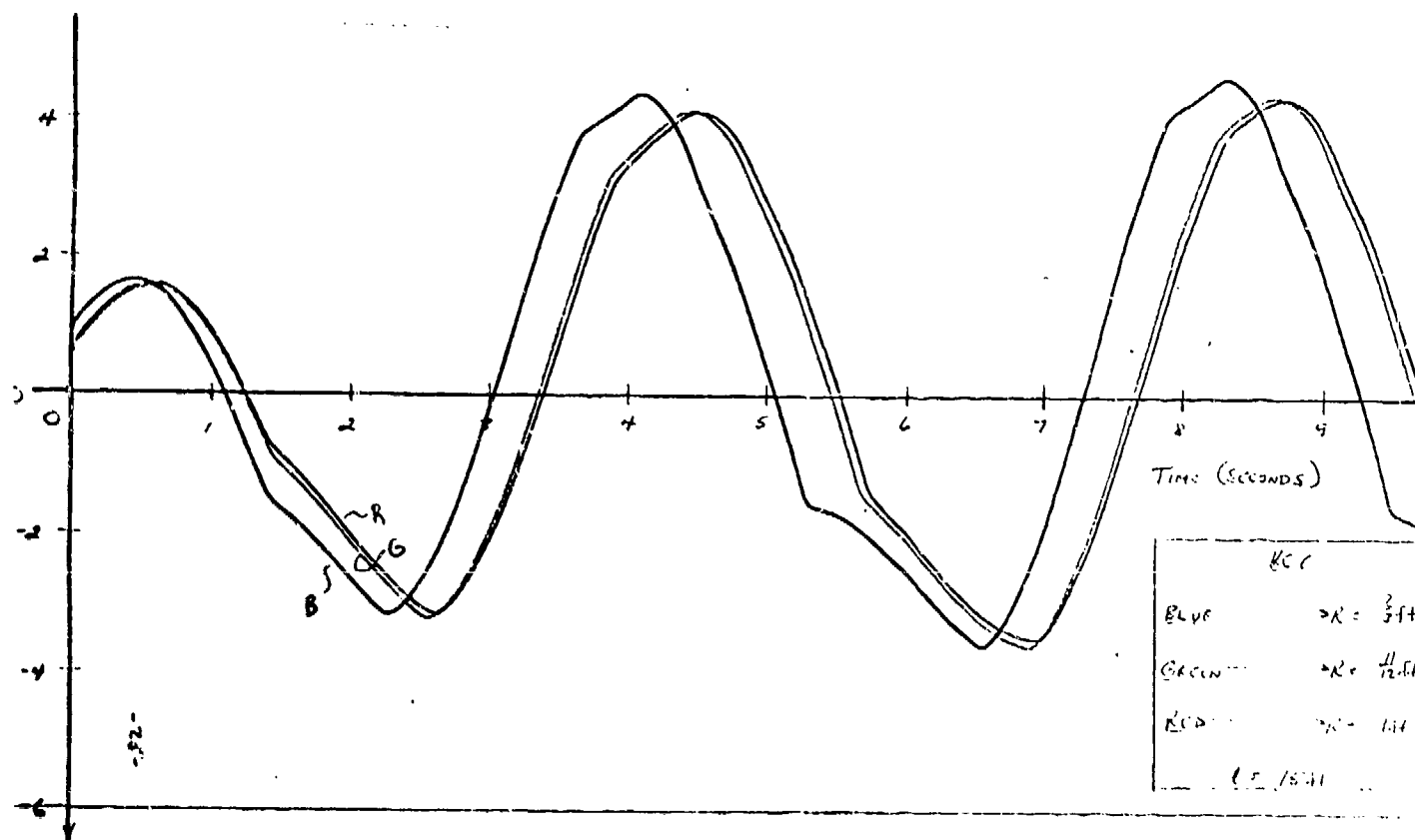


Figure No. 27. Acceleration vs time for  $R = 2/3, 11/12, 1$  ft,  $\ell = 15$  ft



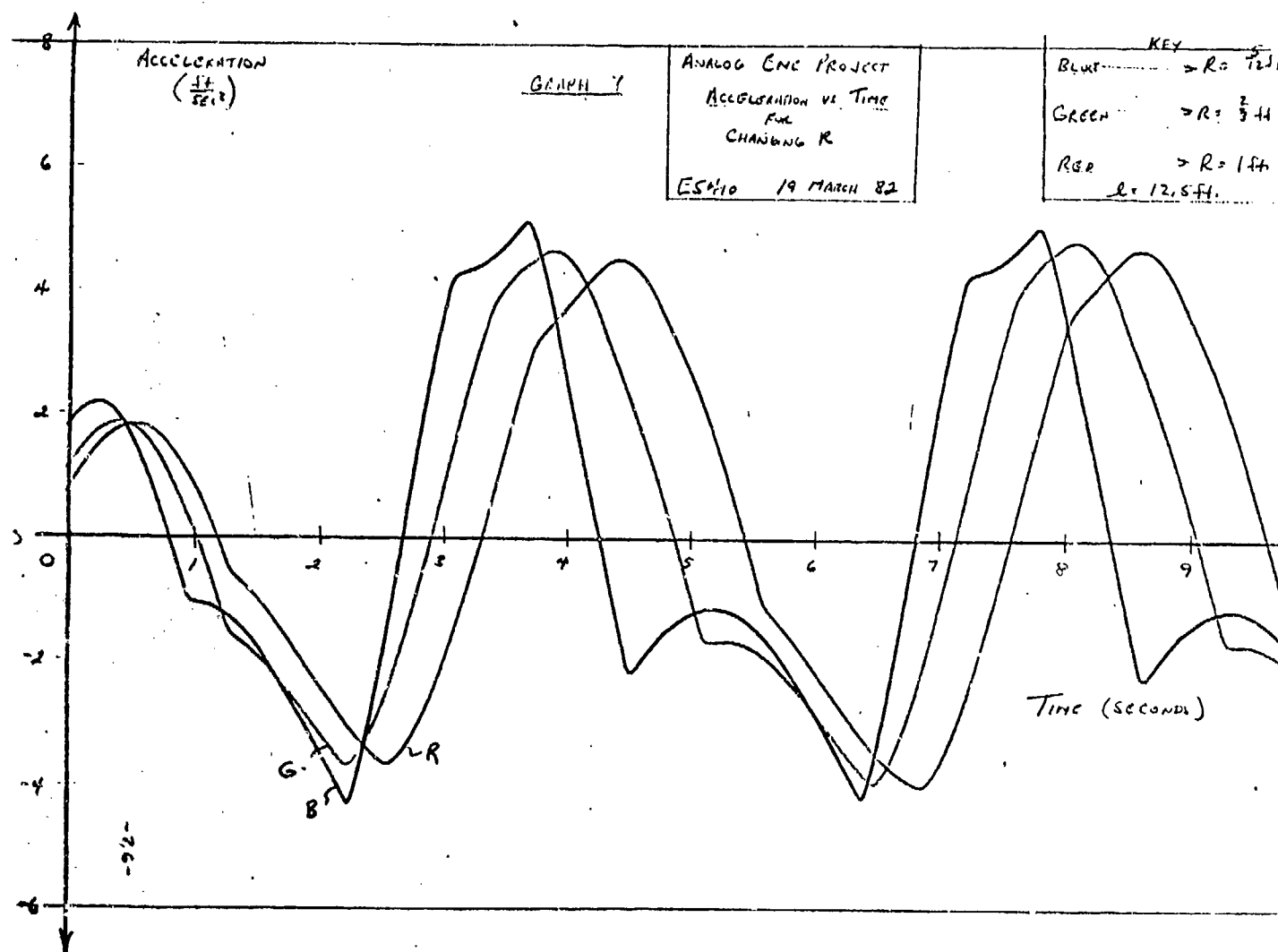


Figure No. 28. Acceleration vs time for  $R = 5/12, 2/3, 1$  ft,  $\ell = 12.5$  ft



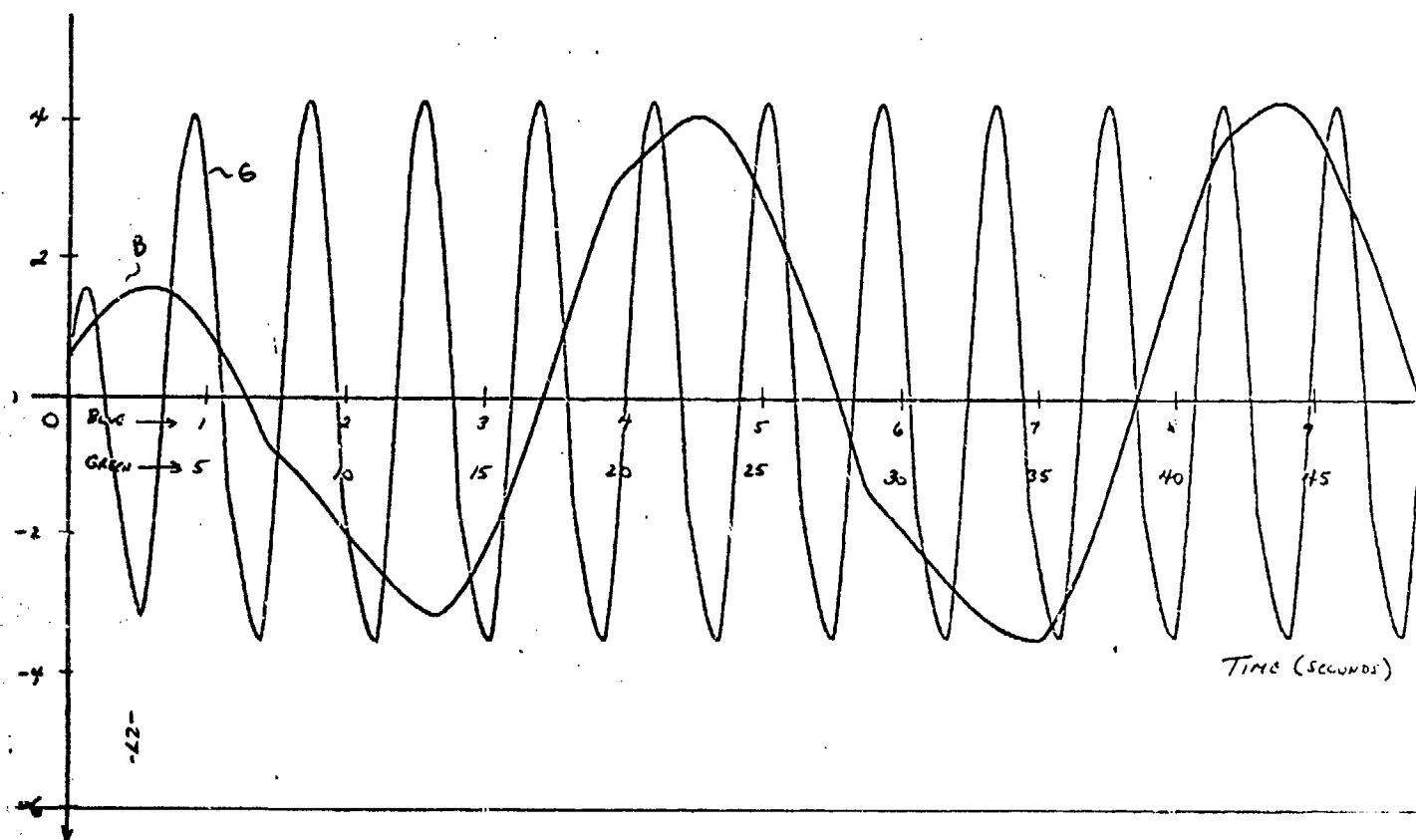


Figure No. 29. Acceleration vs time for  $R = 1$  ft,  $\ell = 15$  ft



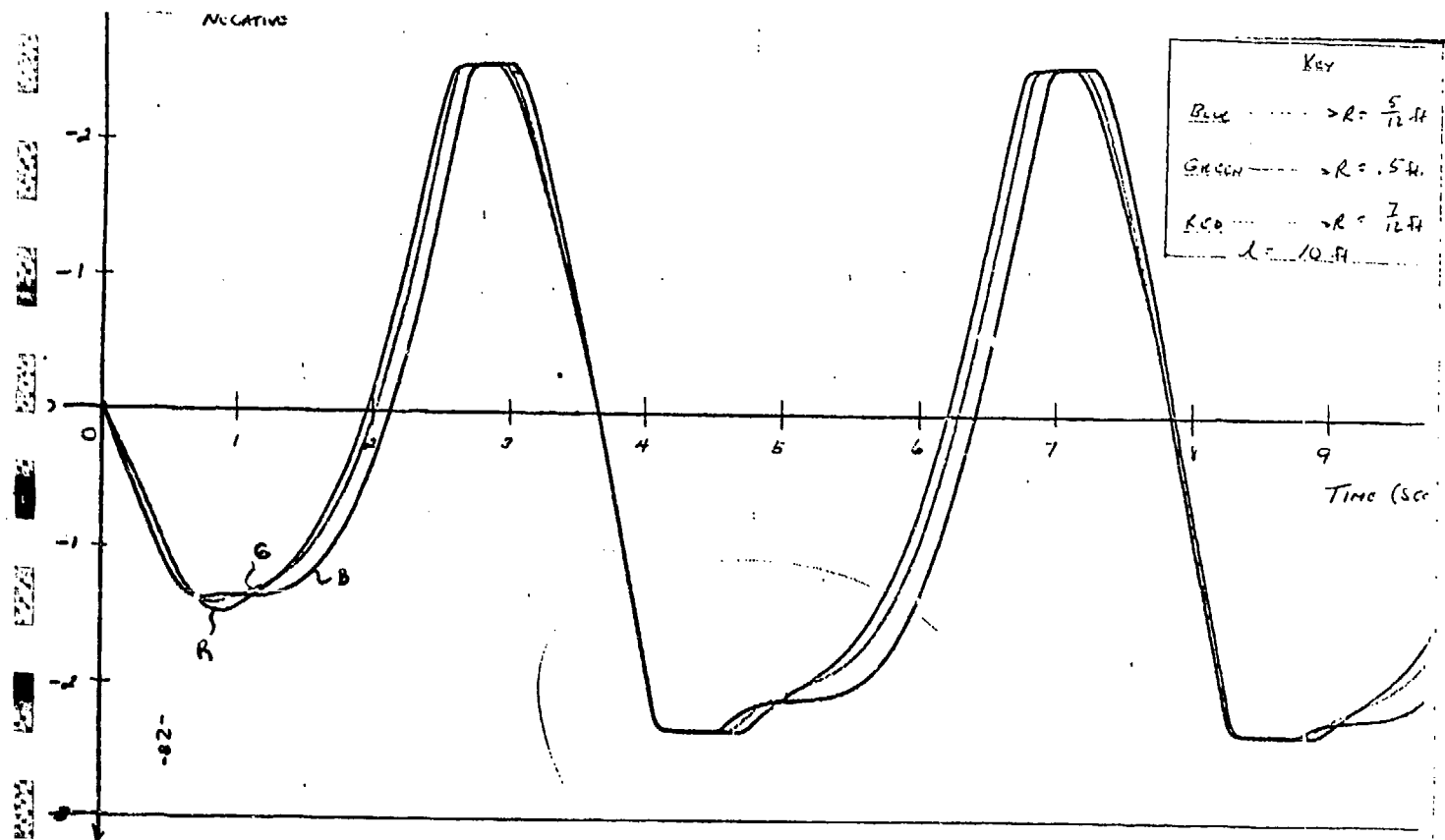


Figure No. 30. Velocity vs time for  $R = \frac{5}{12}, \frac{1}{2}, \frac{7}{12}$  ft,  $\ell = 10$  ft



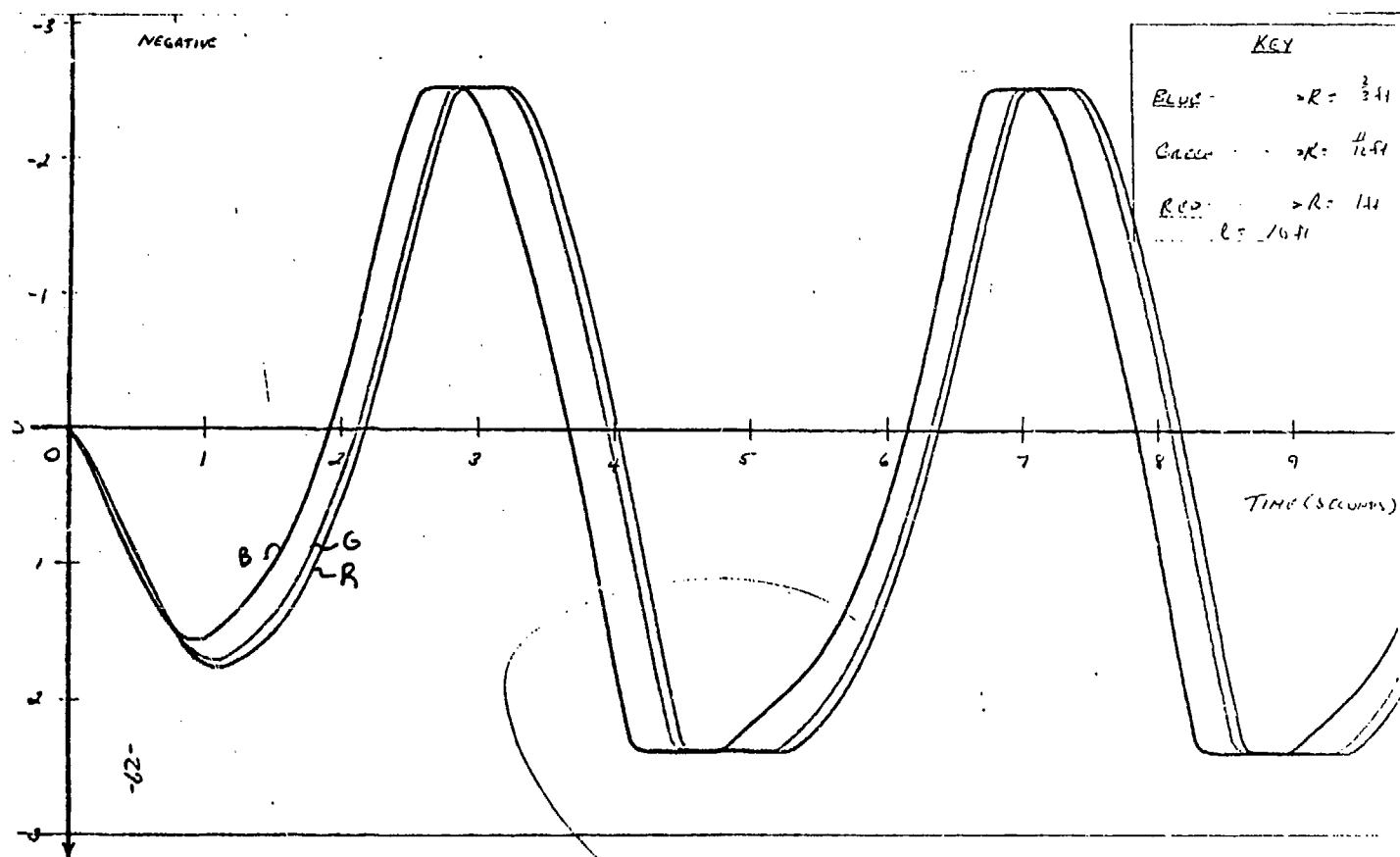


Figure No. 31. Velocity vs time for  $R = 2/3, 11/12, 1$  ft,  $l = 10$  ft



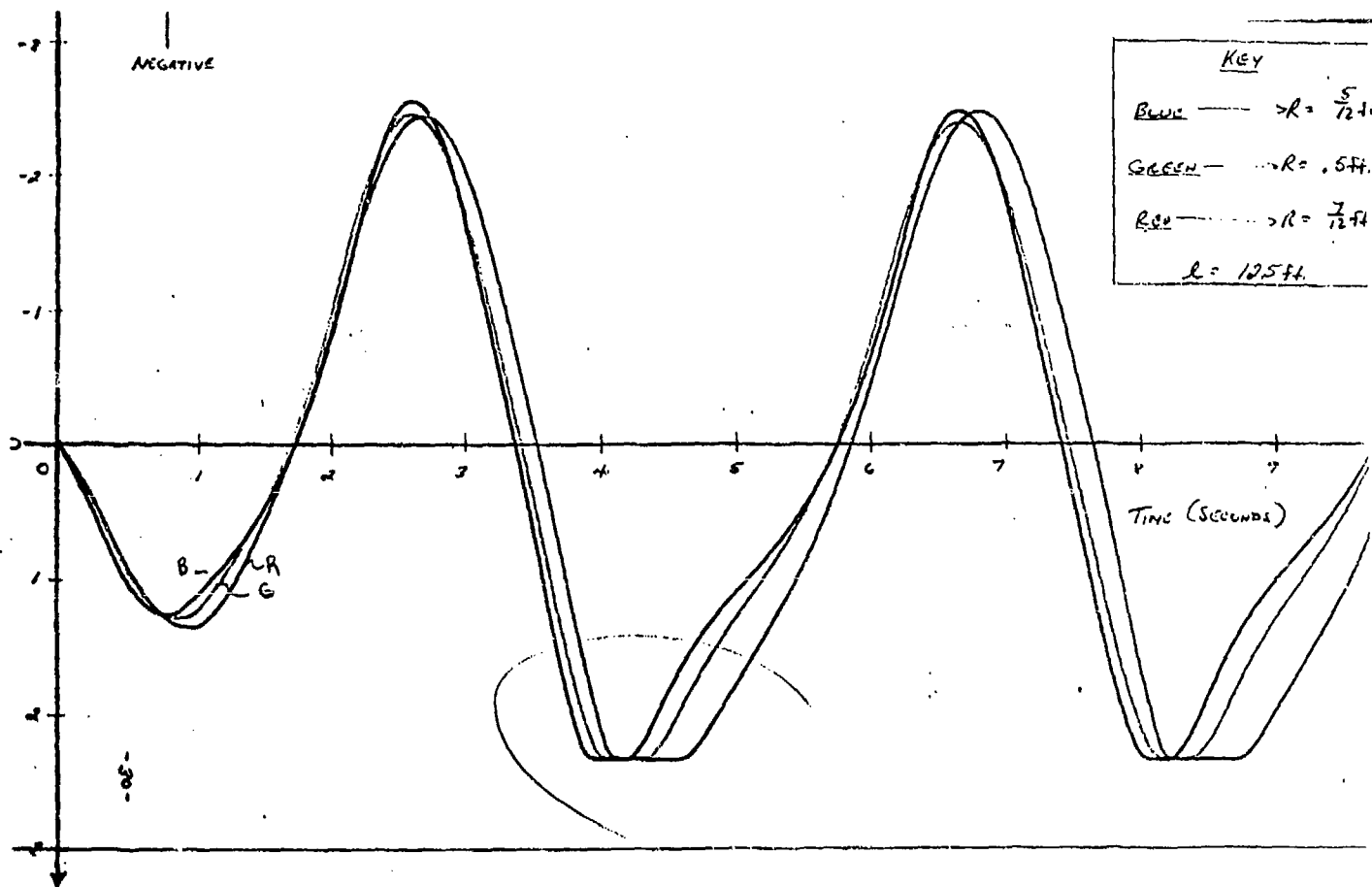


Figure No. 32. Velocity vs time for  $R = 5/12, 1/2, 7/12 \text{ ft}$ ,  $l = 12.5 \text{ ft}$



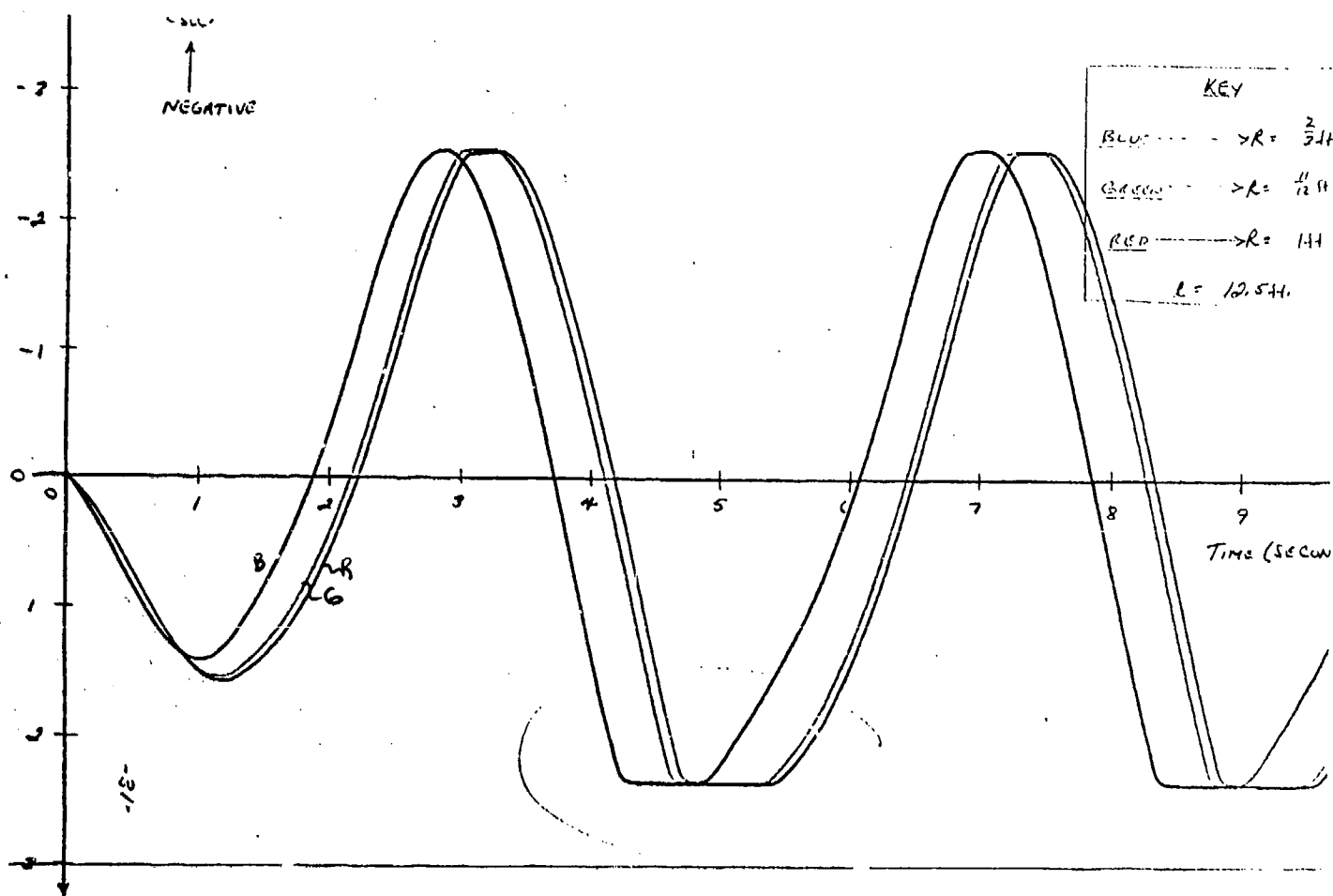


Figure No. 33. Velocity vs time for  $R = 2/3, 11/12, 1 \text{ ft}$ ,  $l = 12.5 \text{ ft}$



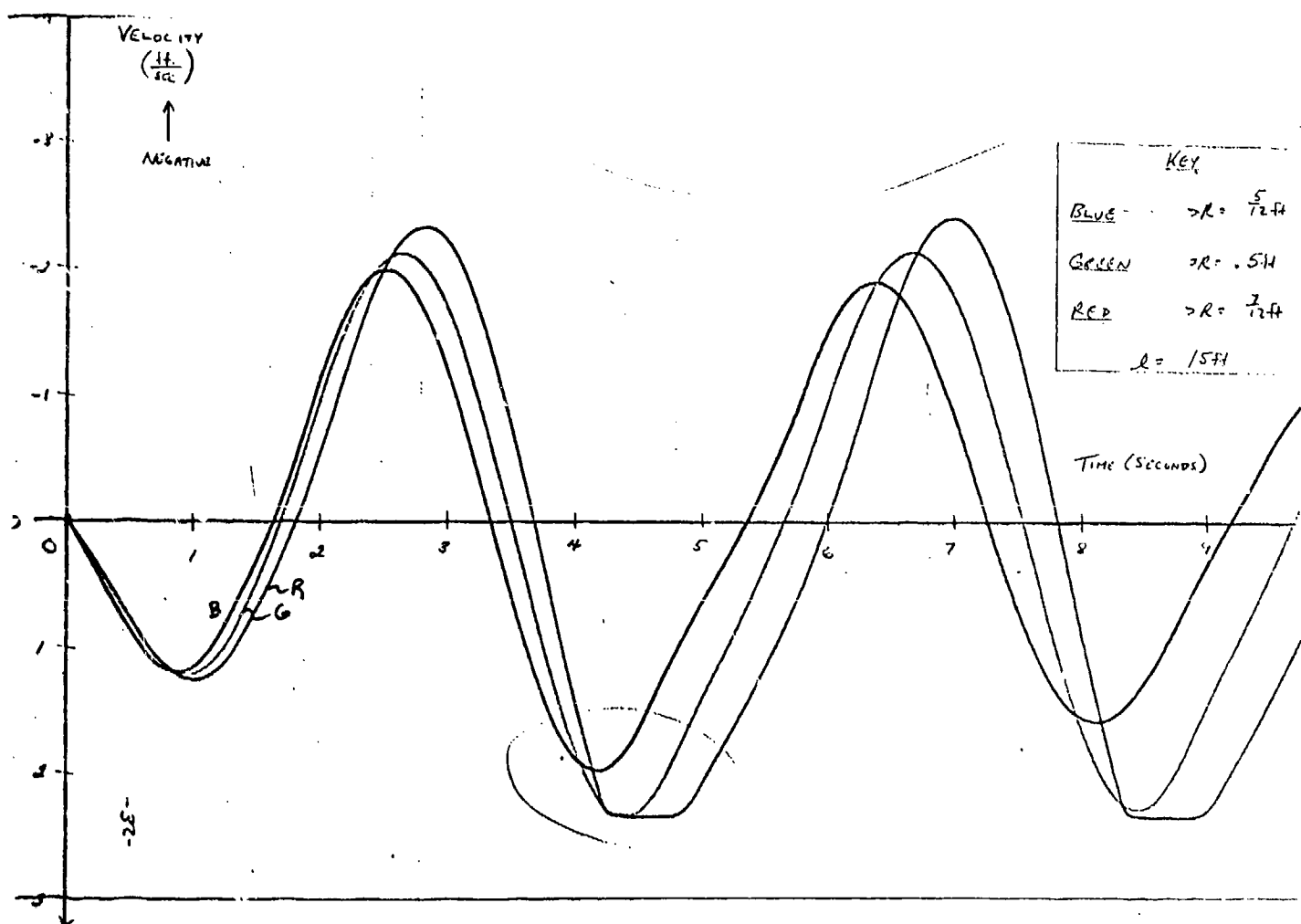


Figure No. 34. Velocity vs time for  $R = 5/12, 1/2, 7/12$  ft,  $l = 15$  ft



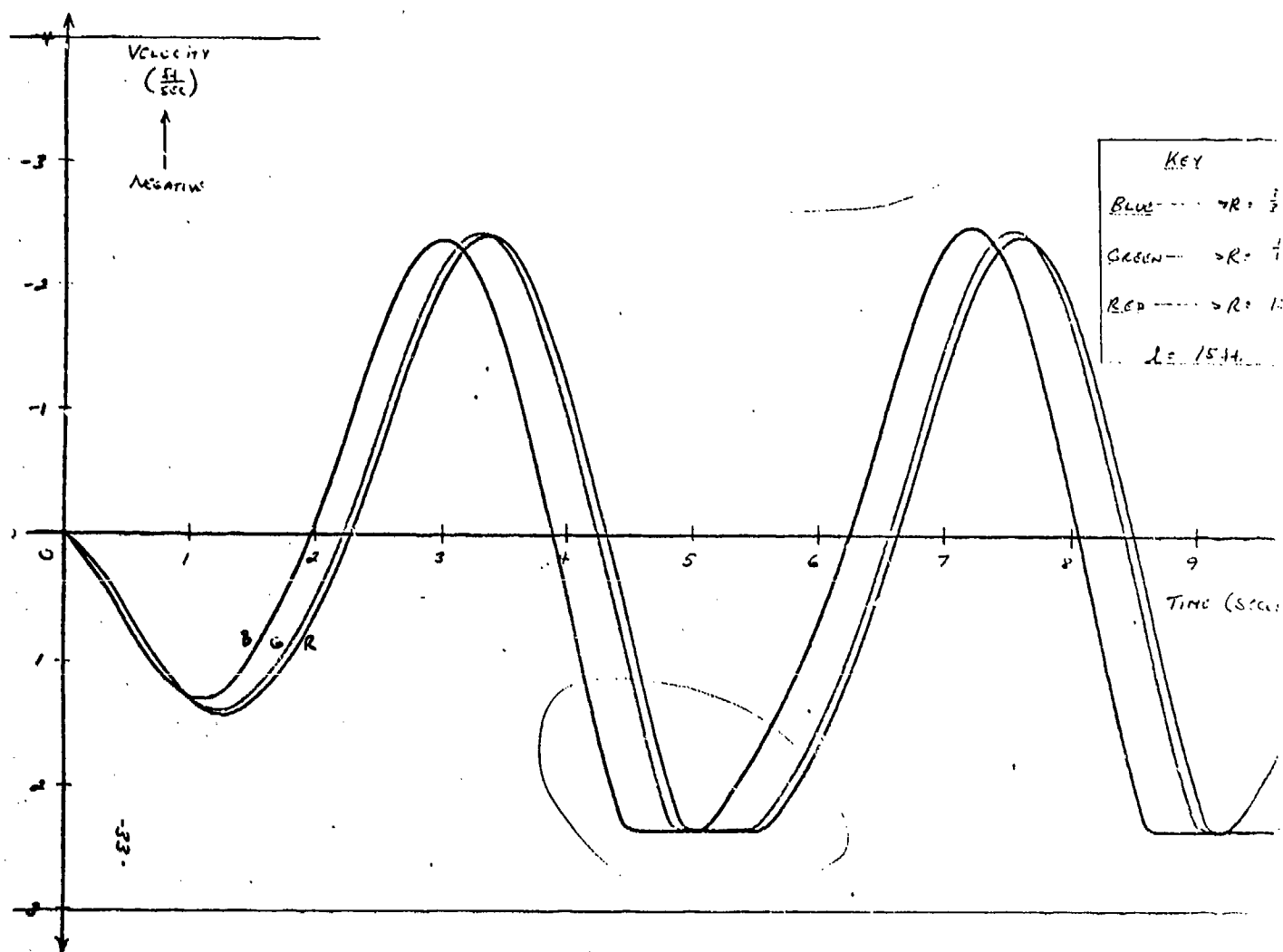


Figure No. 35. Velocity vs time for  $R = 2/3, 11/12, 1$  ft,  $L = 15$  ft



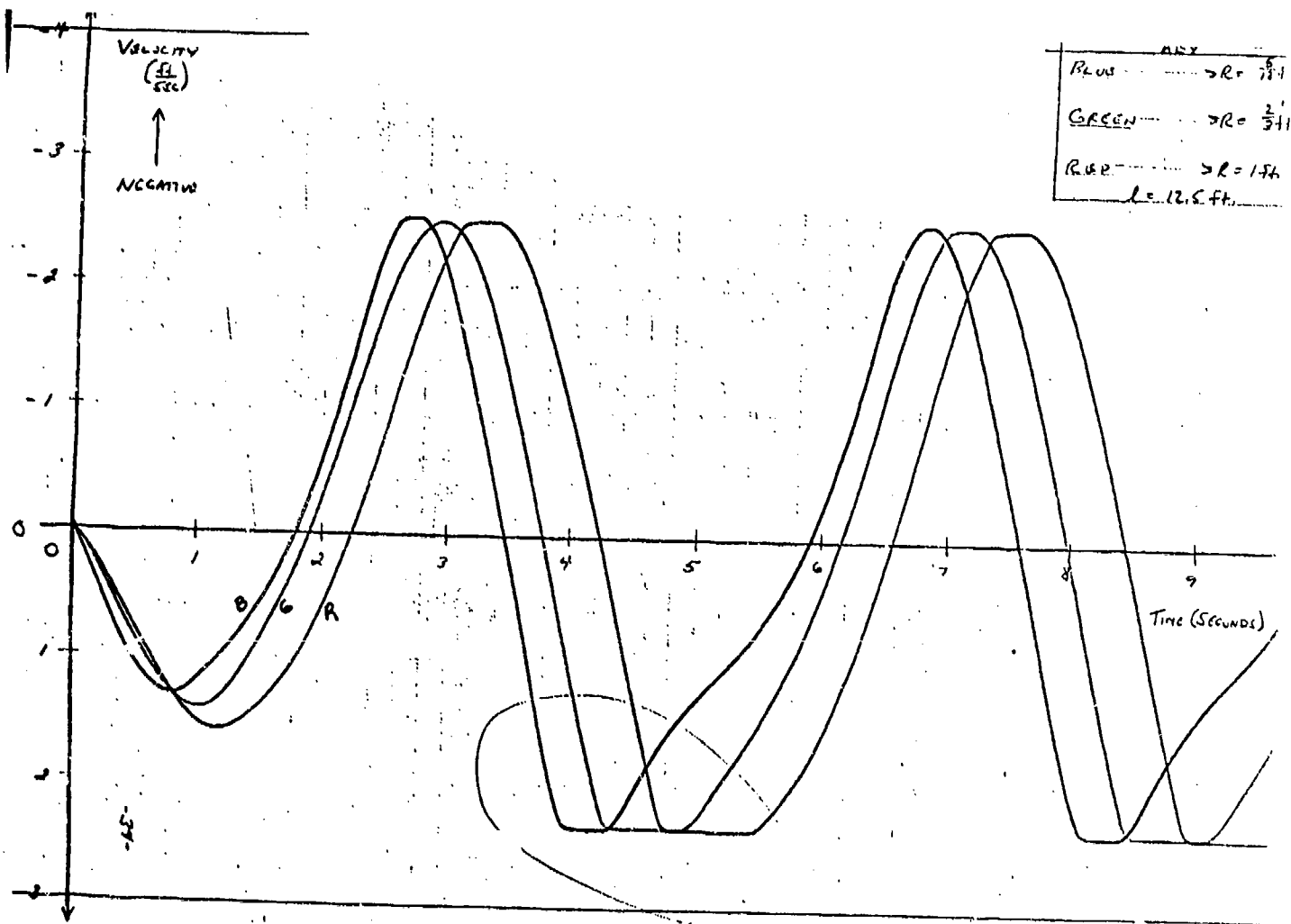


Figure No. 36. Velocity vs time for  $R = 5/12, 2/3, 1 ft, l = 12.5 ft$



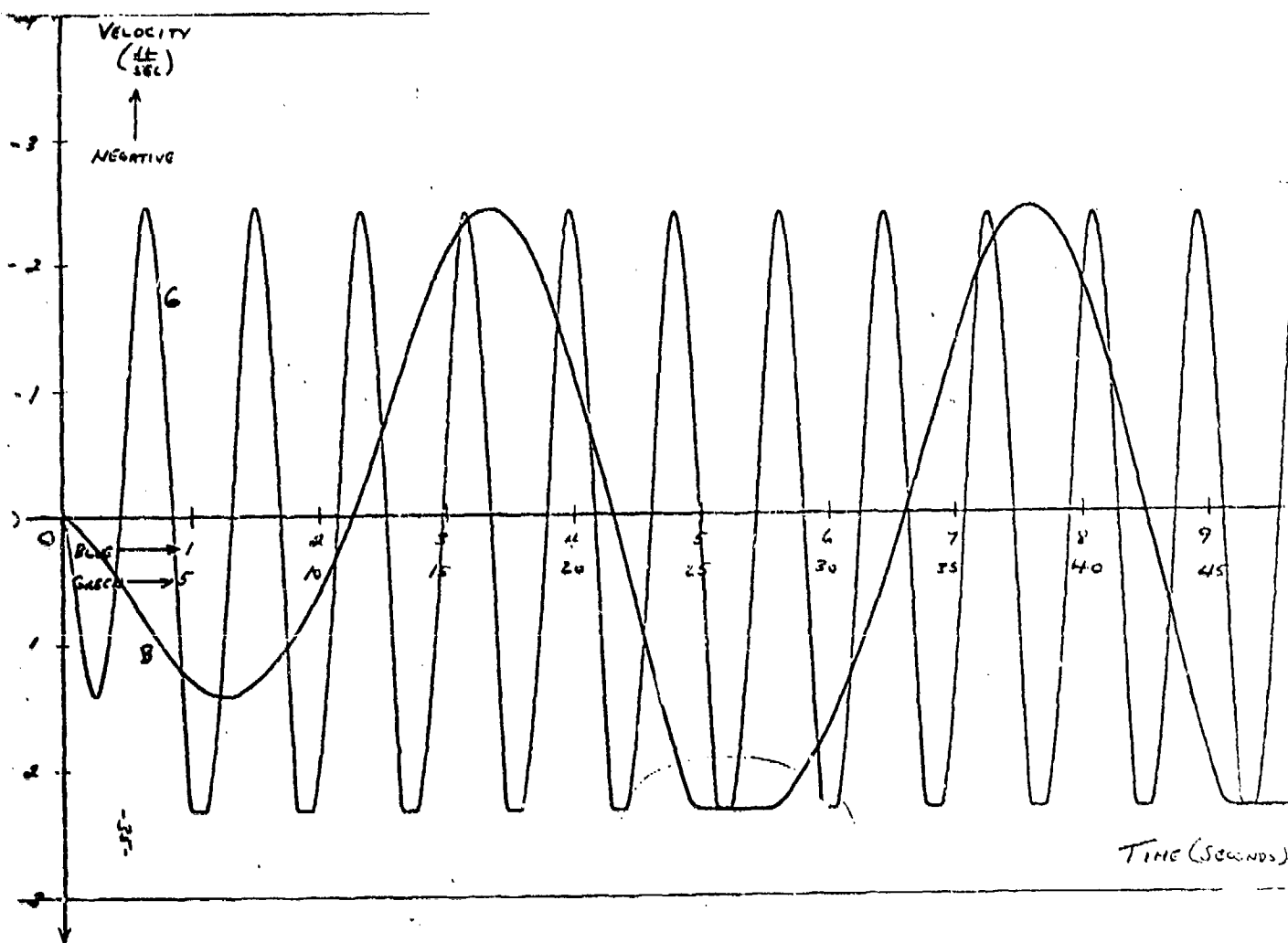


Figure No. 37. Velocity vs time for  $R = 1$  ft,  $l = 15$  ft



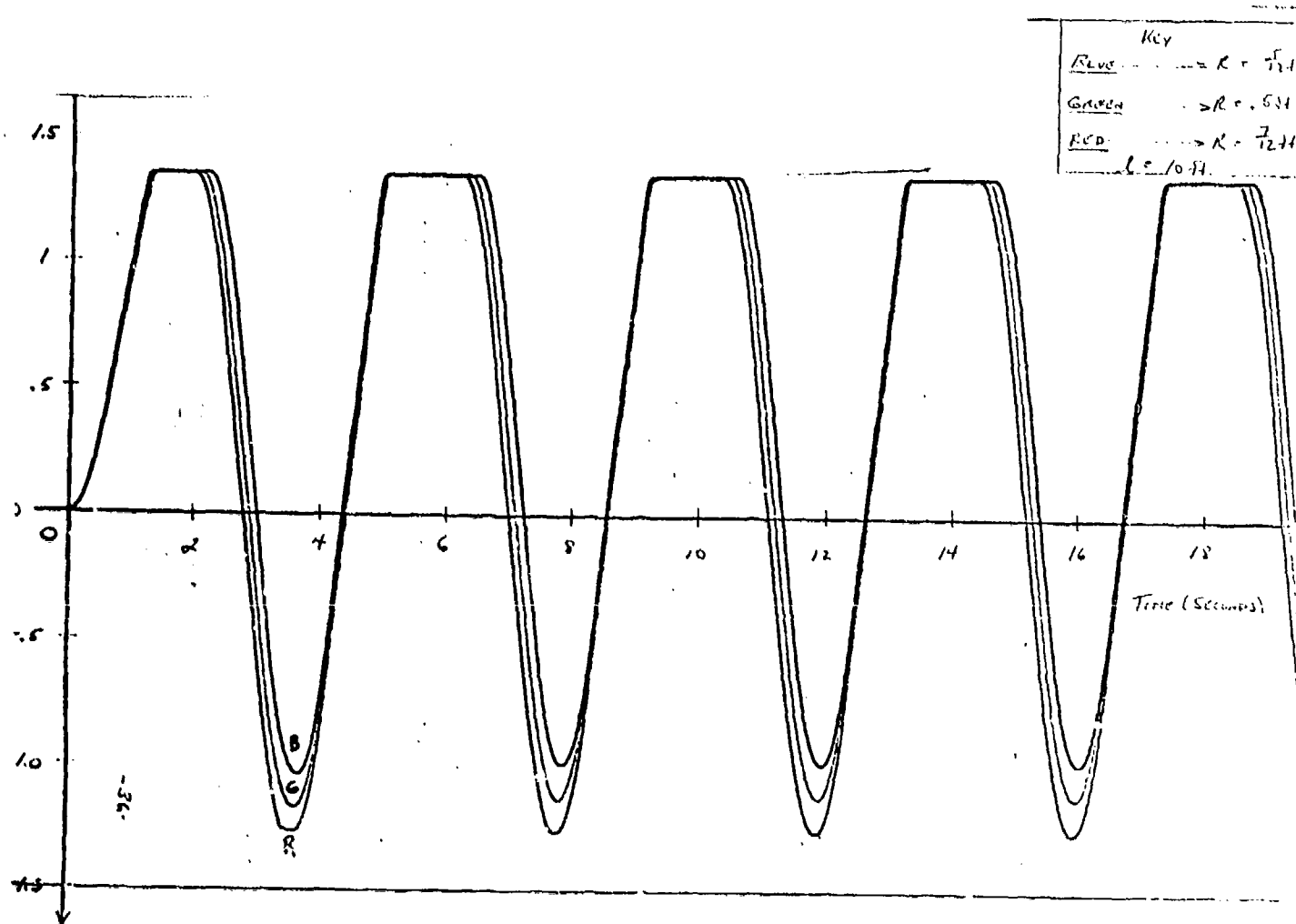


Figure No. 38. Displacement vs time for  $R = 5/12, 1/2, 7/12$  ft,  $\ell = 10$  ft



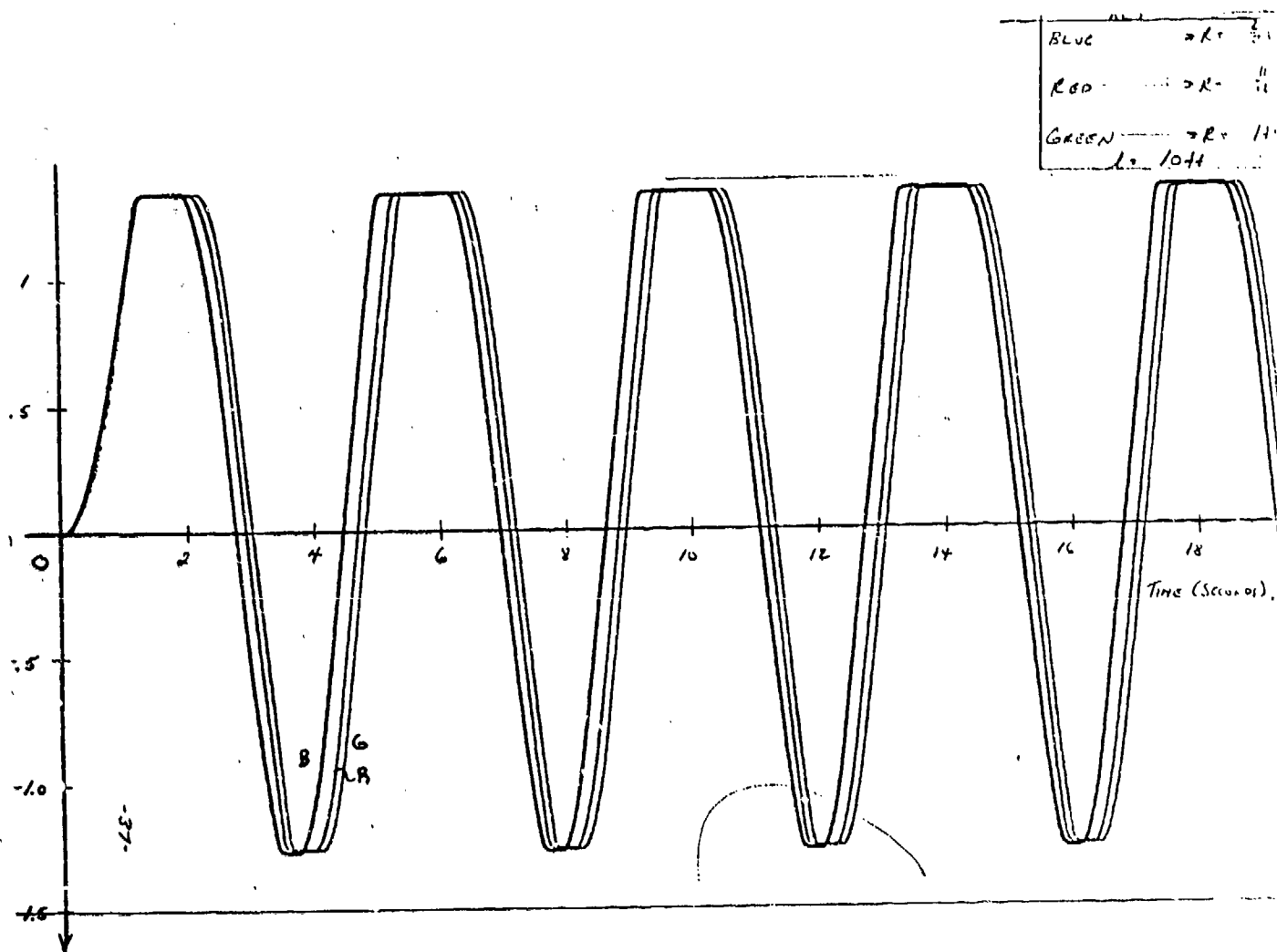


Figure No. 39. Displacement vs time for  $R = 2/3, 11/12, 1 \text{ ft}$ ,  $l = 10 \text{ ft}$



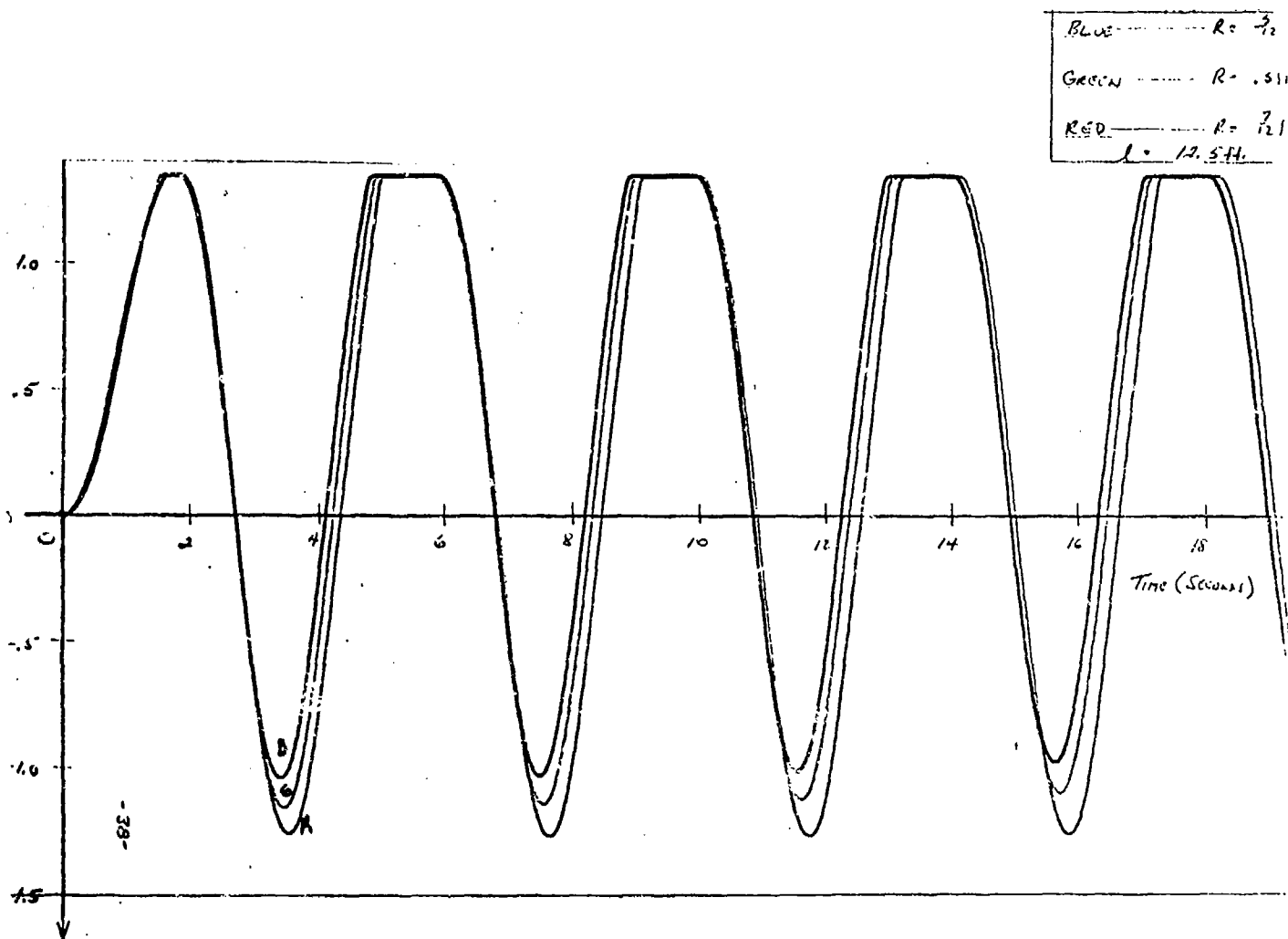


Figure No. 40. Displacement vs time for  $R = 5/12, 1/2, 7/12 \text{ ft}$ ,  $l = 12.5 \text{ ft}$



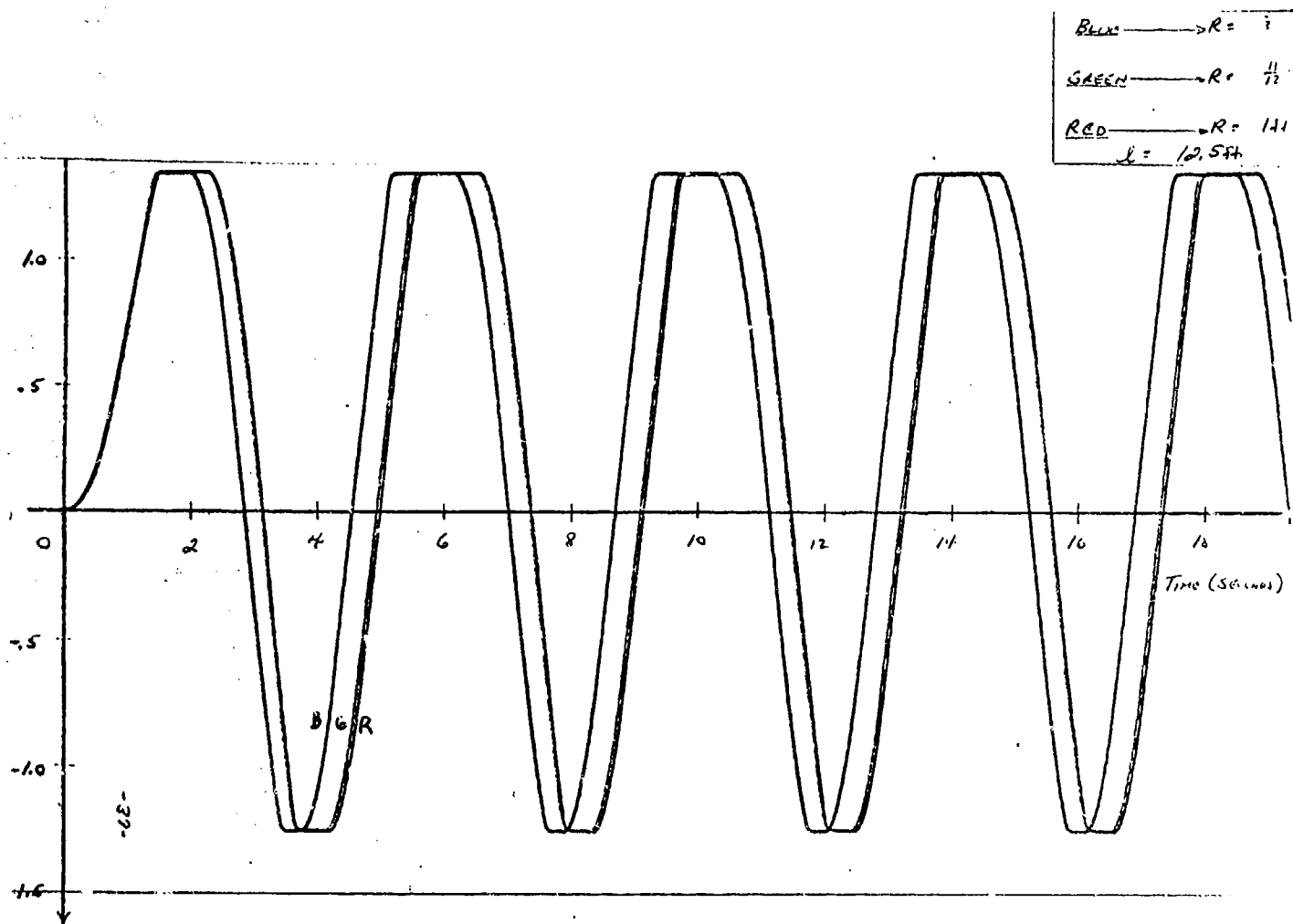


Figure No. 41. Displacement vs time for  $R = 2/3, 11/12, 1 \text{ ft}$ ,  $\lambda = 12.5 \text{ ft}$



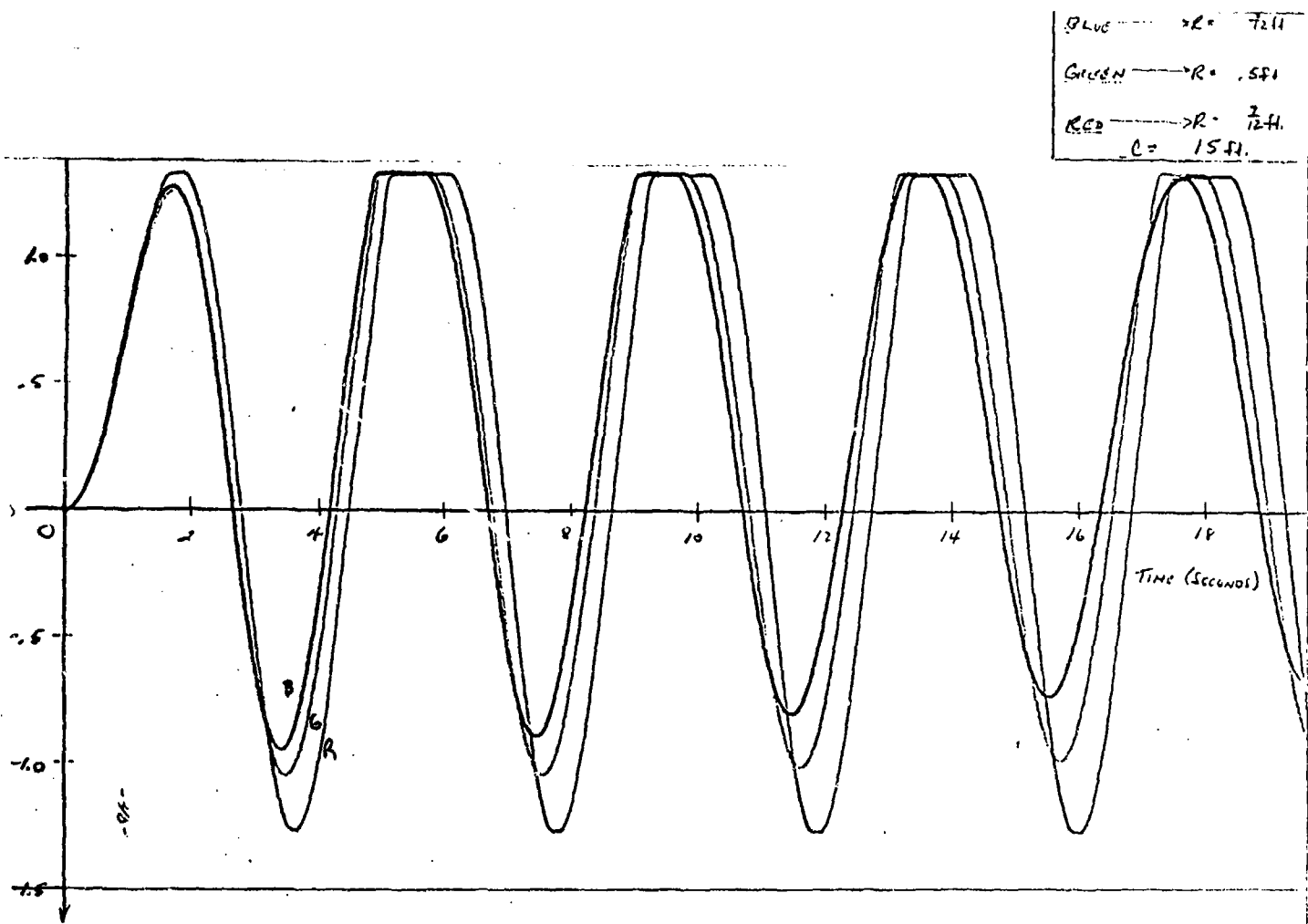


Figure No. 42. Displacement vs time for  $R = 5/12, 1/2, 7/12 \text{ ft.}, \ell = 15 \text{ ft}$



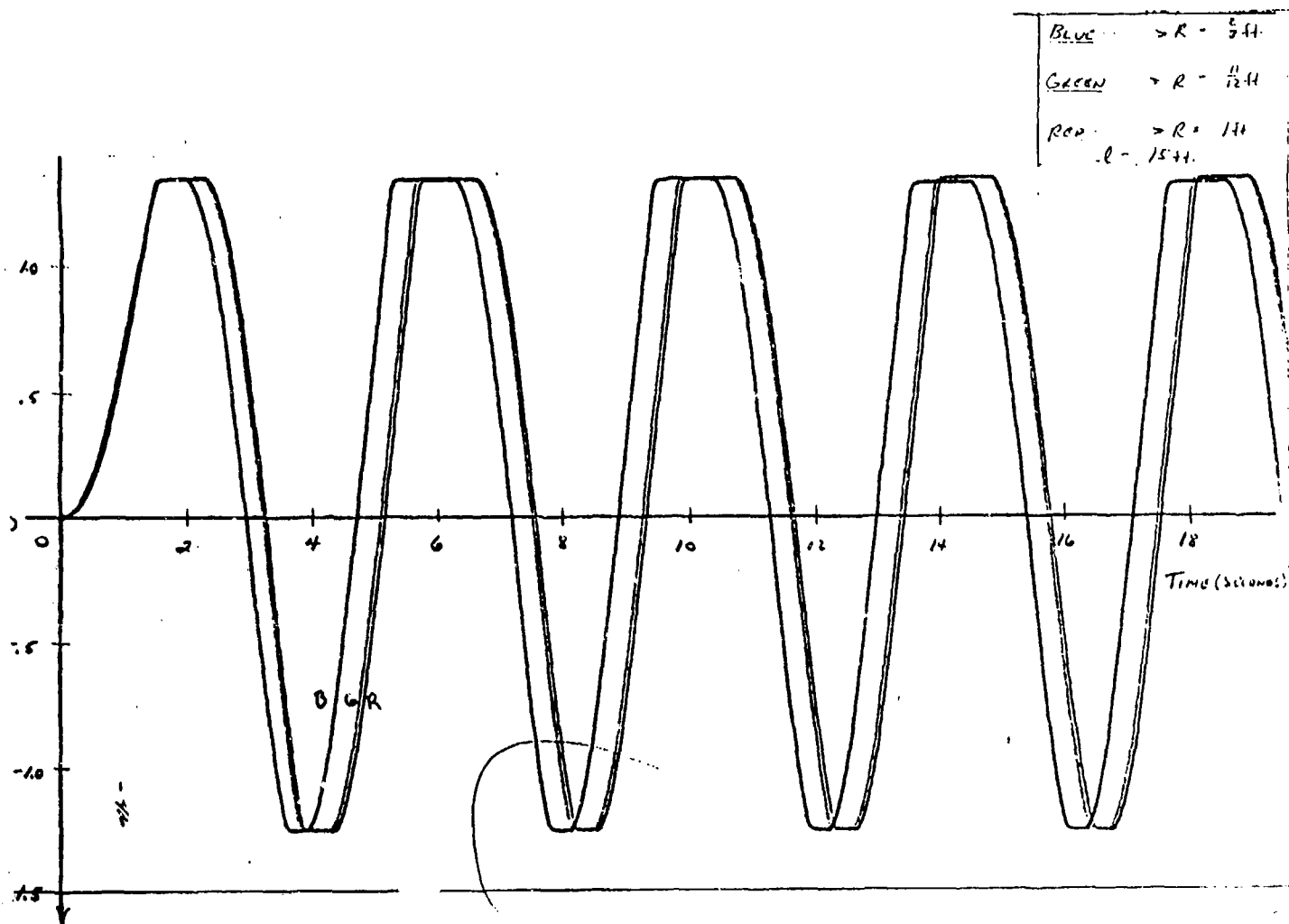


Figure No. 43. Displacement vs time for  $R = 2/3, 11/12, 1$  ft,  $l = 15$  ft



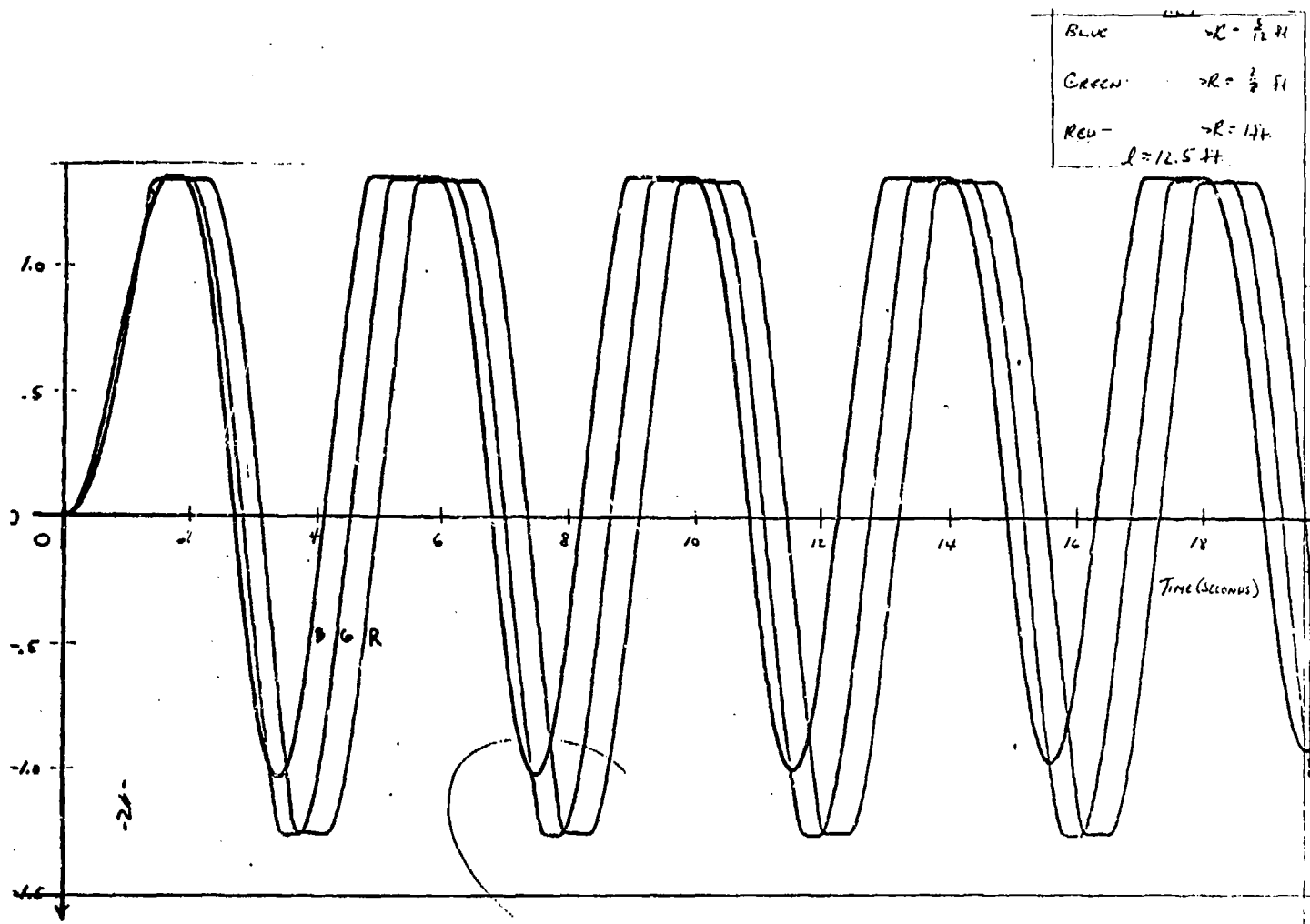


Figure No. 44. Displacement vs time for  $R = 5/12, 2/3, 1 \text{ ft}$ ,  $l = 15 \text{ ft}$



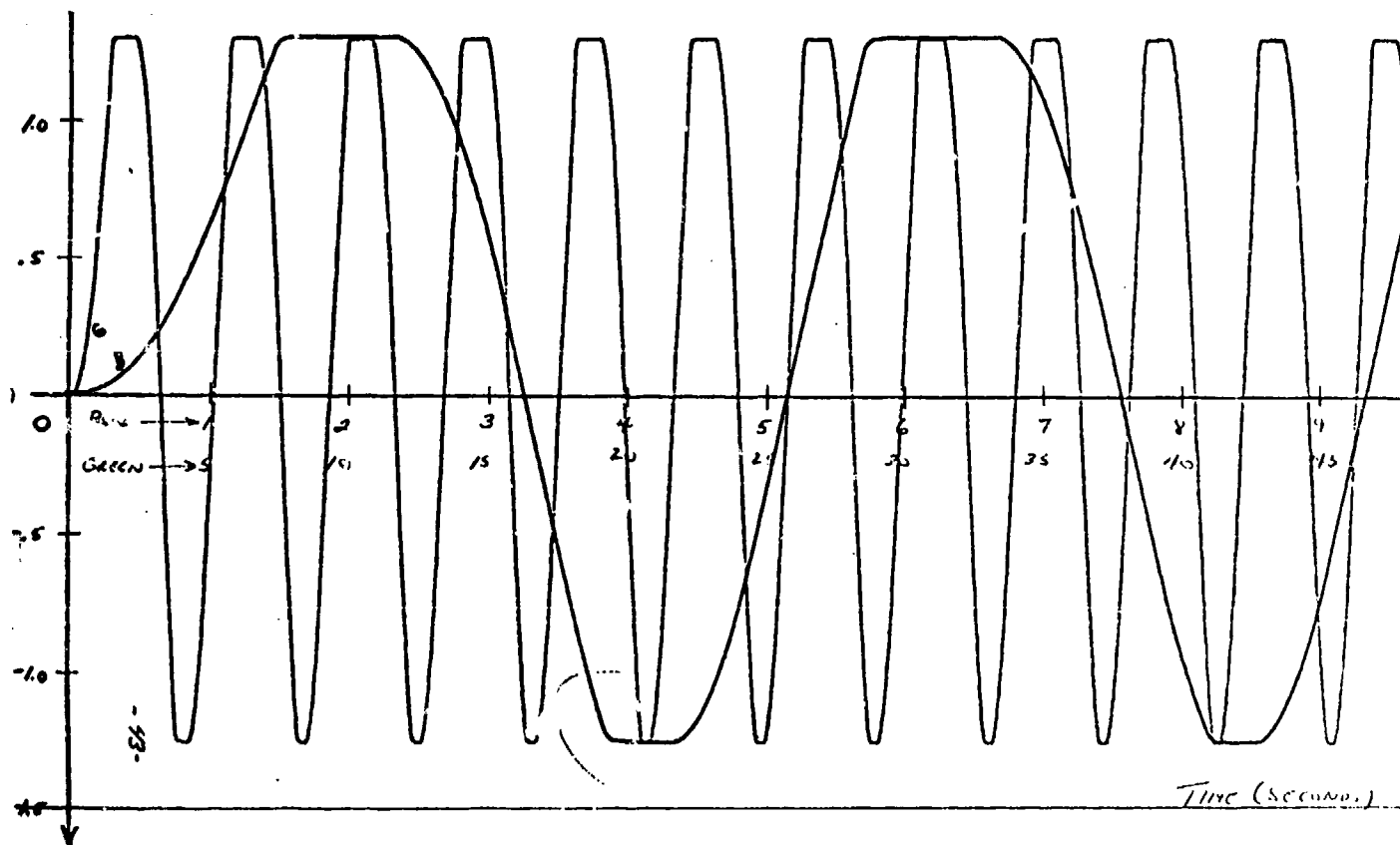


Figure No. 45. Displacement vs time for  $R = 1$  ft,  $l = 15$  ft



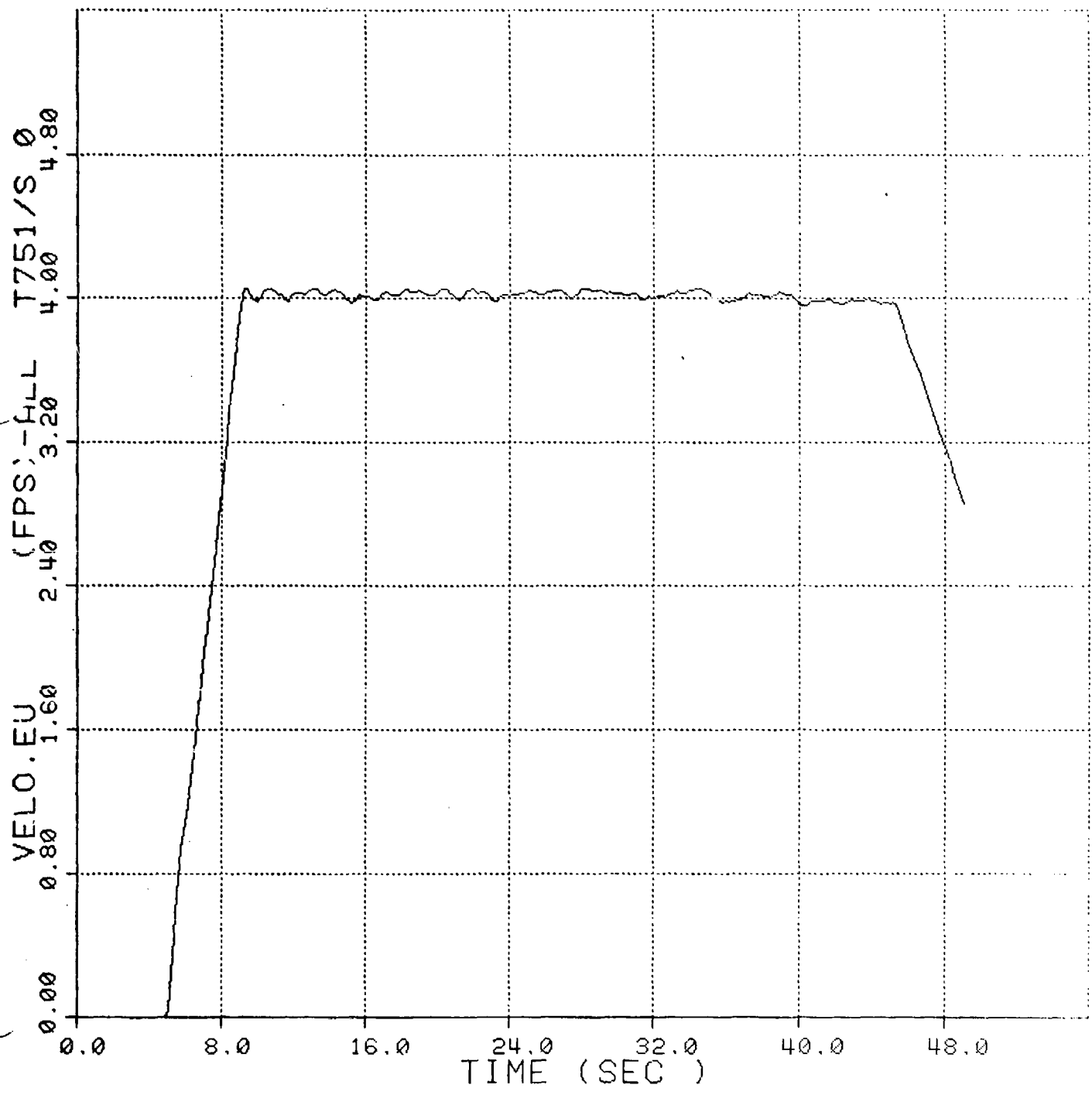


Figure No. 46. Towed Submersible's Velocity vs Time, Case 2



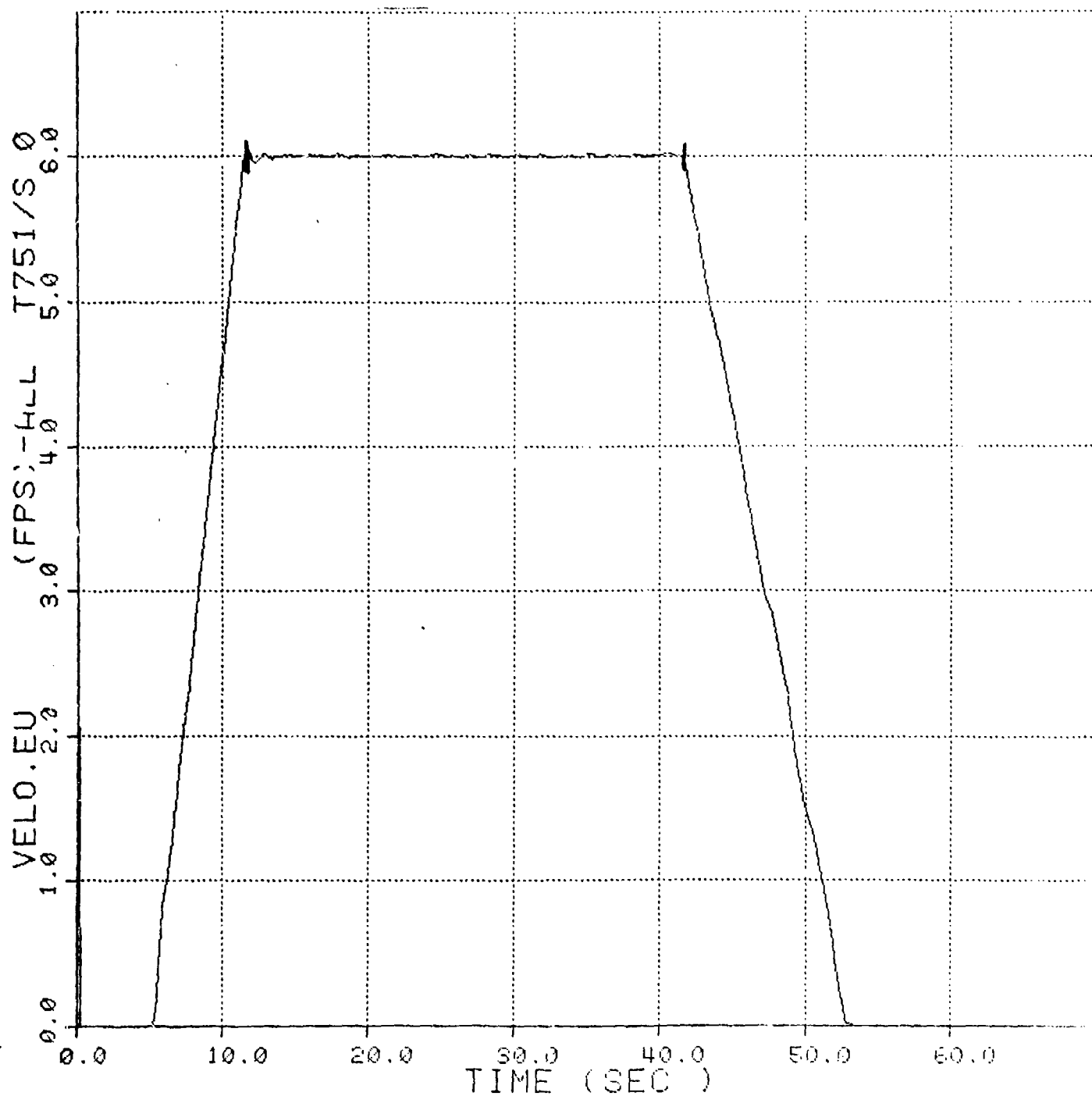


Figure No. 47. Towed Submersible's Velocity vs Time, Case 3



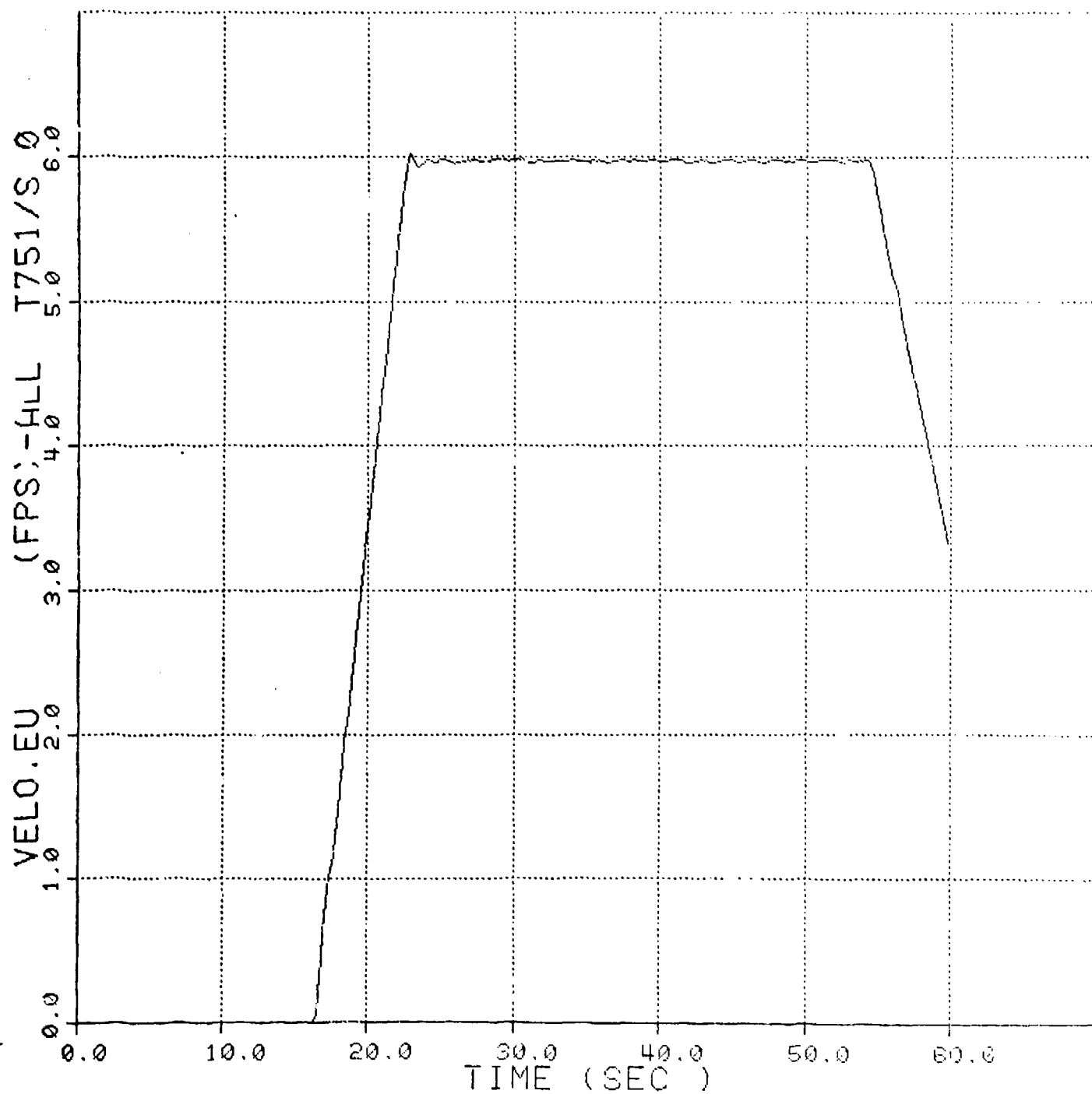


Figure No. 48. Towed Submersible's Velocity vs Time, Case 4



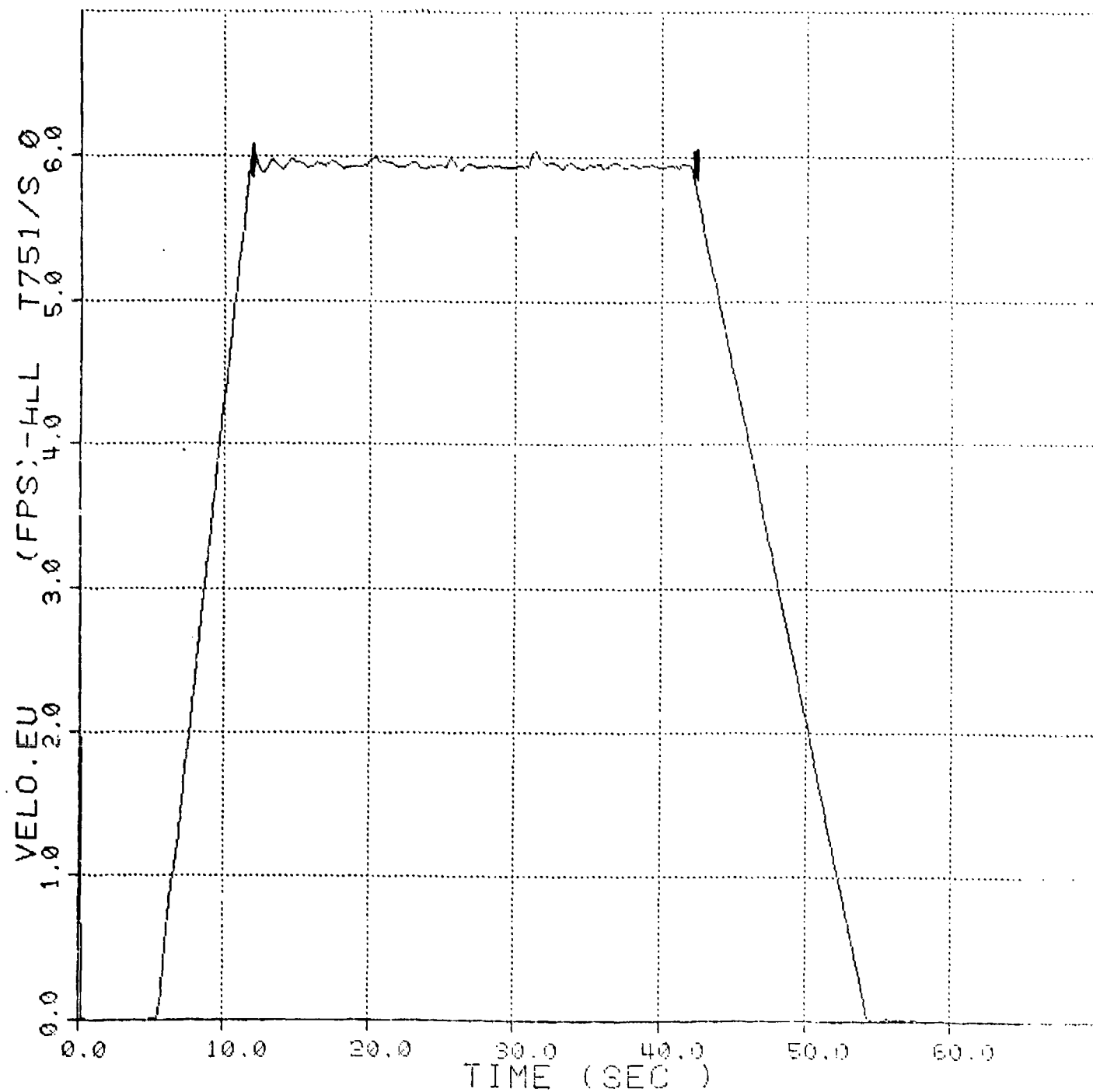


Figure No. 49. Towed Submersible's Velocity vs Time, Case 5



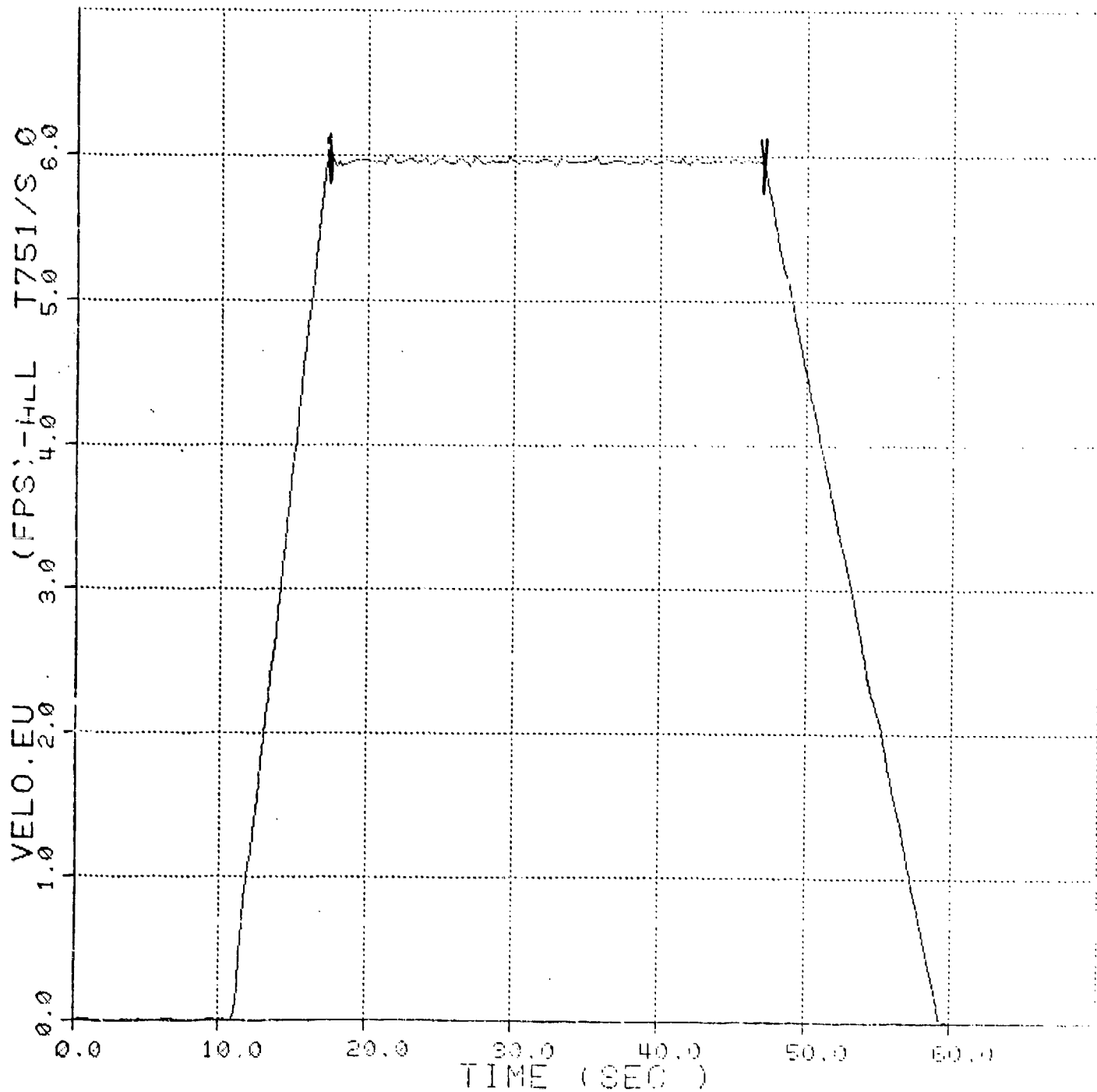


Figure No. 50. Towed Submersible's Velocity vs Time, Case 6



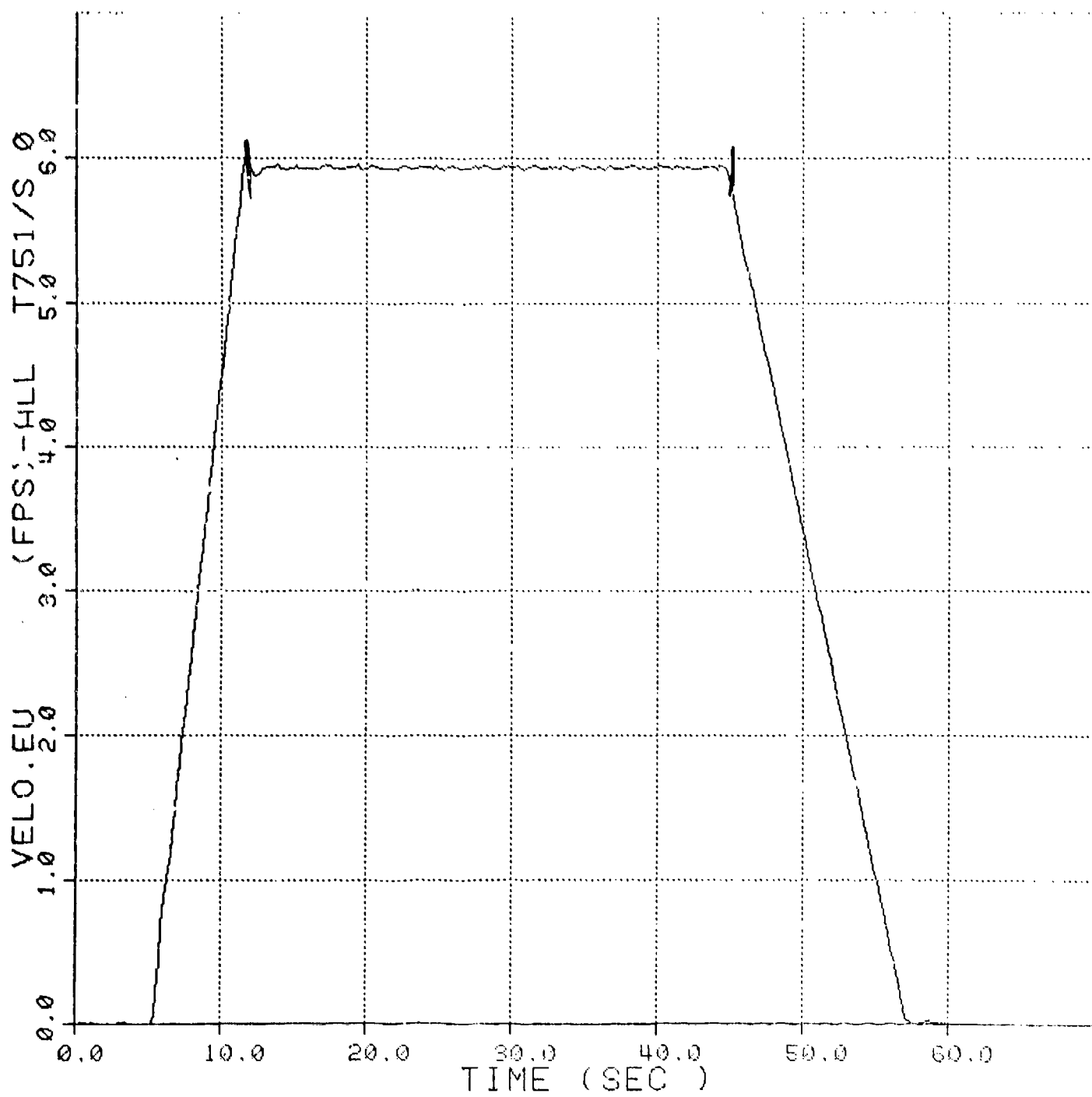


Figure No. 51. Towed Submersible's Velocity vs Time, Case 7



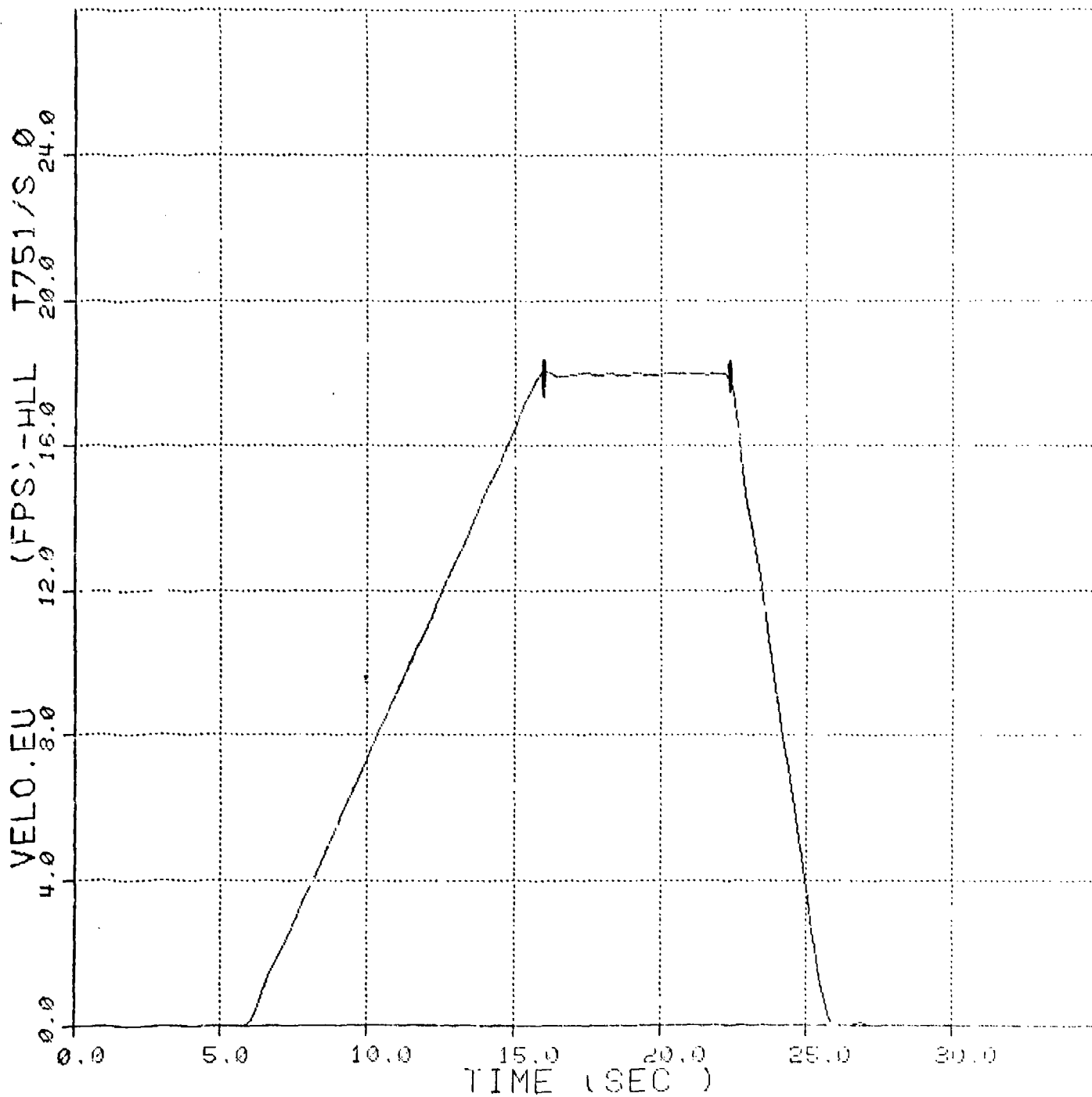


Figure No. 52. Towed Submersible's Velocity vs Time, Case 8



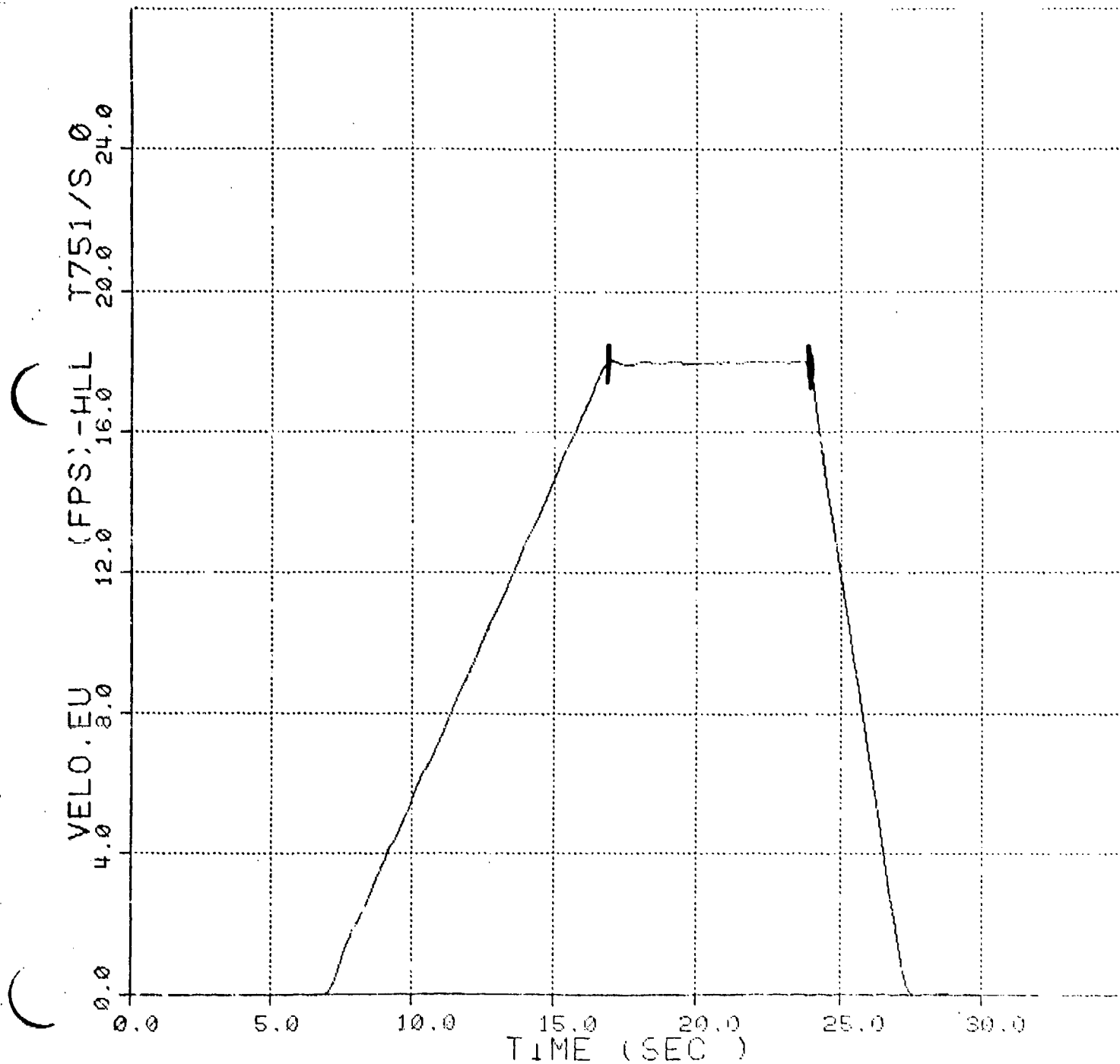


Figure No. 53. Towed Submersible's Velocity vs Time, Case 9



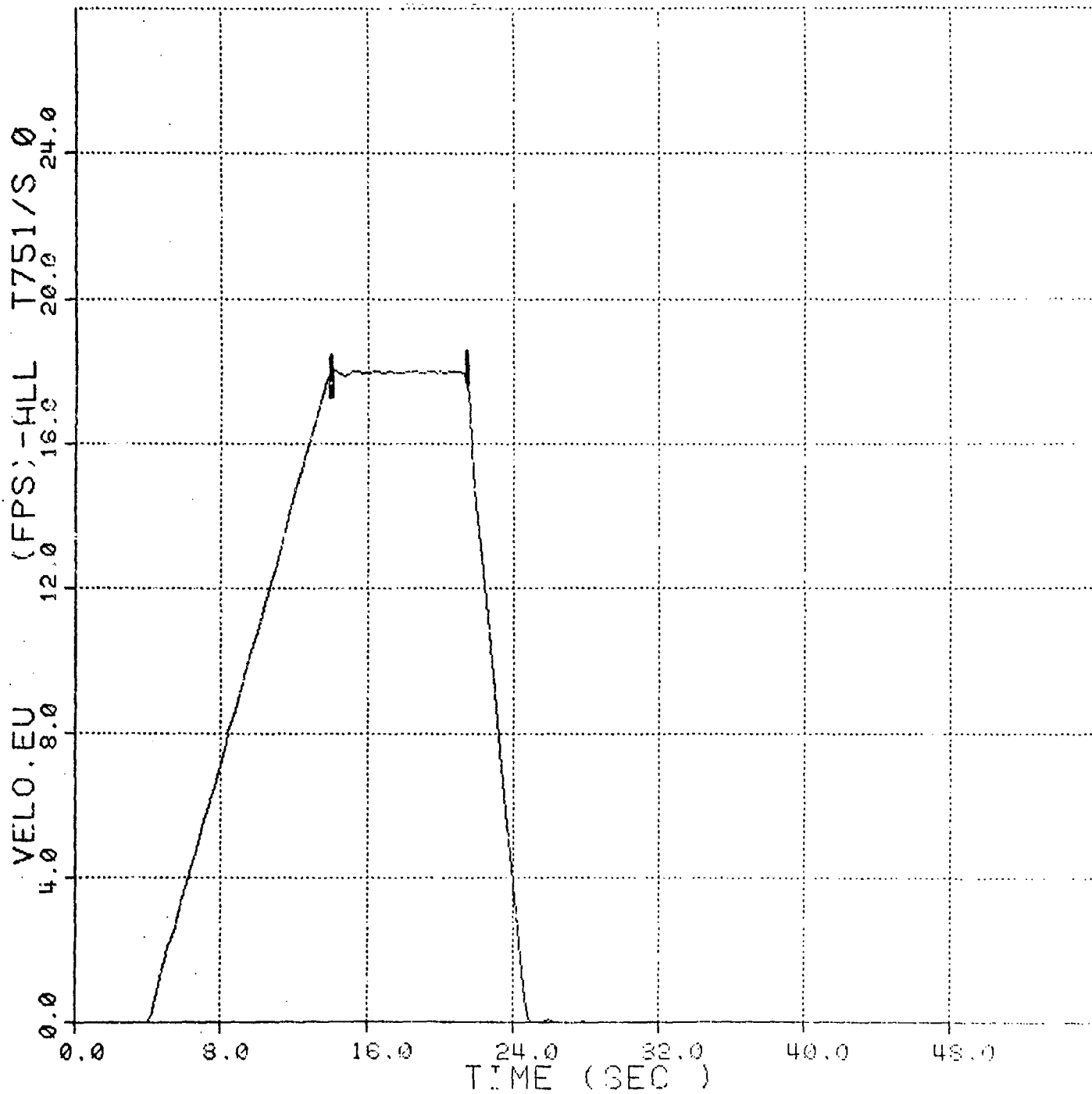


Figure No. 54. Towed Submersible's Velocity vs Time, Case 10



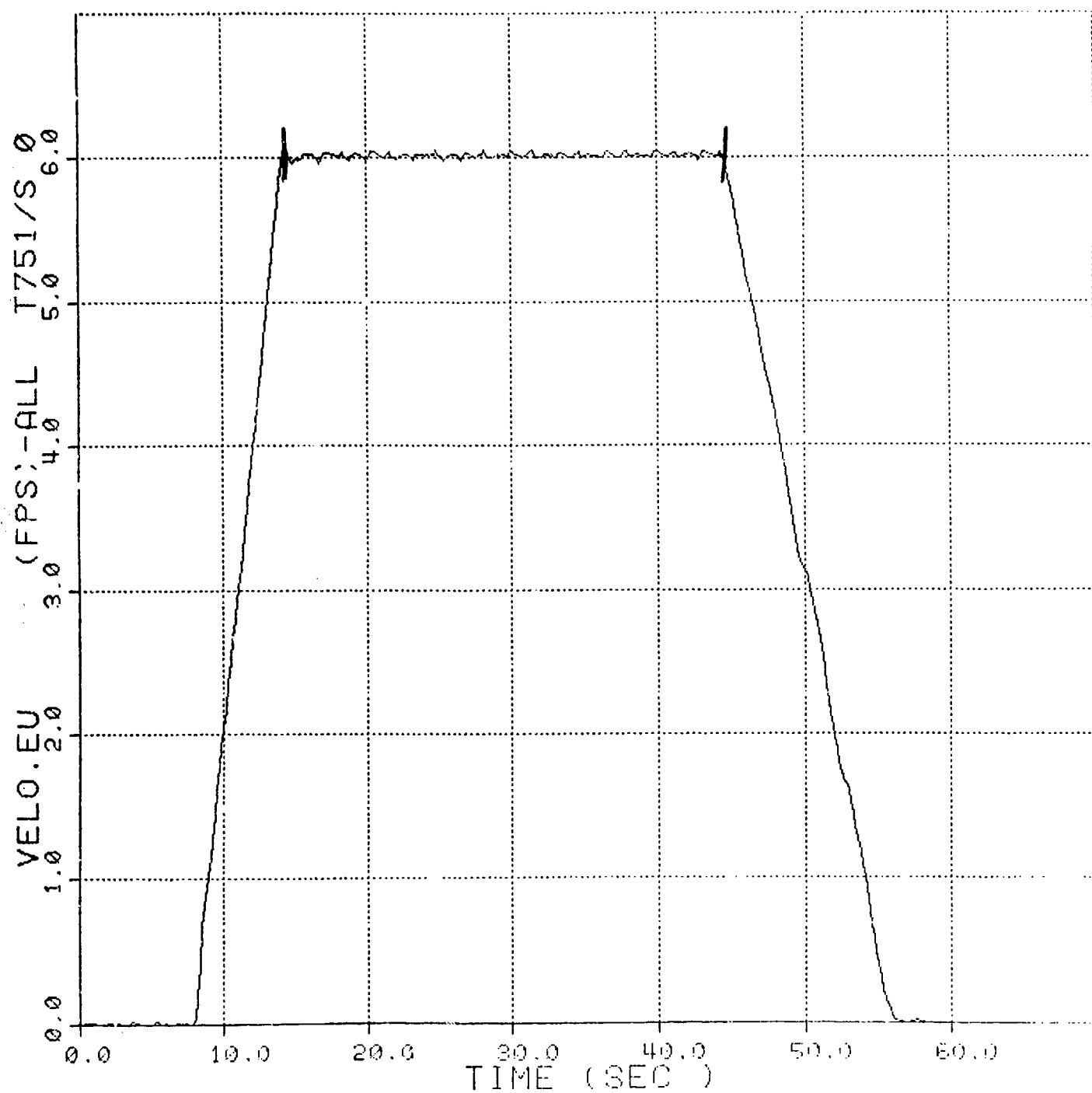


Figure No. 55. Towed Submersible's Velocity vs Time, Case 11



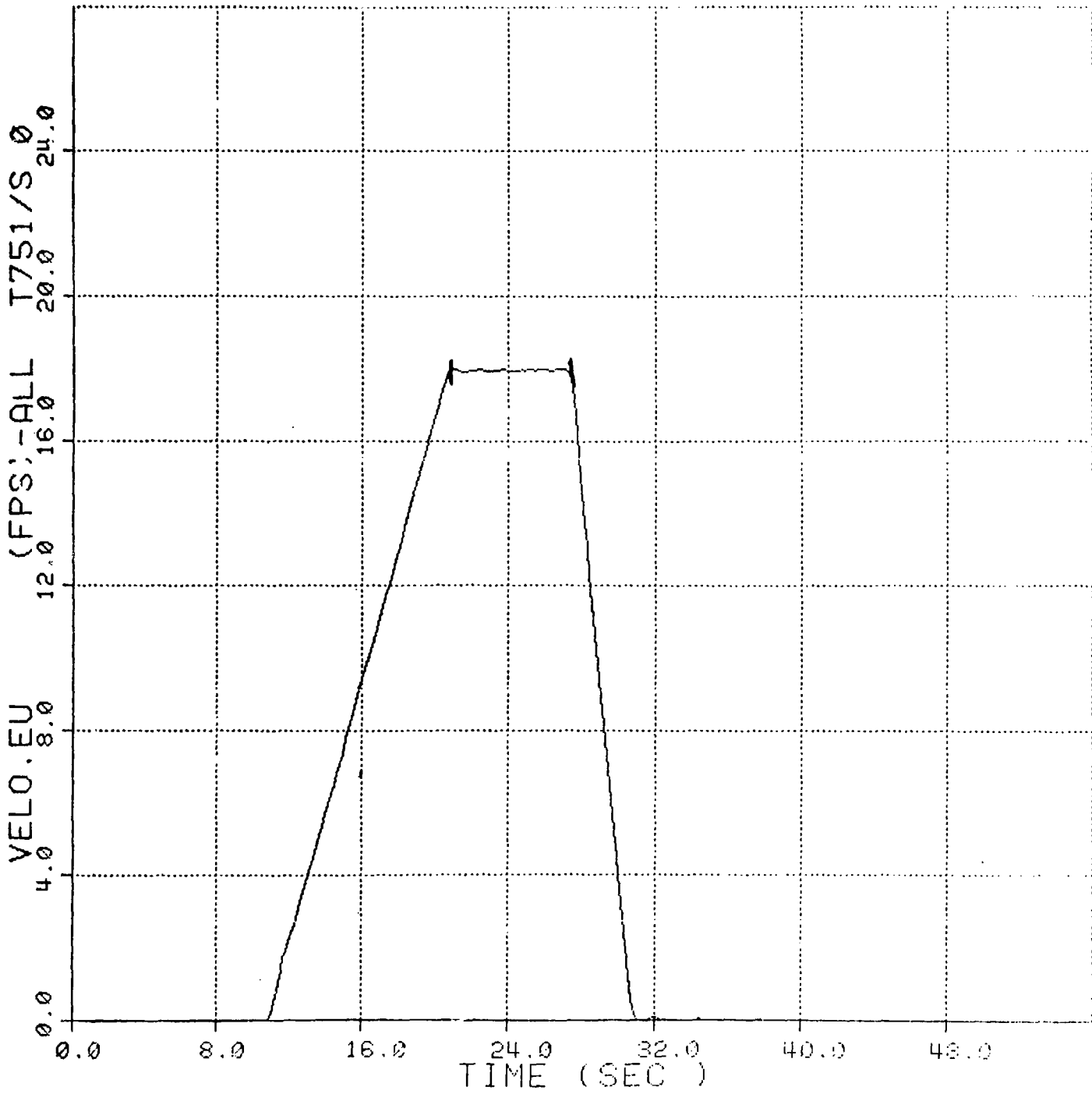


Figure No. 56. Towed Submersible's Velocity vs Time, Case 12



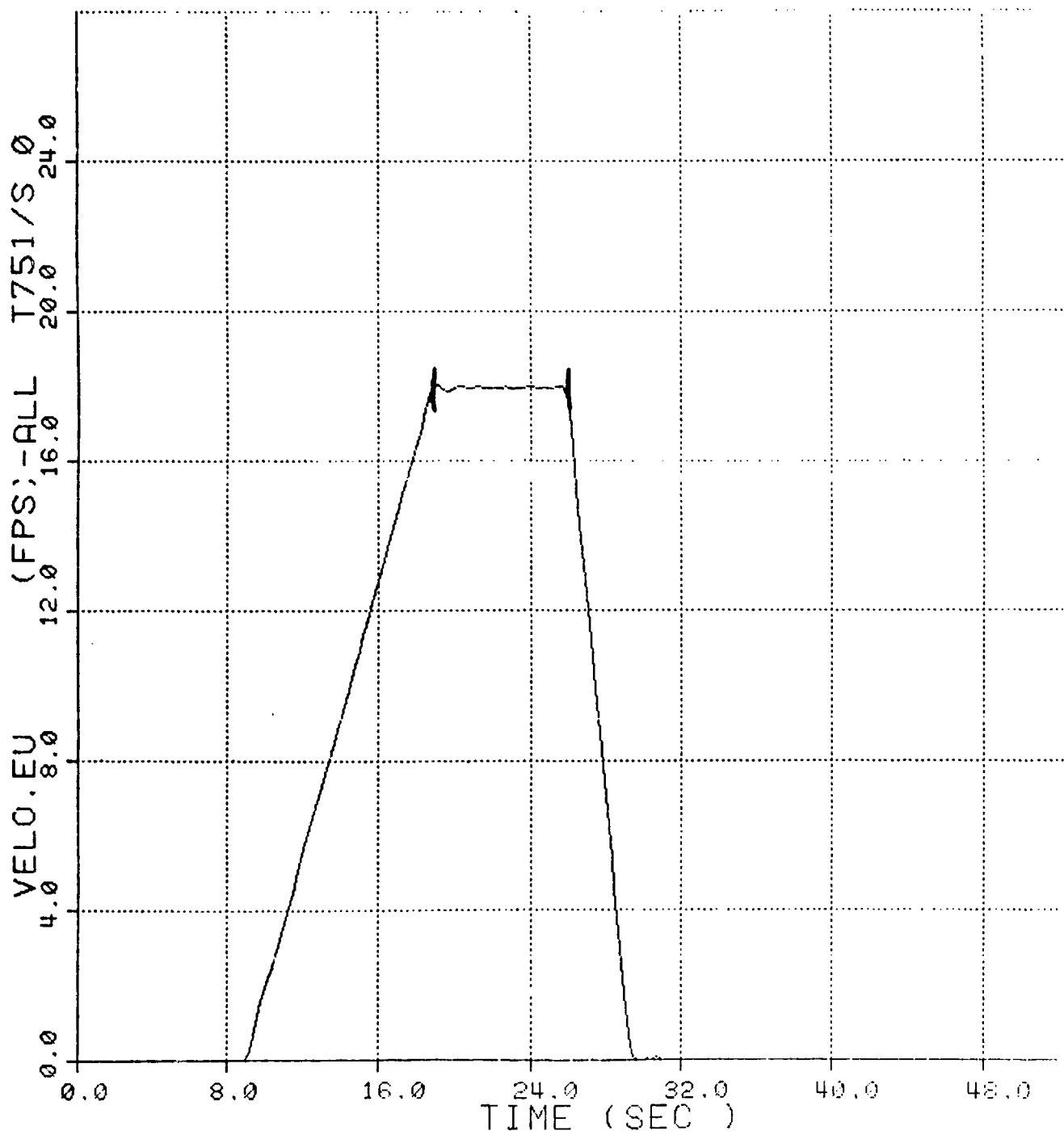


Figure No. 57. Towed Submersible's Velocity vs Time, Case 13



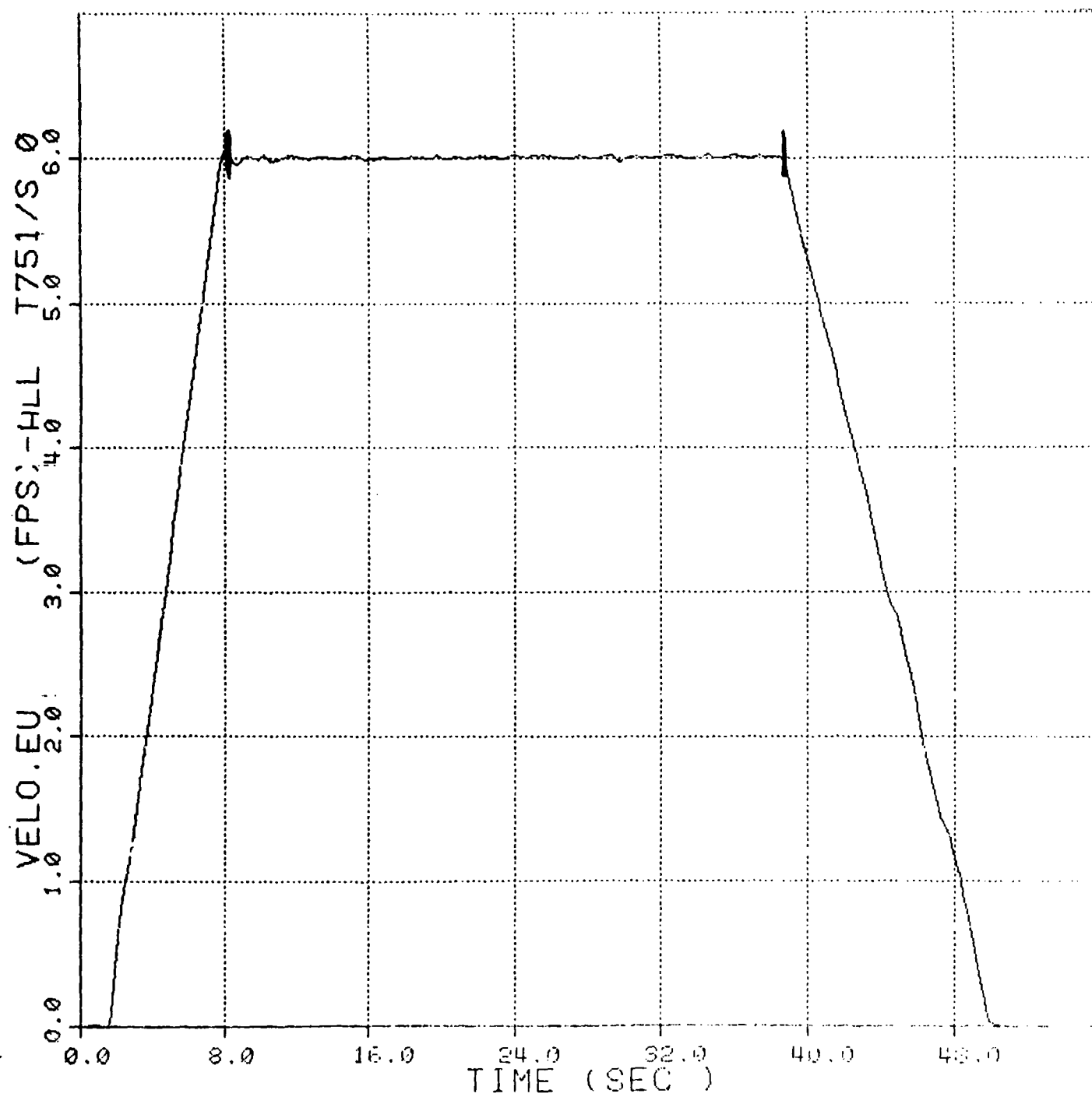


Figure No. 58. Towed Submersible's Velocity vs Time, Case 14



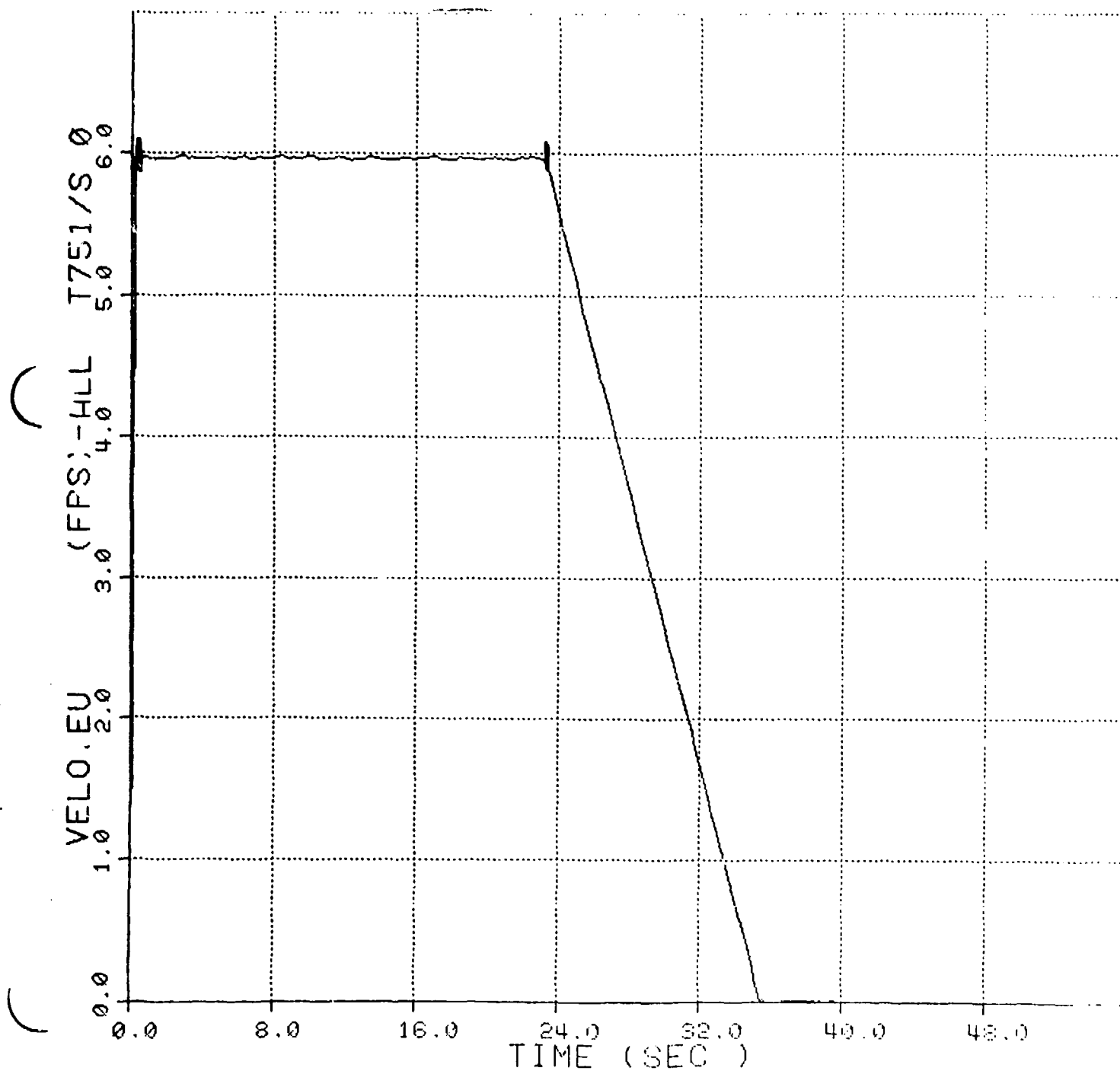


Figure No. 59. Towed Submersible's Velocity vs Time, Case 15



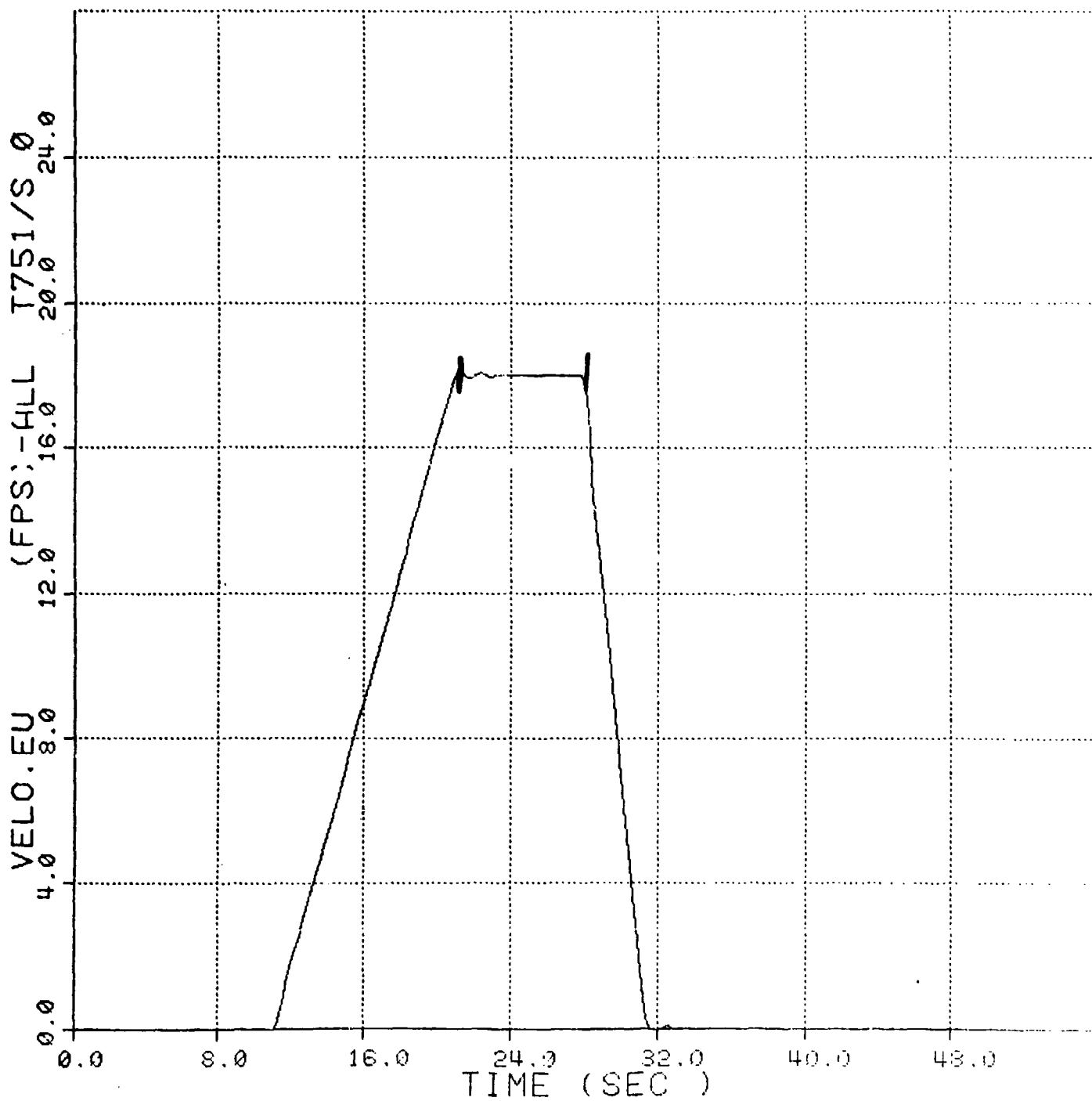


Figure No. 60. Towed Submersible's Velocity vs Time, Case 16



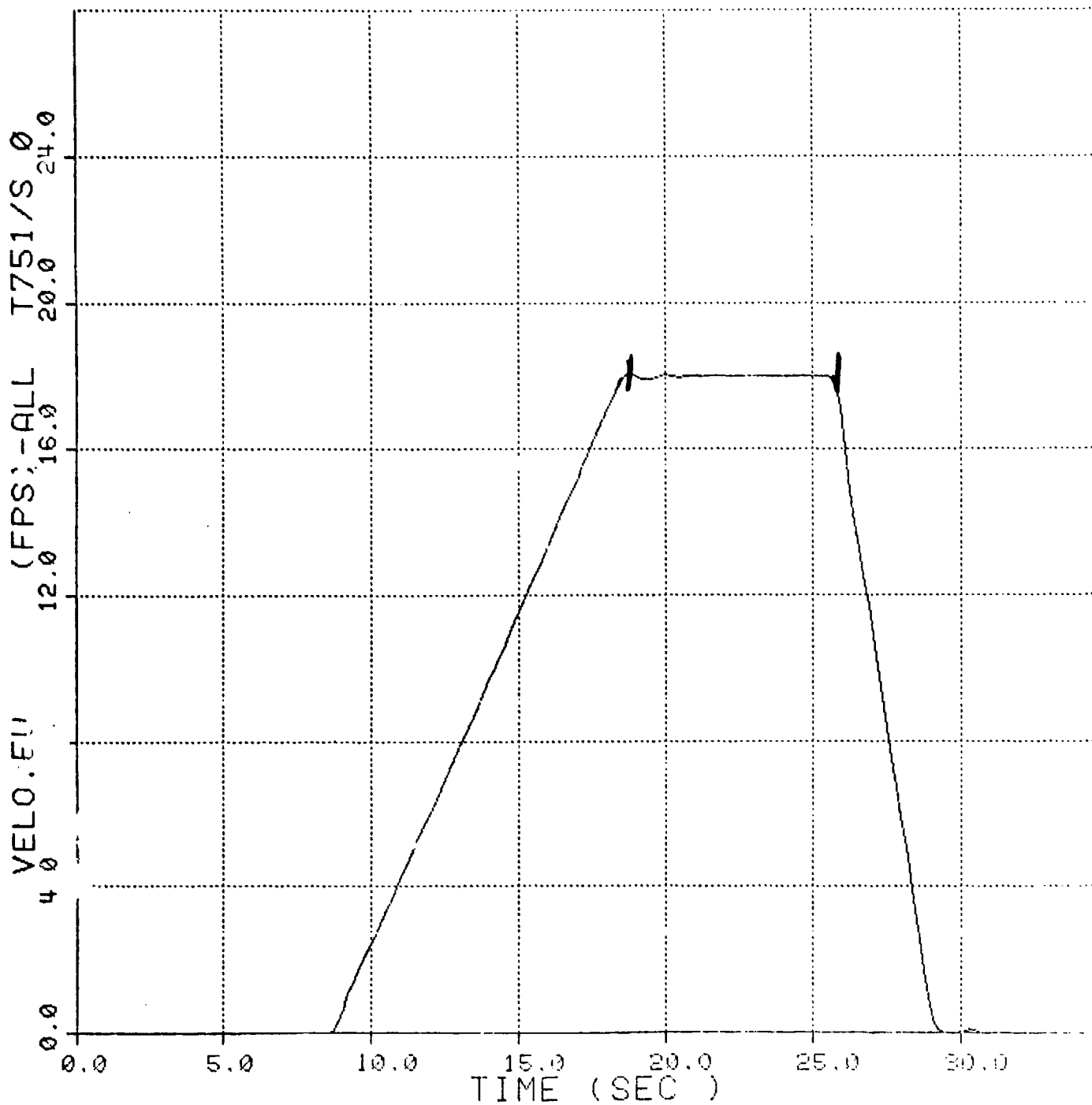


Figure No. 61. Towed Submersible's Velocity vs Time, Case 17



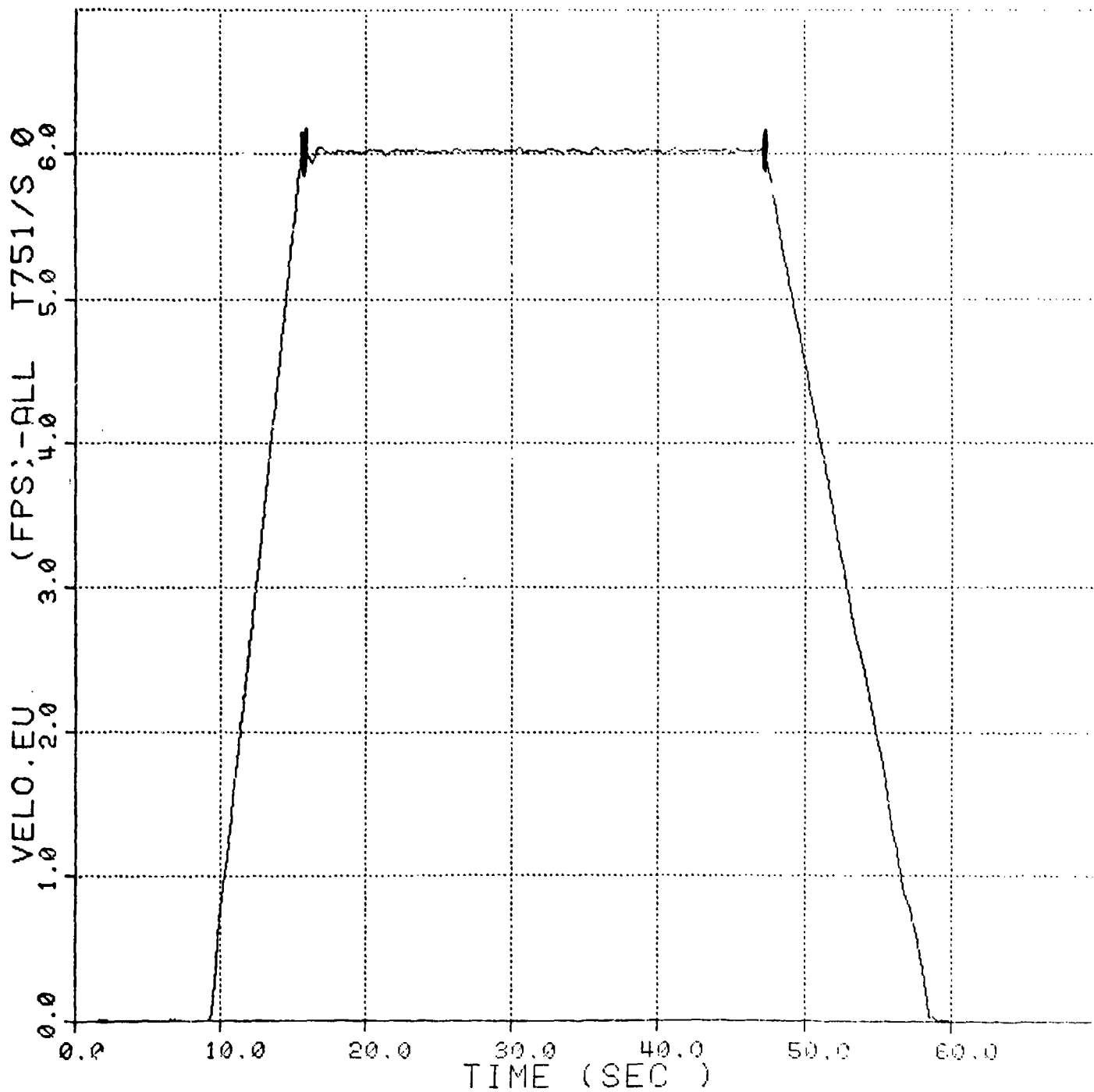


Figure No. 62. Towed Submersible's Velocity vs Time, Case 18



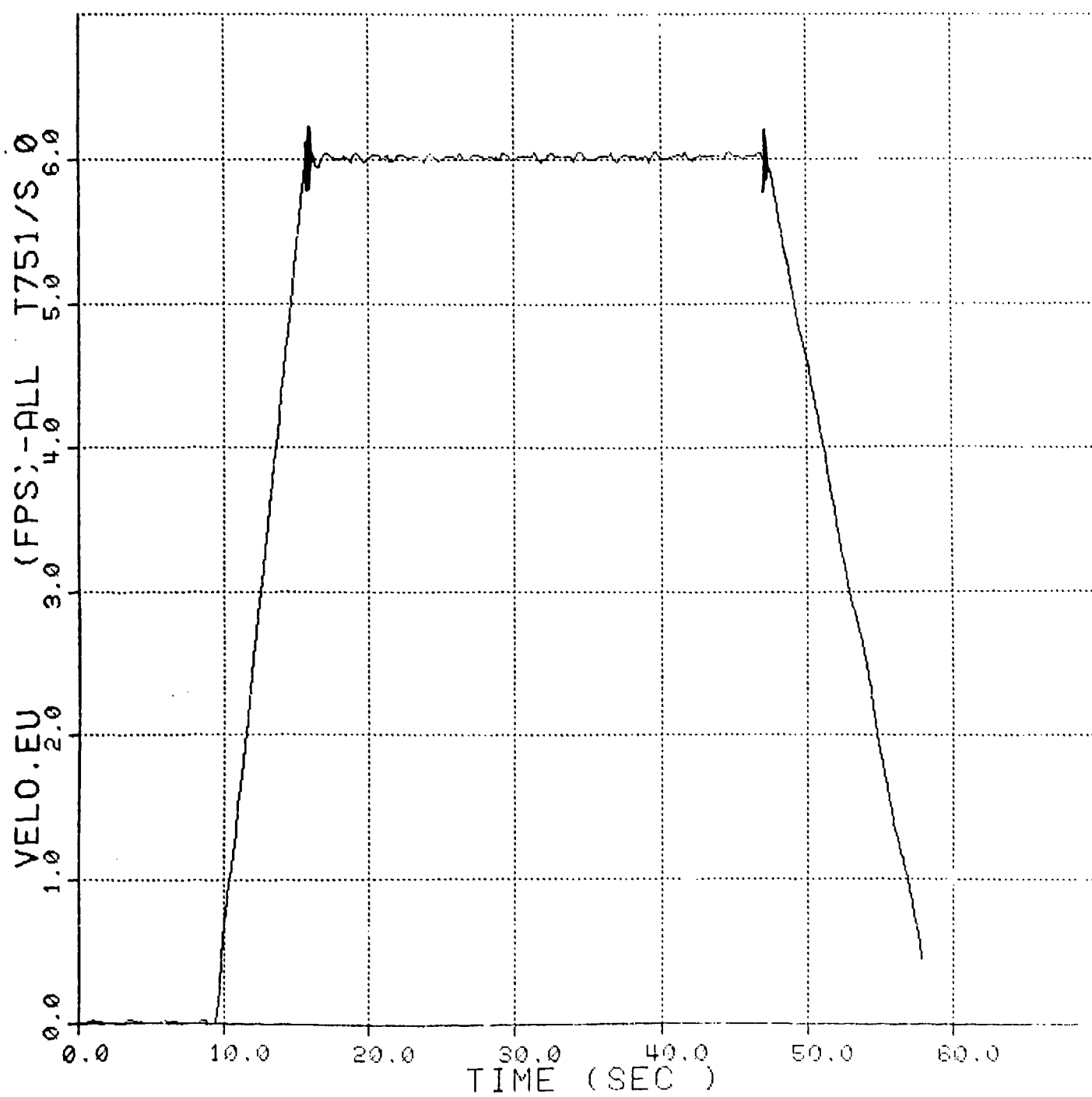


Figure No. 63. Towed Submersible's Velocity vs Time, Case 19



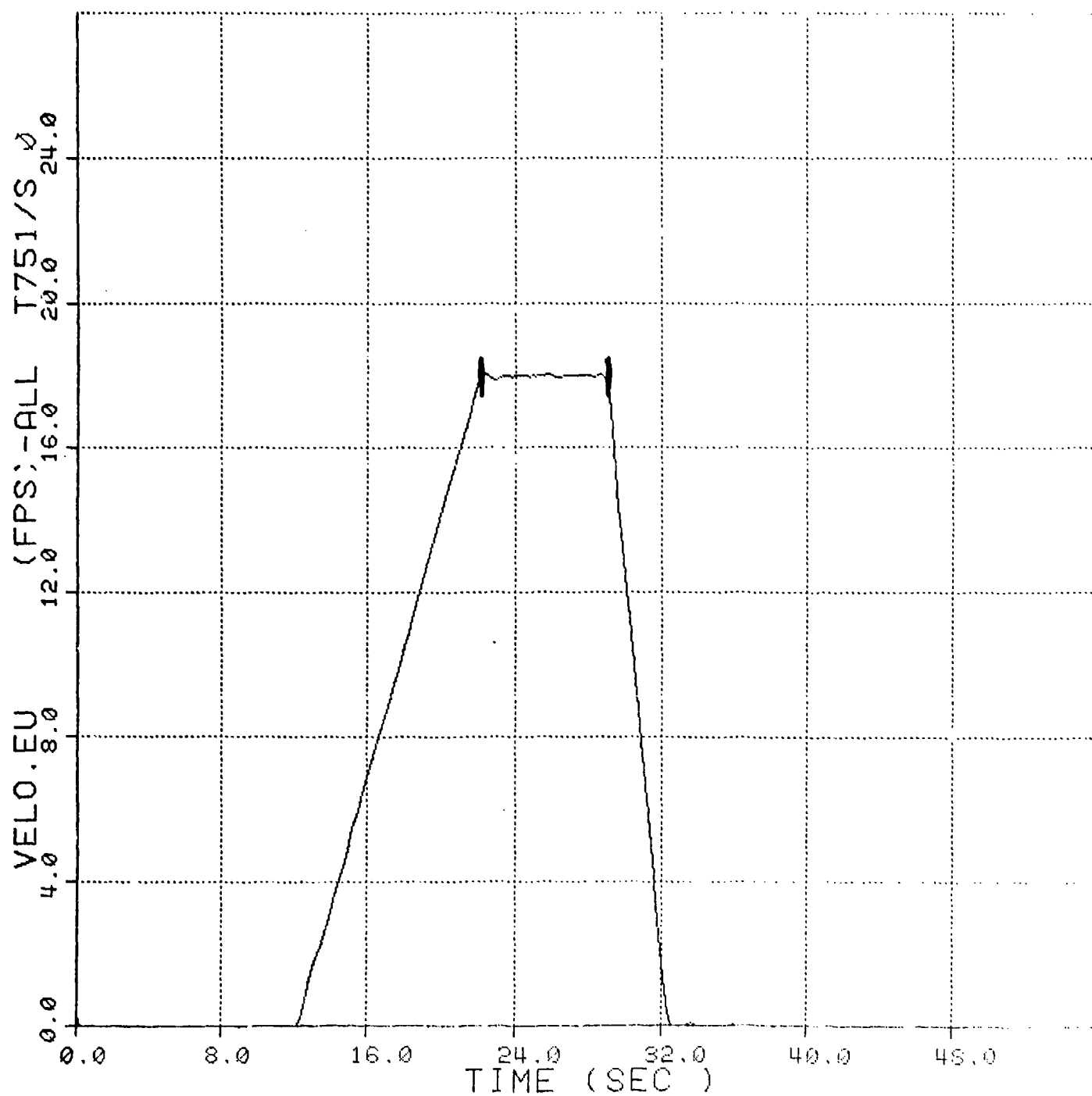


Figure No. 64. Towed Submersible's Velocity vs Time, Case 20



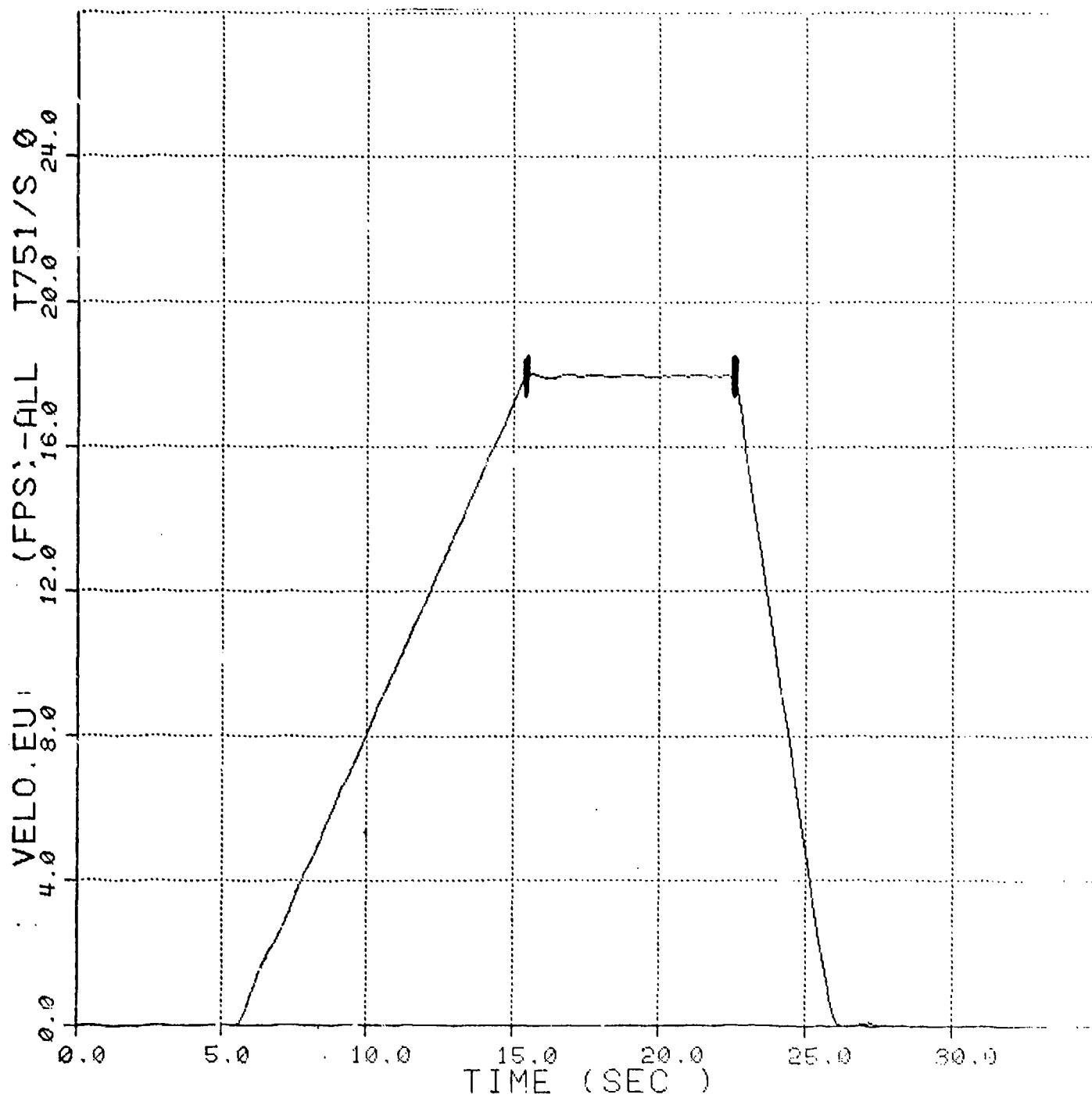


Figure No. 65. Towed Submersible's Velocity vs Time, Case 21



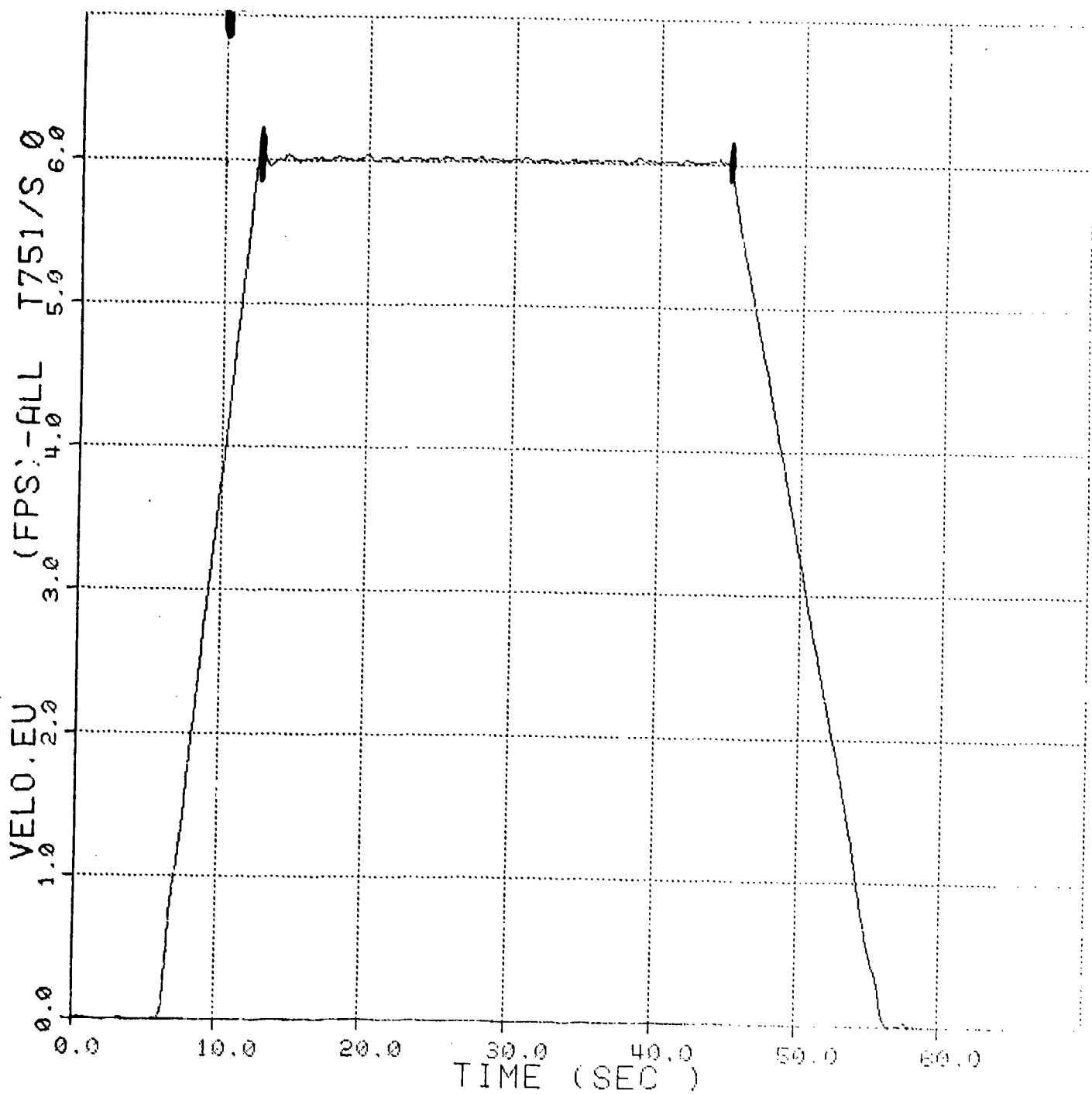


Figure No. 66. Towed Submersible's Velocity vs Time, Case 22



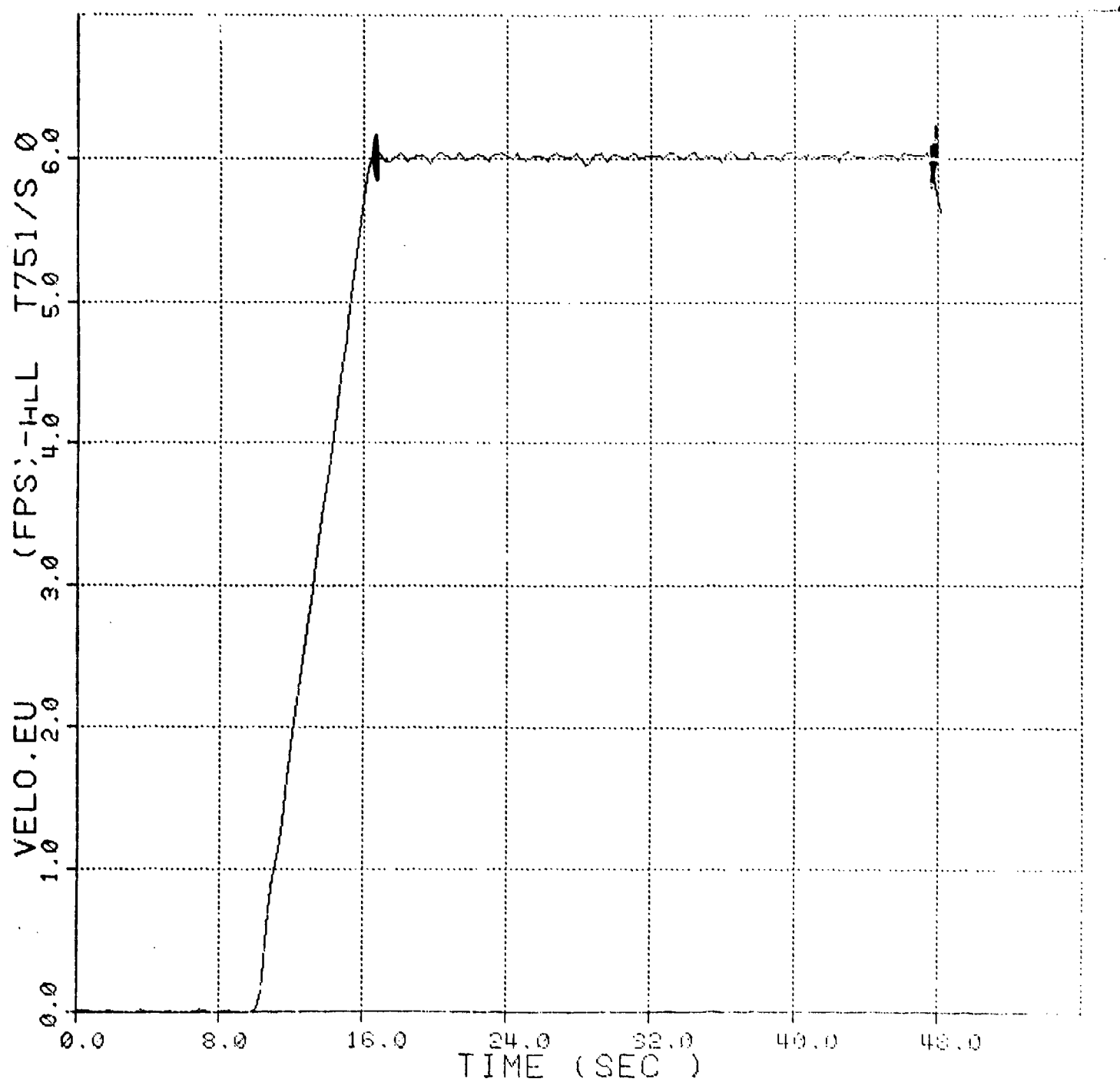


Figure No. 67. Towed Submersible's Velocity vs Time, Case 23



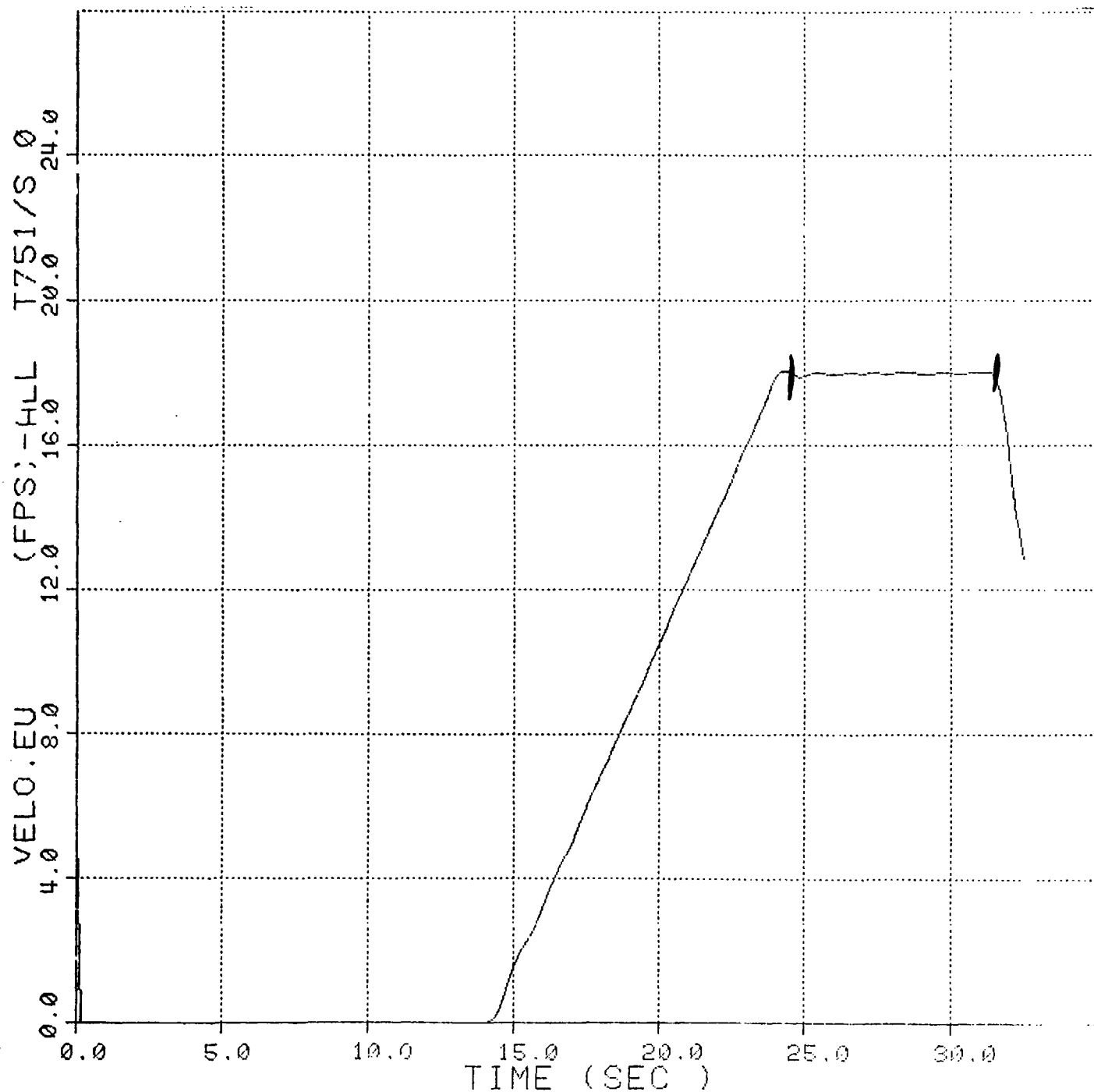


Figure No. 68. Towed Submersible's Velocity vs Time, Case 24



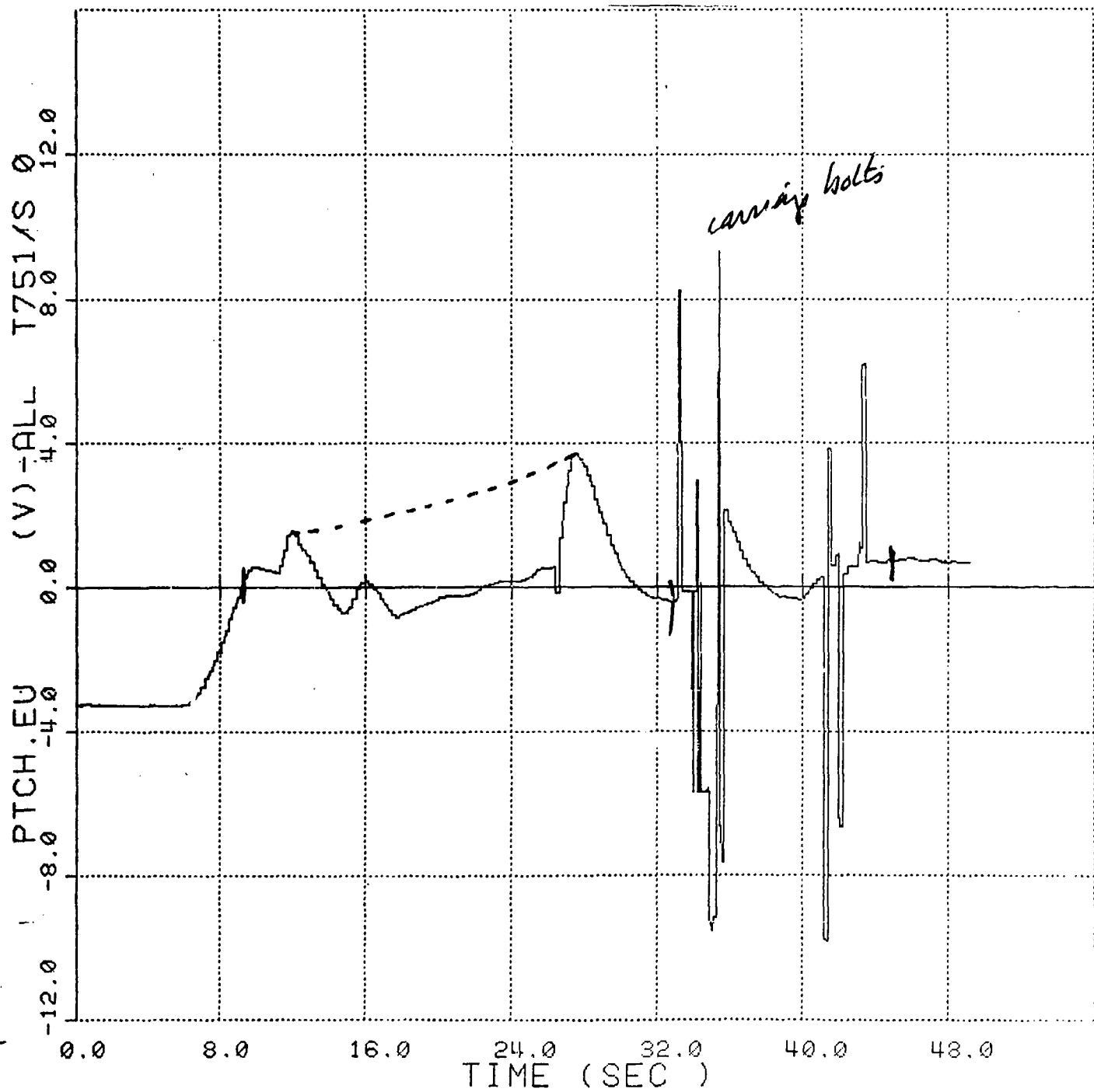


Figure No. 69. Towed Submersible's Pitch vs Time, Case 2



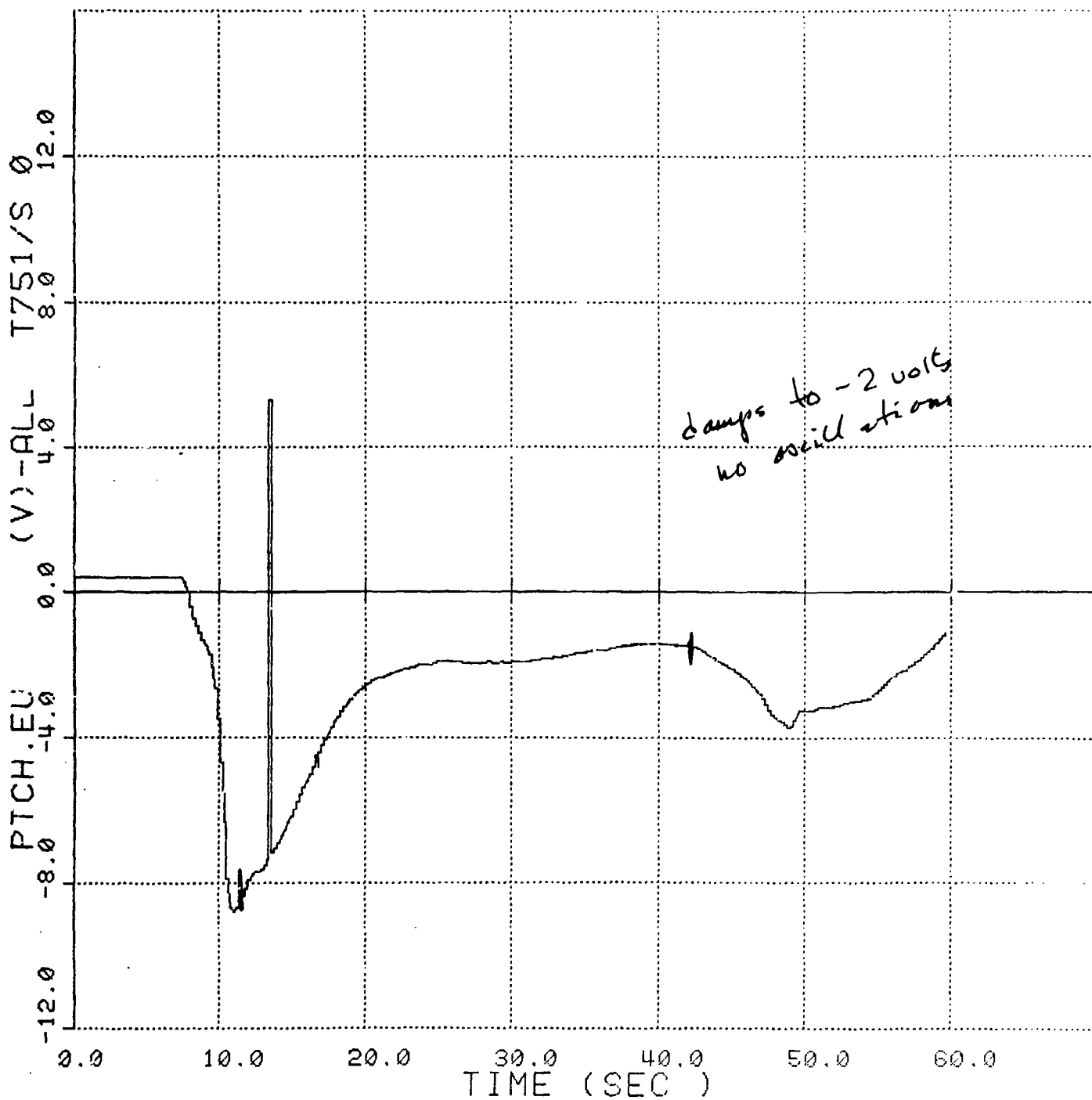


Figure No. 70. Towed Submersible's Pitch vs Time, Case 3



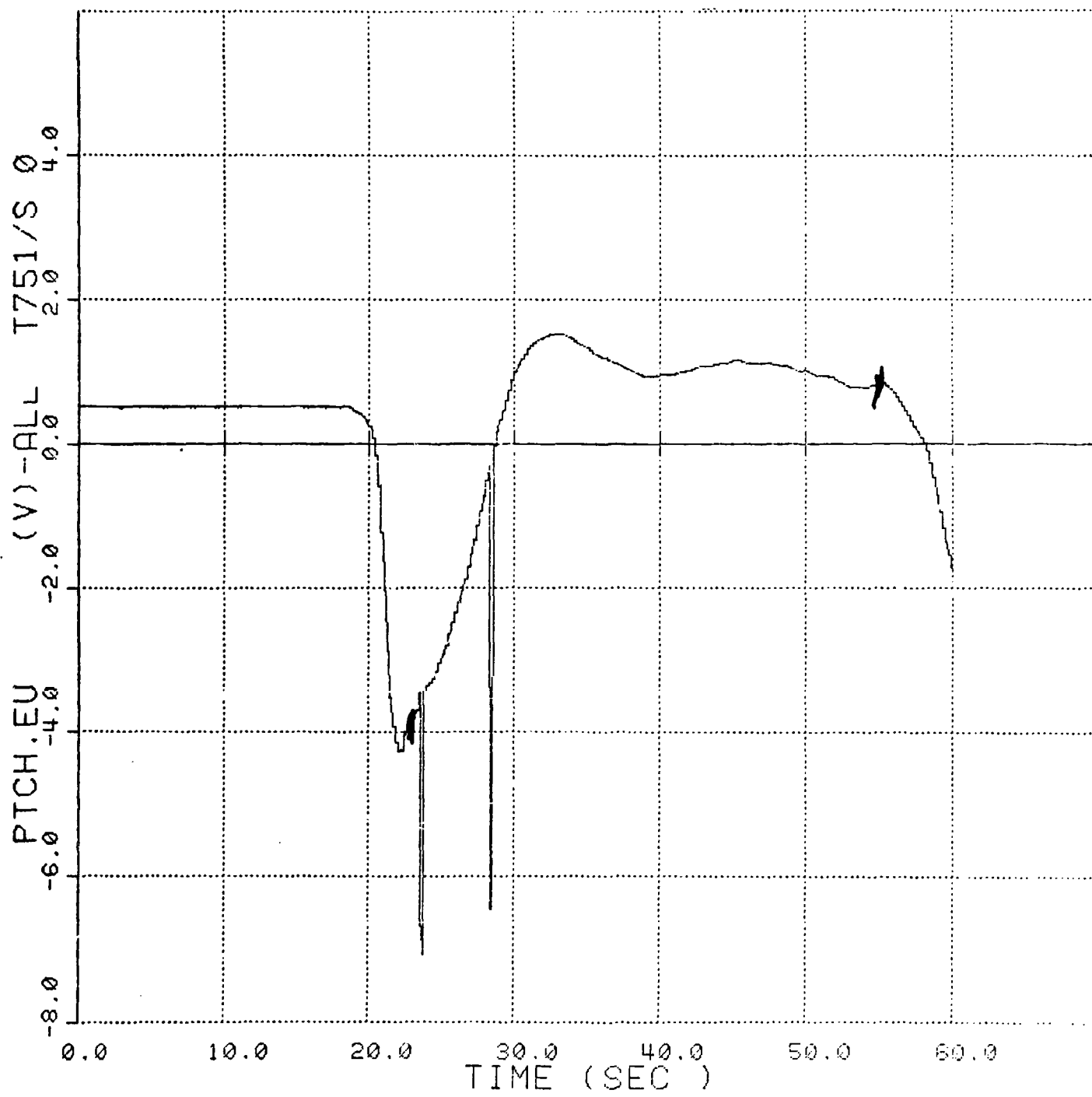


Figure No. 71. Towed Submersible's Pitch vs Time, Case 4



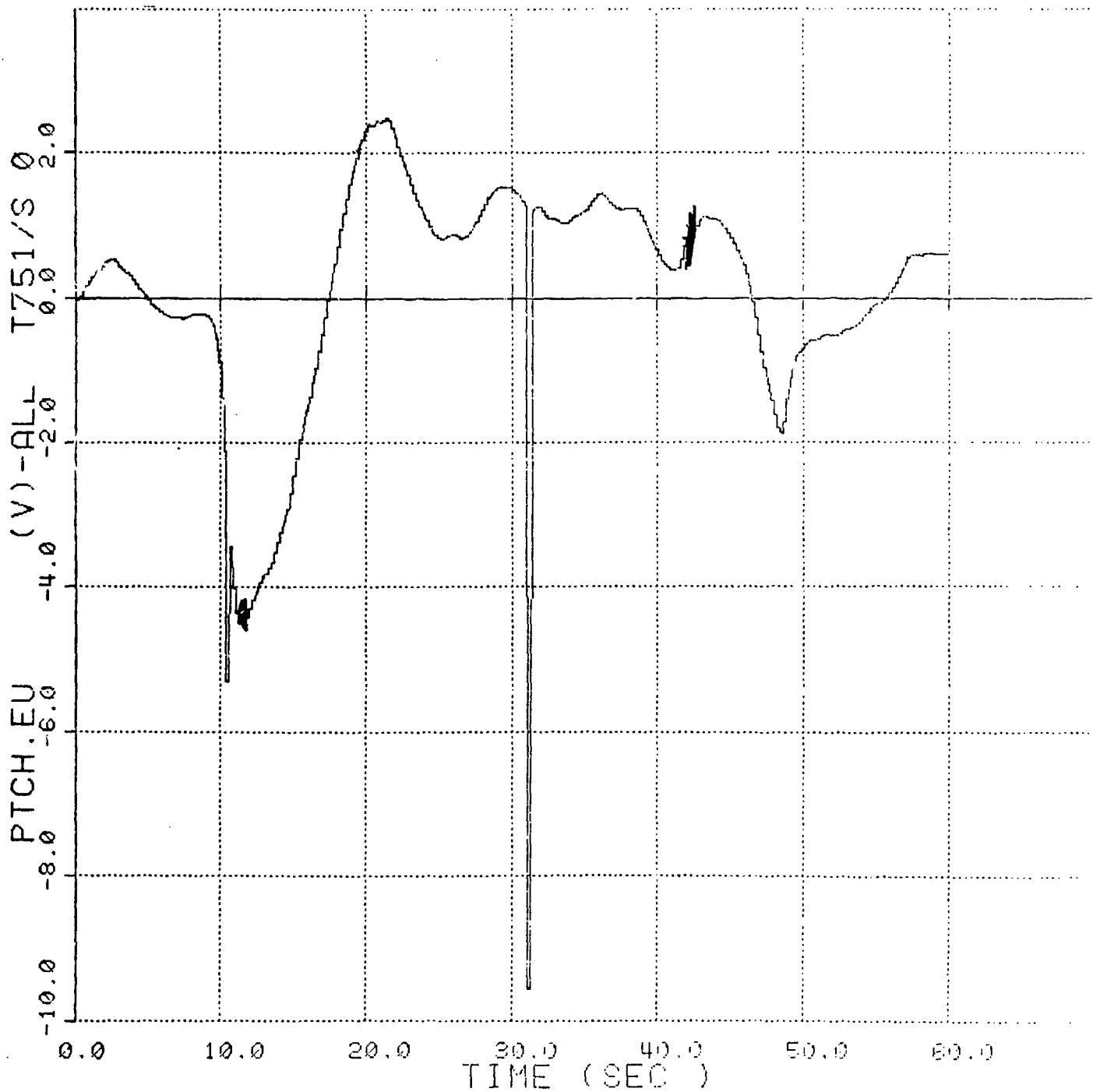


Figure No. 72. Towed Submersible's Pitch vs Time, Case 5



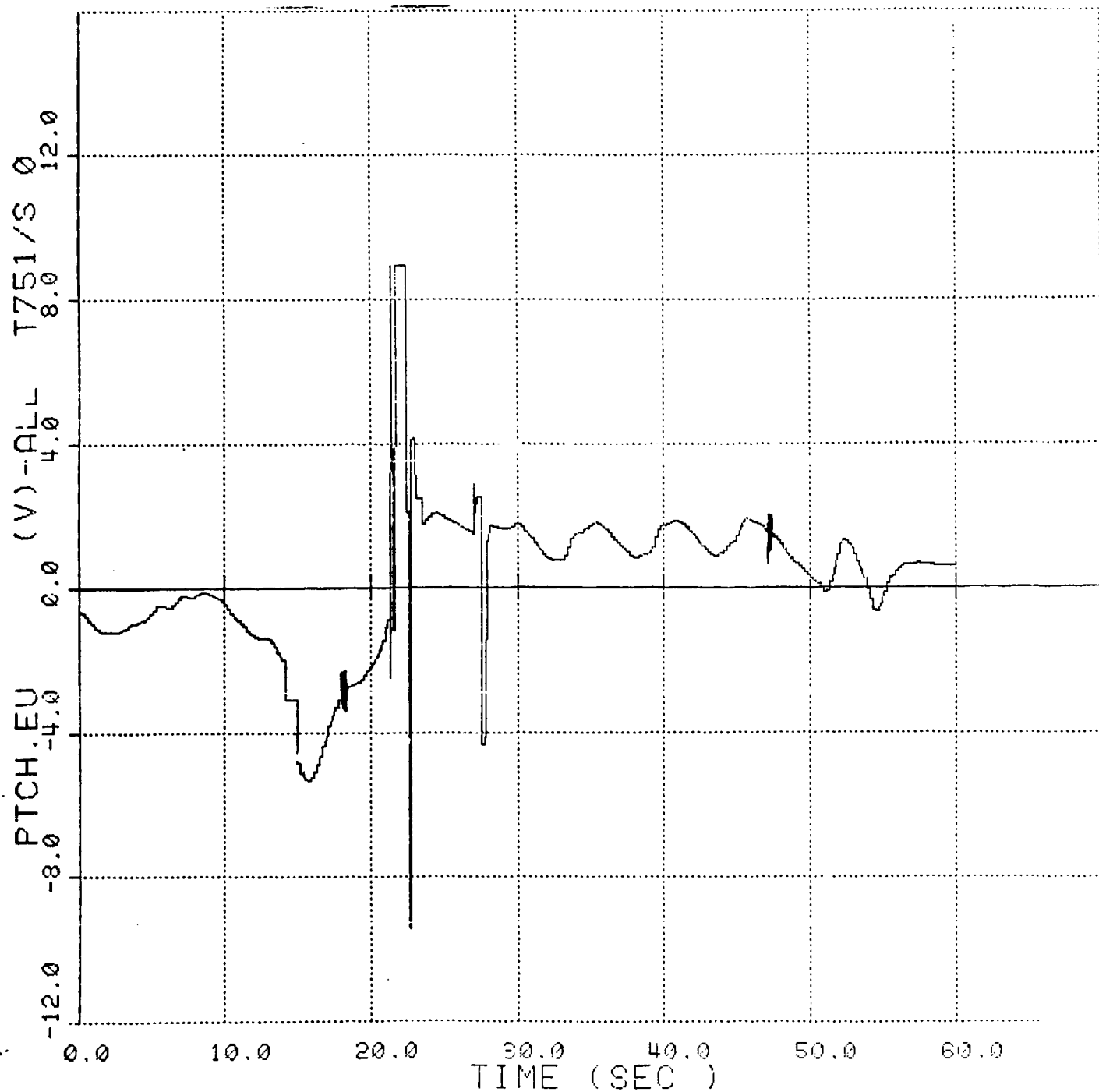


Figure No. 73. Towed Submersible's Pitch vs Time, Case 6



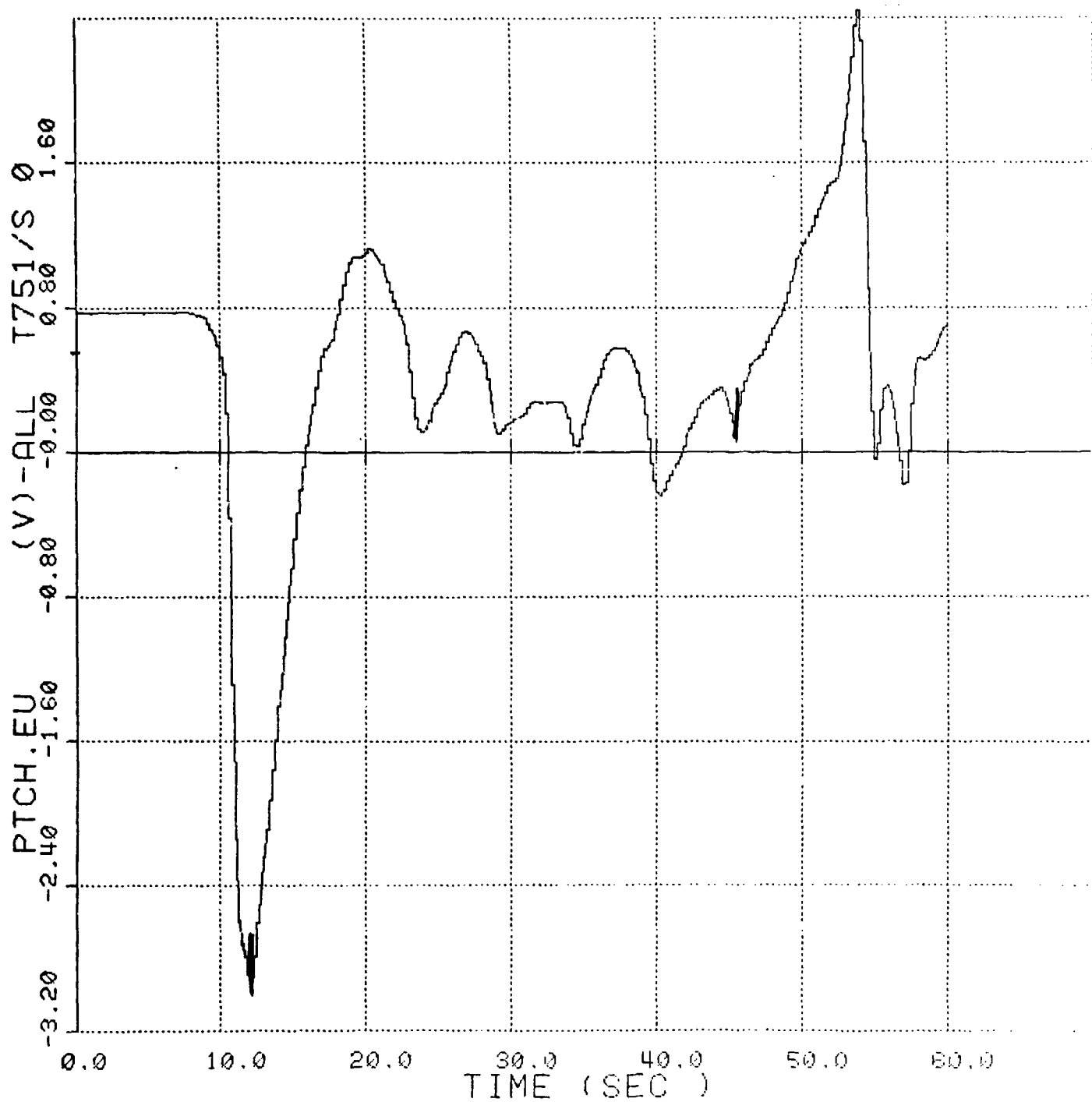


Figure No. 74. Towed Submersible's Pitch vs Time, Case 7



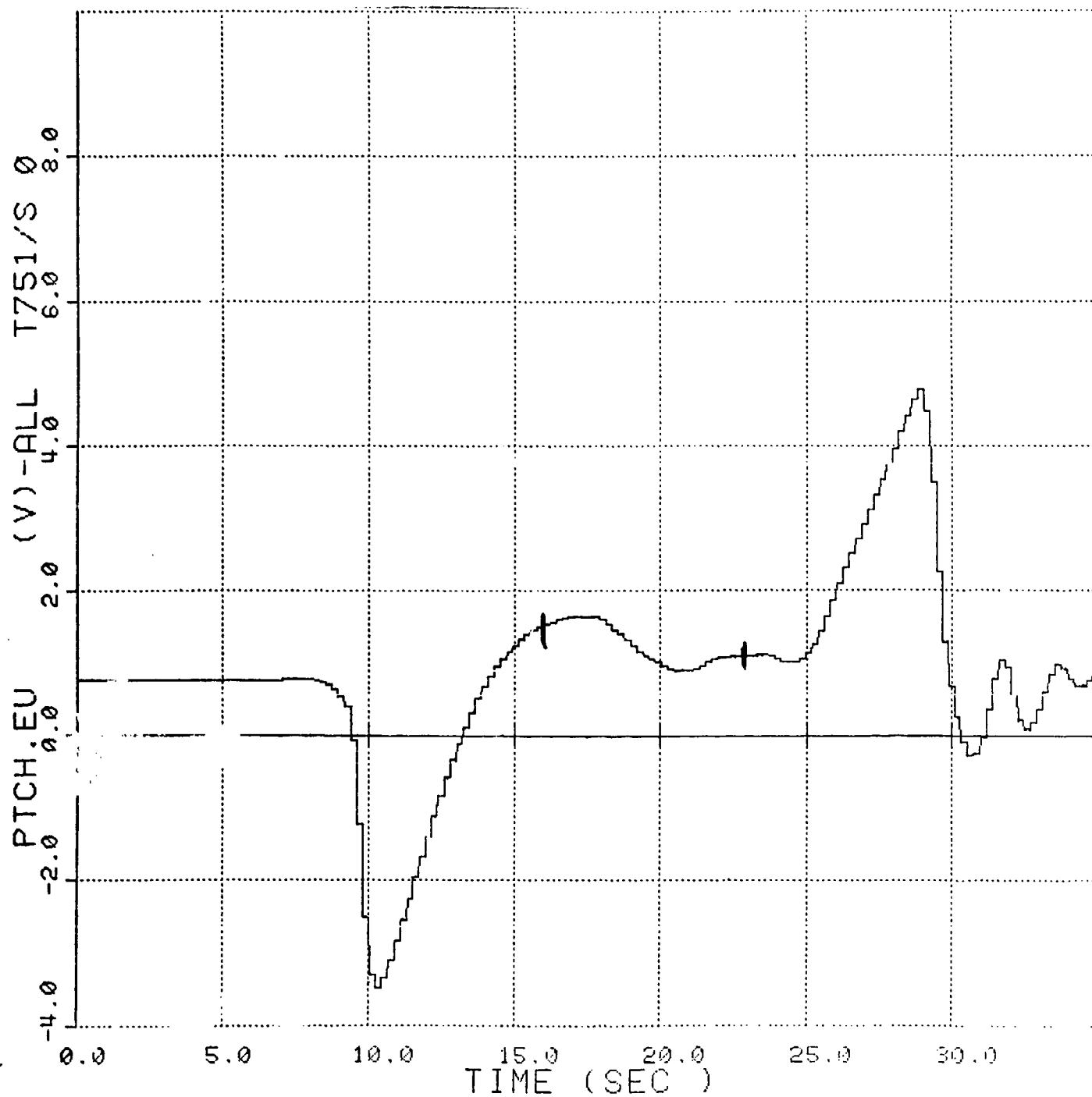


Figure No. 75. Towed Submersible's Pitch vs Time, Case 8



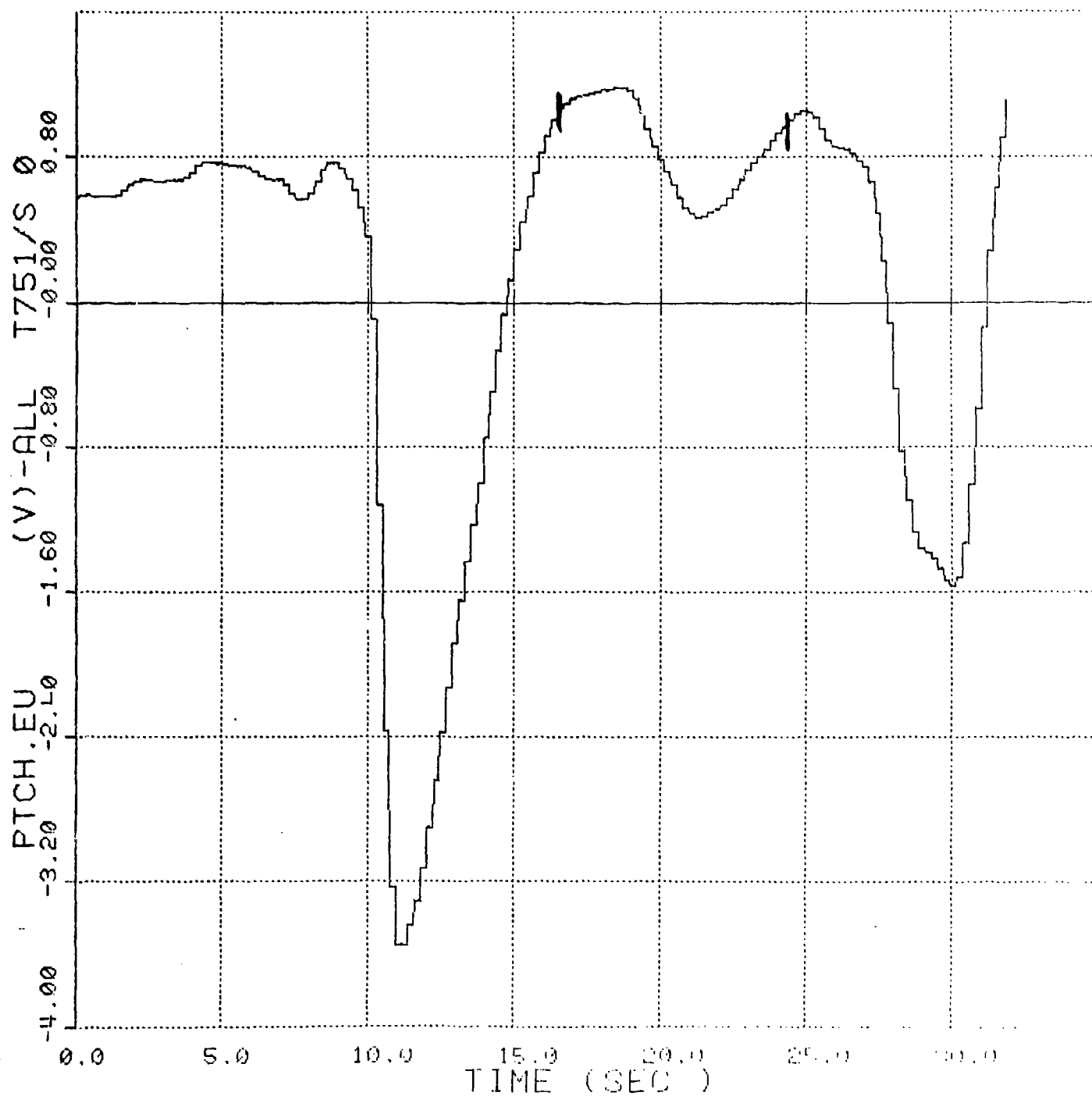


Figure No. 76. Towed Submersible's Pitch vs Time, Case 9



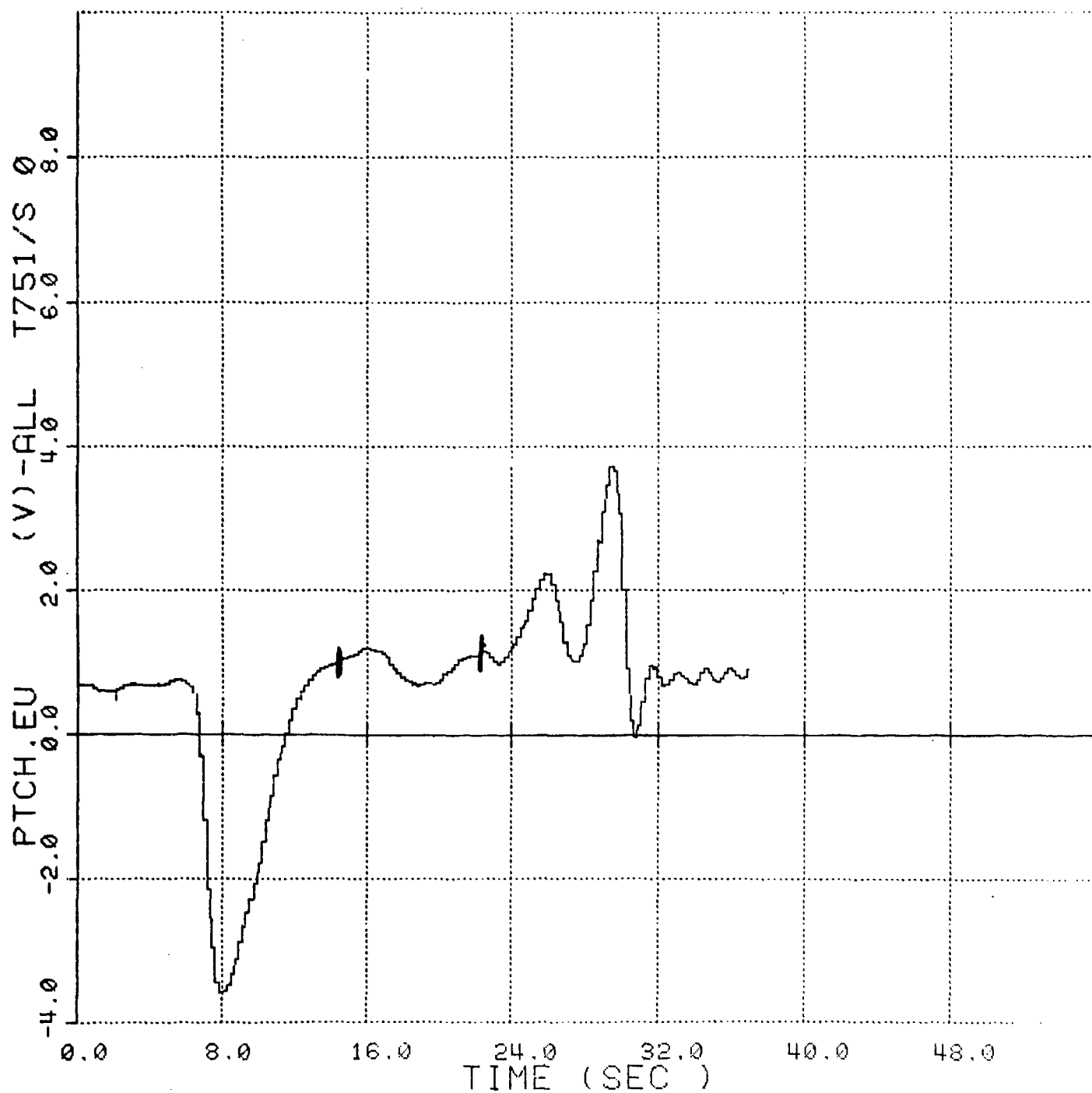


Figure No. 77. Towed Submersible's Pitch vs Time, Case 10



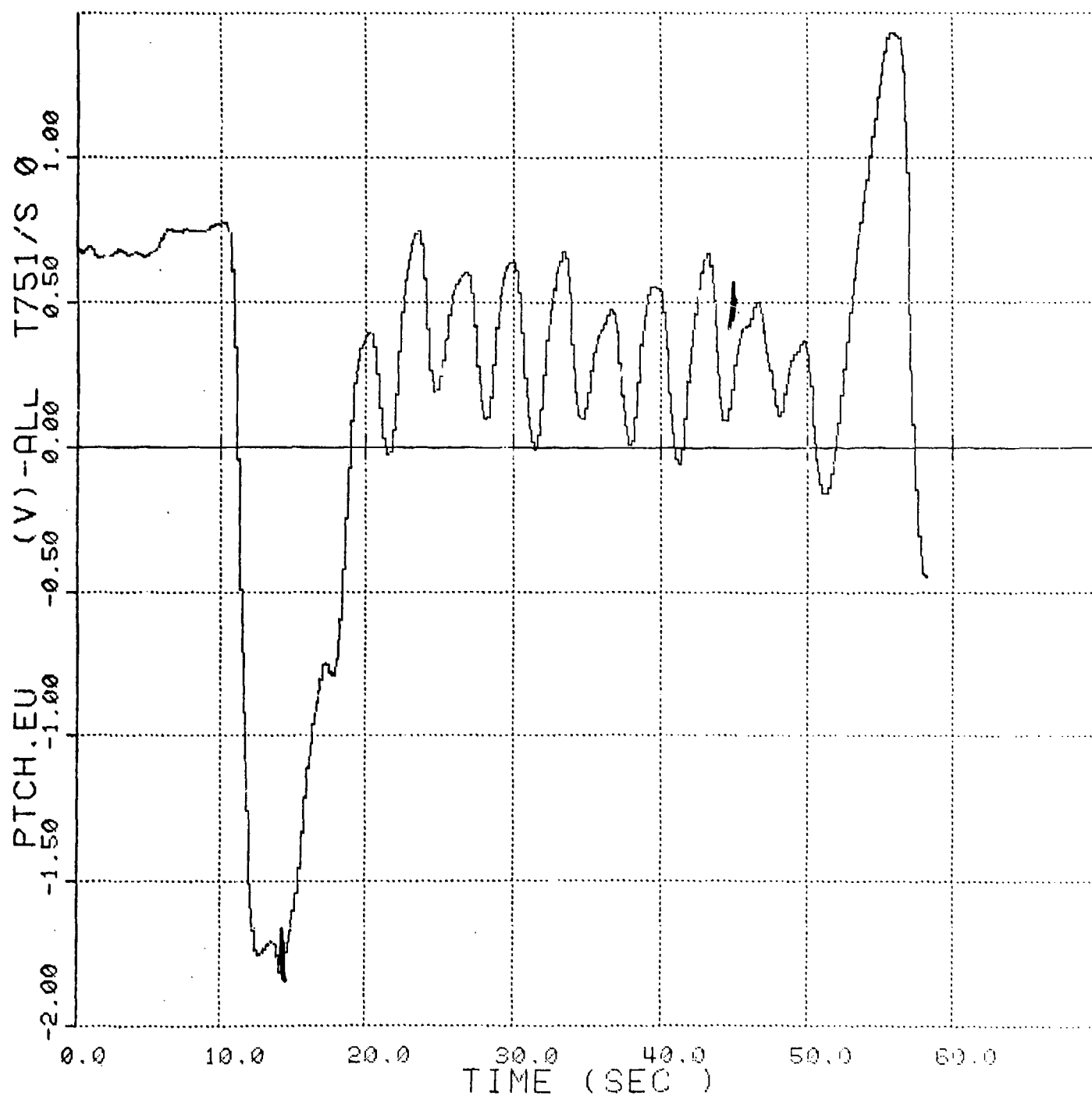


Figure No. 78. Towed Submersible's Pitch vs Time, Case 11



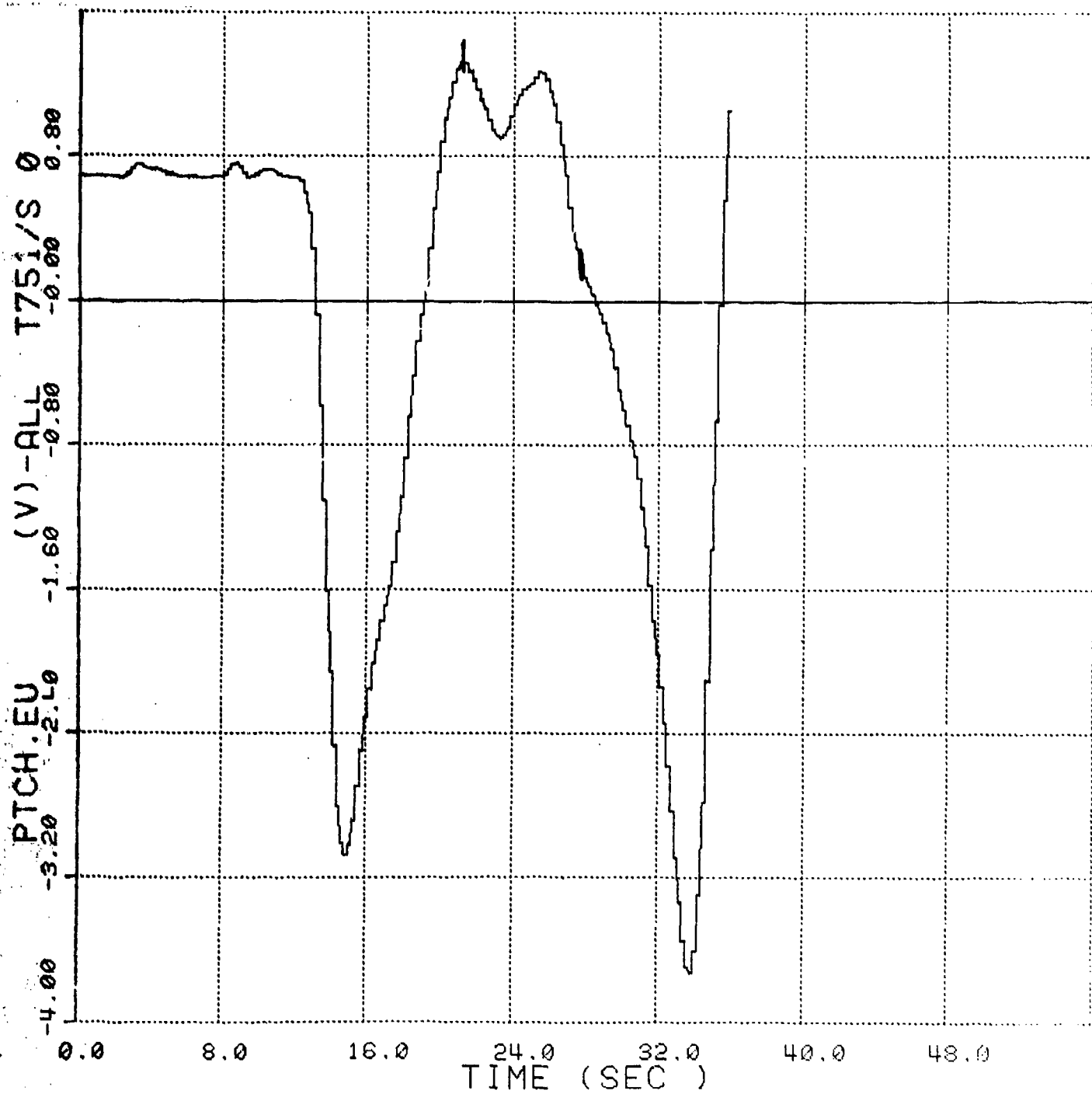


Figure No. 79. Towed Submersible's Pitch vs Time, Case 12



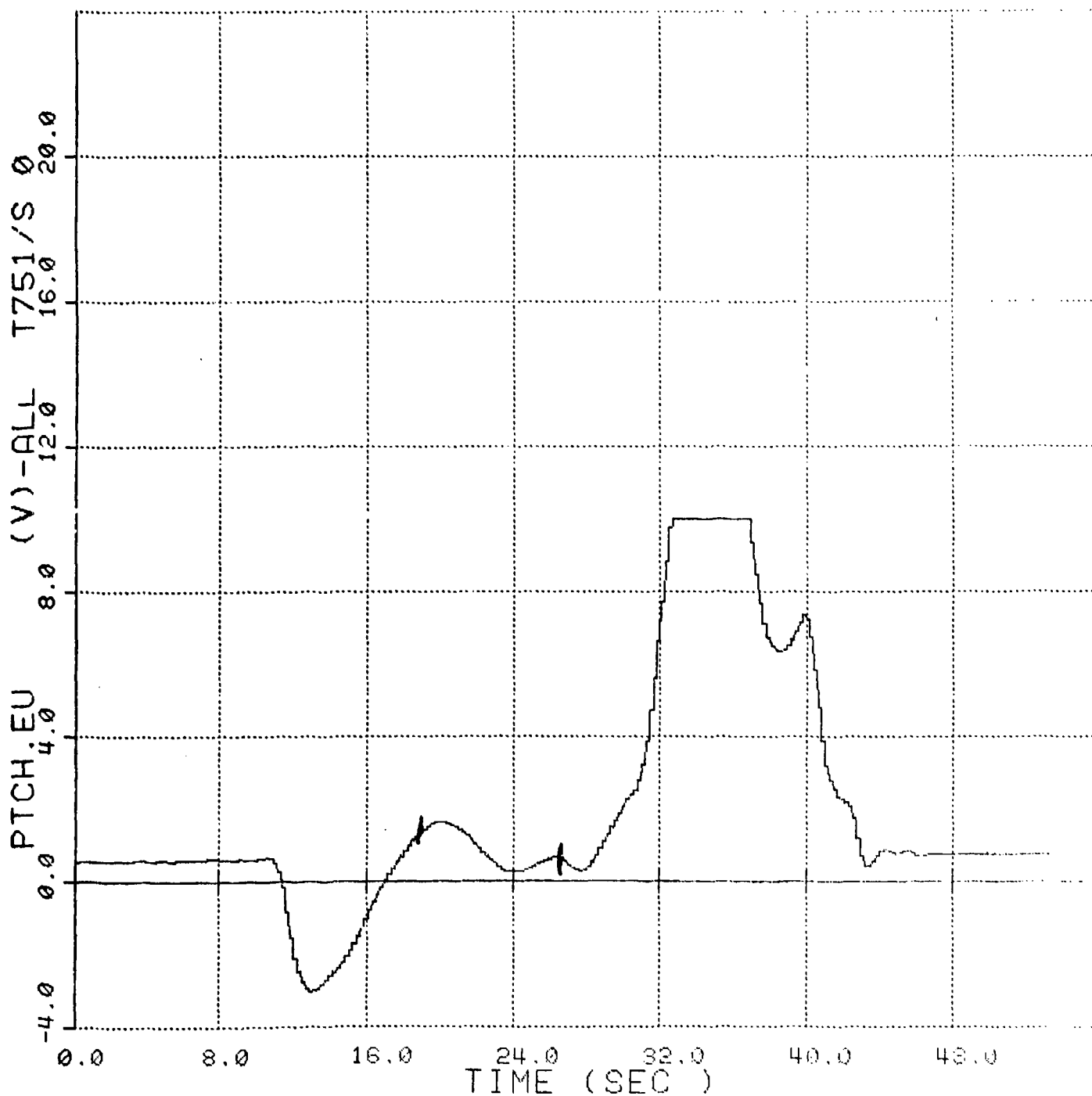


Figure No. 80. Towed Submersible's Pitch vs Time, Case 13



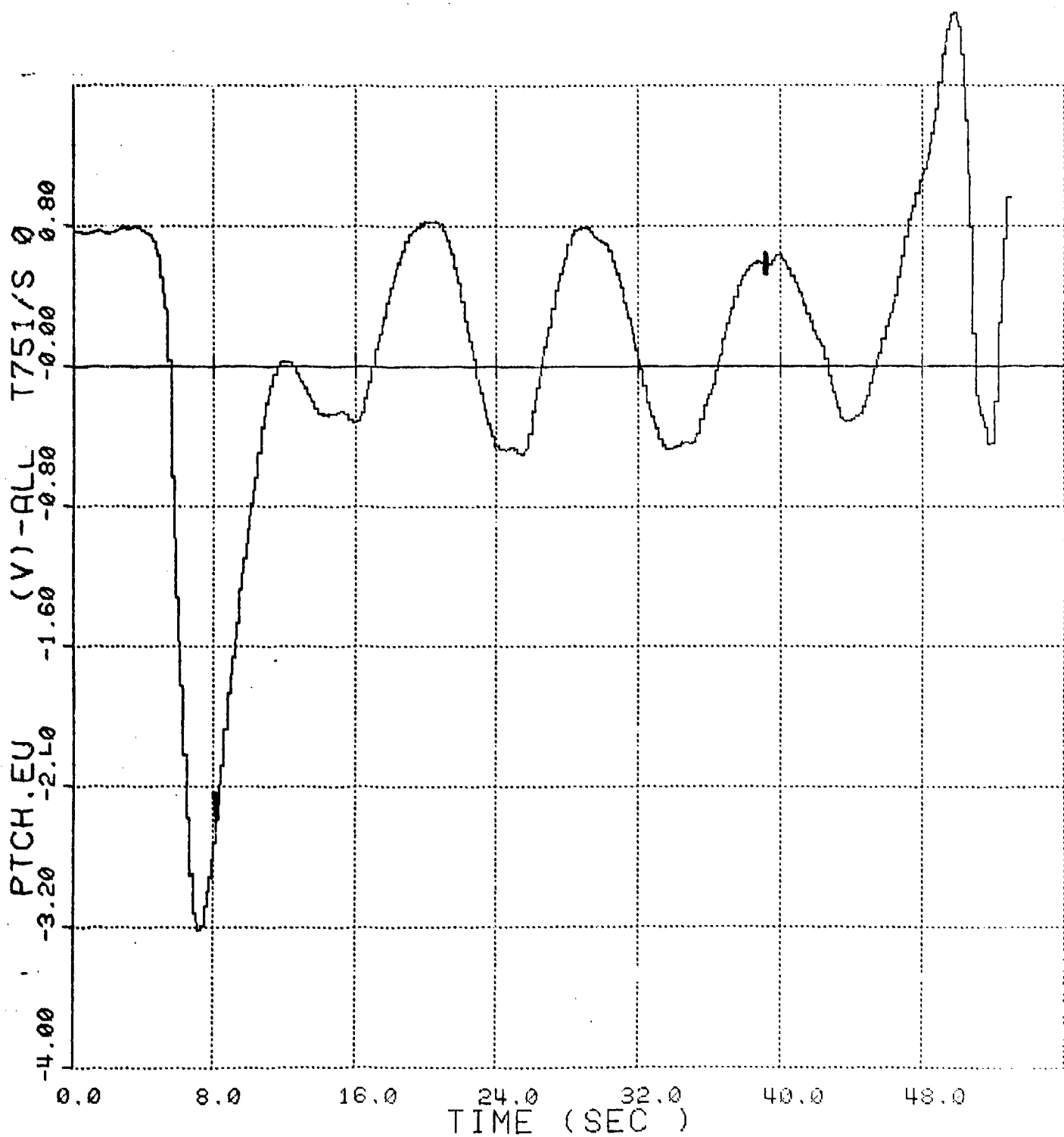


Figure No. 81. Towed Submersible's Pitch vs Time, Case 14



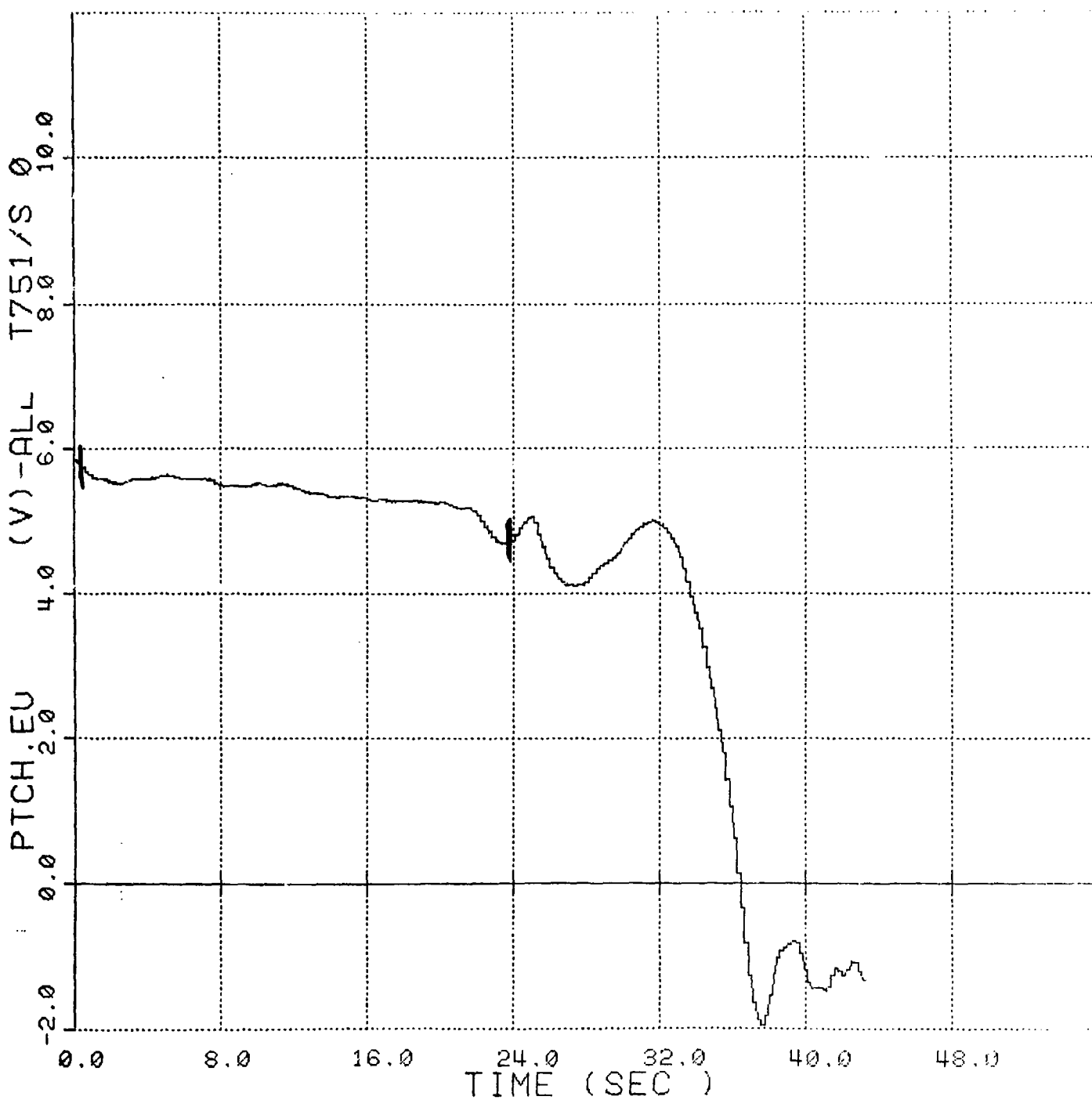


Figure No. 82. Towed Submersible's Pitch vs Time, Case 15



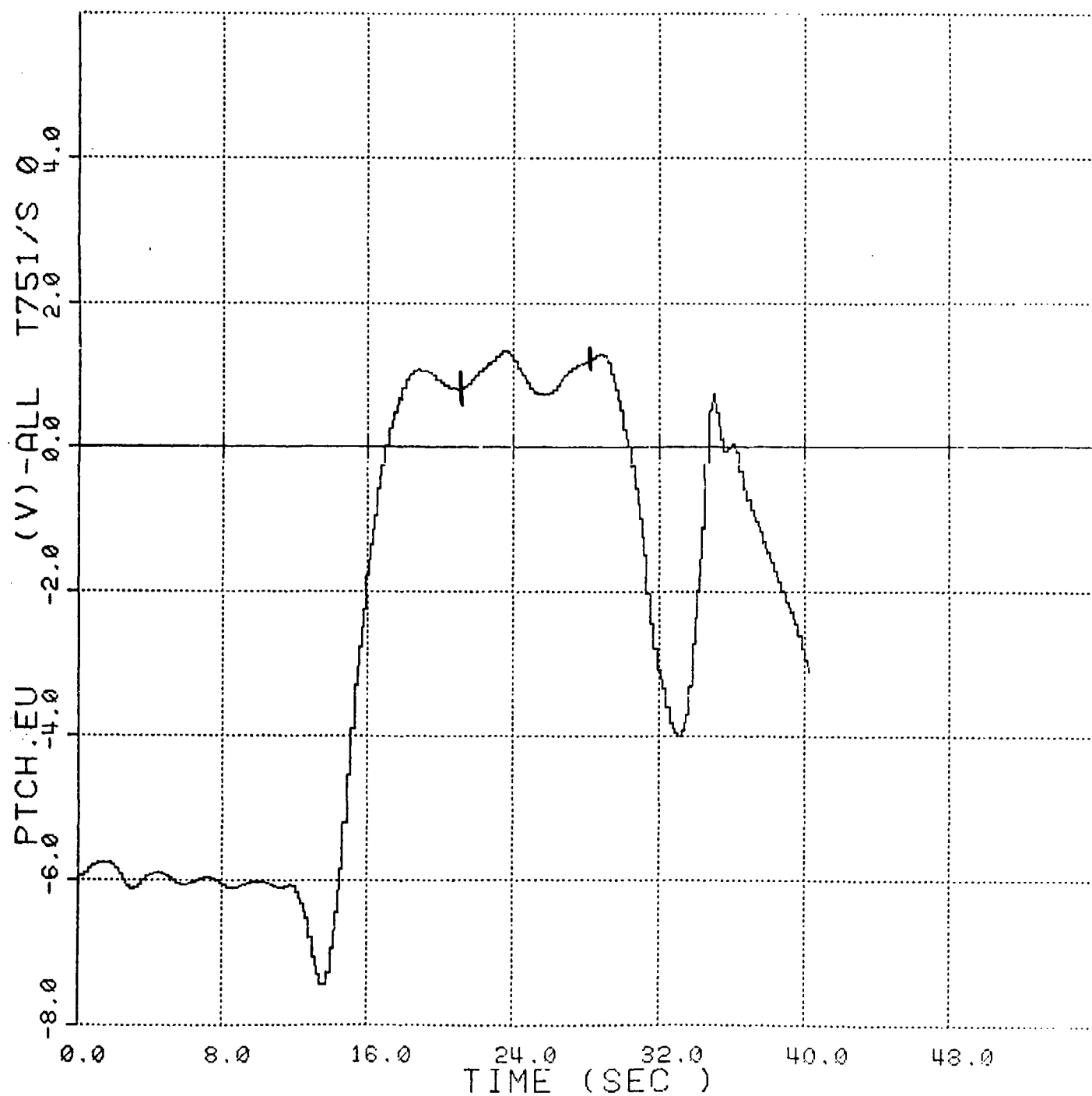


Figure No. 83. Towed Submersible's Pitch vs Time, Case 16



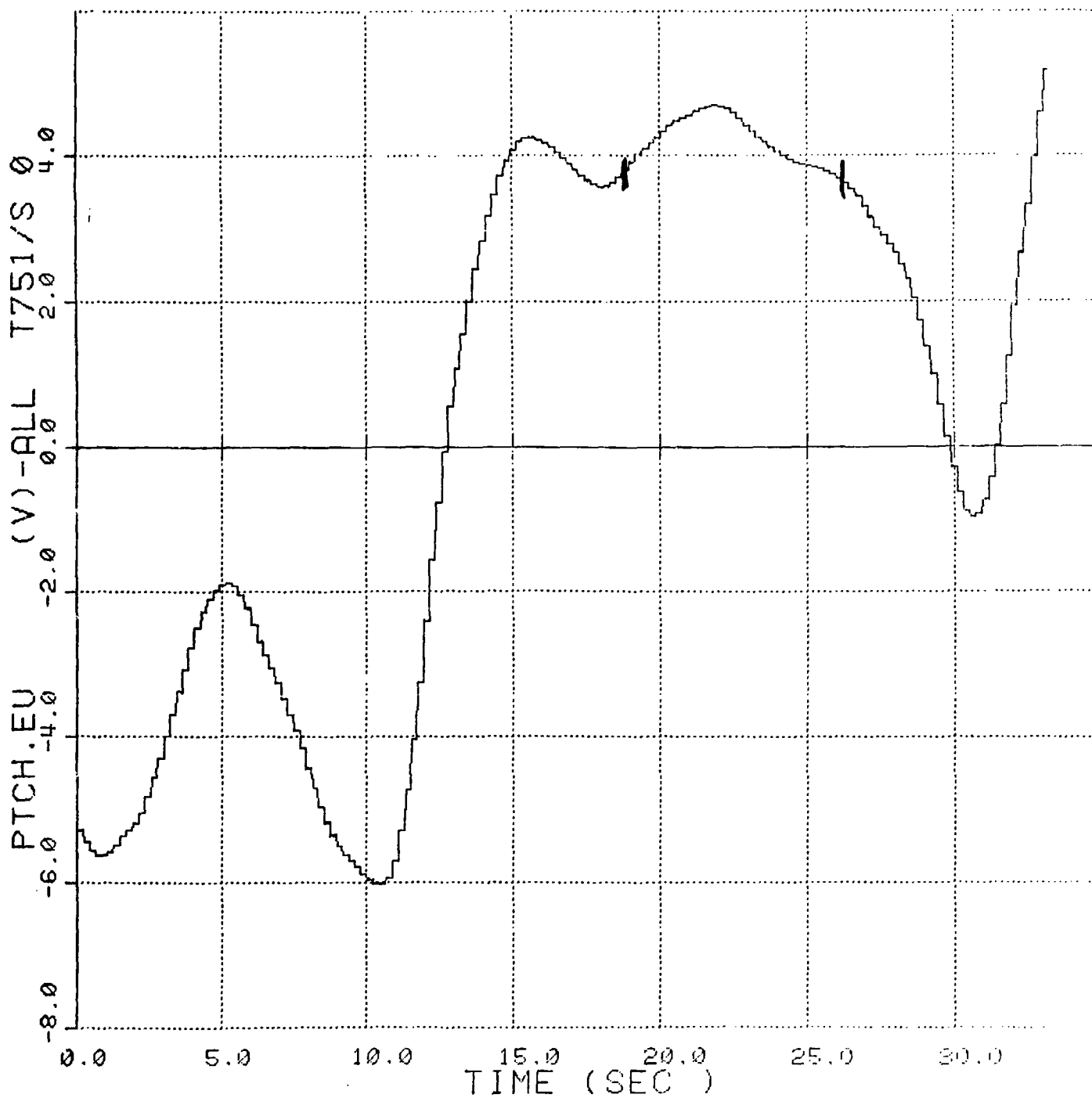


Figure No. 84. Towed Submersible's Pitch vs Time, Case 17



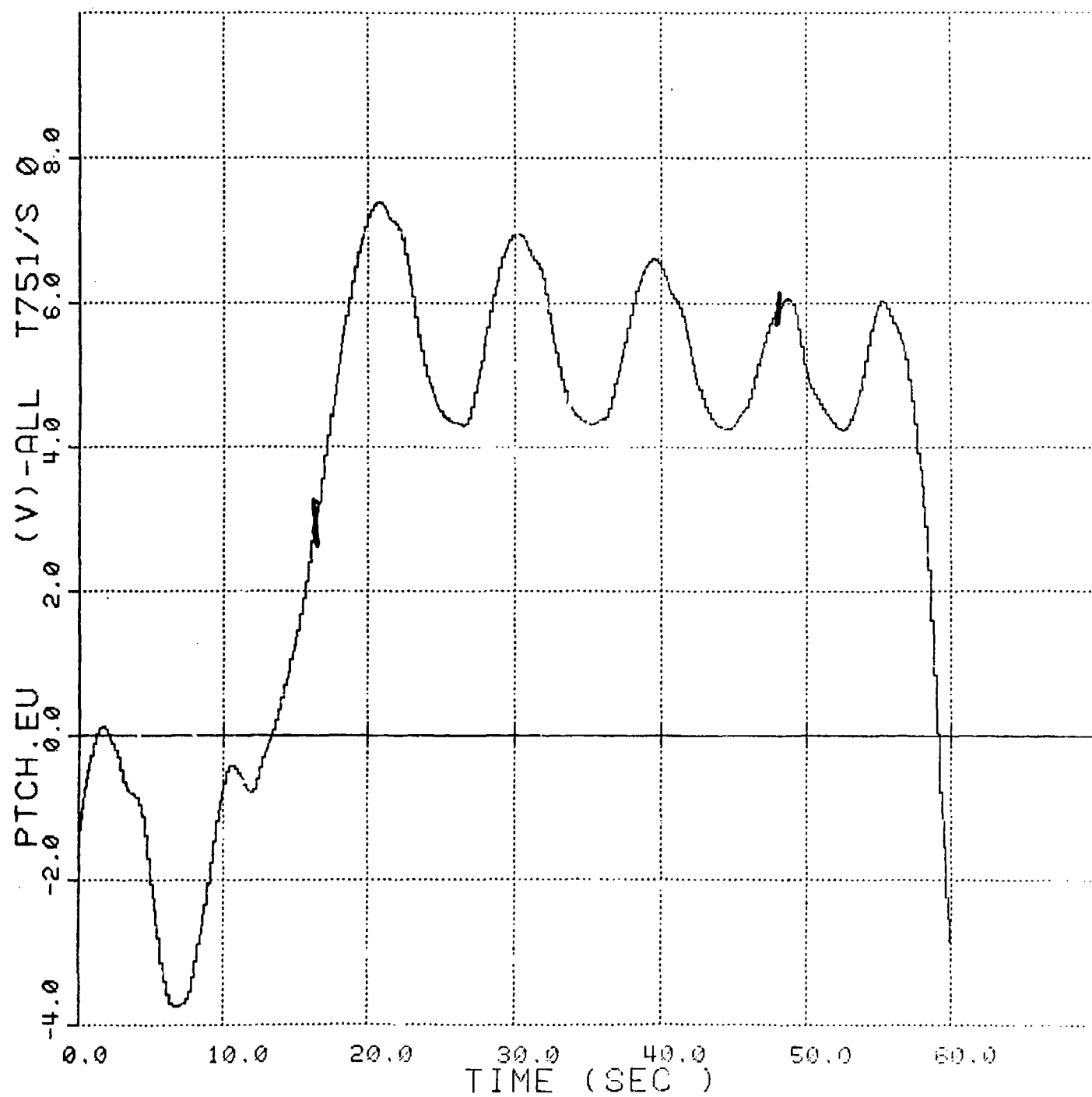


Figure No. 85. Towed Submersible's Pitch vs Time, Case 18



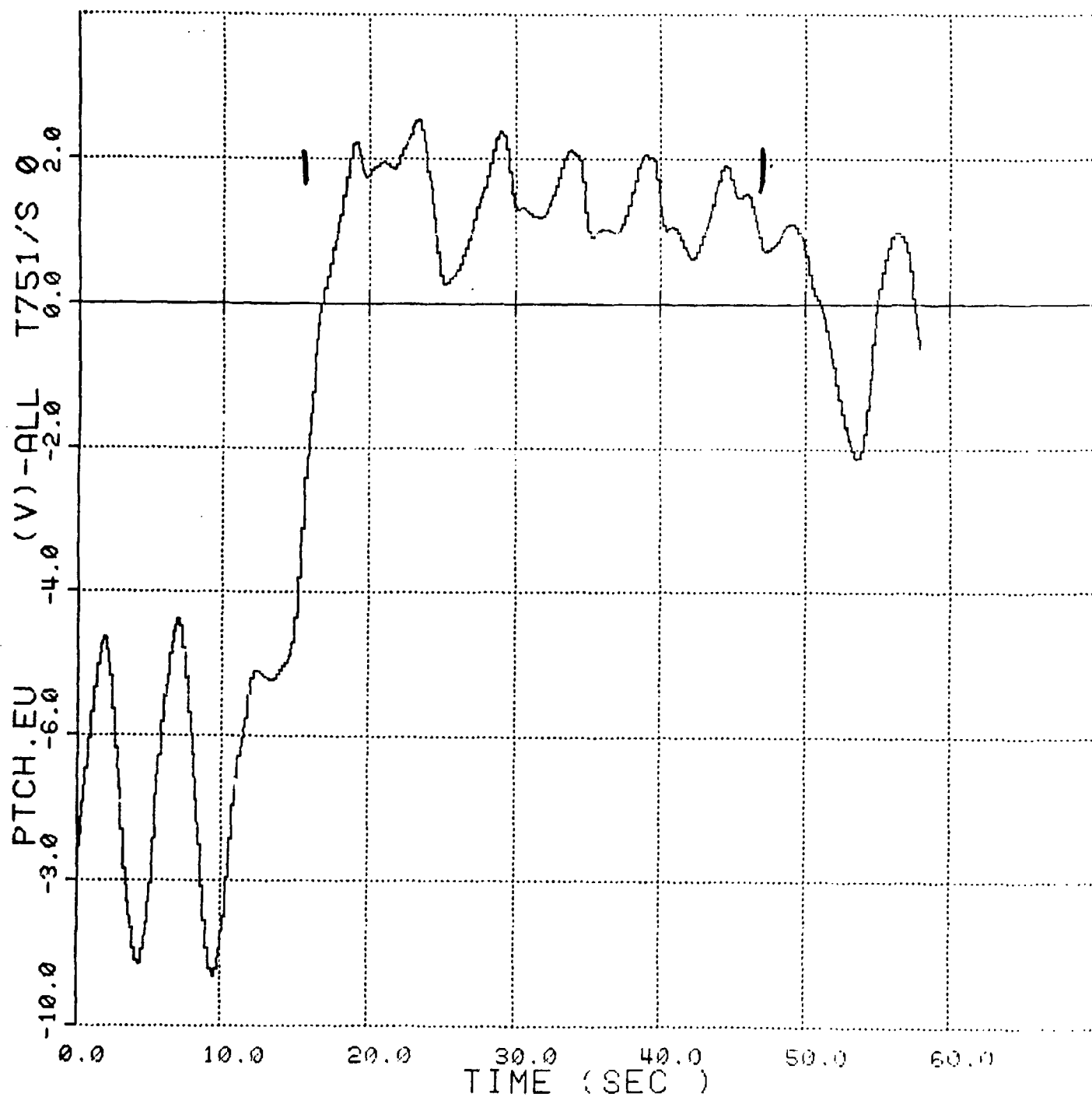


Figure No. 86. Towed Submersible's Pitch vs Time, Case 19



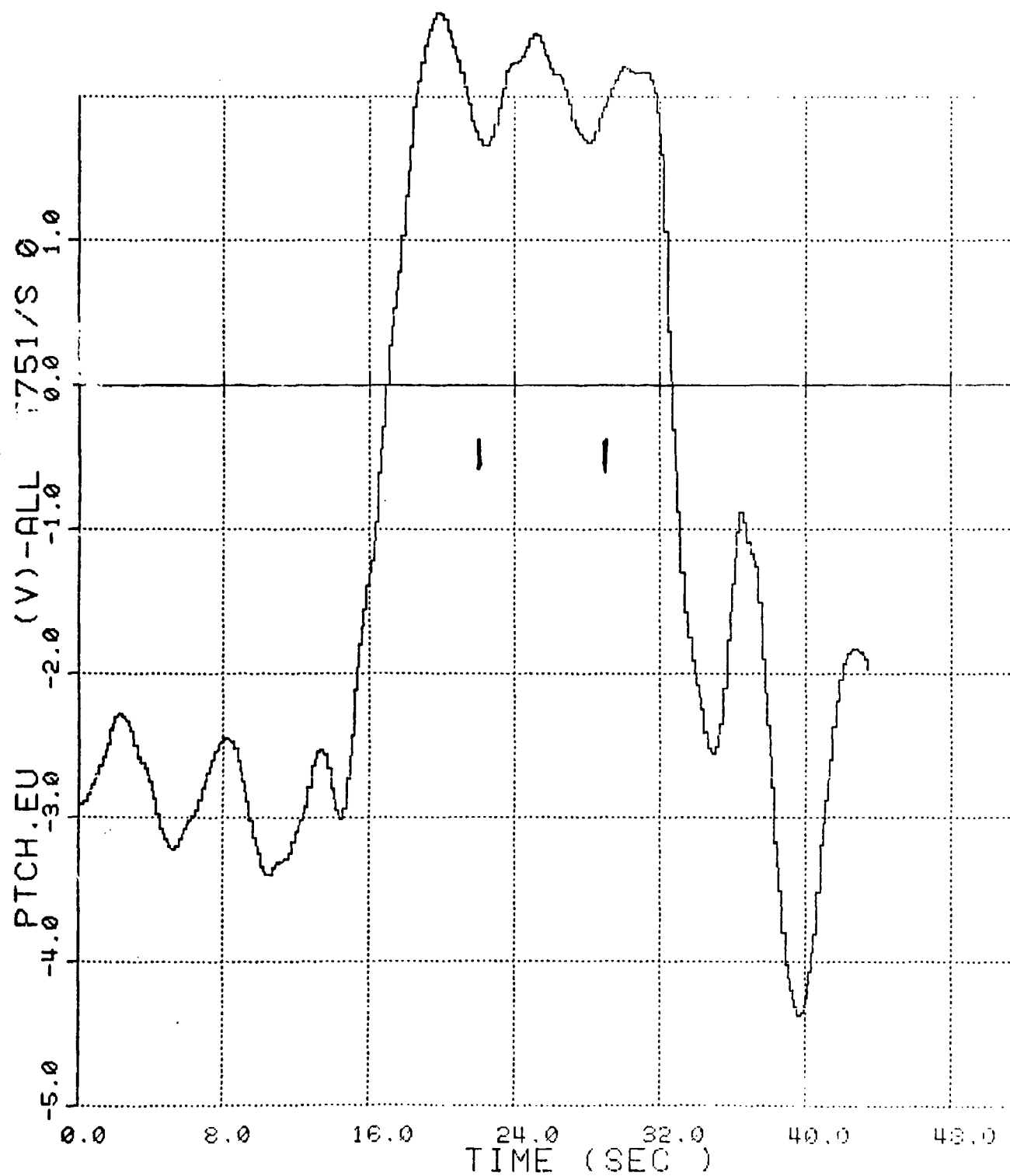


Figure No. 87. Towed Submersible's Pitch vs Time, Case 20



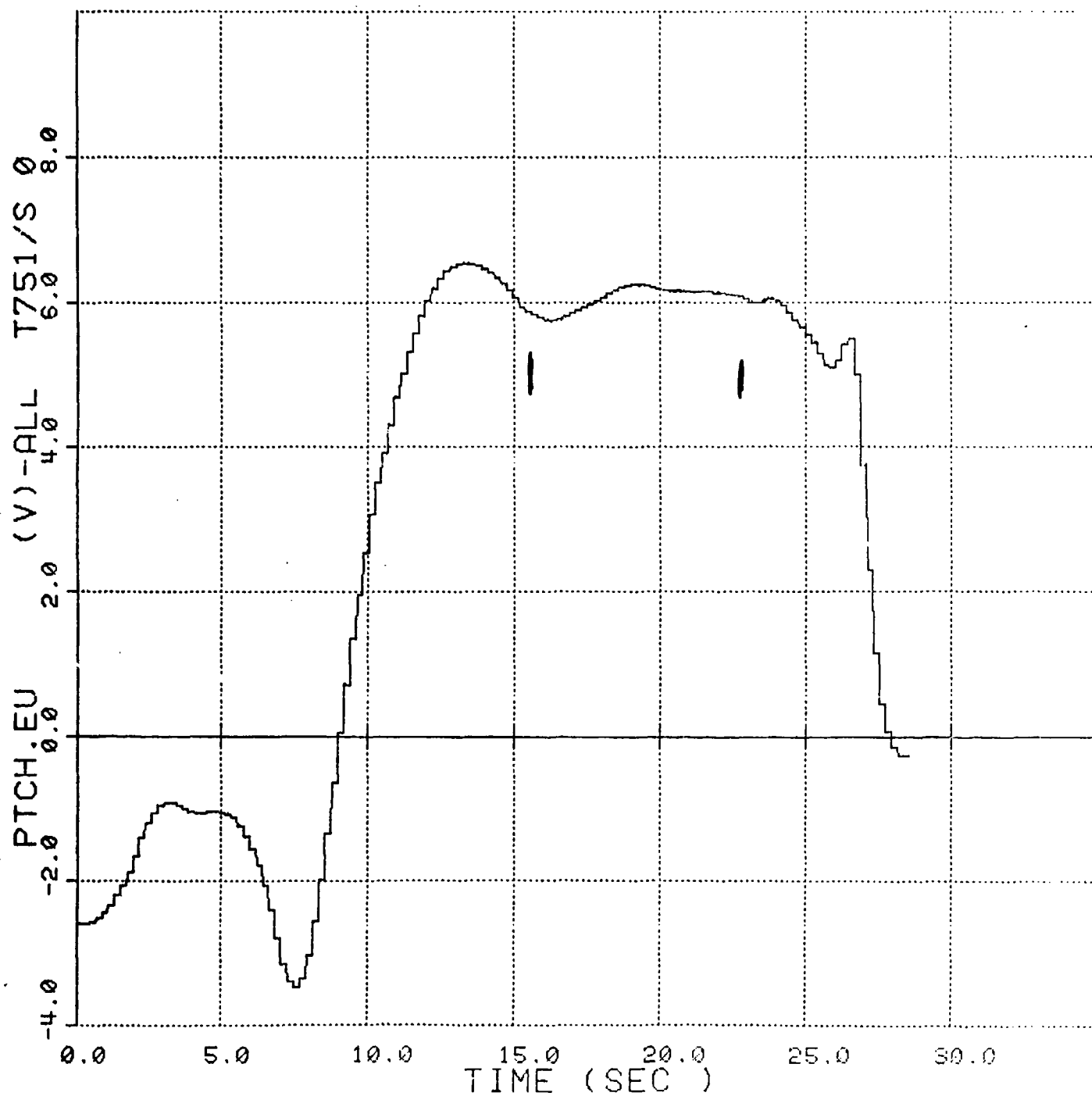


Figure No. 88. Towed Submersible's Pitch vs Time, Case 21



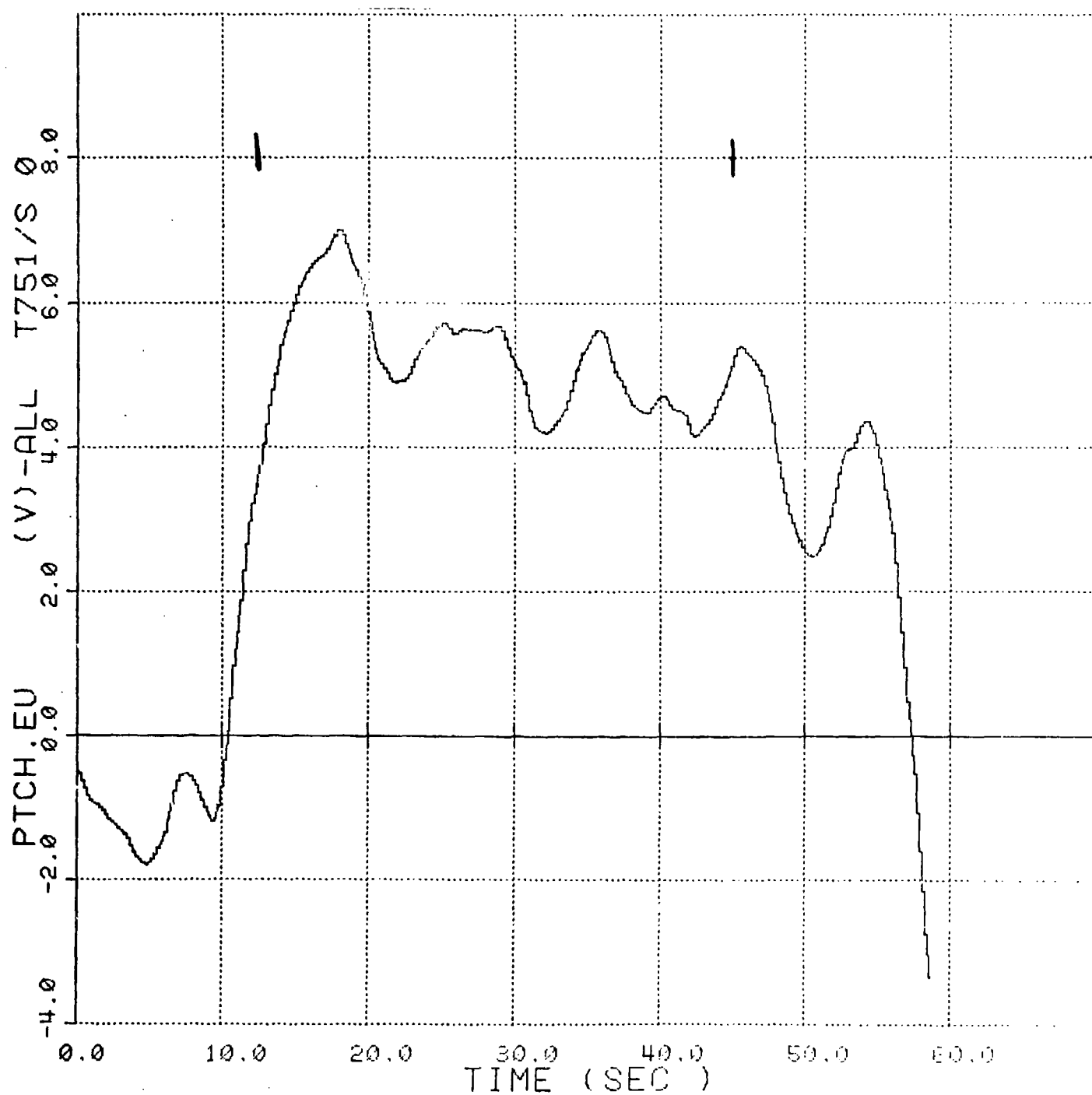


Figure No. 89. Towed Submersible's Pitch vs Time, Case 22



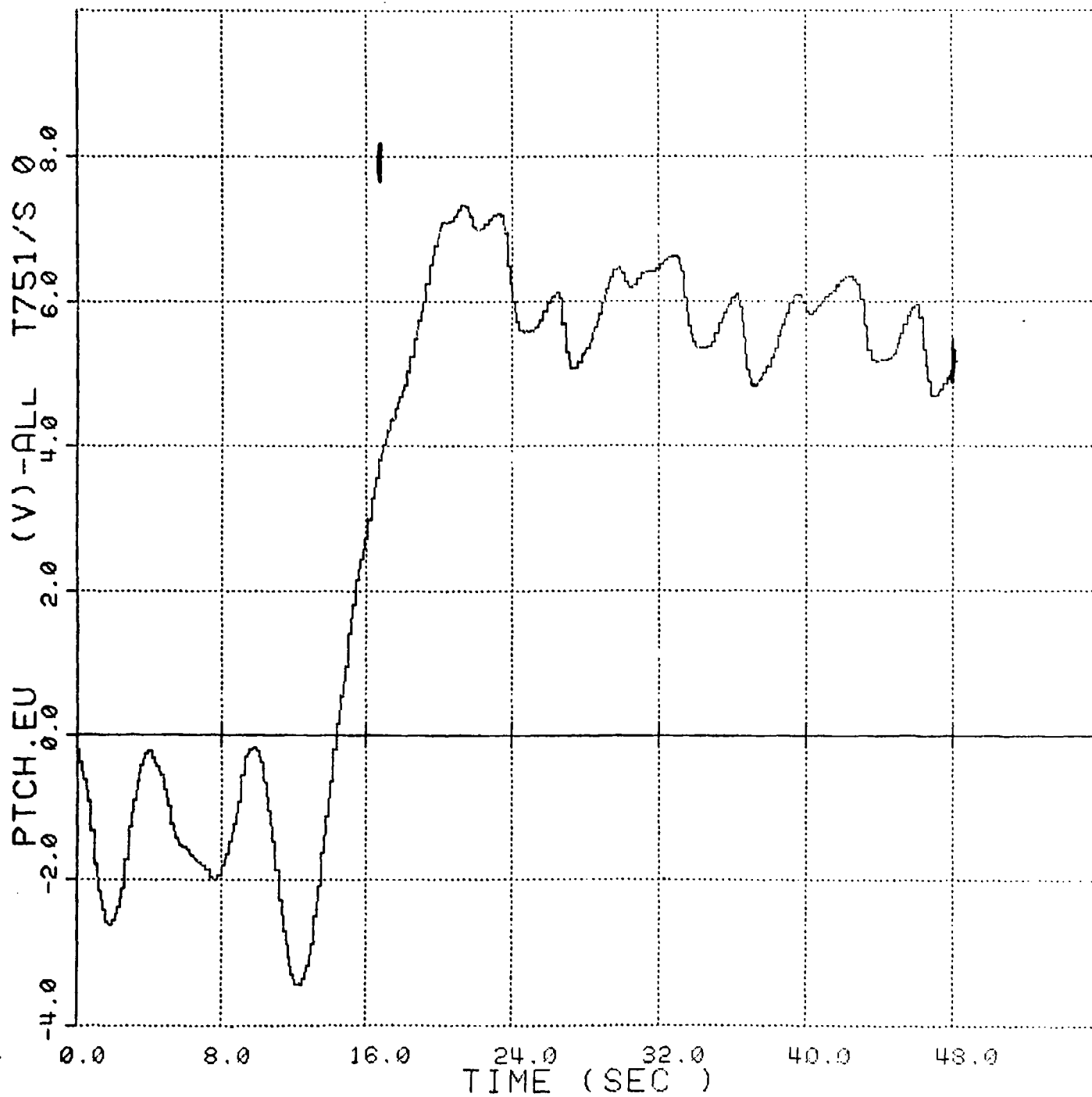


Figure No. 90. Towed Submersible's Pitch vs Time, Case 23



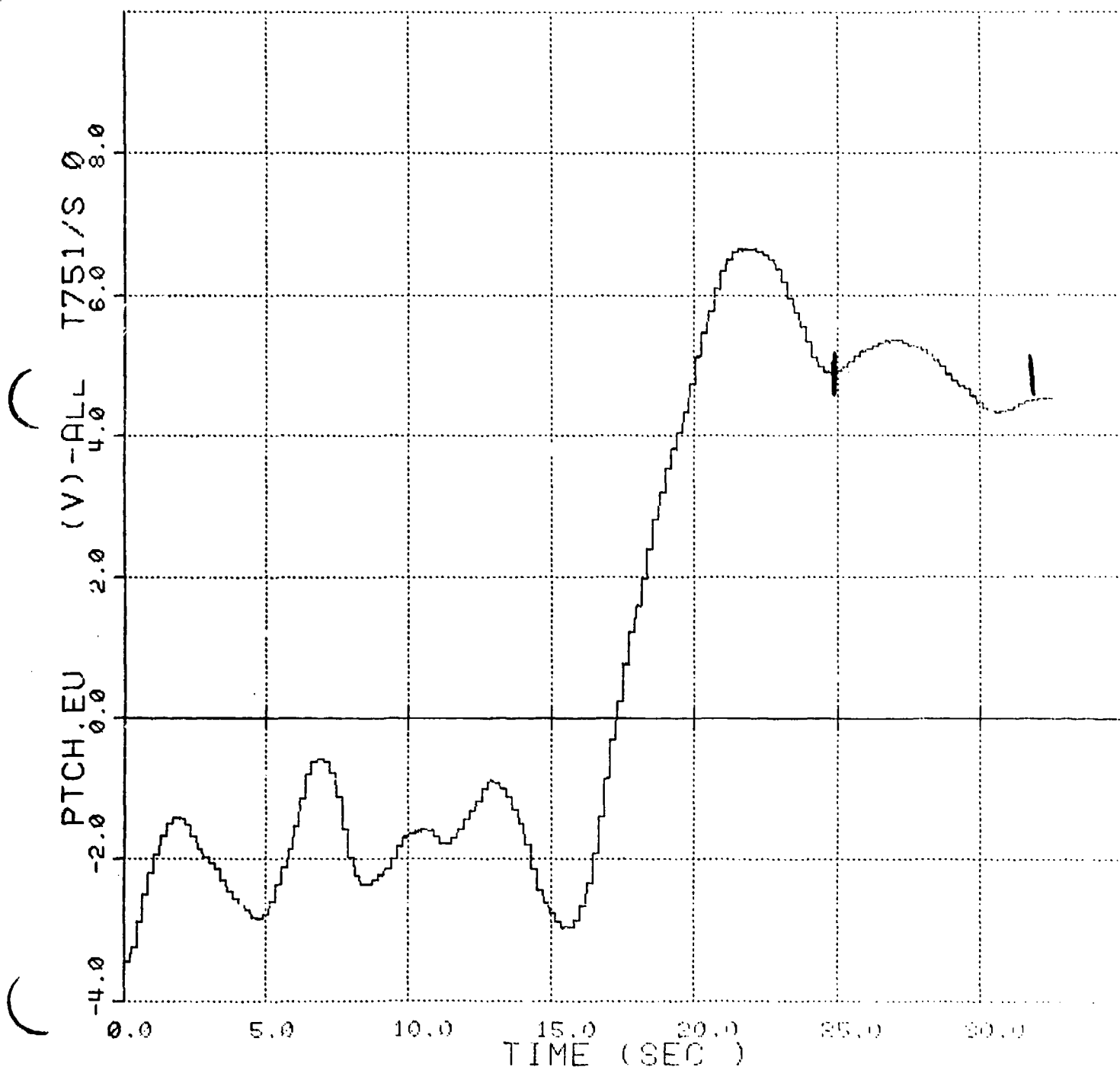


Figure No. 91. Towed Submersible's Pitch vs Time, Case 24







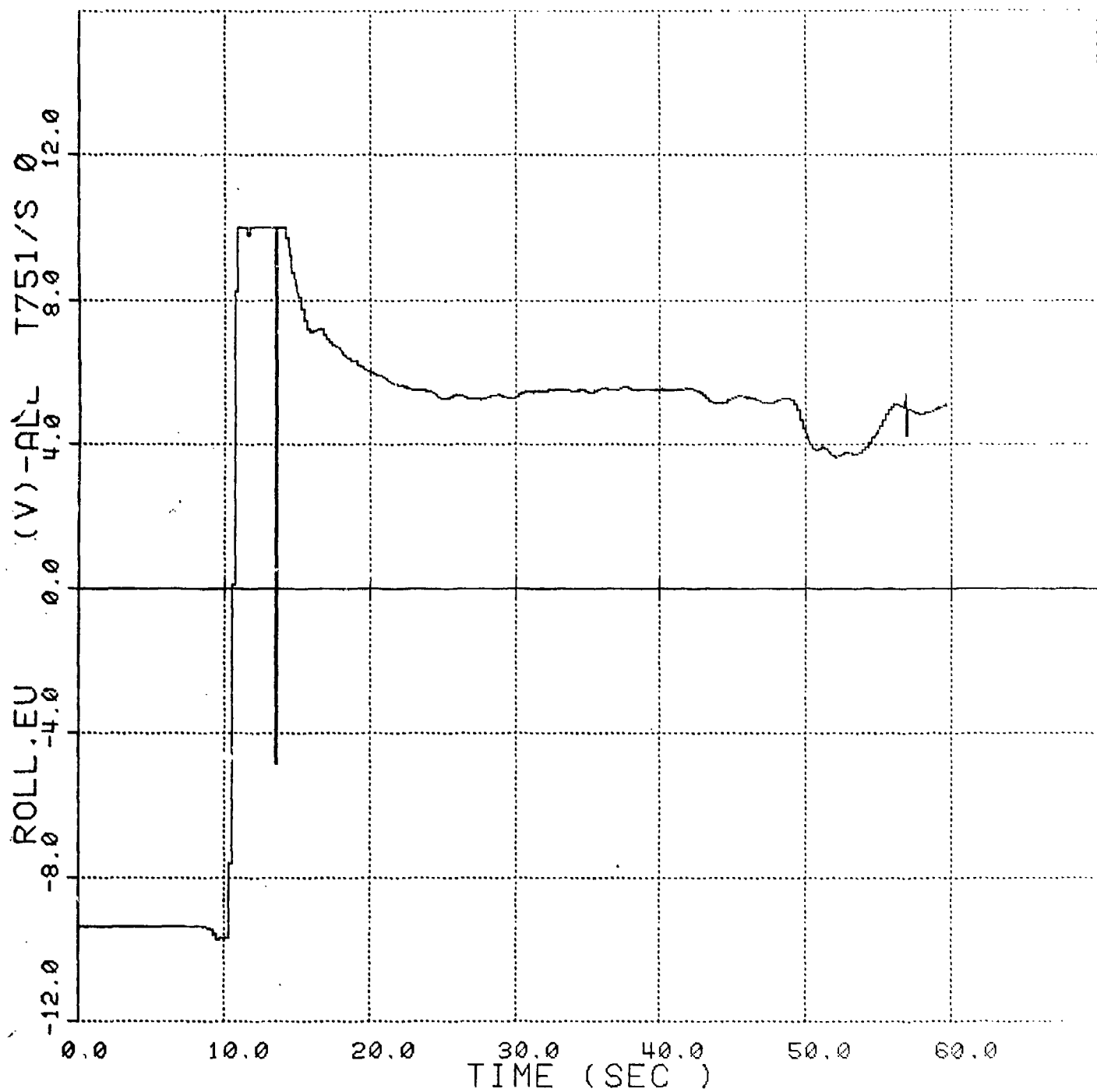


Figure No. 93. Towed Submersible's Roll vs Time, Case 3



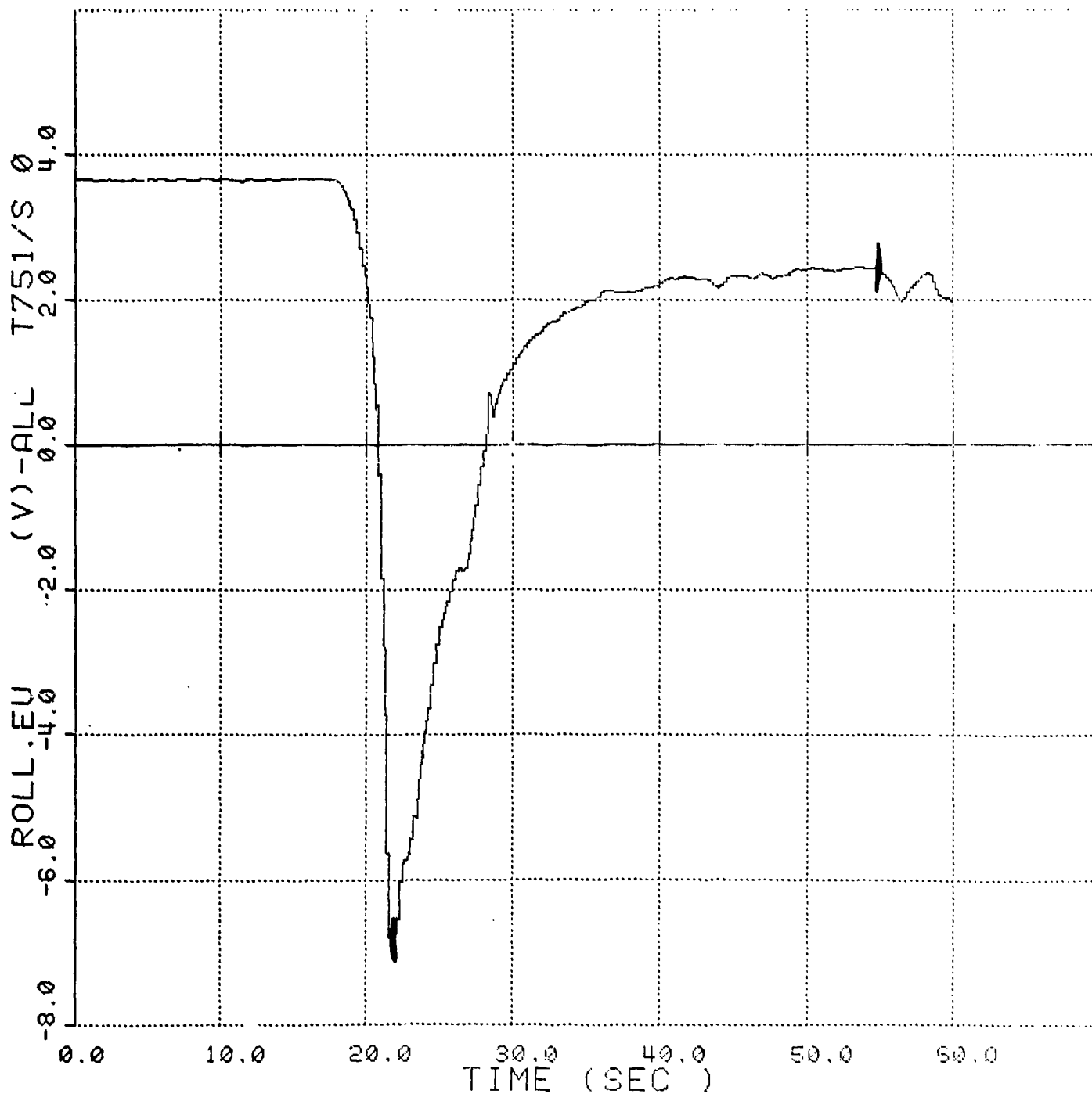


Figure No. 94. Towed Submersible's Roll vs Time, Case 4



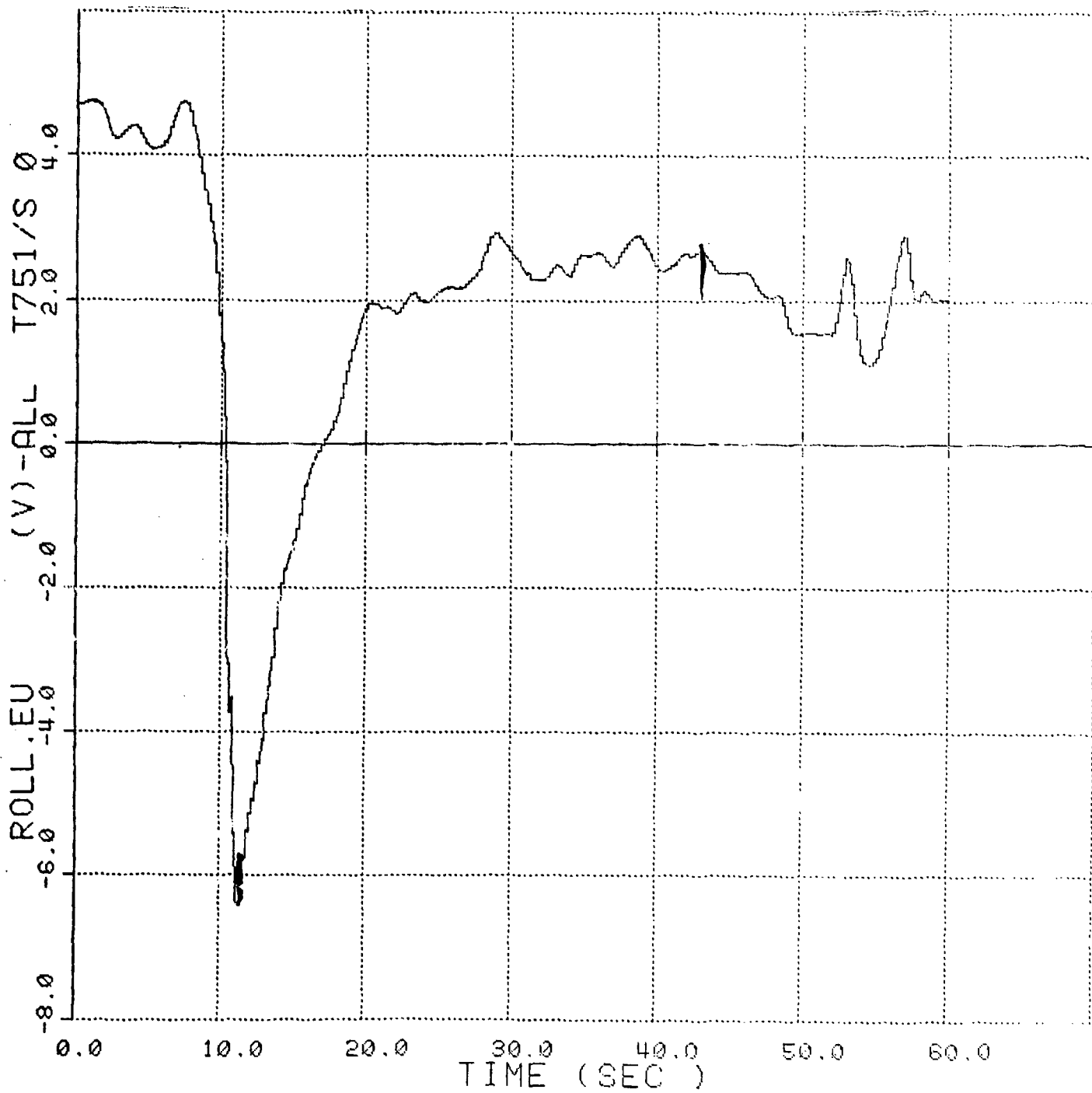


Figure No. 95. Towed Submersible's Roll vs Time, Case 5



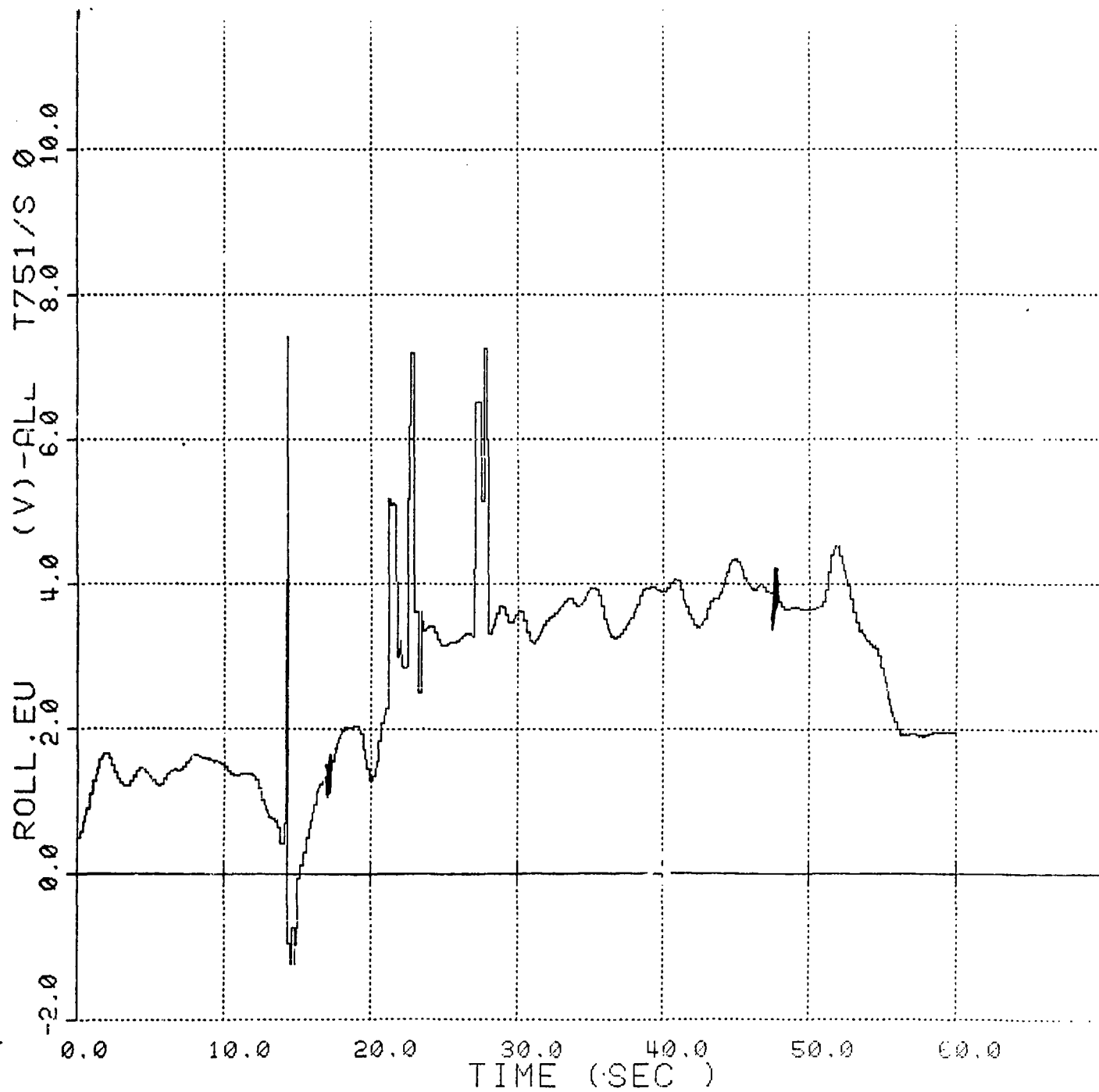


Figure No. 96. Towed Submersible's Roll vs Time, Case 6



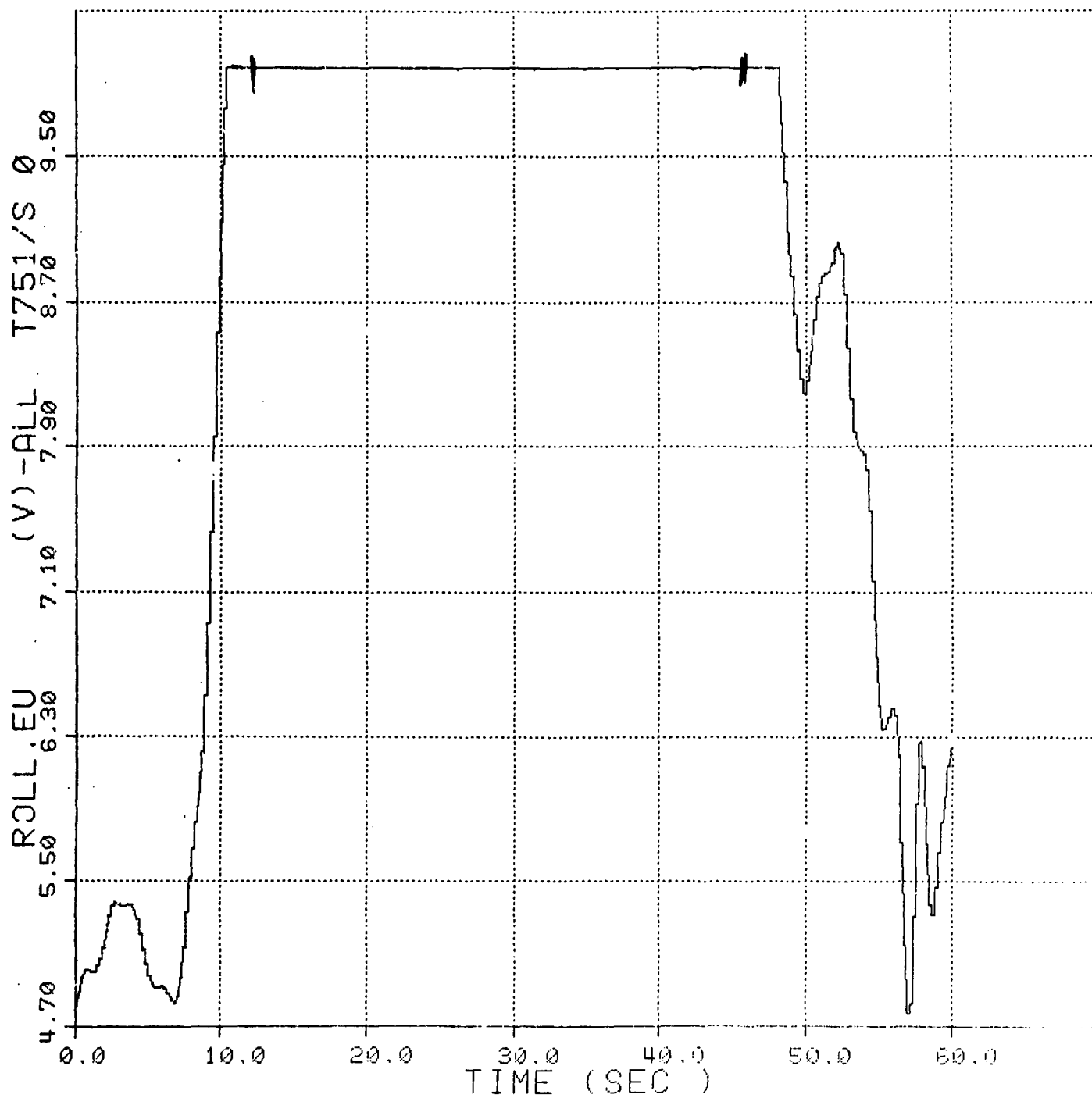


Figure No. 97. Towed Submersible's Roll vs Time, Case 7



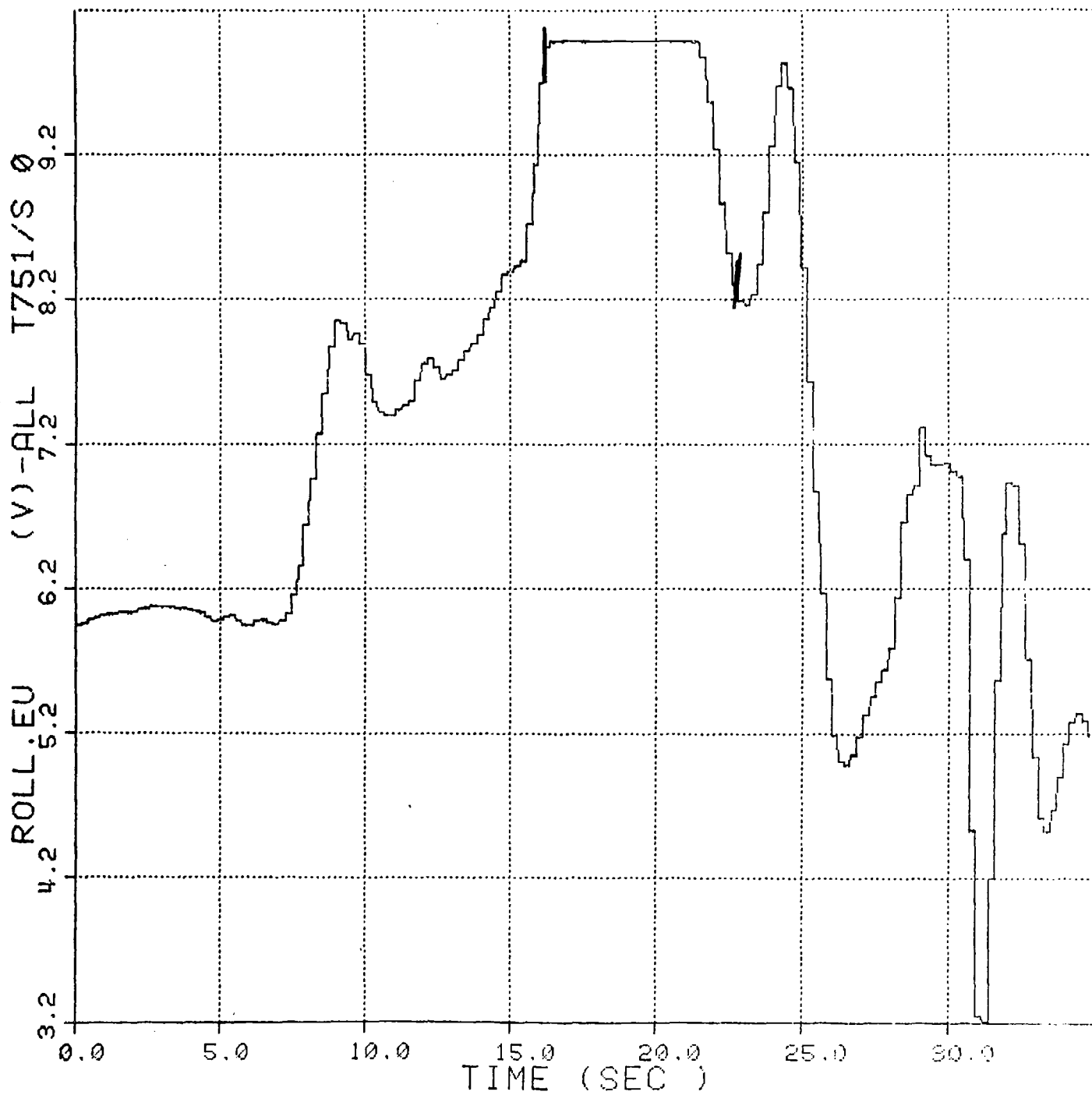


Figure No. 98. Towed Submersible's Roll vs Time, Case 8



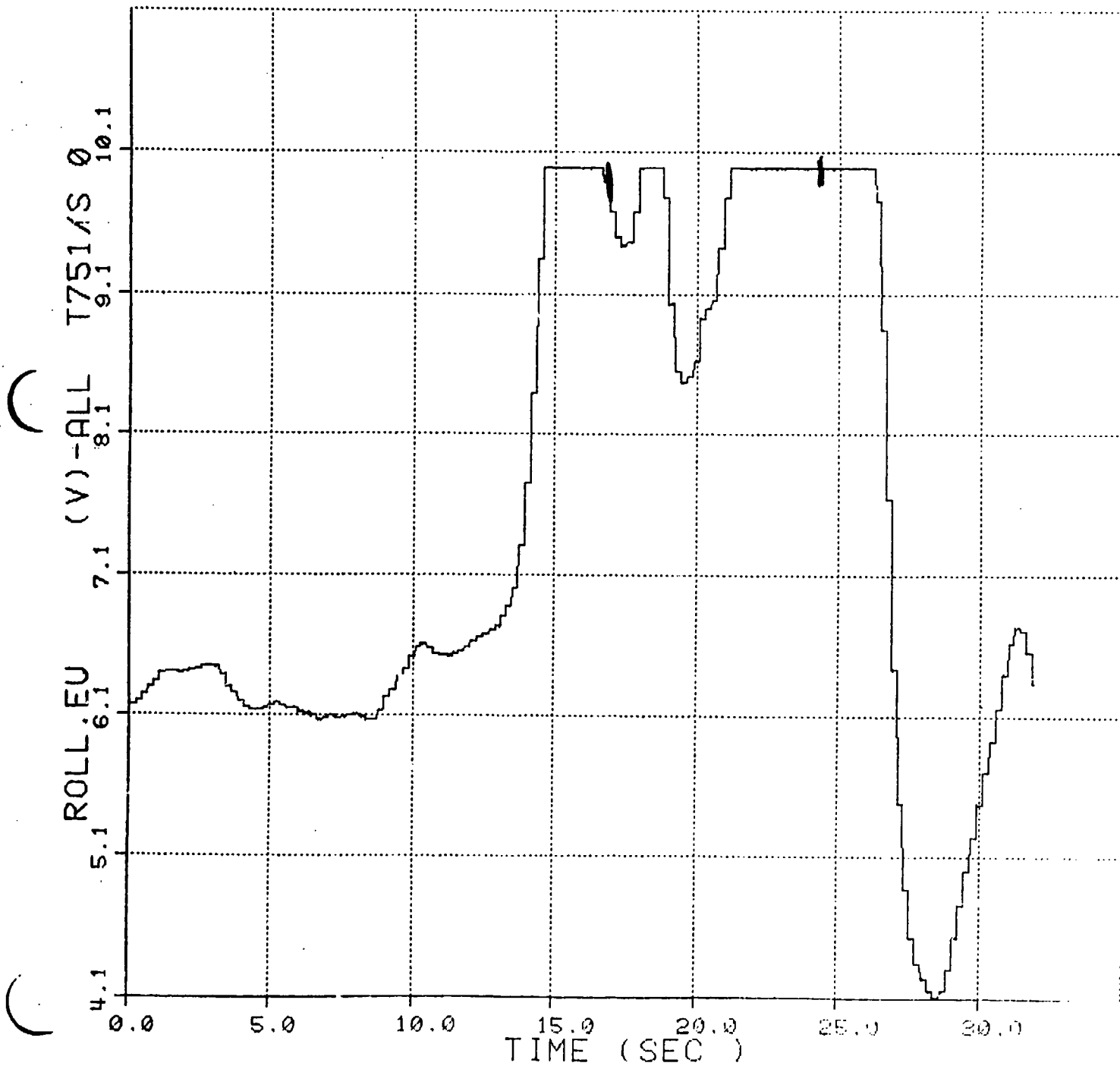


Figure No. 99. Towed Submersible's Roll vs Time, Case 9



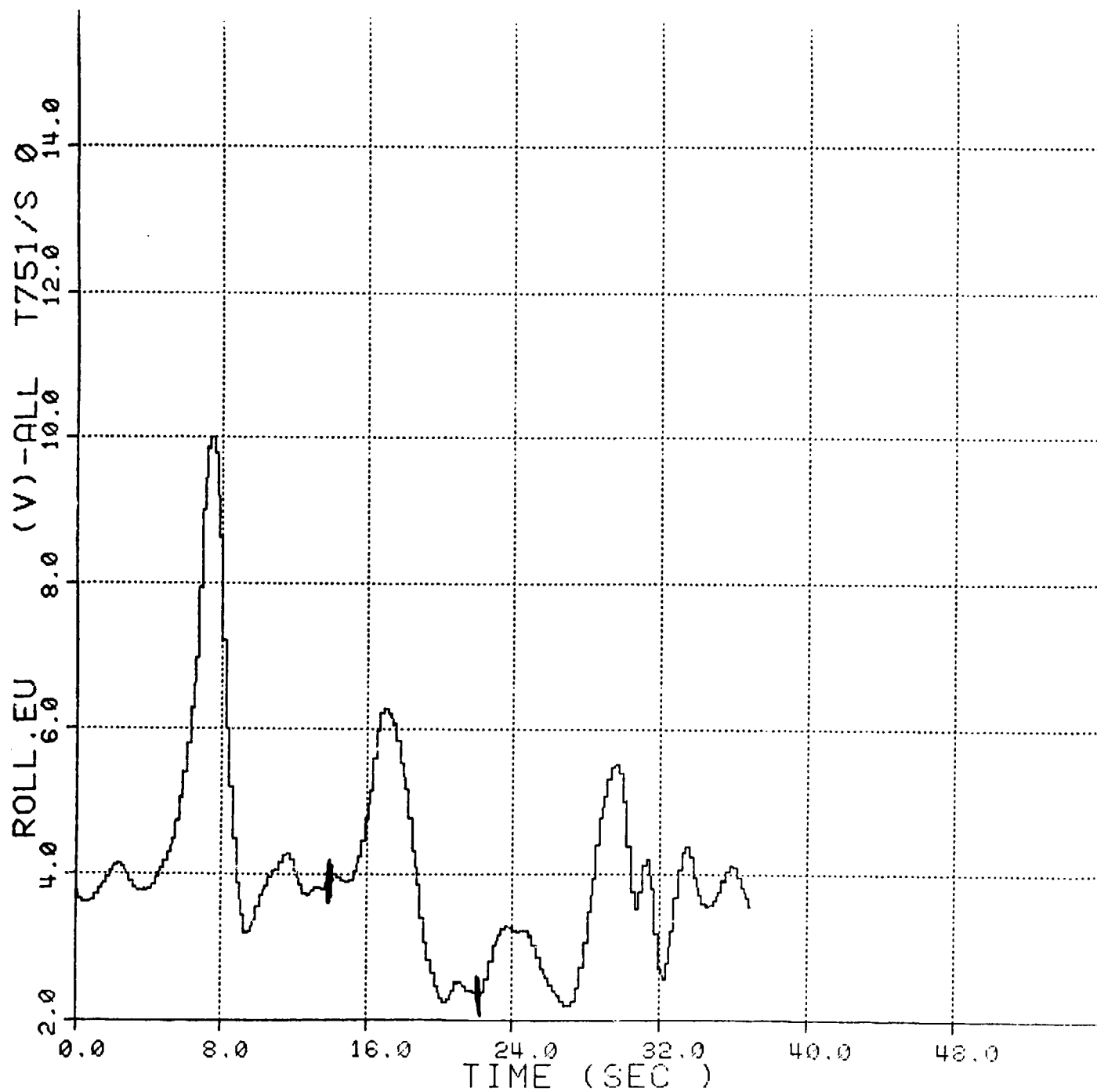


Figure No.100. Towed Submersible's Roll vs Time, Case 10



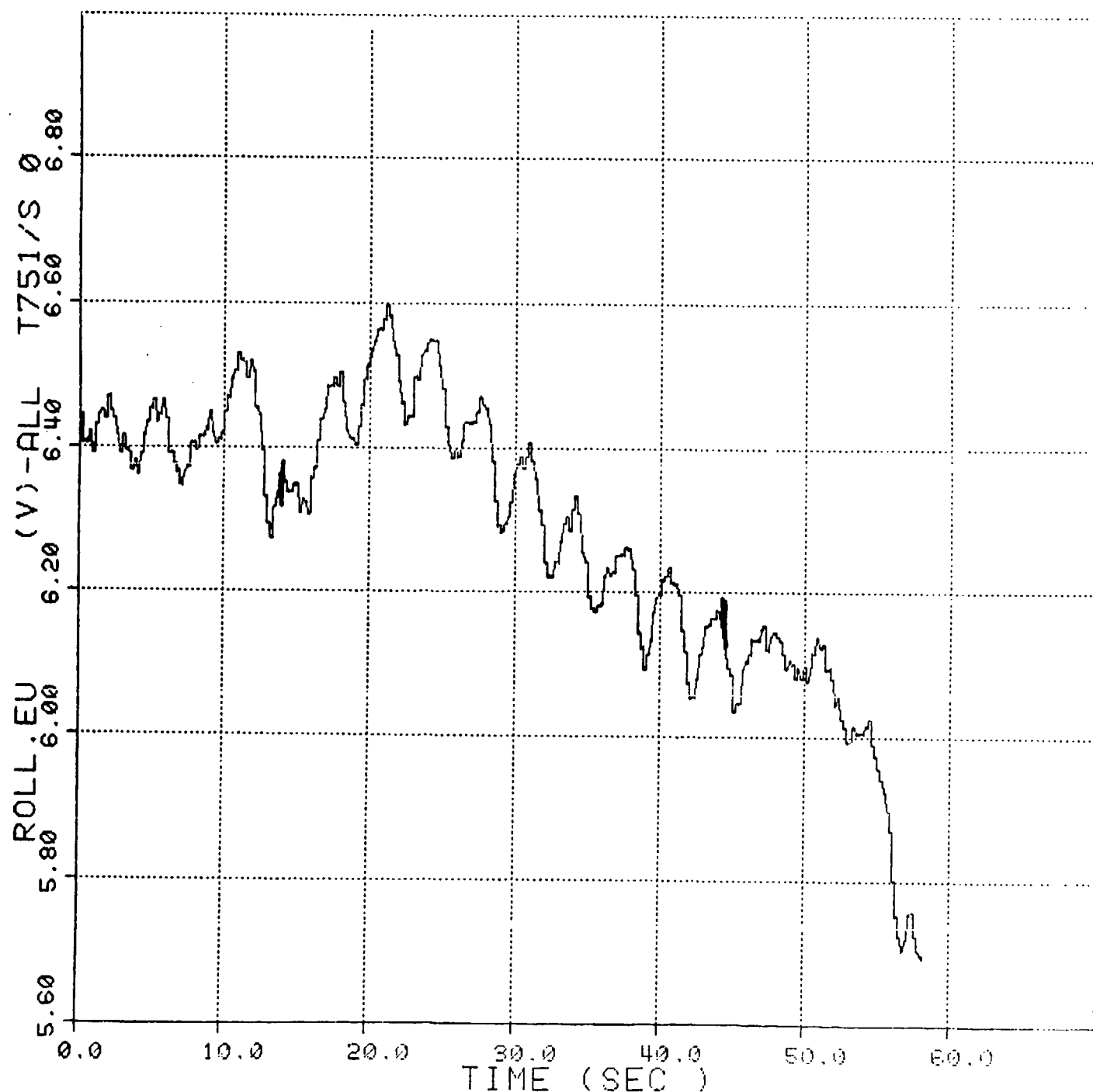


Figure No.101. Towed Submersible's Roll vs Time, Case 11



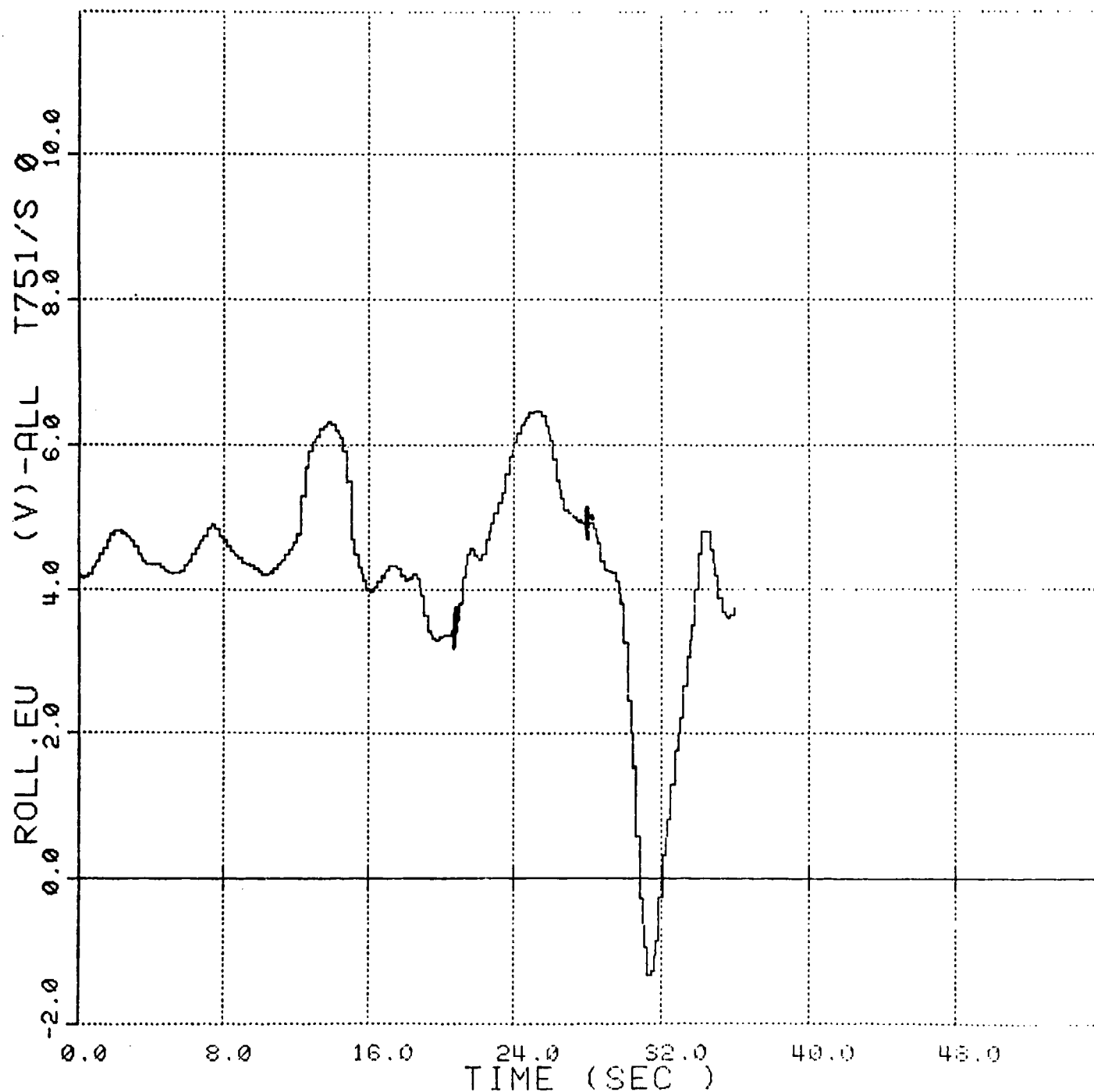


Figure No.102. Towed Submersible's Roll vs Time, Case 12



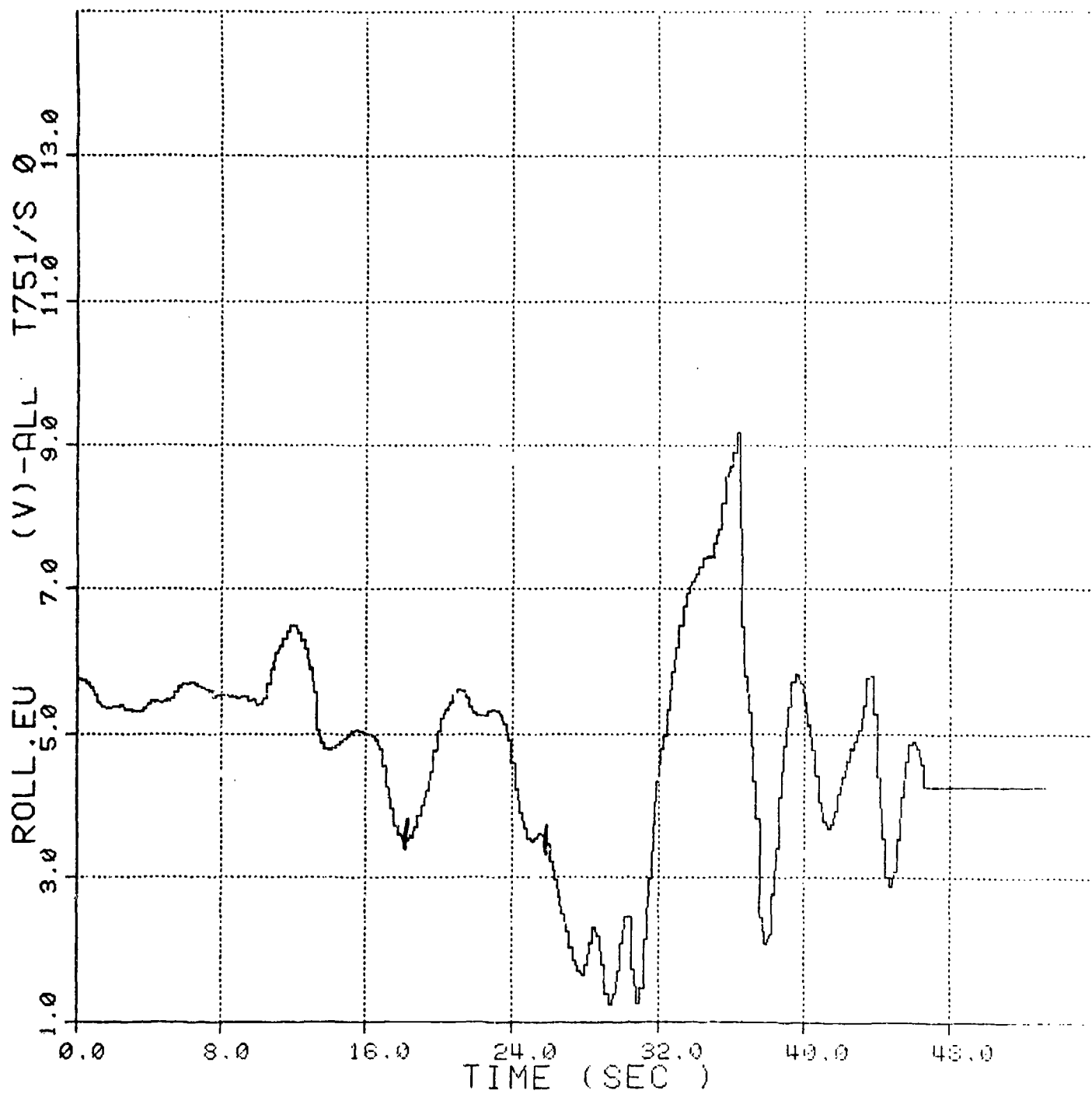


Figure No.103. Towed Submersible's Roll vs Time, Case 13



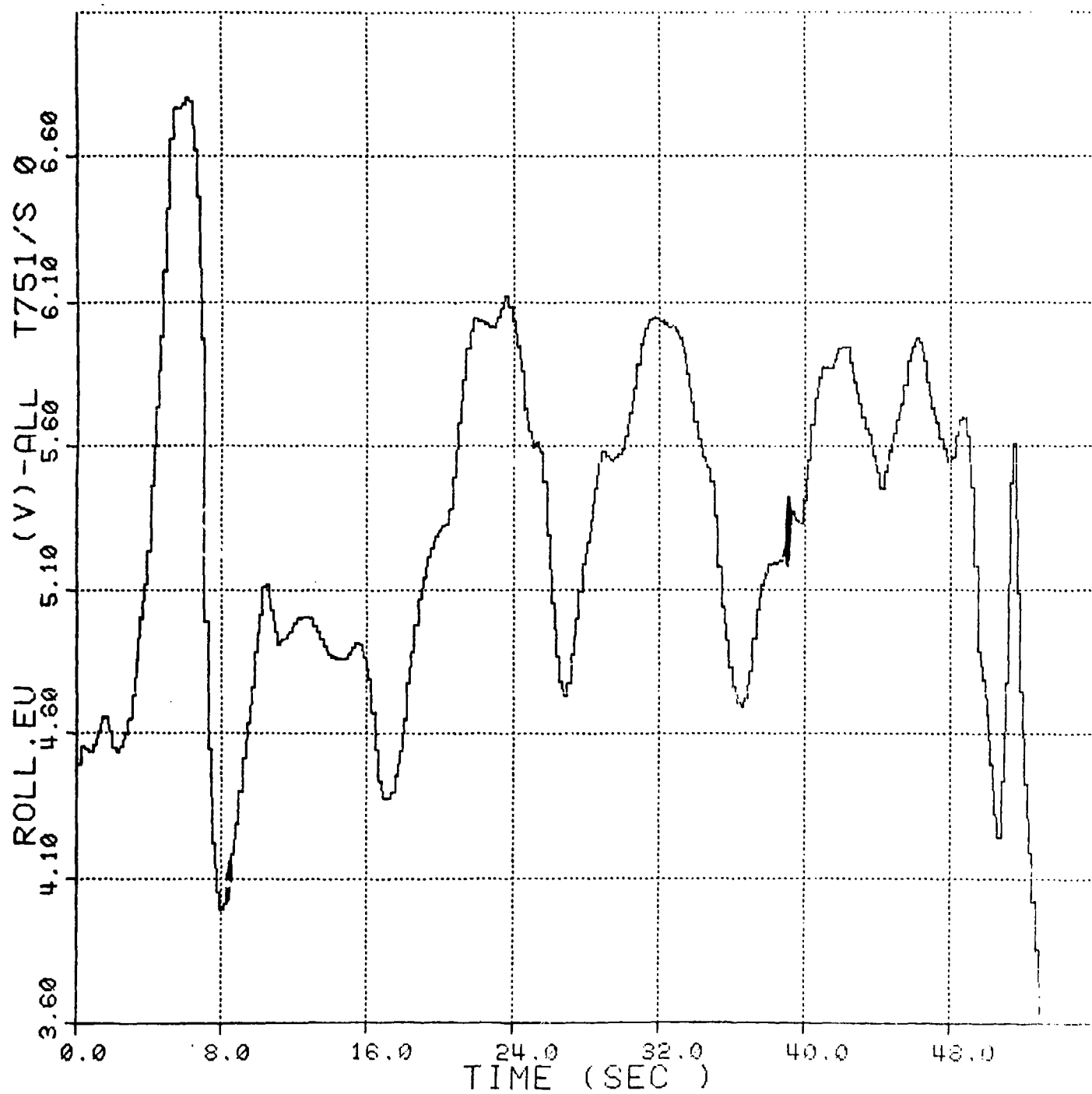


Figure No. 104. Towed Submersible's Roll vs Time, Case 14



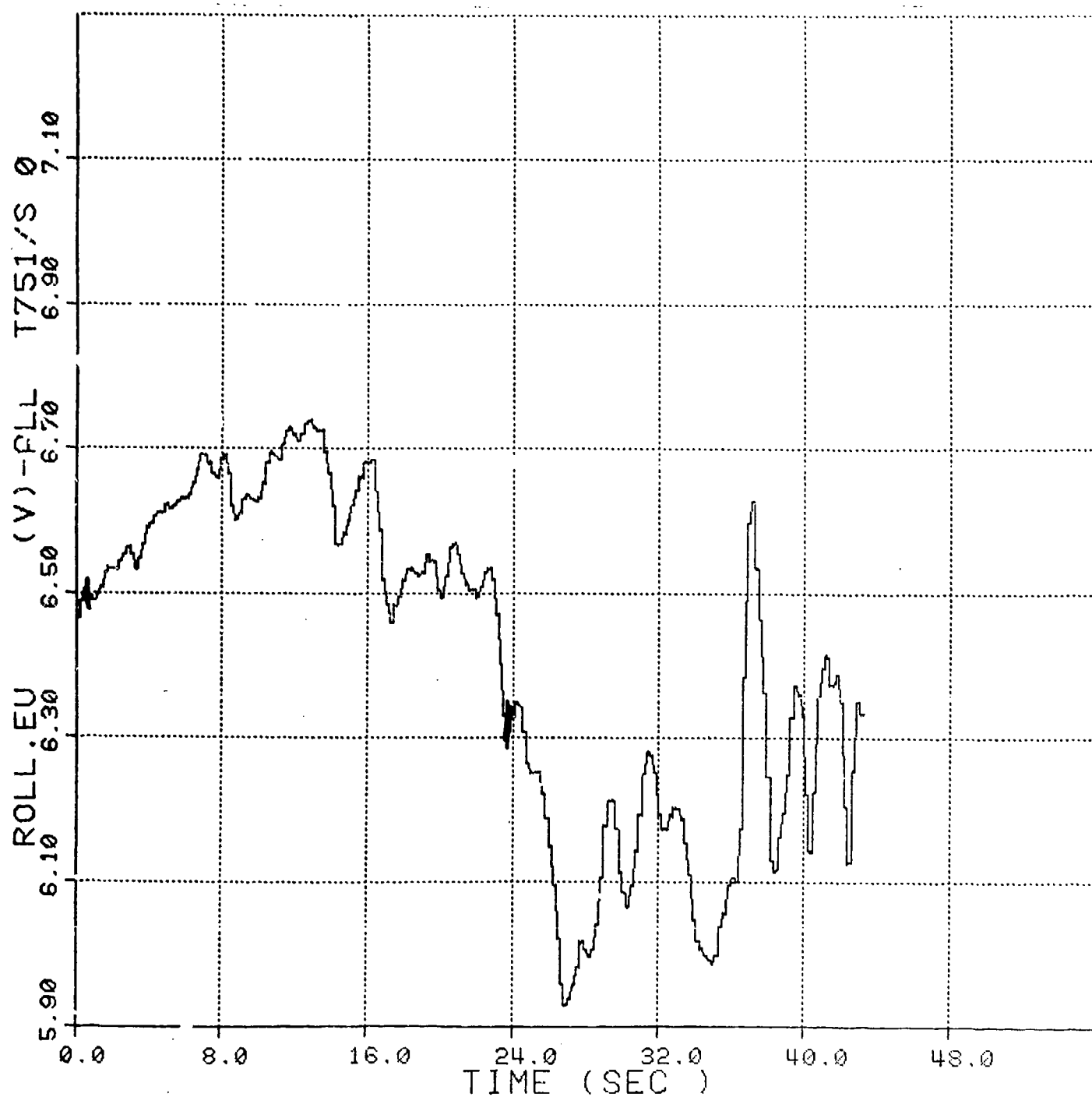


Figure No. 105. Towed Submersible's Roll vs Time, Case 15



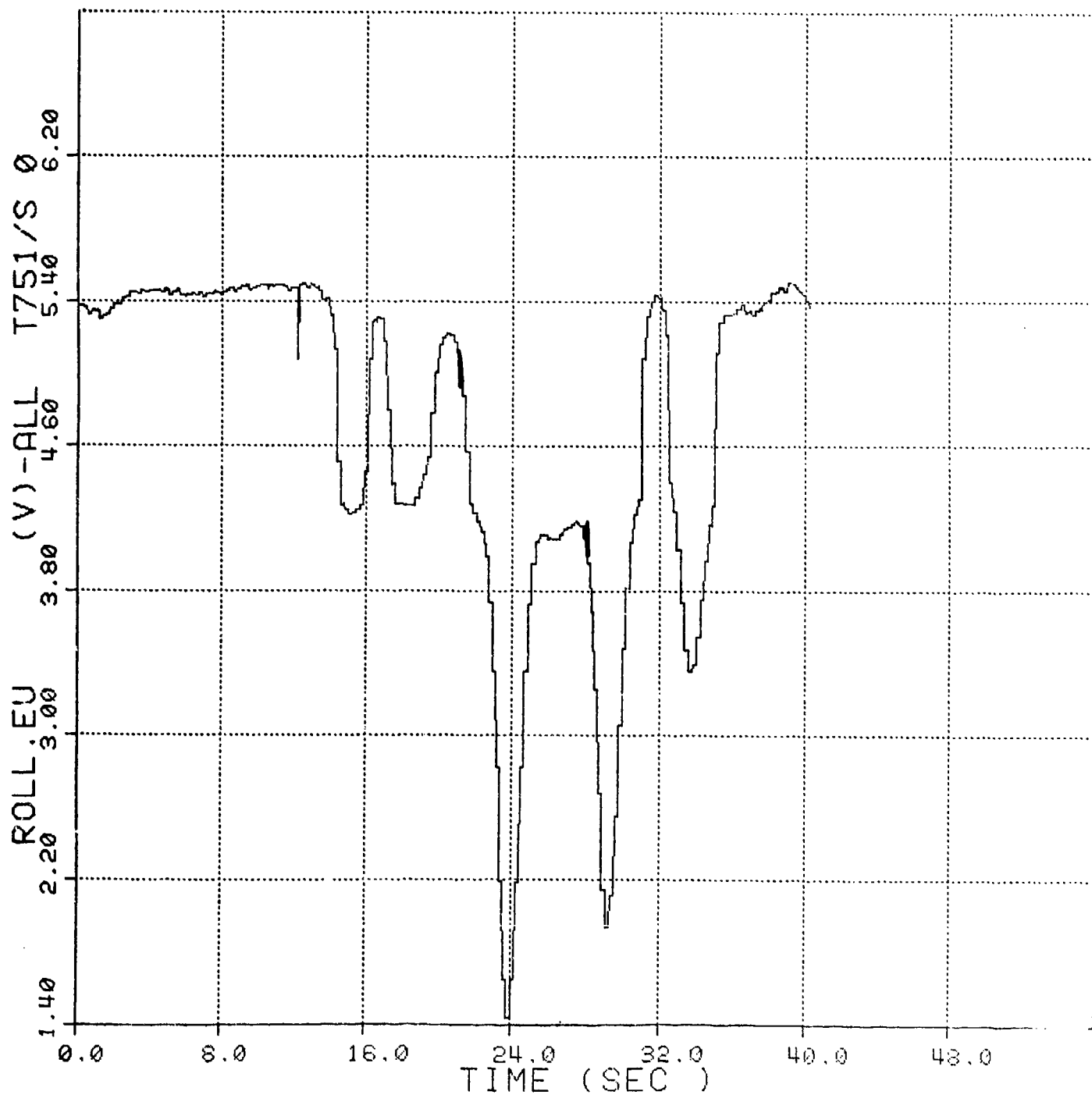


Figure No. 106. Towed Submersible's Roll vs Time, Case 16



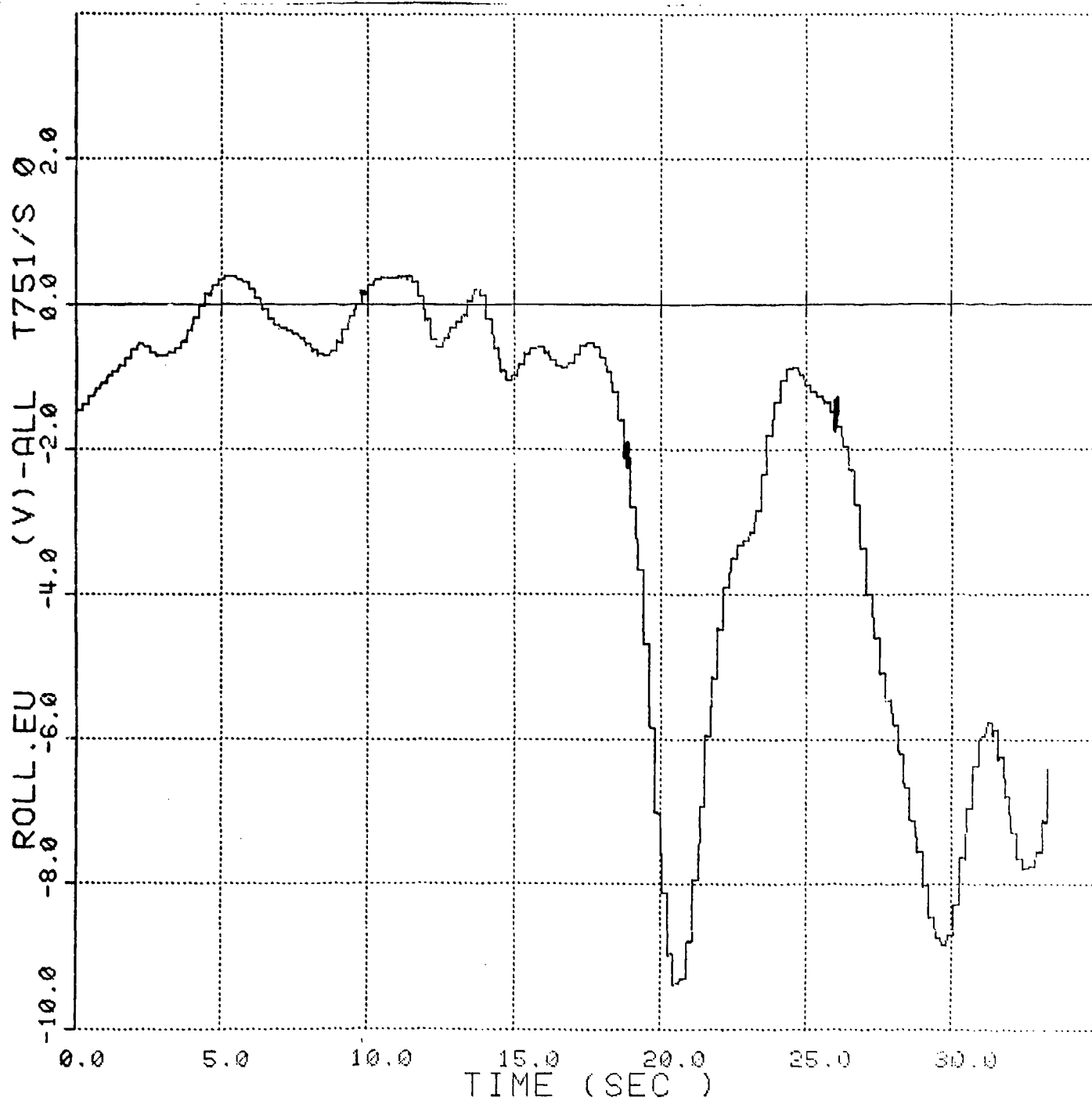


Figure No. 107. Towed Submersible's Roll vs Time, Case 17



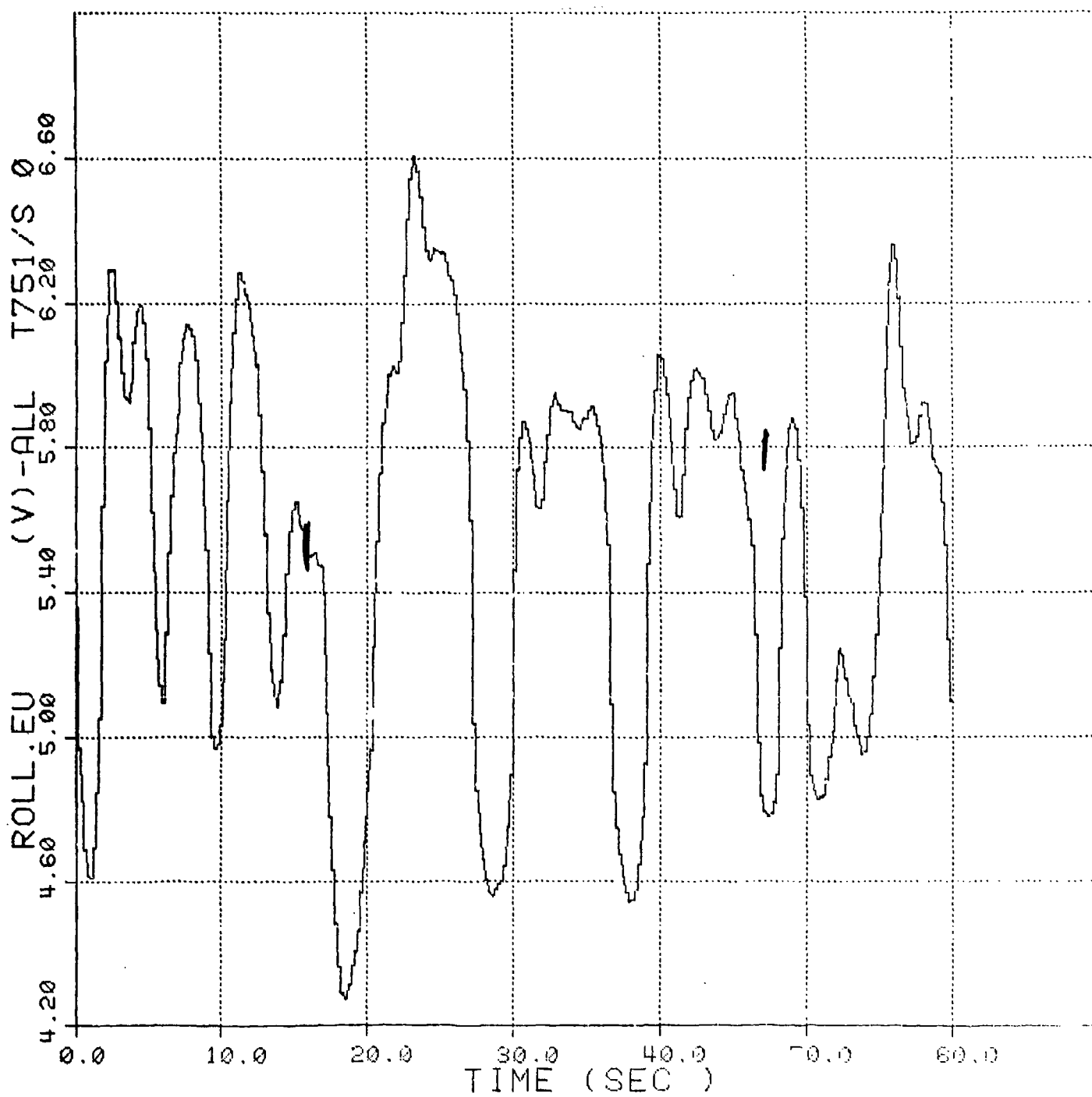


Figure No. 108. Towed Submersible's Roll vs Time, Case 18



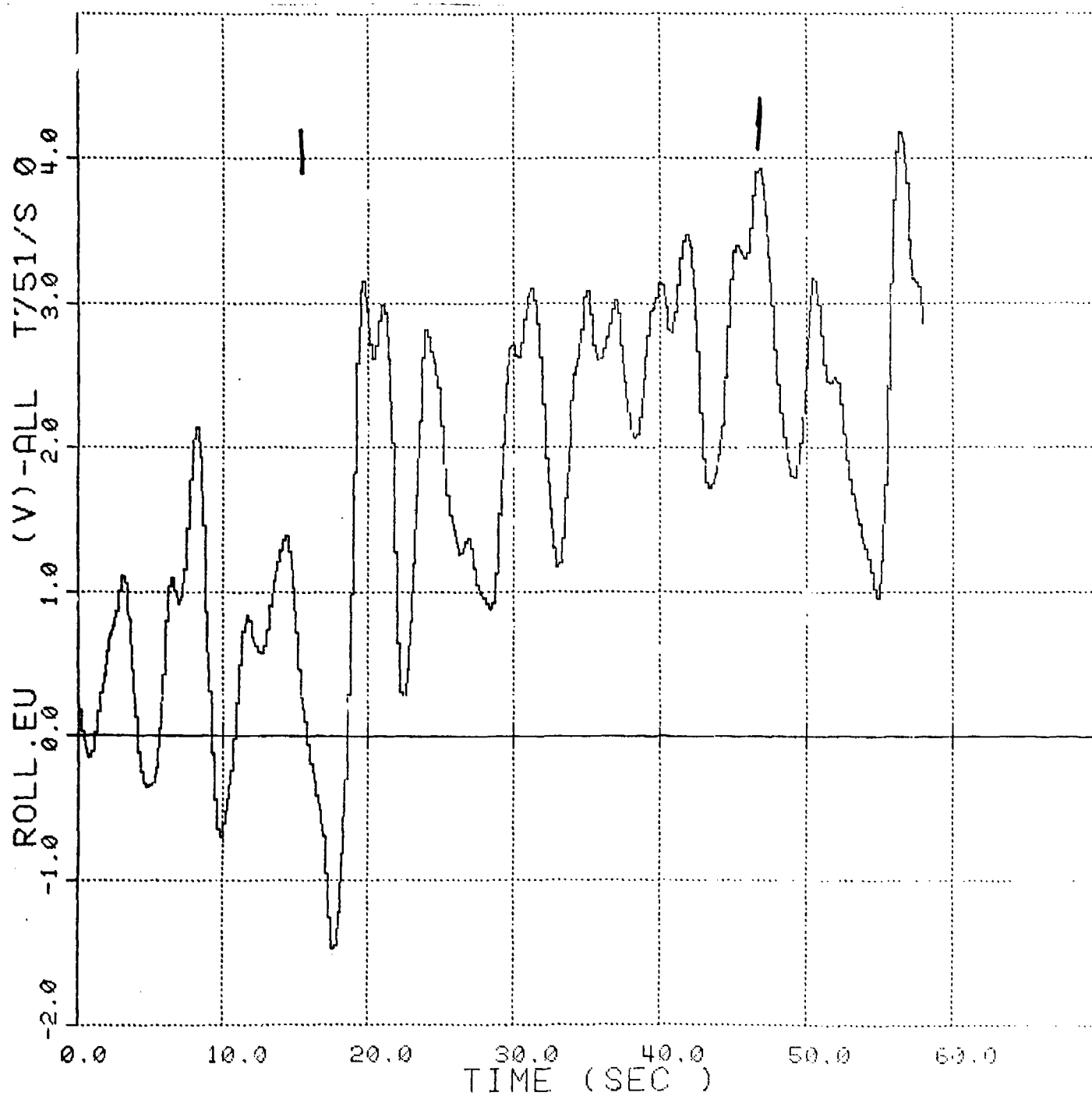


Figure No. 100. Towed Submersible's Roll vs Time, Case 19



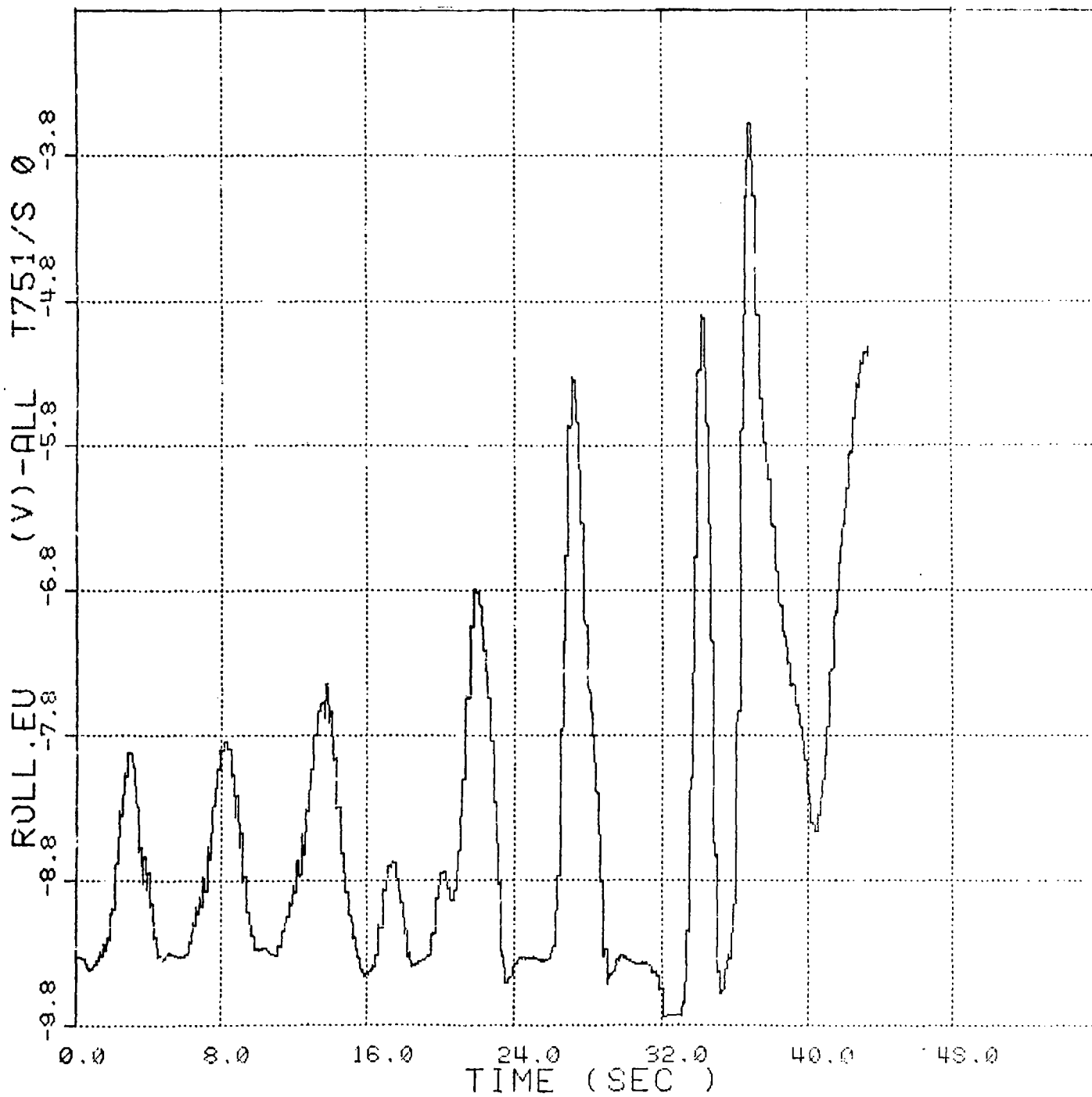


Figure No. 110. Towed Submersible's Roll vs Time, Case 20



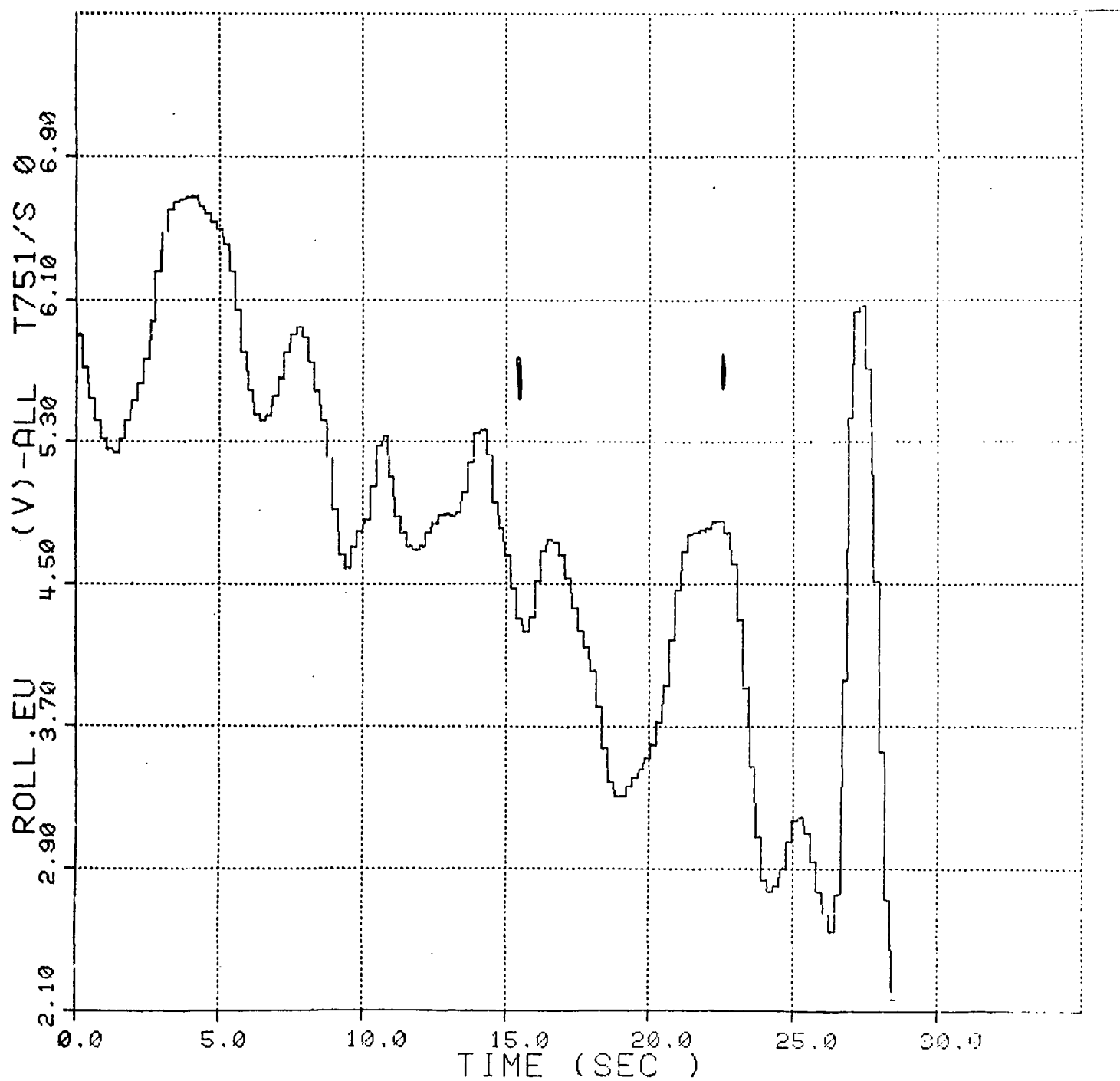


Figure No. 111. Towed Submersible's Roll vs Time, Case 21



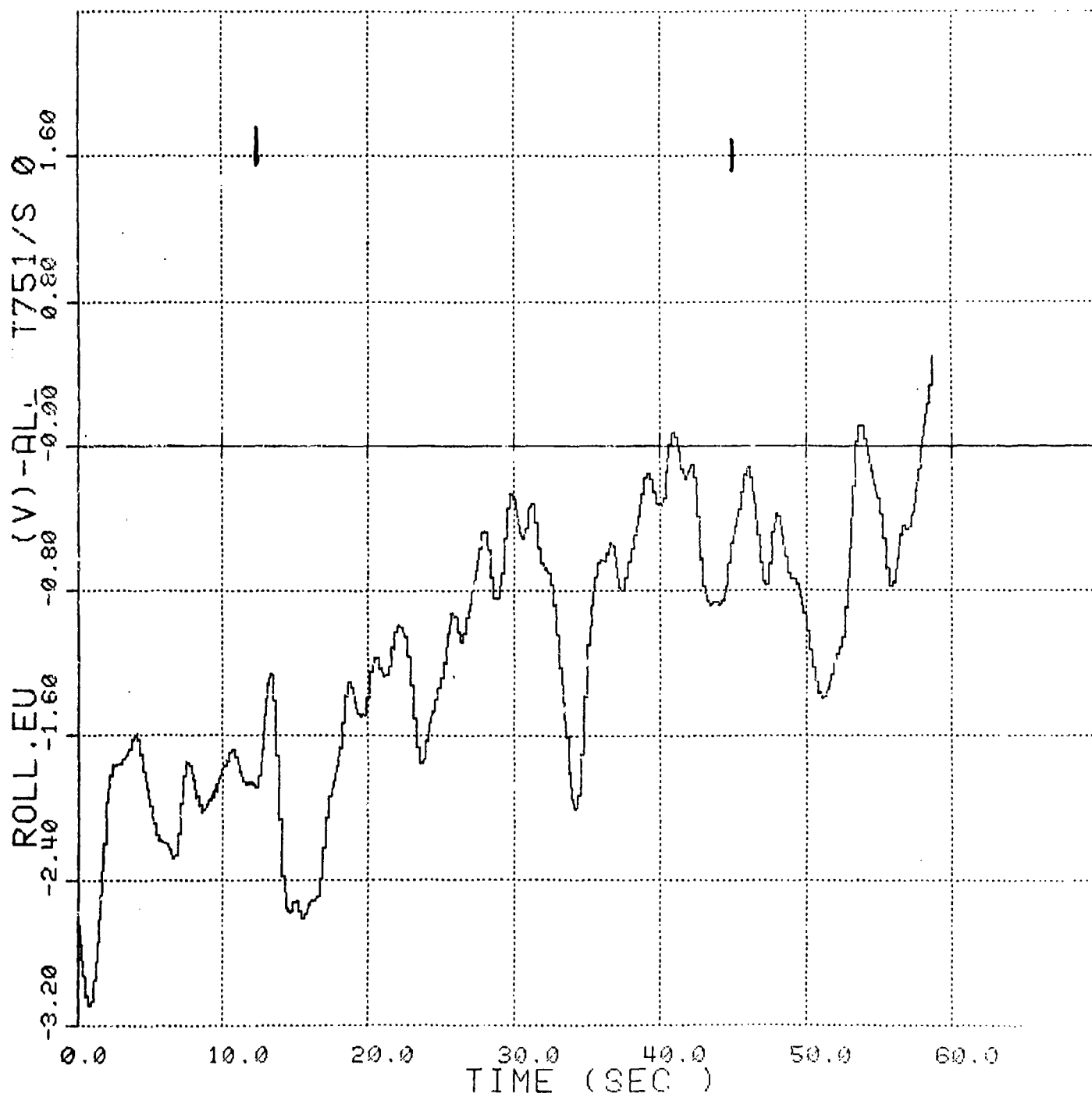


Figure No. 112. Towed Submersible's Roll vs Time, Case 22



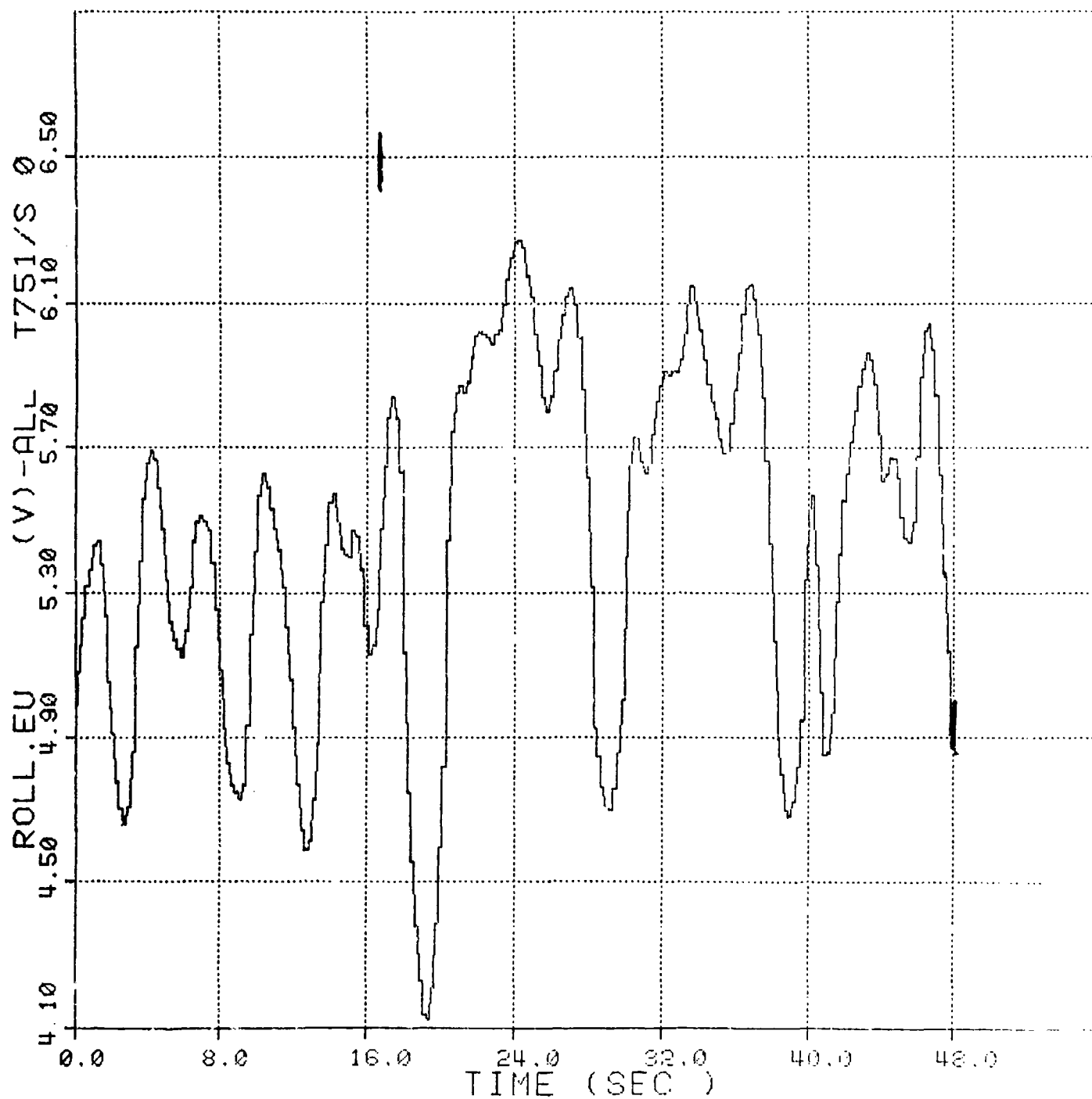


Figure No. 113. Towed Submersible's Roll vs Time, Case 23



114 115 116 117 118 119 120 121 122 123 124 125 126 127 128 129 130 131 132 133 134 135 136 137 138 139 140 141 142 143 144 145 146 147 148 149 150 151 152 153 154 155 156 157 158 159 160 161 162 163 164 165 166 167 168 169 170 171 172 173 174 175 176 177 178 179 180 181 182 183 184 185 186 187 188 189 190 191 192 193 194 195 196 197 198 199 200 201 202 203 204 205 206 207 208 209 210 211 212 213 214 215 216 217 218 219 220 221 222 223 224 225 226 227 228 229 230 231 232 233 234 235 236 237 238 239 240 241 242 243 244 245 246 247 248 249 250 251 252 253 254 255 256 257 258 259 260 261 262 263 264 265 266 267 268 269 270 271 272 273 274 275 276 277 278 279 280 281 282 283 284 285 286 287 288 289 290 291 292 293 294 295 296 297 298 299 300 301 302 303 304 305 306 307 308 309 310 311 312 313 314 315 316 317 318 319 320 321 322 323 324 325 326 327 328 329 330 331 332 333 334 335 336 337 338 339 340 341 342 343 344 345 346 347 348 349 350 351 352 353 354 355 356 357 358 359 360 361 362 363 364 365 366 367 368 369 370 371 372 373 374 375 376 377 378 379 380 381 382 383 384 385 386 387 388 389 390 391 392 393 394 395 396 397 398 399 400 401 402 403 404 405 406 407 408 409 410 411 412 413 414 415 416 417 418 419 420 421 422 423 424 425 426 427 428 429 430 431 432 433 434 435 436 437 438 439 440 441 442 443 444 445 446 447 448 449 450 451 452 453 454 455 456 457 458 459 460 461 462 463 464 465 466 467 468 469 470 471 472 473 474 475 476 477 478 479 480 481 482 483 484 485 486 487 488 489 490 491 492 493 494 495 496 497 498 499 500 501 502 503 504 505 506 507 508 509 510 511 512 513 514 515 516 517 518 519 520 521 522 523 524 525 526 527 528 529 530 531 532 533 534 535 536 537 538 539 540 541 542 543 544 545 546 547 548 549 550 551 552 553 554 555 556 557 558 559 560 561 562 563 564 565 566 567 568 569 570 571 572 573 574 575 576 577 578 579 580 581 582 583 584 585 586 587 588 589 590 591 592 593 594 595 596 597 598 599 600 601 602 603 604 605 606 607 608 609 610 611 612 613 614 615 616 617 618 619 620 621 622 623 624 625 626 627 628 629 630 631 632 633 634 635 636 637 638 639 640 641 642 643 644 645 646 647 648 649 650 651 652 653 654 655 656 657 658 659 660 661 662 663 664 665 666 667 668 669 670 671 672 673 674 675 676 677 678 679 680 681 682 683 684 685 686 687 688 689 690 691 692 693 694 695 696 697 698 699 700 701 702 703 704 705 706 707 708 709 710 711 712 713 714 715 716 717 718 719 720 721 722 723 724 725 726 727 728 729 730 731 732 733 734 735 736 737 738 739 740 741 742 743 744 745 746 747 748 749 750 751 752 753 754 755 756 757 758 759 760 761 762 763 764 765 766 767 768 769 770 771 772 773 774 775 776 777 778 779 780 781 782 783 784 785 786 787 788 789 790 791 792 793 794 795 796 797 798 799 800 801 802 803 804 805 806 807 808 809 810 811 812 813 814 815 816 817 818 819 820 821 822 823 824 825 826 827 828 829 830 831 832 833 834 835 836 837 838 839 840 841 842 843 844 845 846 847 848 849 850 851 852 853 854 855 856 857 858 859 860 861 862 863 864 865 866 867 868 869 870 871 872 873 874 875 876 877 878 879 880 881 882 883 884 885 886 887 888 889 890 891 892 893 894 895 896 897 898 899 900 901 902 903 904 905 906 907 908 909 910 911 912 913 914 915 916 917 918 919 920 921 922 923 924 925 926 927 928 929 930 931 932 933 934 935 936 937 938 939 940 941 942 943 944 945 946 947 948 949 950 951 952 953 954 955 956 957 958 959 960 961 962 963 964 965 966 967 968 969 970 971 972 973 974 975 976 977 978 979 980 981 982 983 984 985 986 987 988 989 990 991 992 993 994 995 996 997 998 999 1000

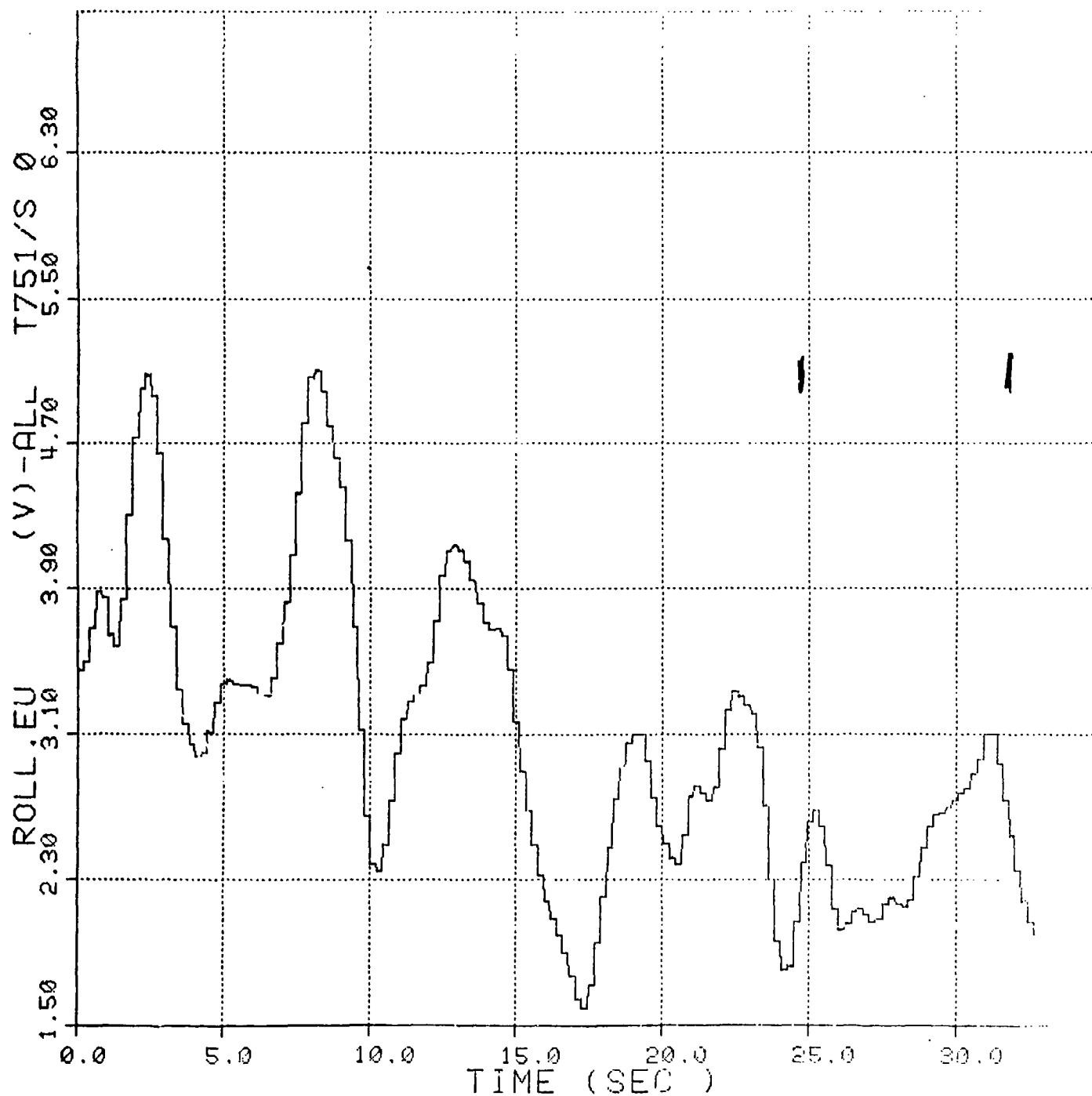


Figure No. 114. Towed Submersible's Roll vs Time, Case 24



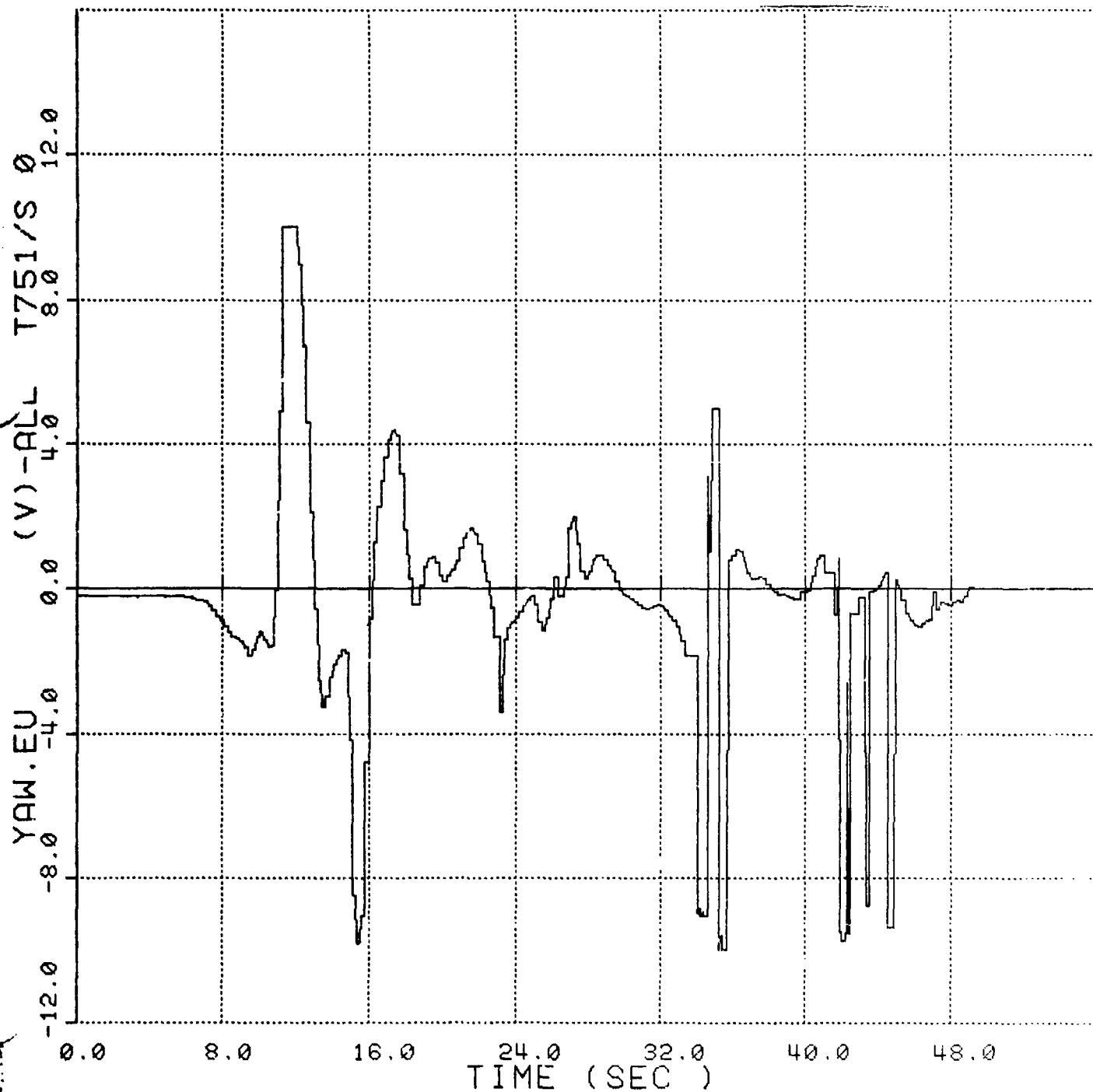


Figure No. 115. Towed Submersible's Yaw vs Time, Case 2



116  
T751/S  
0  
-ALL  
(V)  
-2.0  
-4.0  
-6.0  
-8.0  
-10.0  
YAW.EU

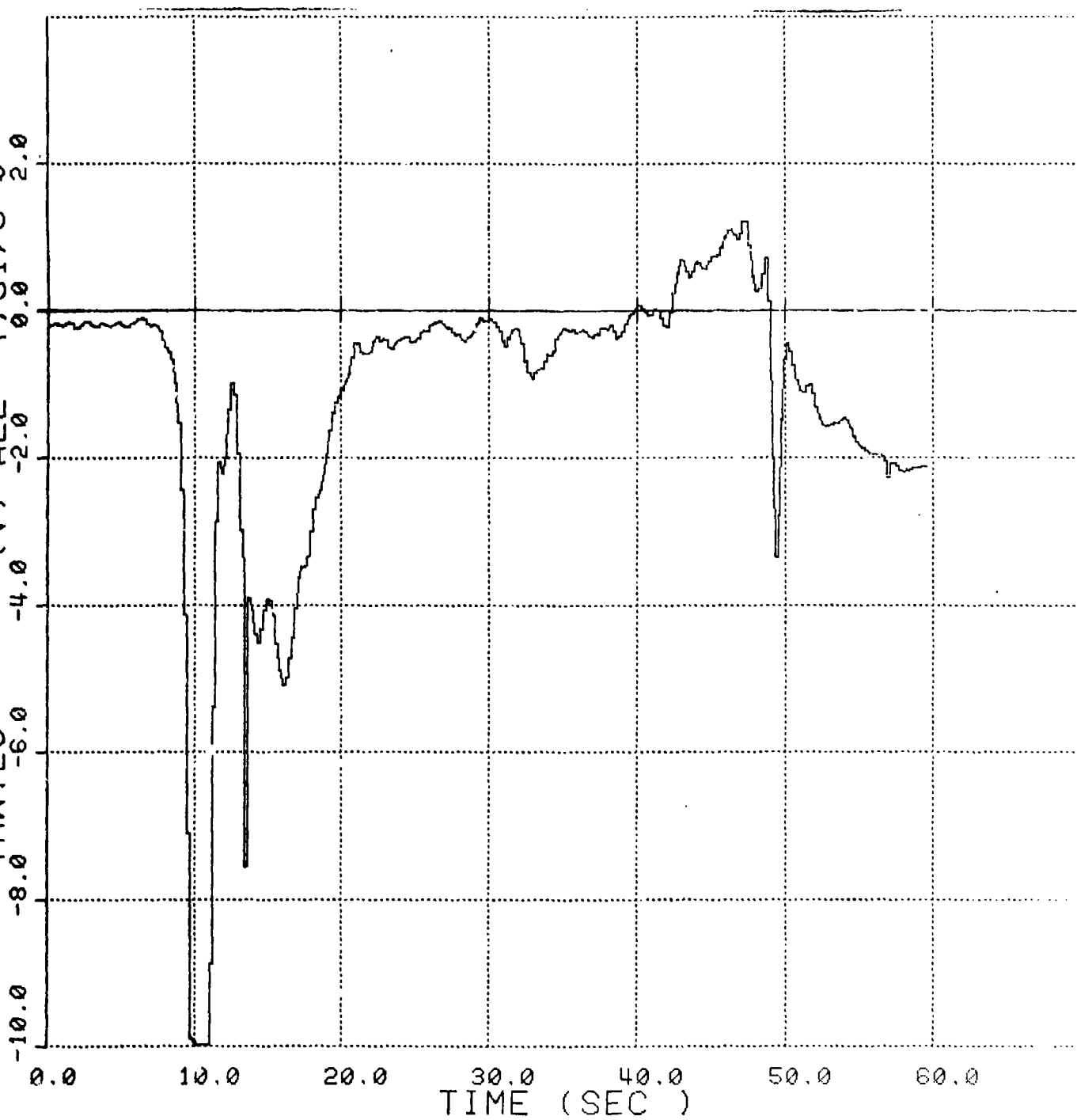


Figure No. 116. Towed Submersible's Yaw vs Time, Case 3



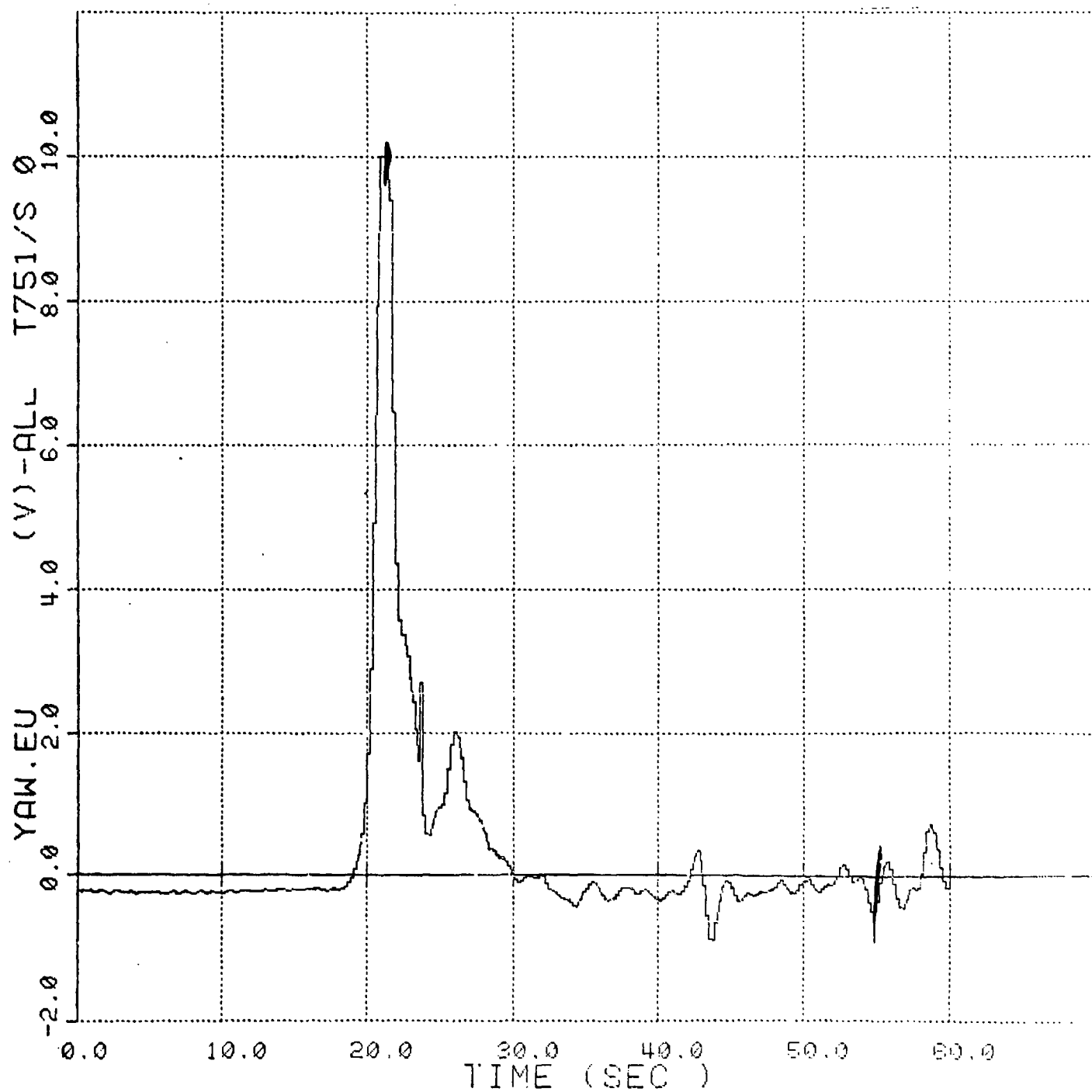


Figure No. 117. Towed Submersible's Yaw vs Time, Case 4



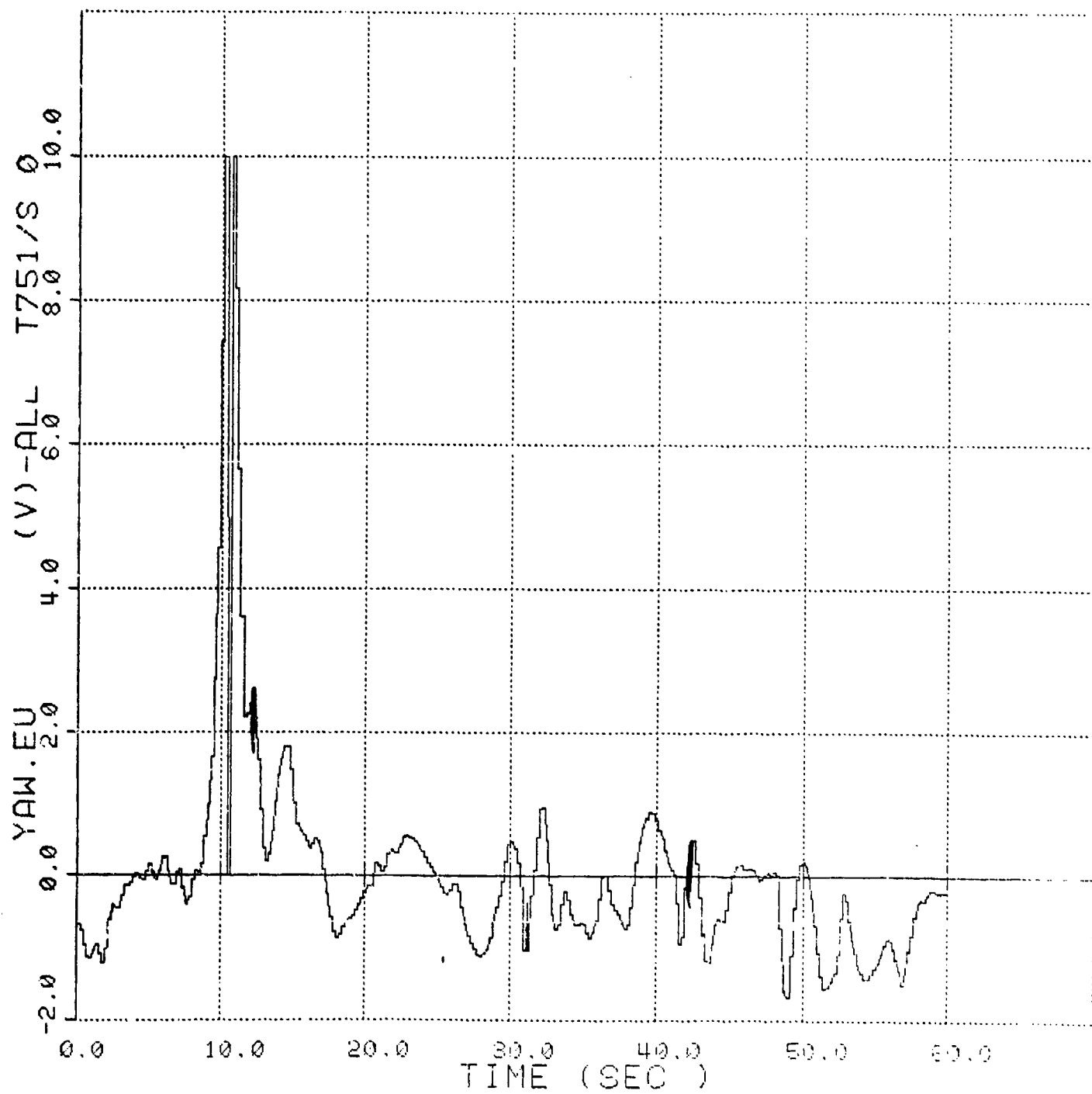


Figure No. 118. Towel Submersible's Yaw vs Time, Case 5



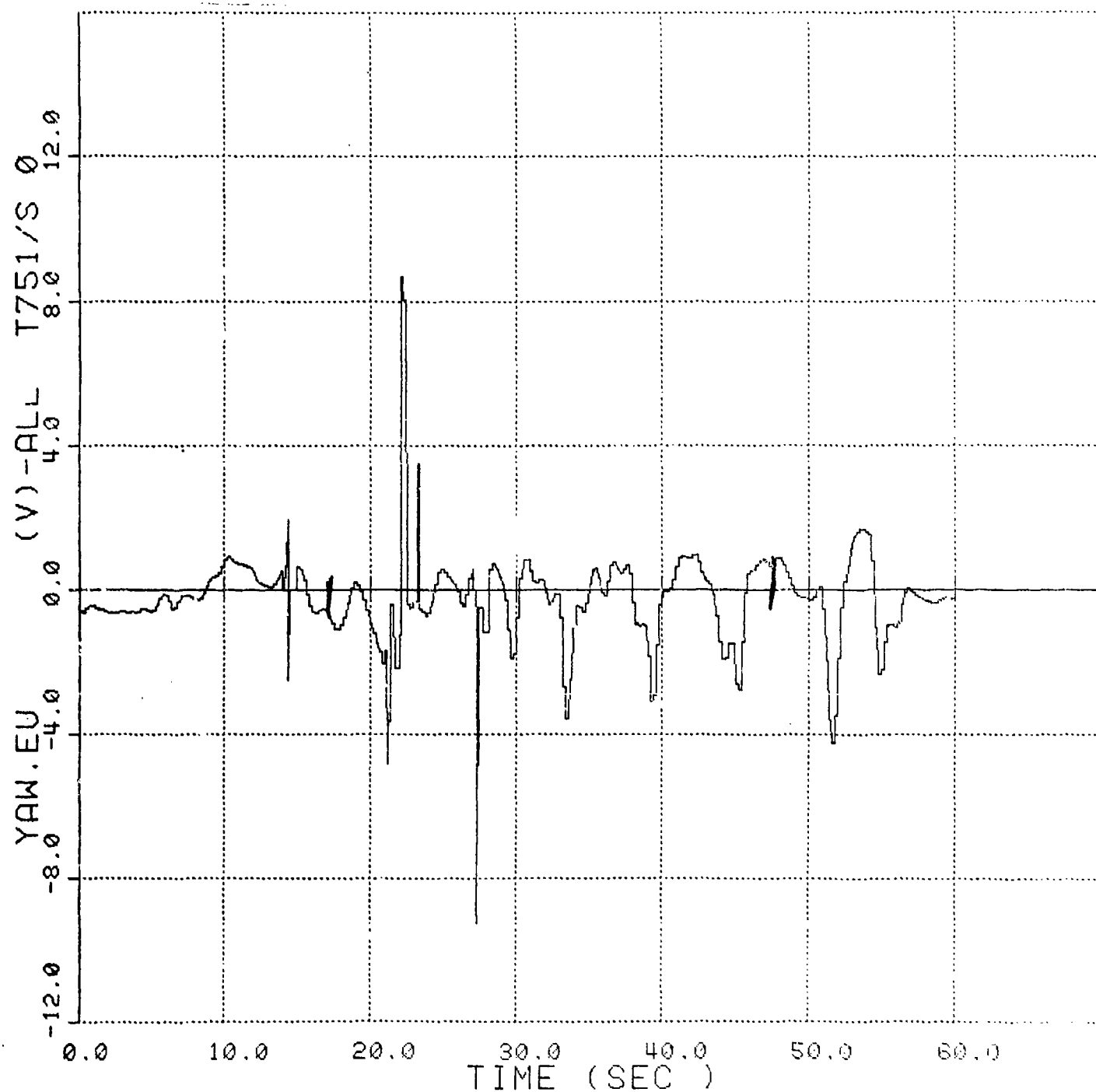


Figure No. 119. Towed Submersible's Yaw vs Time, Case 6



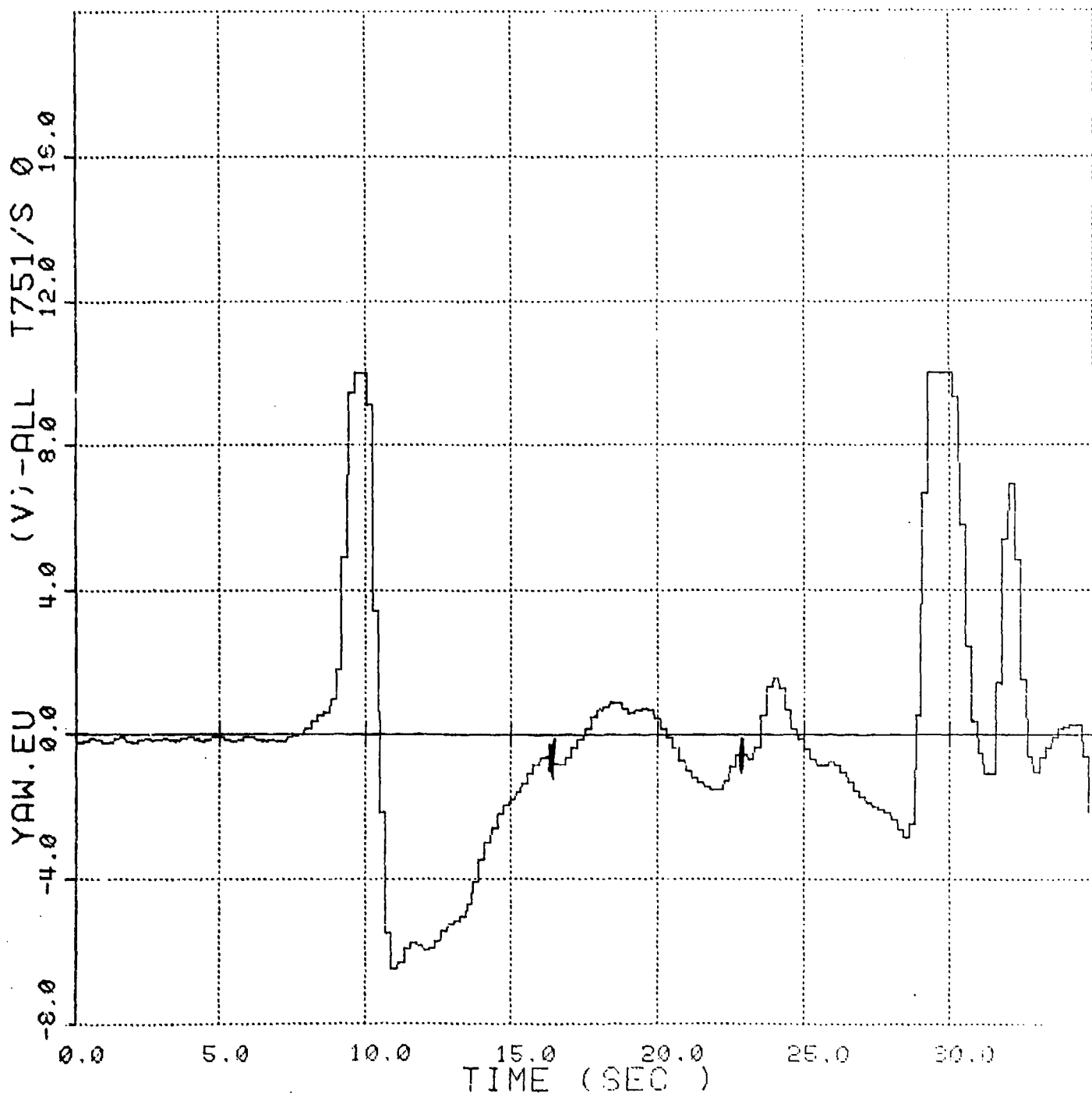


Figure No. 120. Towed Submersible's Yaw vs Time, Case 8



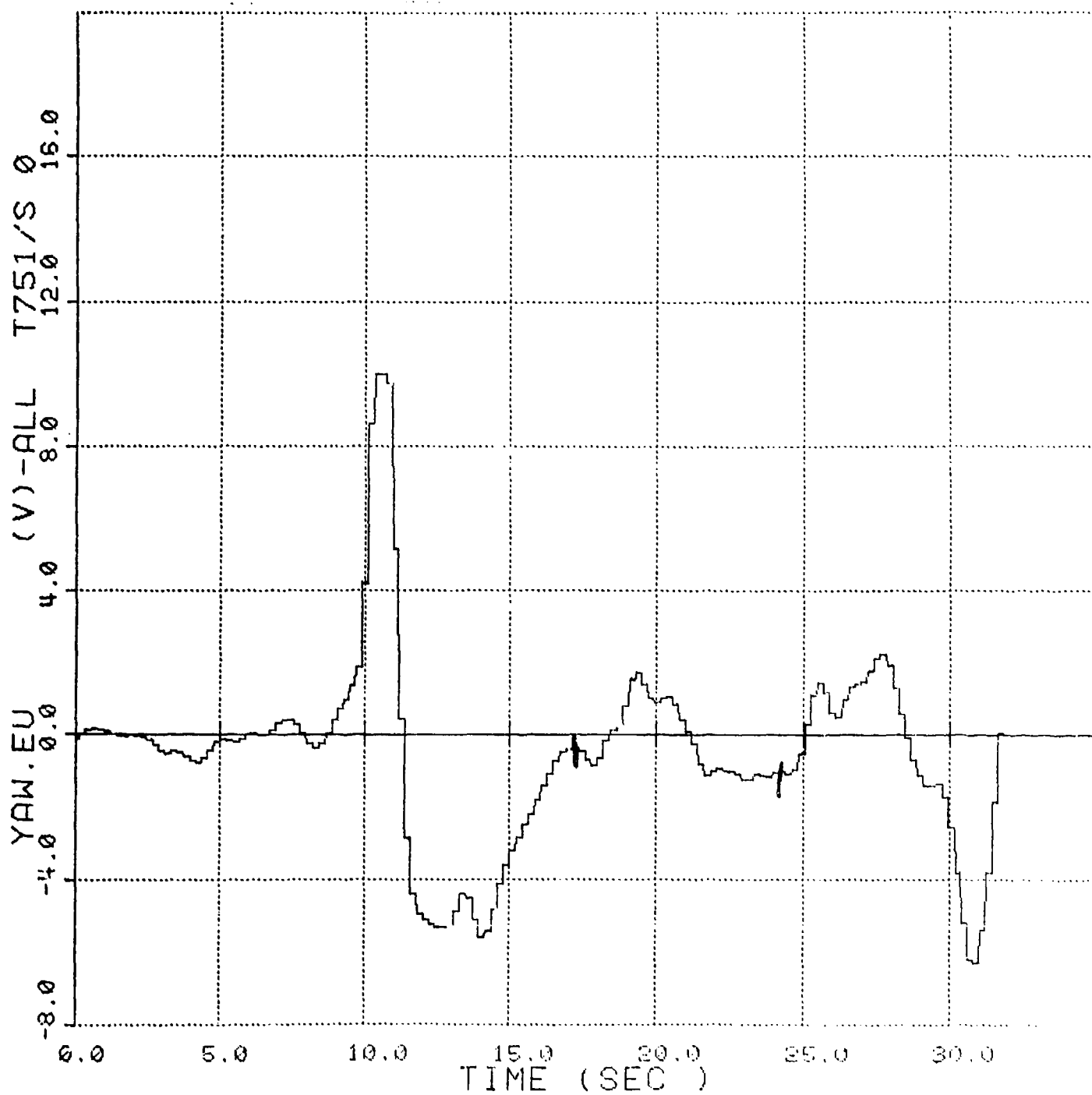


Figure No. 121. Towed Submersible's Yaw vs Time, Case 9



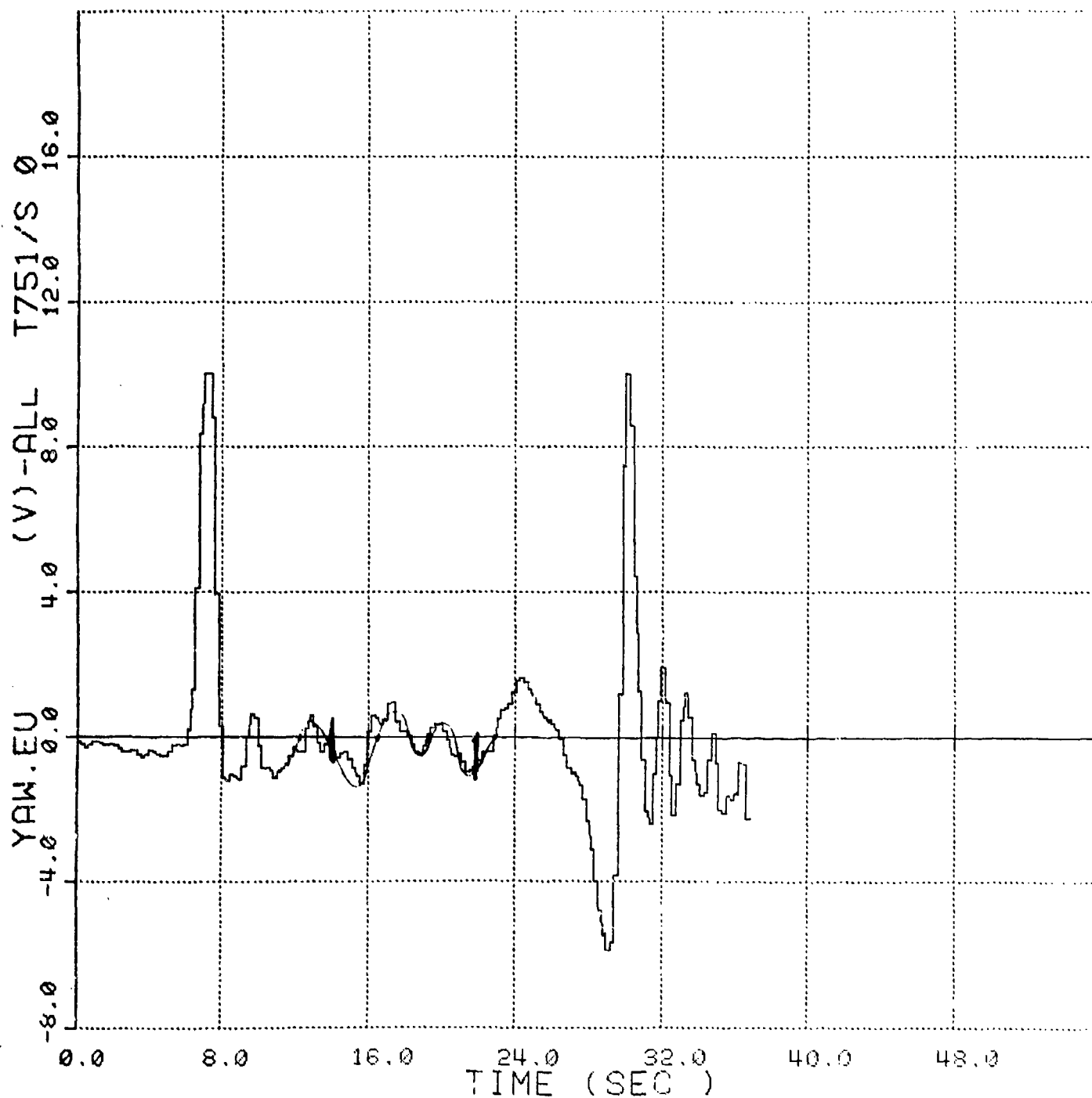


Figure No. 122. Towed Submersible's Yaw vs Time, Case 10



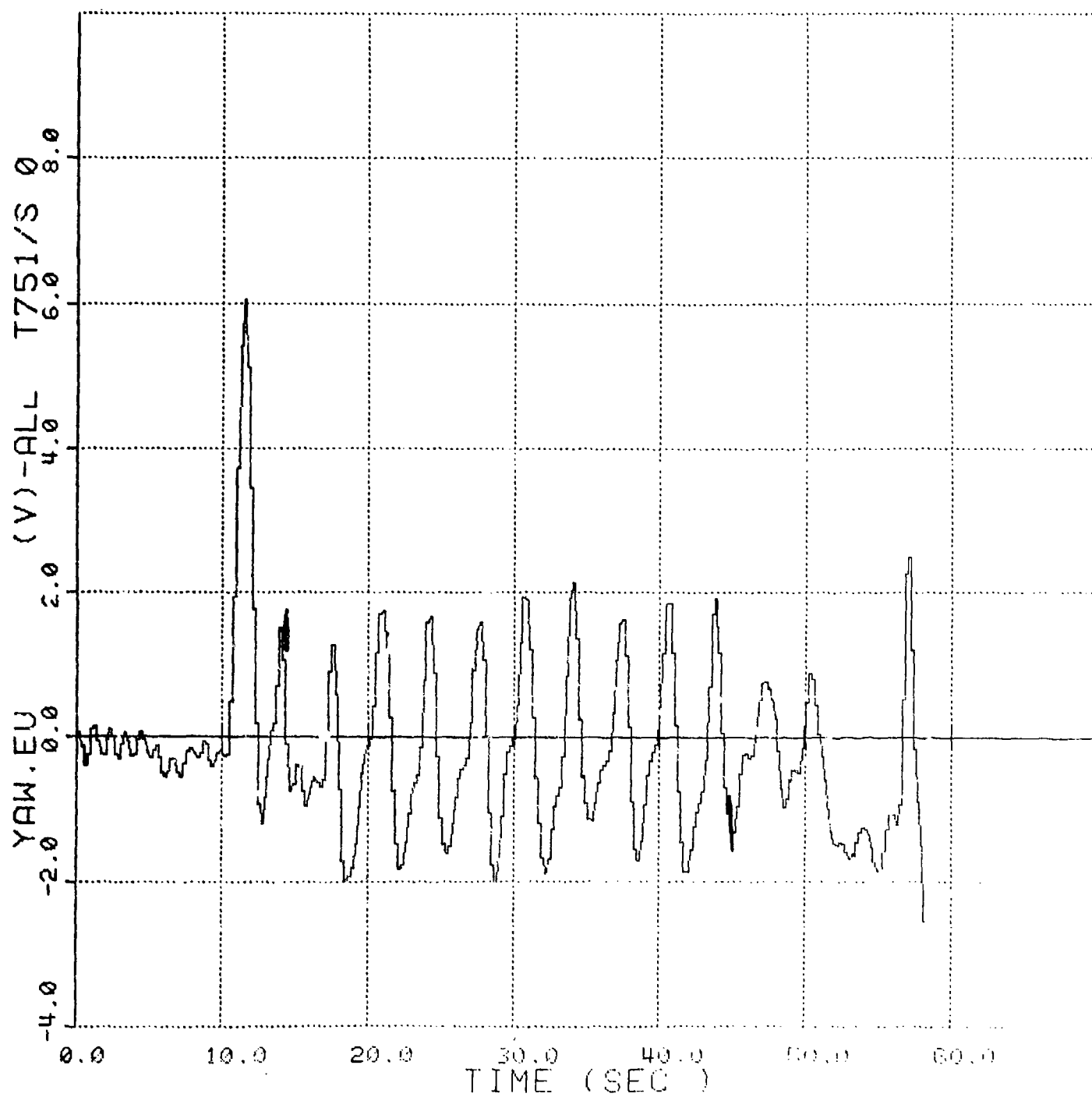


Figure No. 12 . Towed Submersible's Yaw vs Time, Case 11



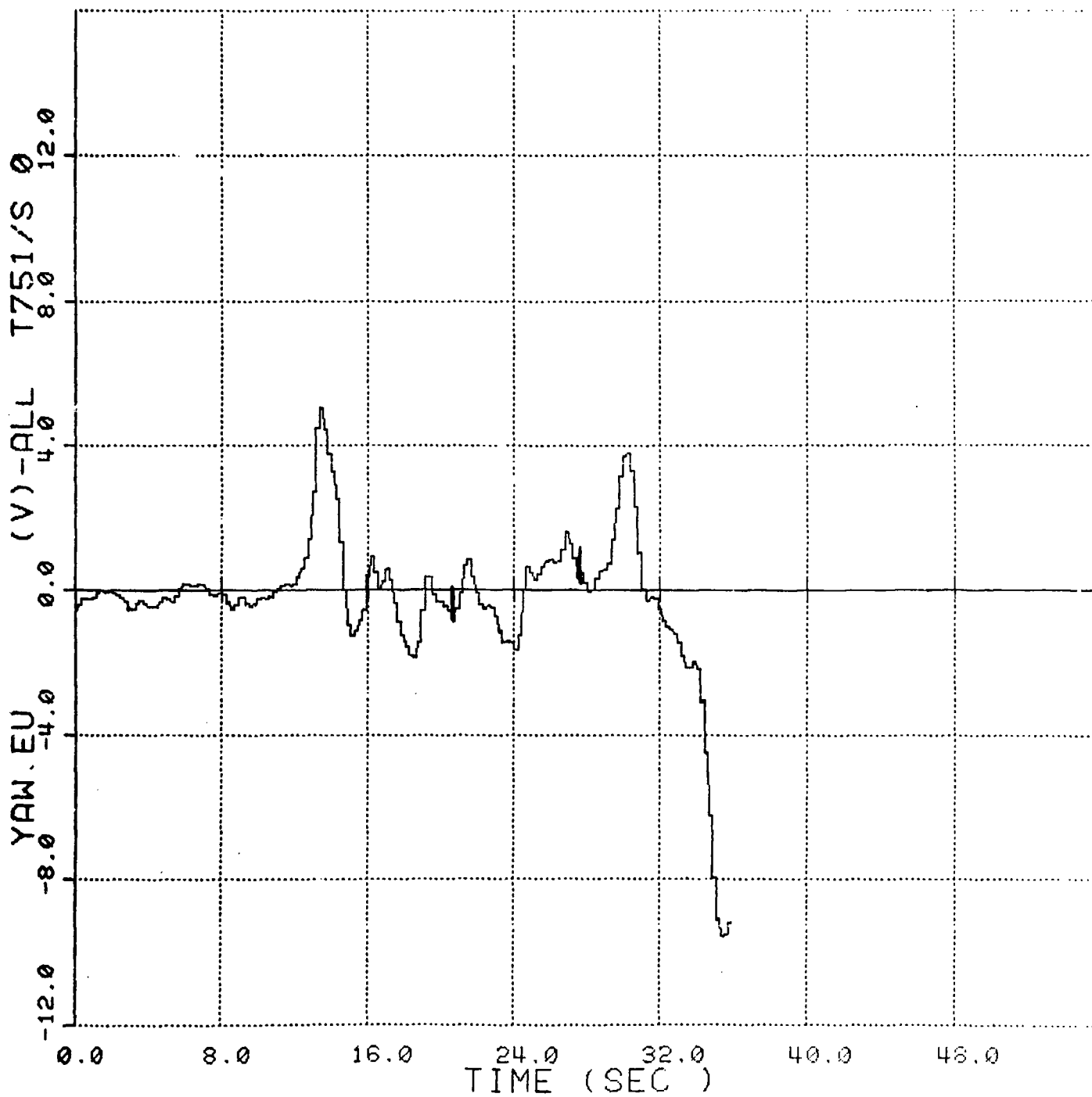


Figure No. 124. Towed Submersible's Yaw vs Time, Case 12



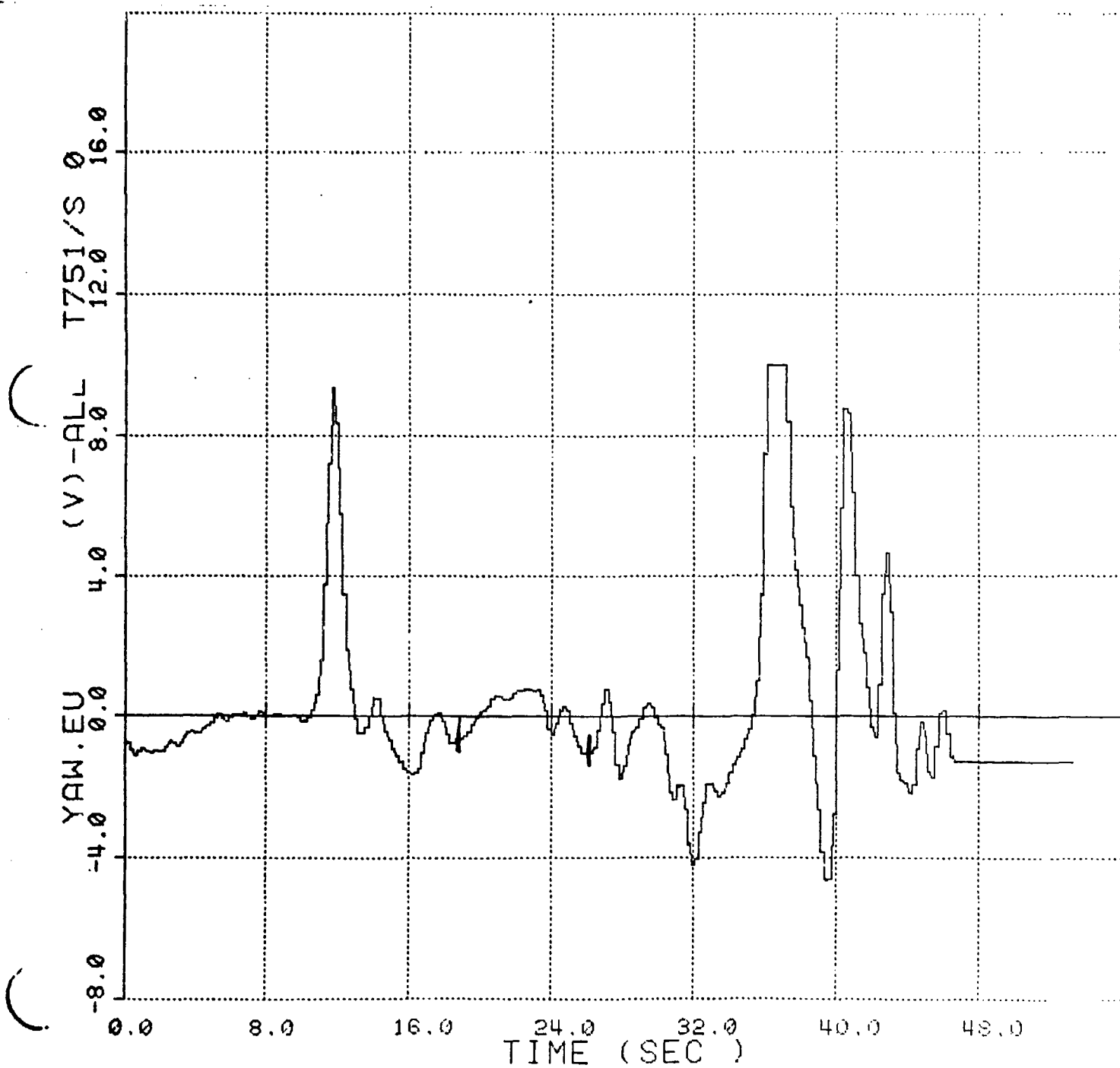


Figure No. 125. Towed Submersible's Yaw vs Time, Case 13



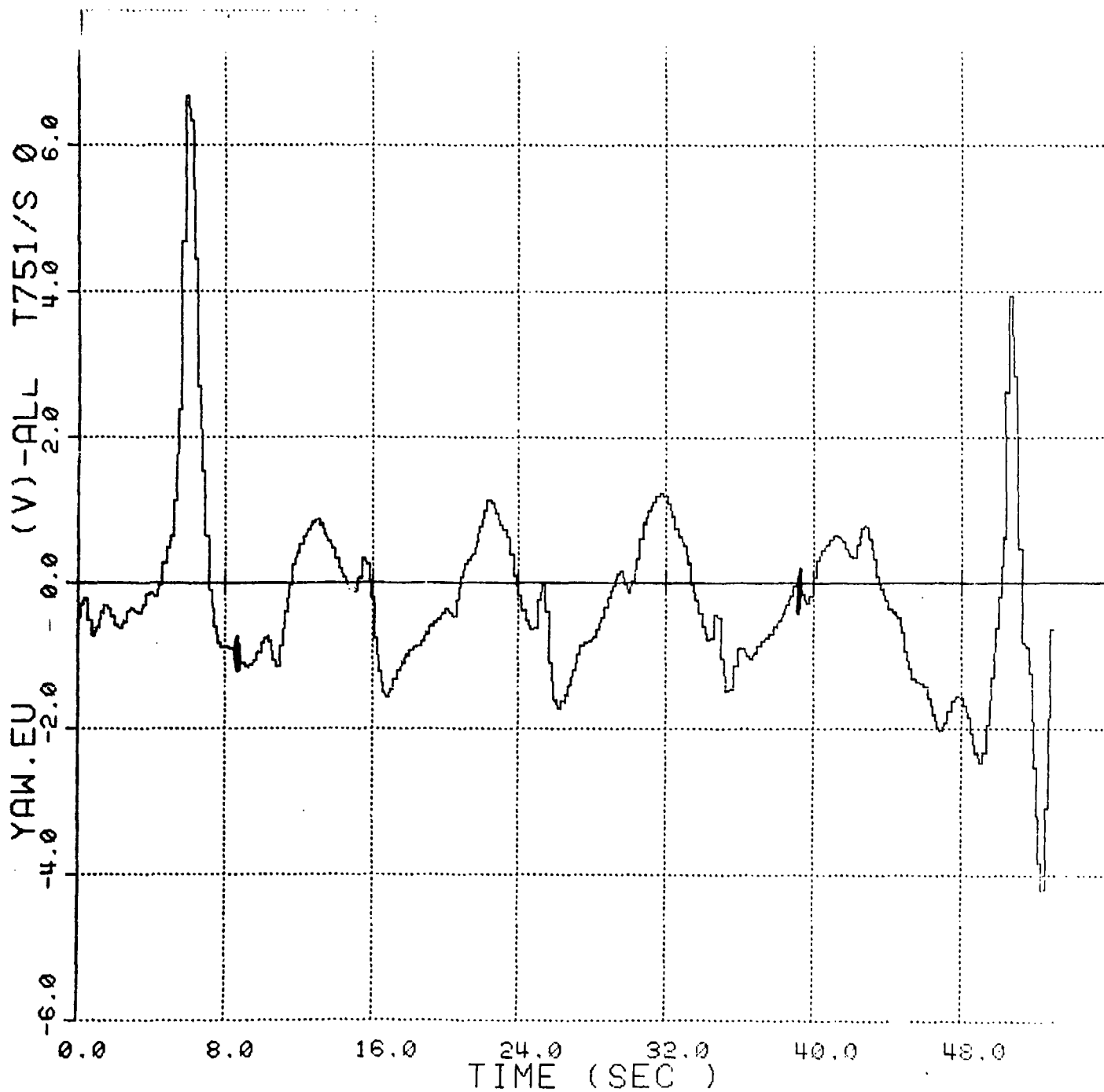


Figure No. 126. Towed Submersible's Yaw vs Time, Case 14



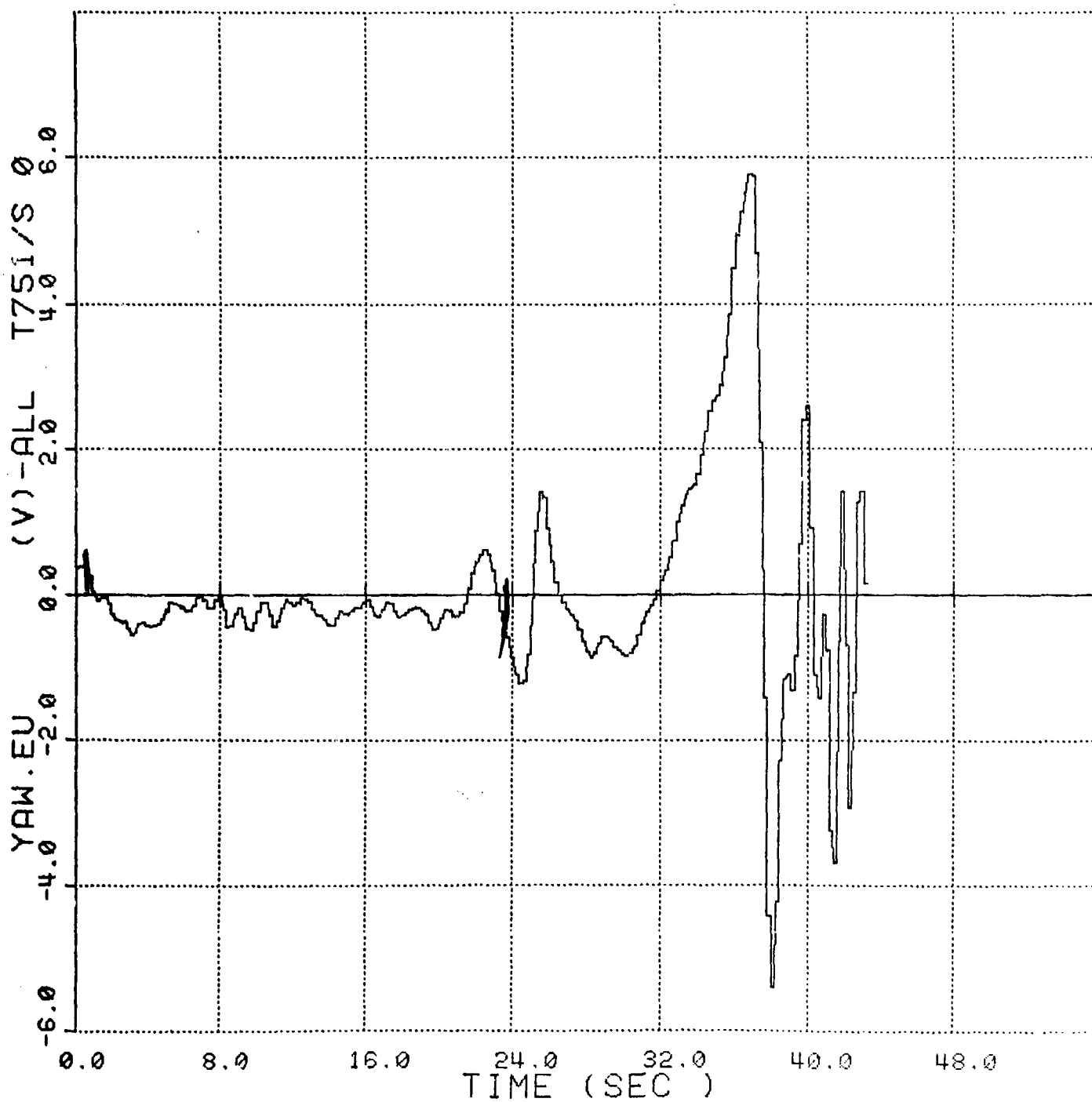


Figure No. 127. Towed Submersible's Yaw vs Time, Case 15



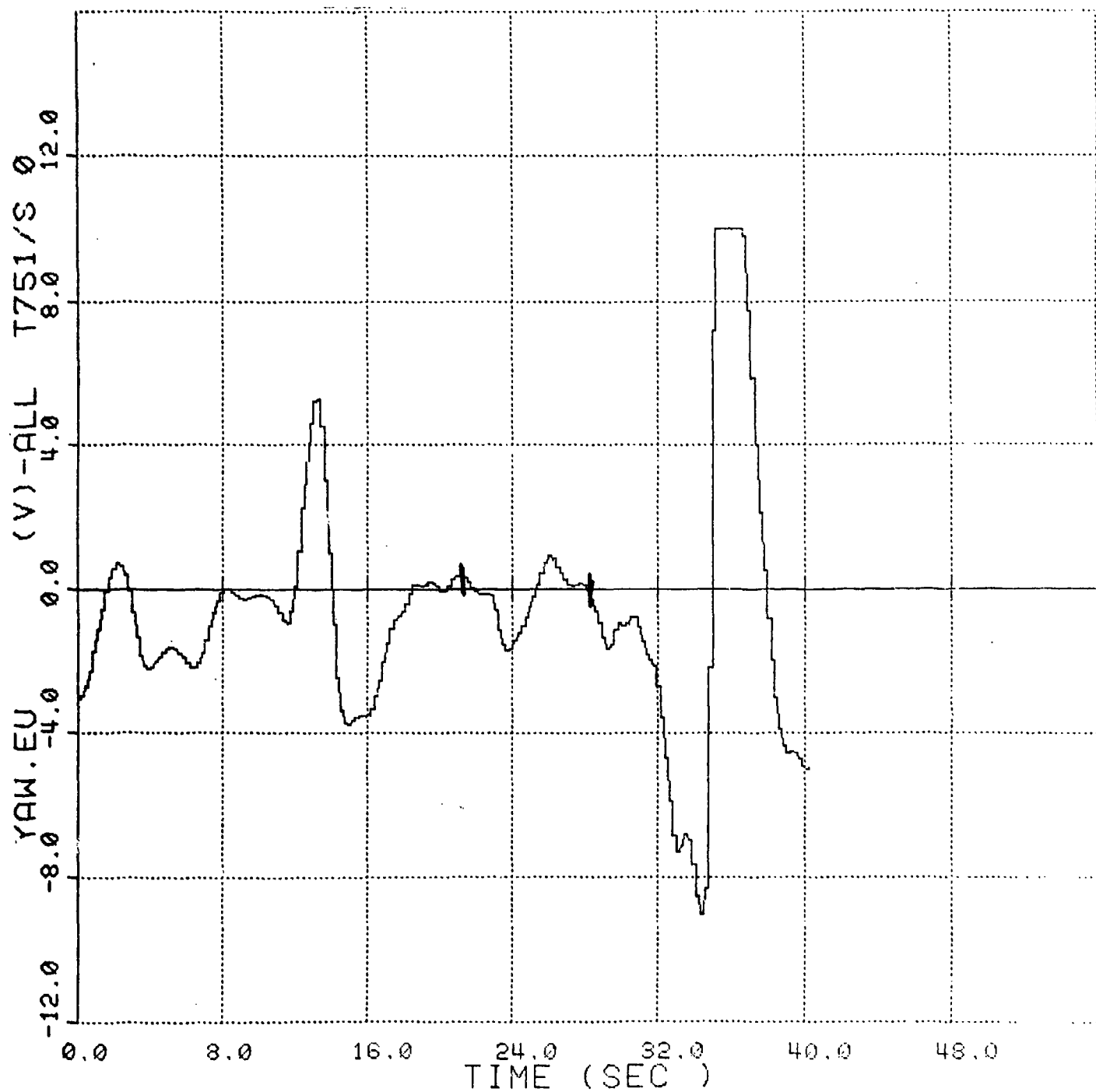


Figure No. 128. Towed Submersible's Yaw vs Time, Case 16



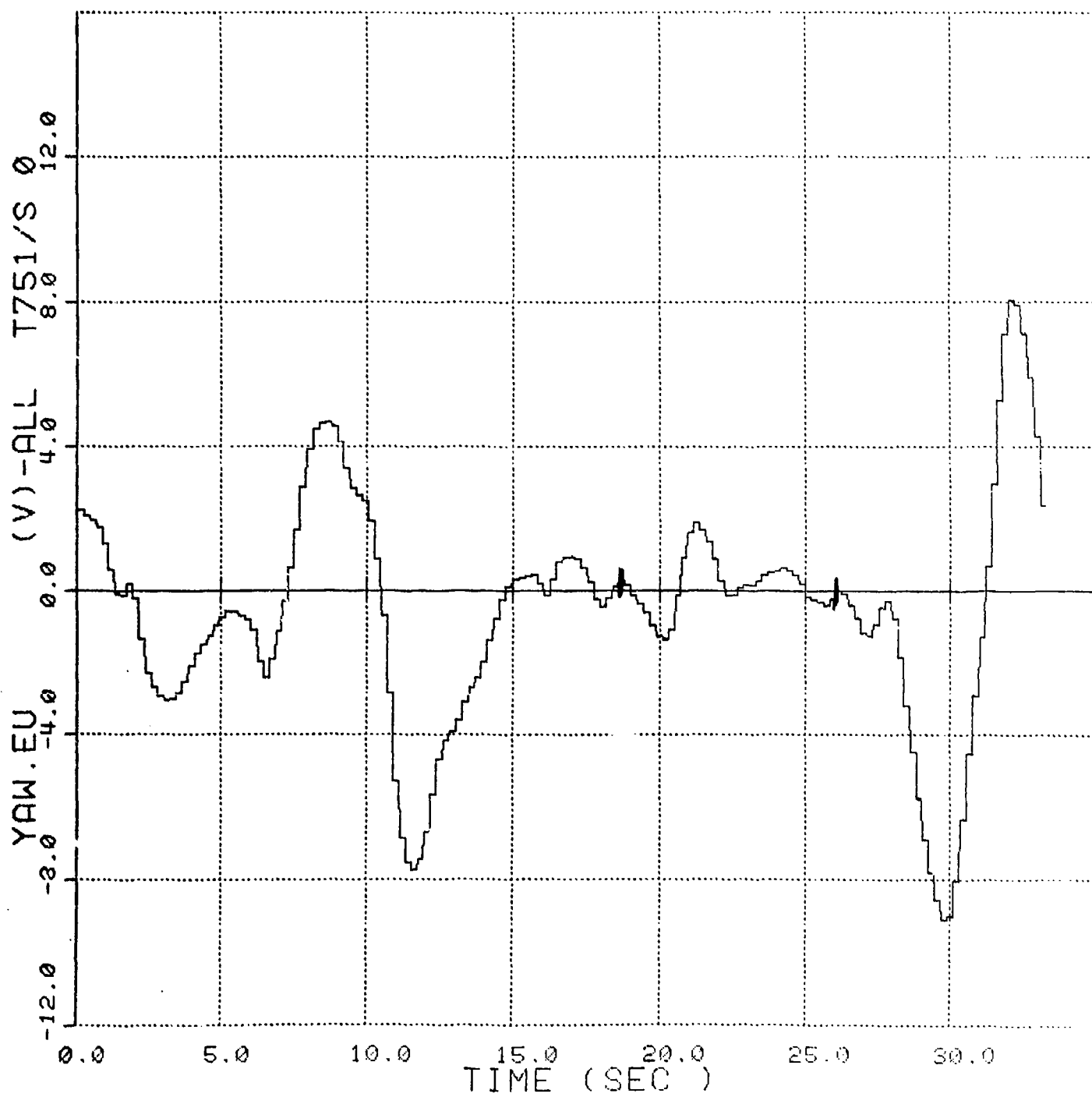


Figure No. 129. Towed Submersible's Yaw vs Time, Case 17



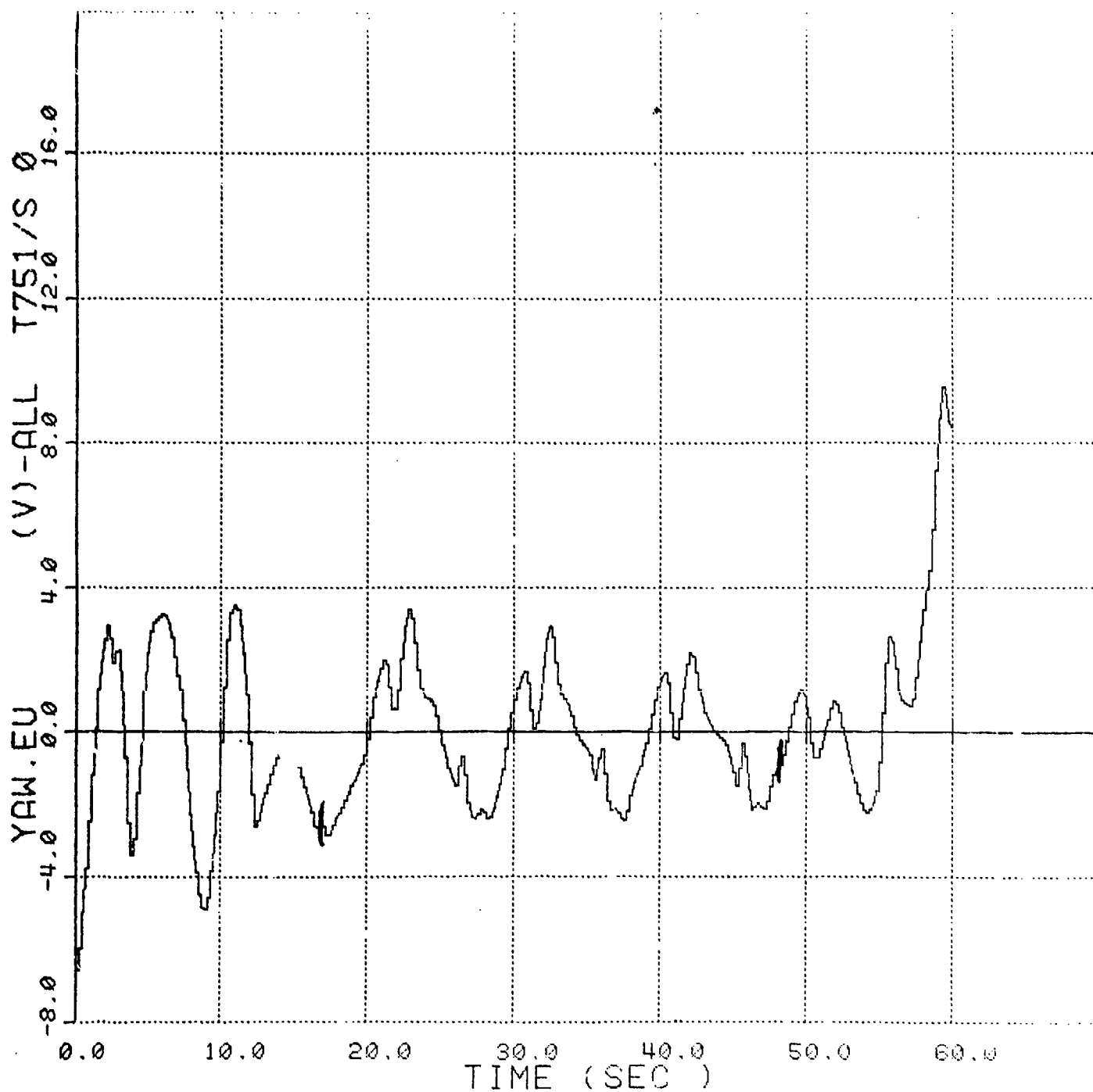


Figure No. 130. Towed Submersible's Yaw vs Time, Case 18



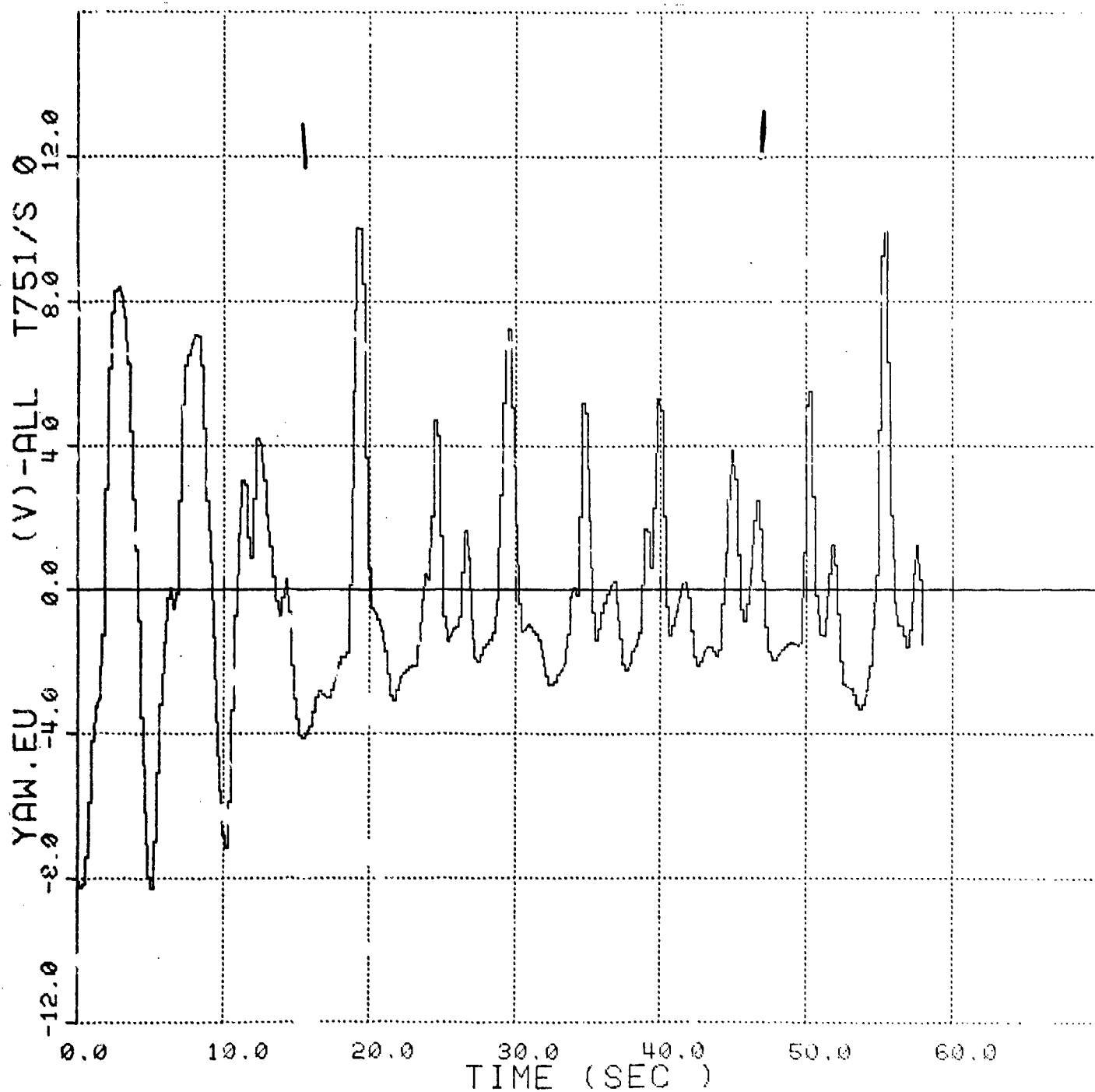


Figure No. 131. Towed Submersible's Yaw vs Time, Case 19



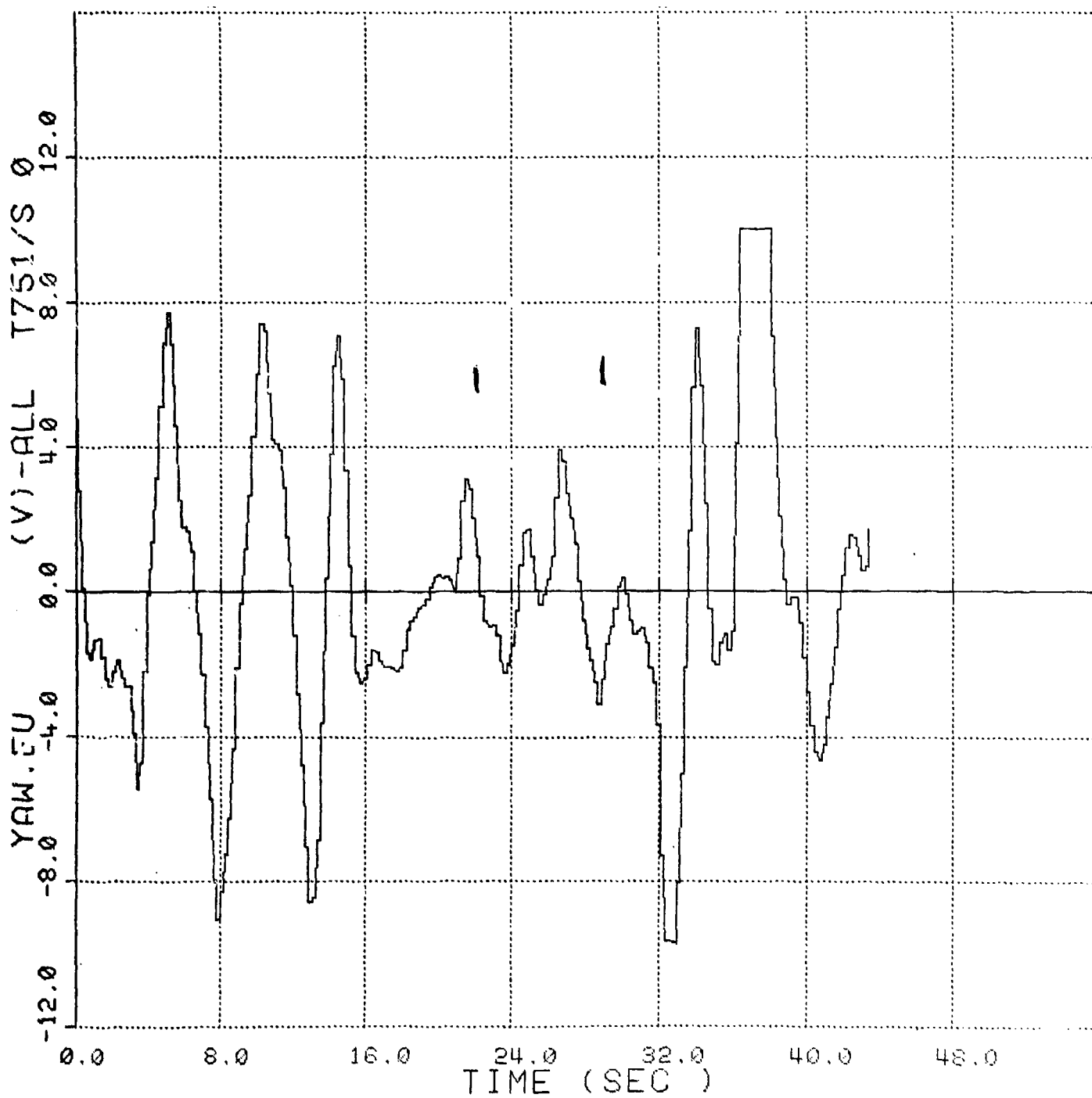


Figure No. 132. Towed Submersible's Yaw vs Time, Case 20



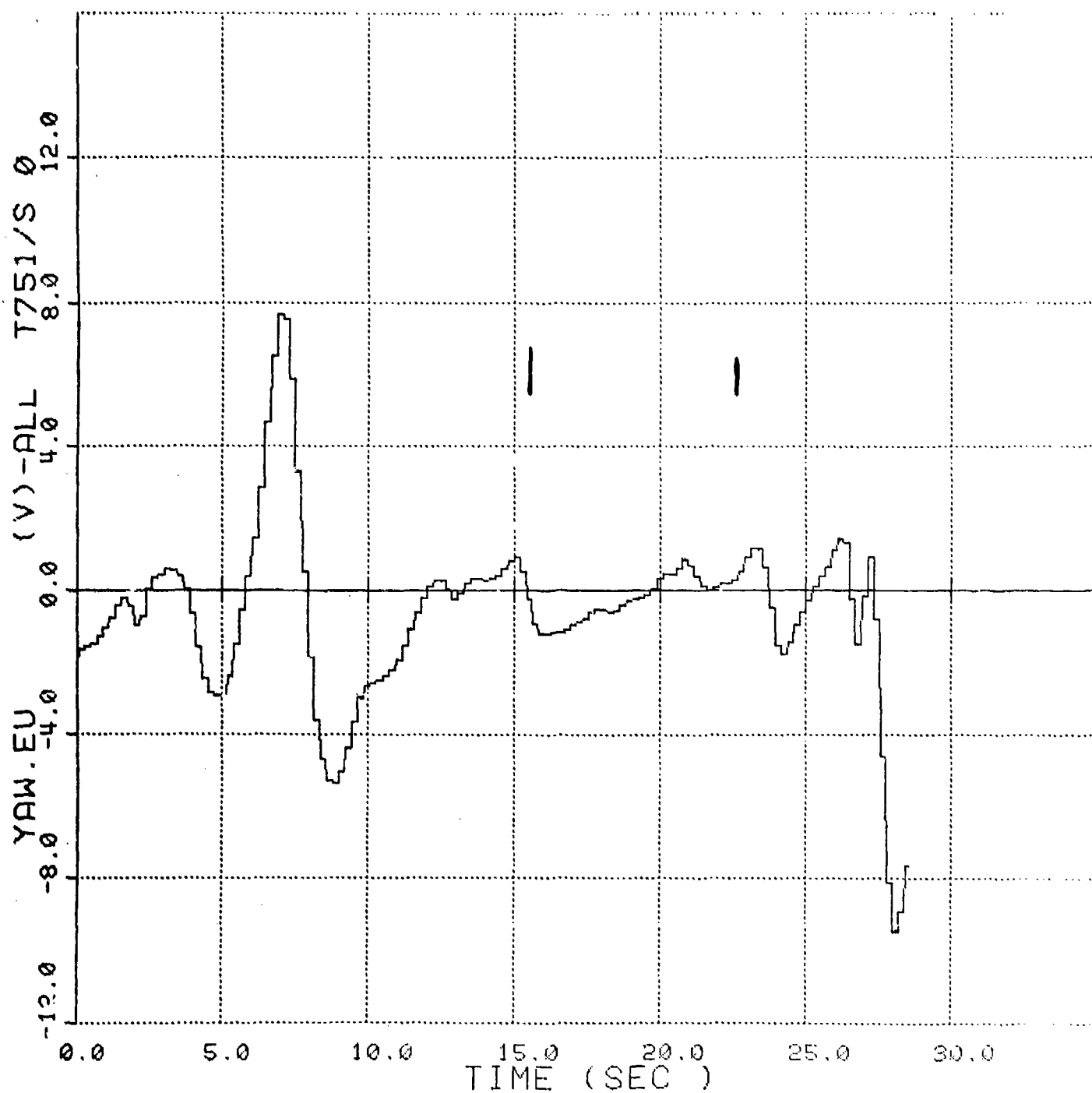


Figure No. 133. Towed Submersible's Yaw vs Time, Case 21



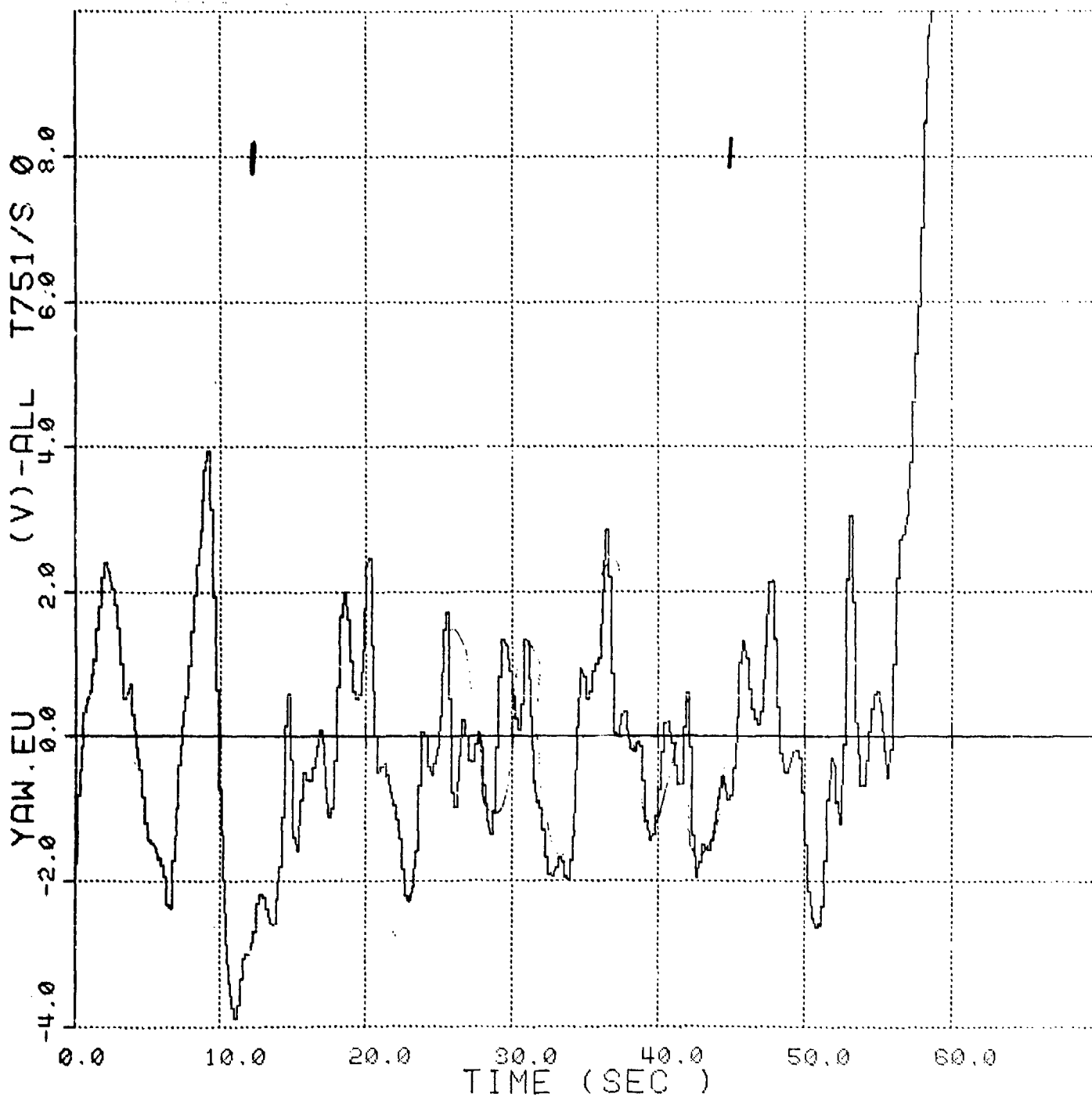


Figure No. 134. Towed Submersible's Yaw vs Time, Case 22



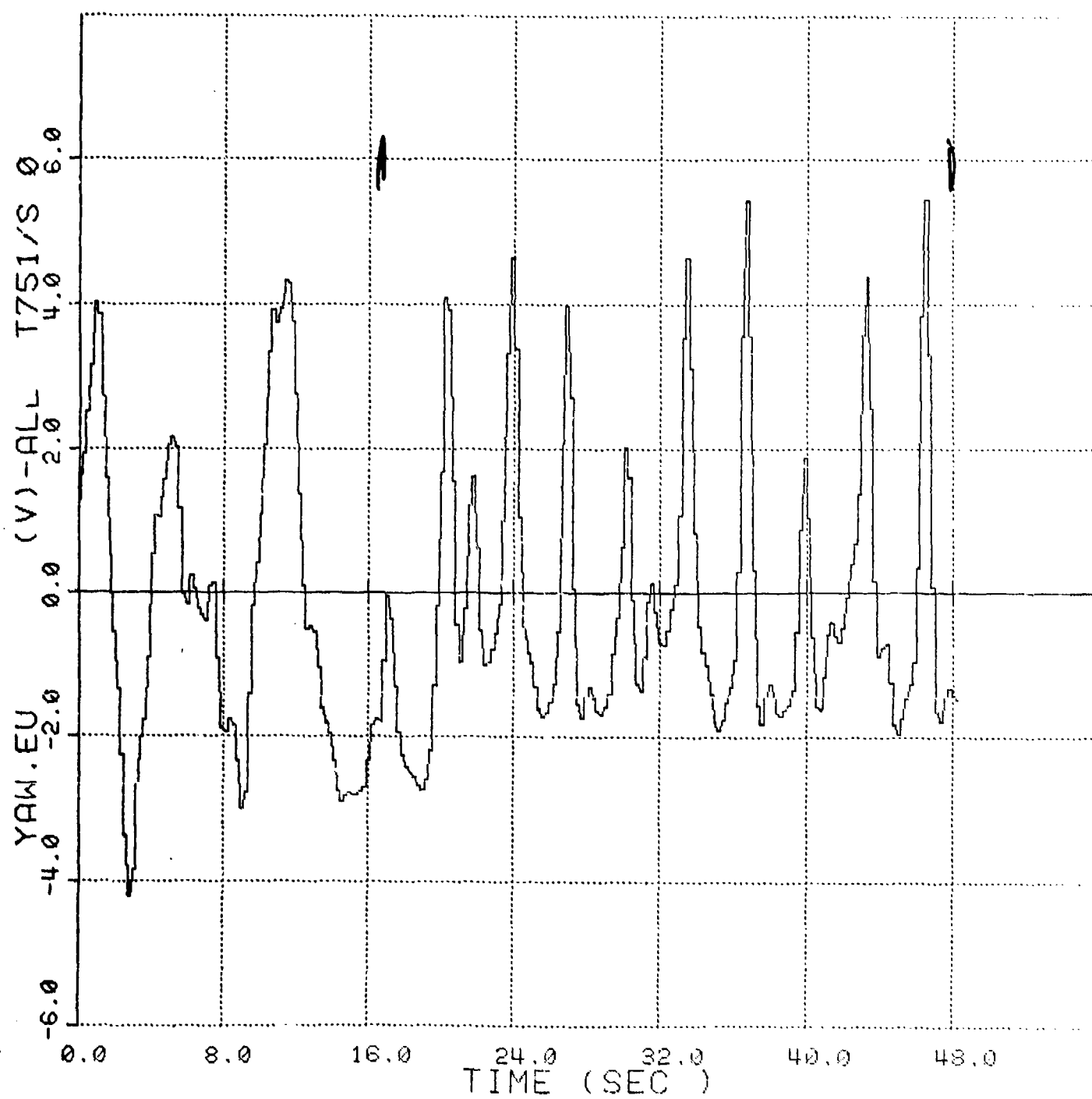


Figure No. 135. Towed Submersible's Yaw vs Time, Case 23



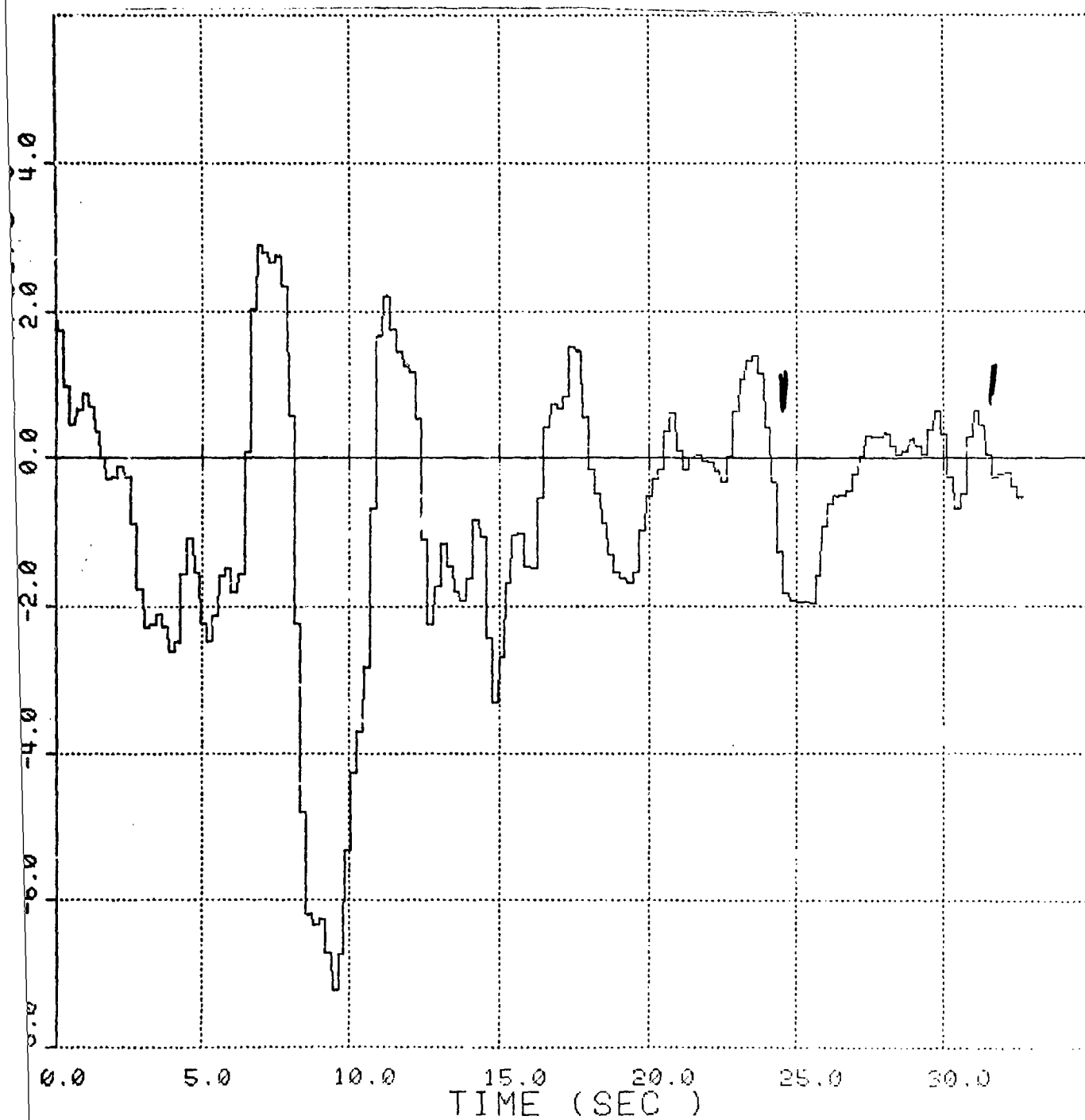


Figure No. 136. Towed Submersible's Yaw vs Time, Case 24



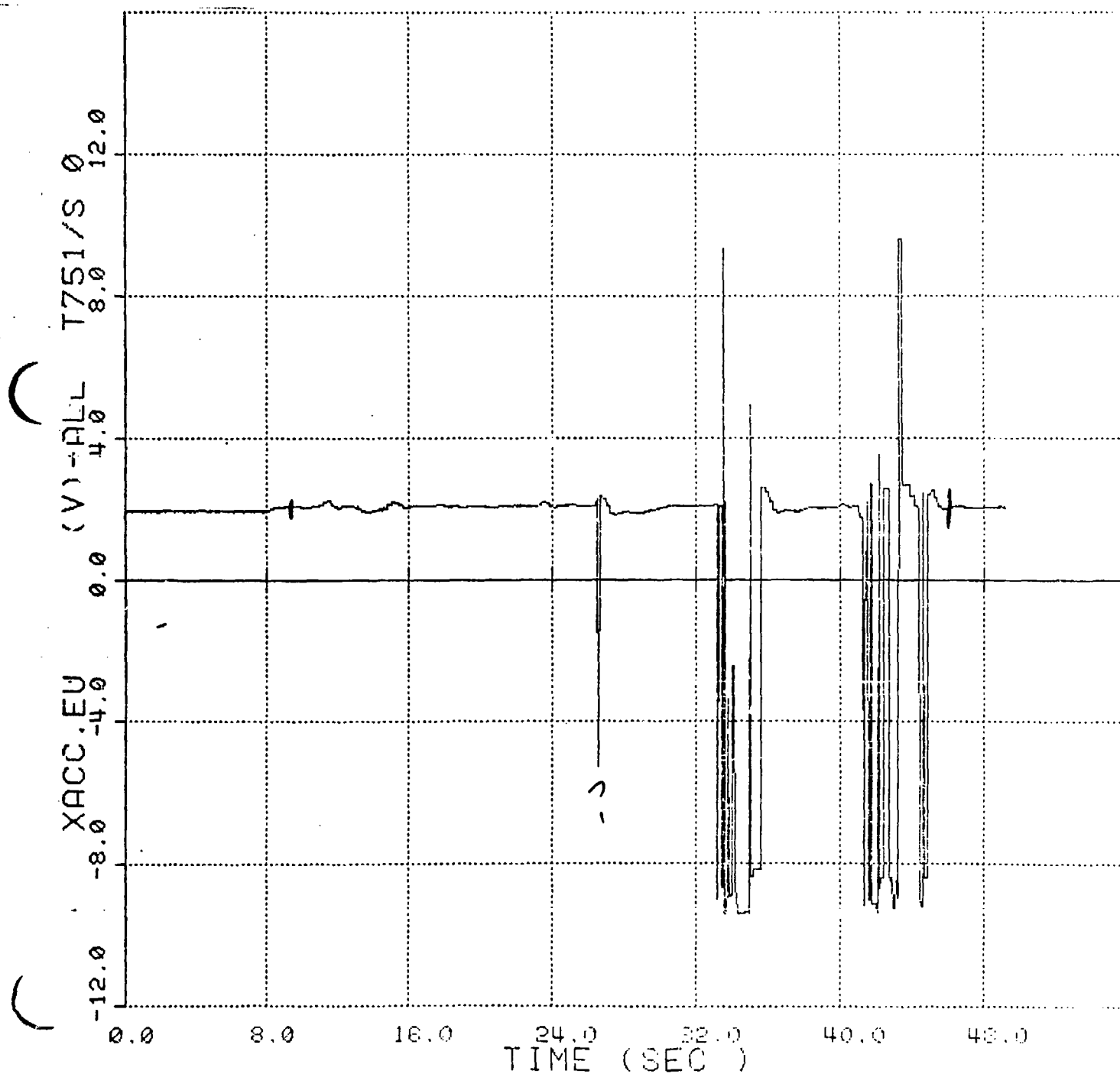


Figure No. 137. Towed Submersible's Longitudinal Acceleration vs Time, Case 2



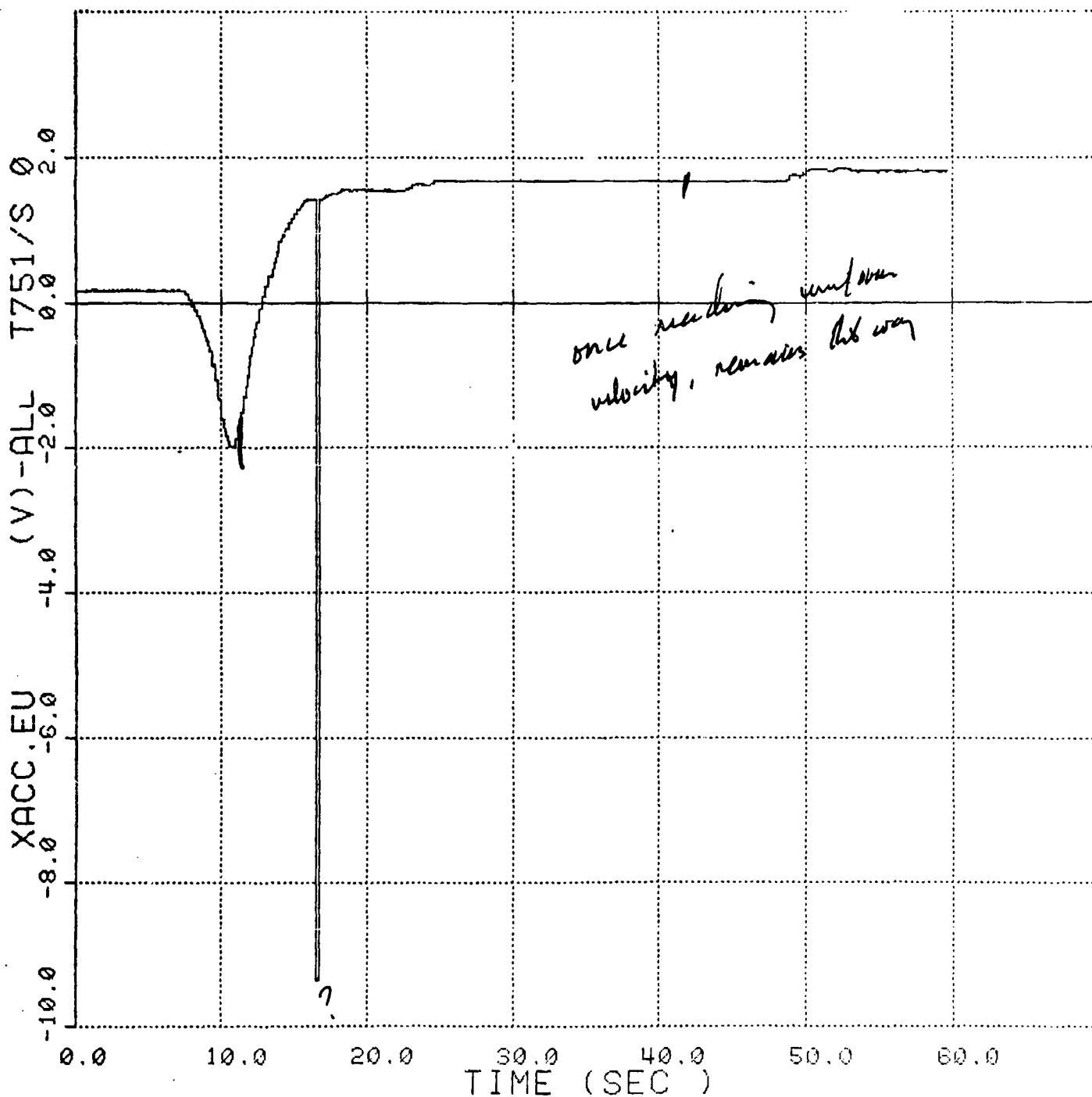


Figure No. 138. Towed Submersible's Longitudinal Acceleration vs Time, Case 3



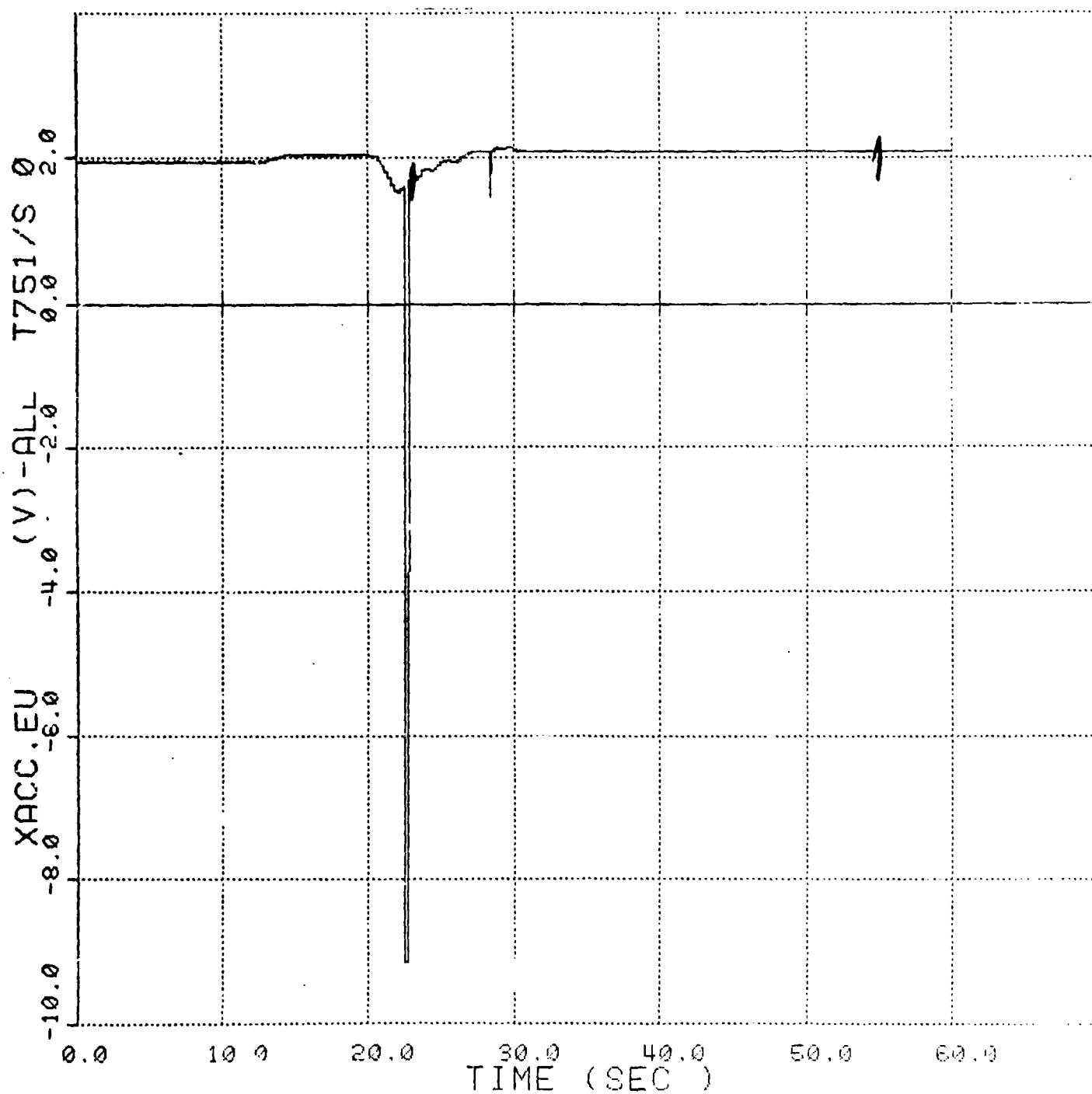


Figure No. 139. Towed Submersible's Longitudinal Acceleration vs Time, Case 4



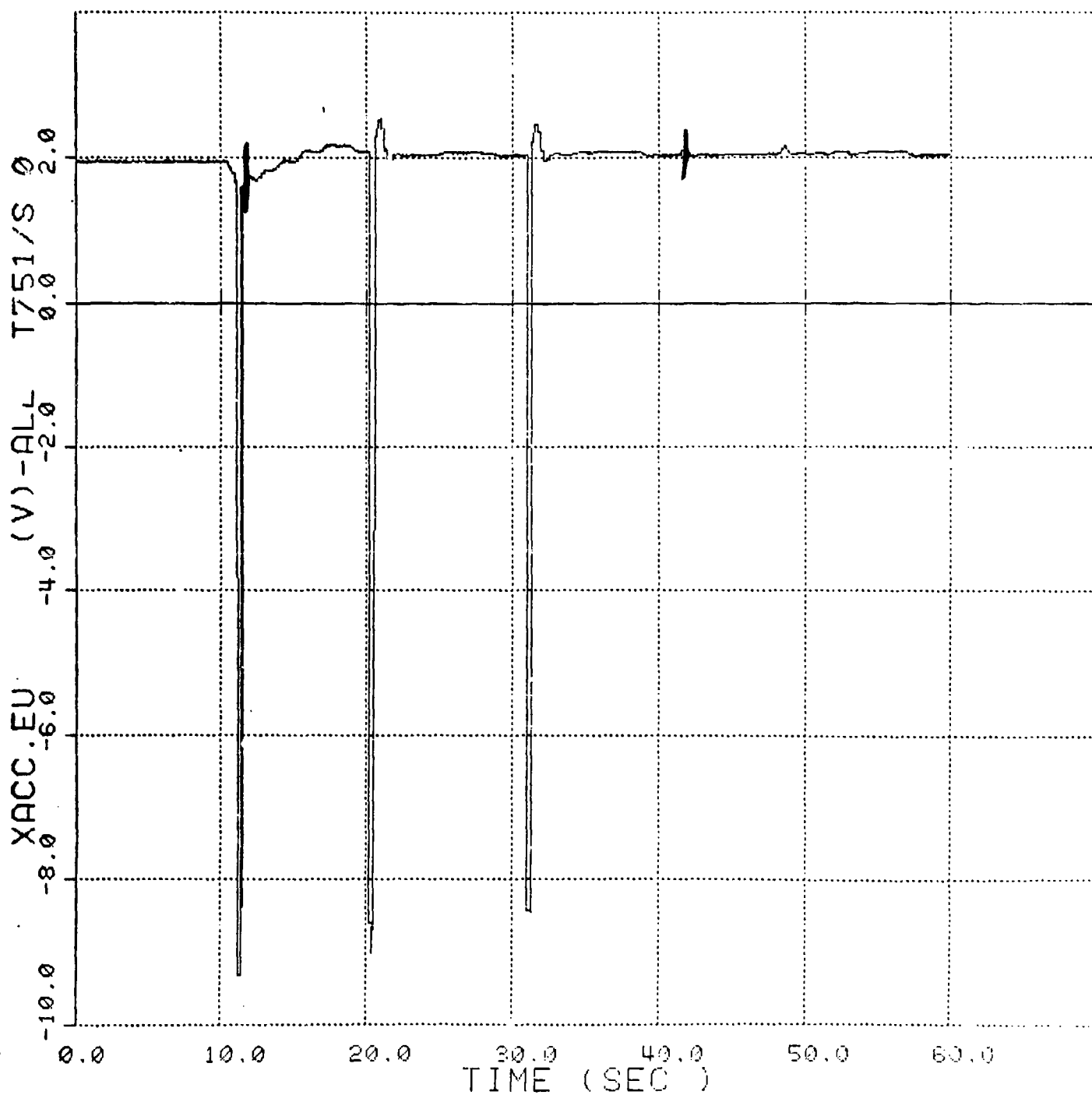


Figure No. 140. Towed Submersible's Longitudinal Acceleration vs Time, Case 5



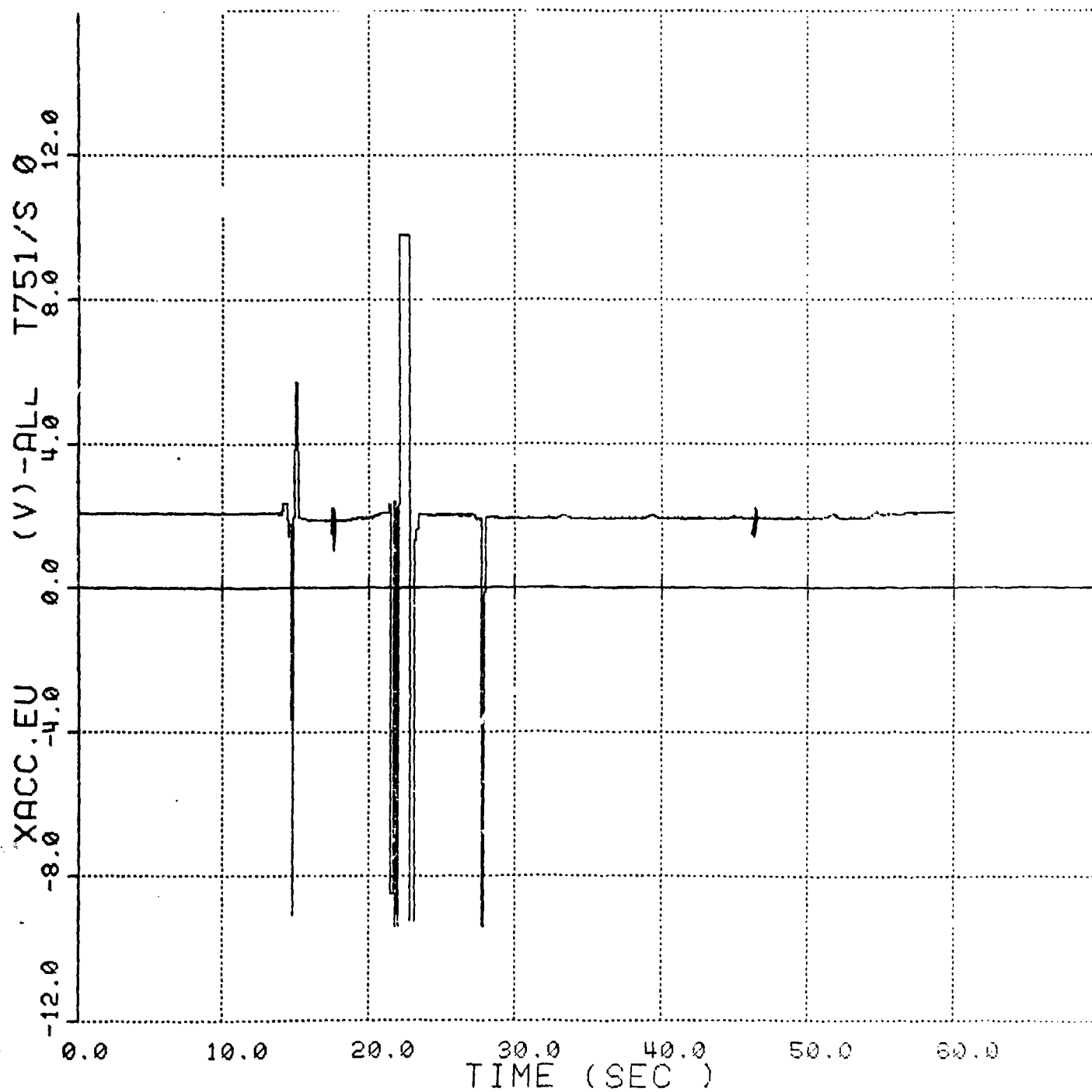


Figure No. 141. Towed Submersible's Longitudinal Acceleration vs Time, Case 6



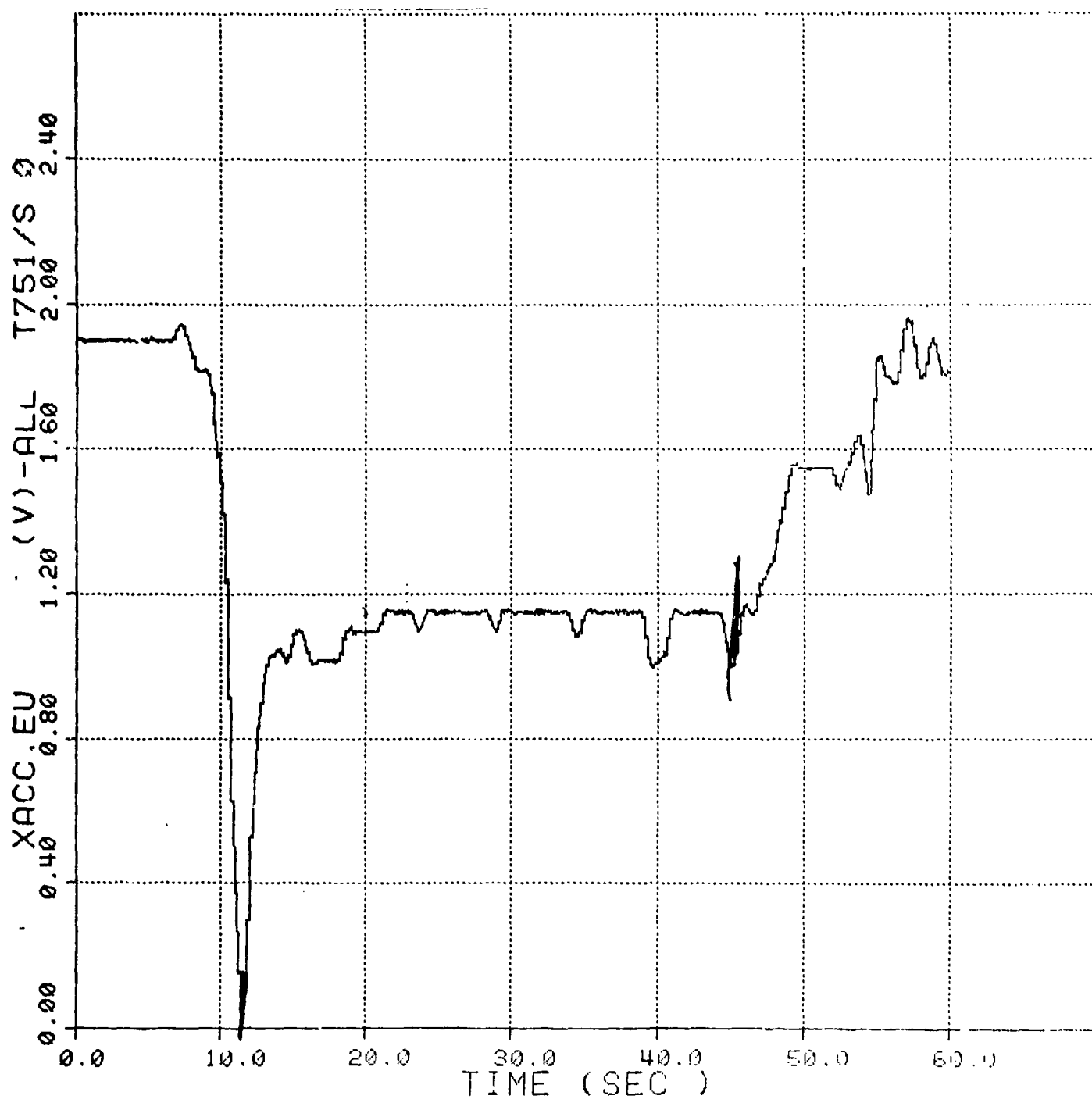


Figure No. 142. Towed Submersible's Longitudinal Acceleration vs Time, Case 7



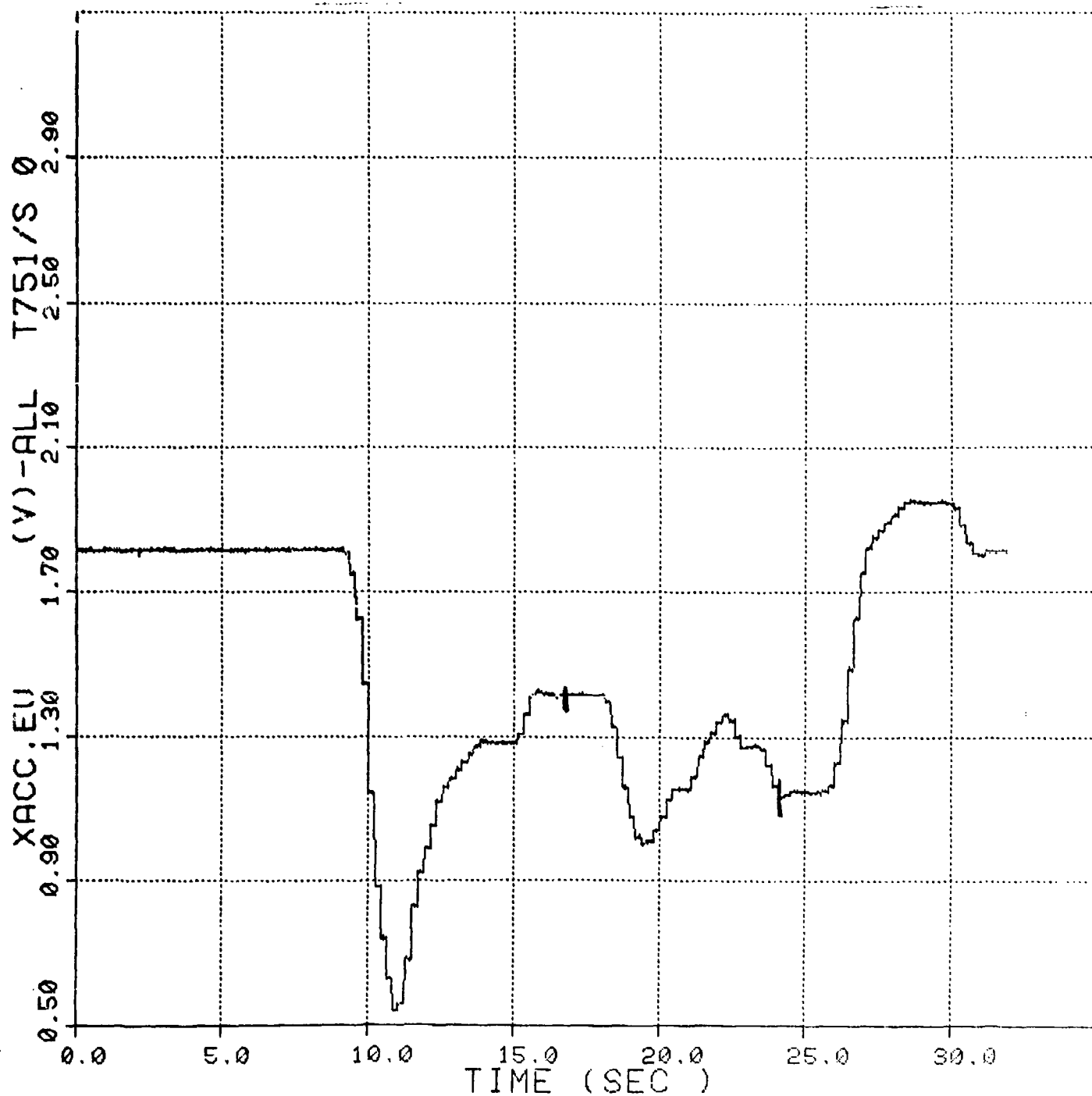


Figure No. 143. Towed Submersible's Longitudinal Acceleration vs Time, Case 9



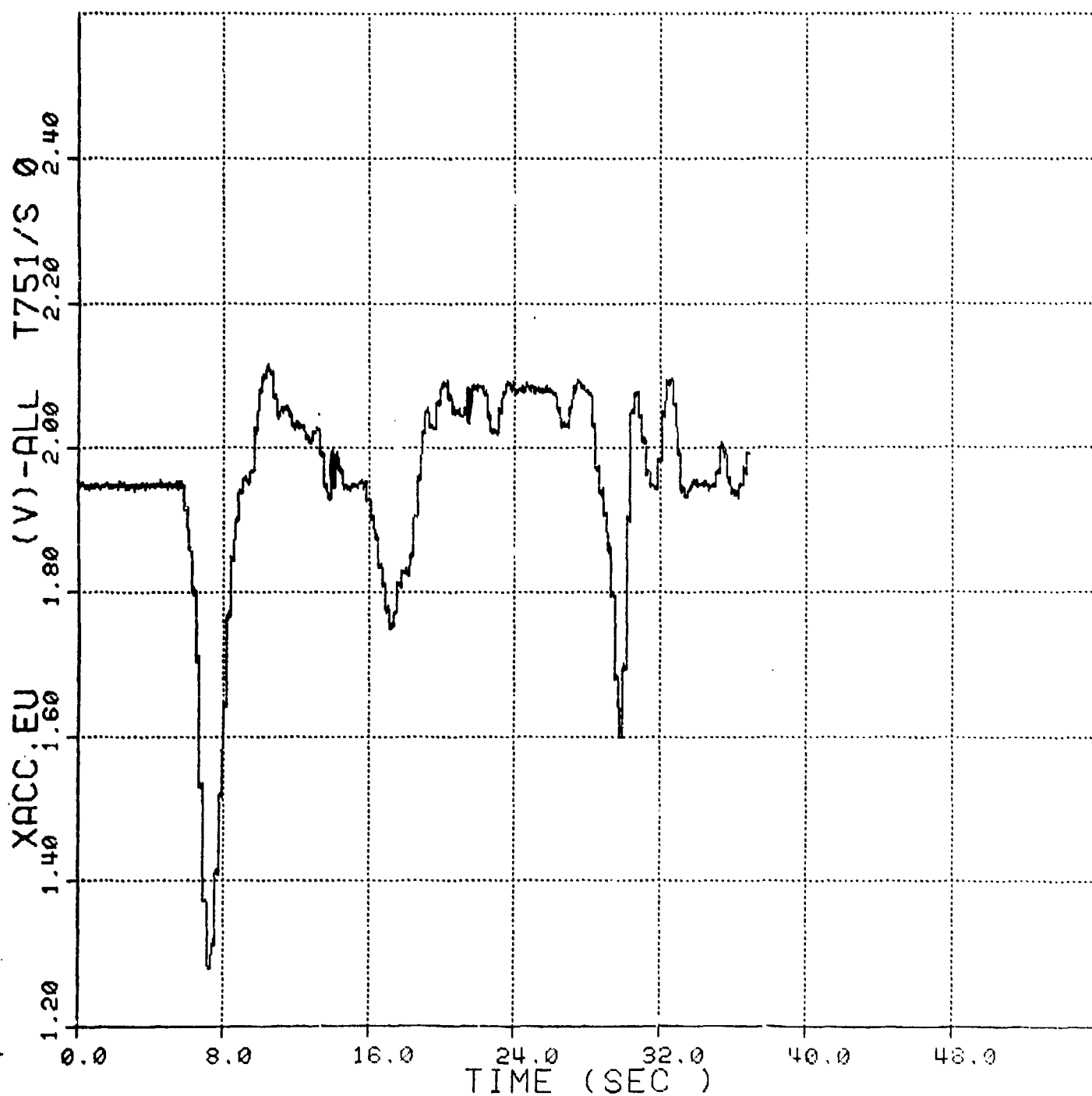


Figure No. 144. Towed Submersible's Longitudinal Acceleration vs Time, Case 10



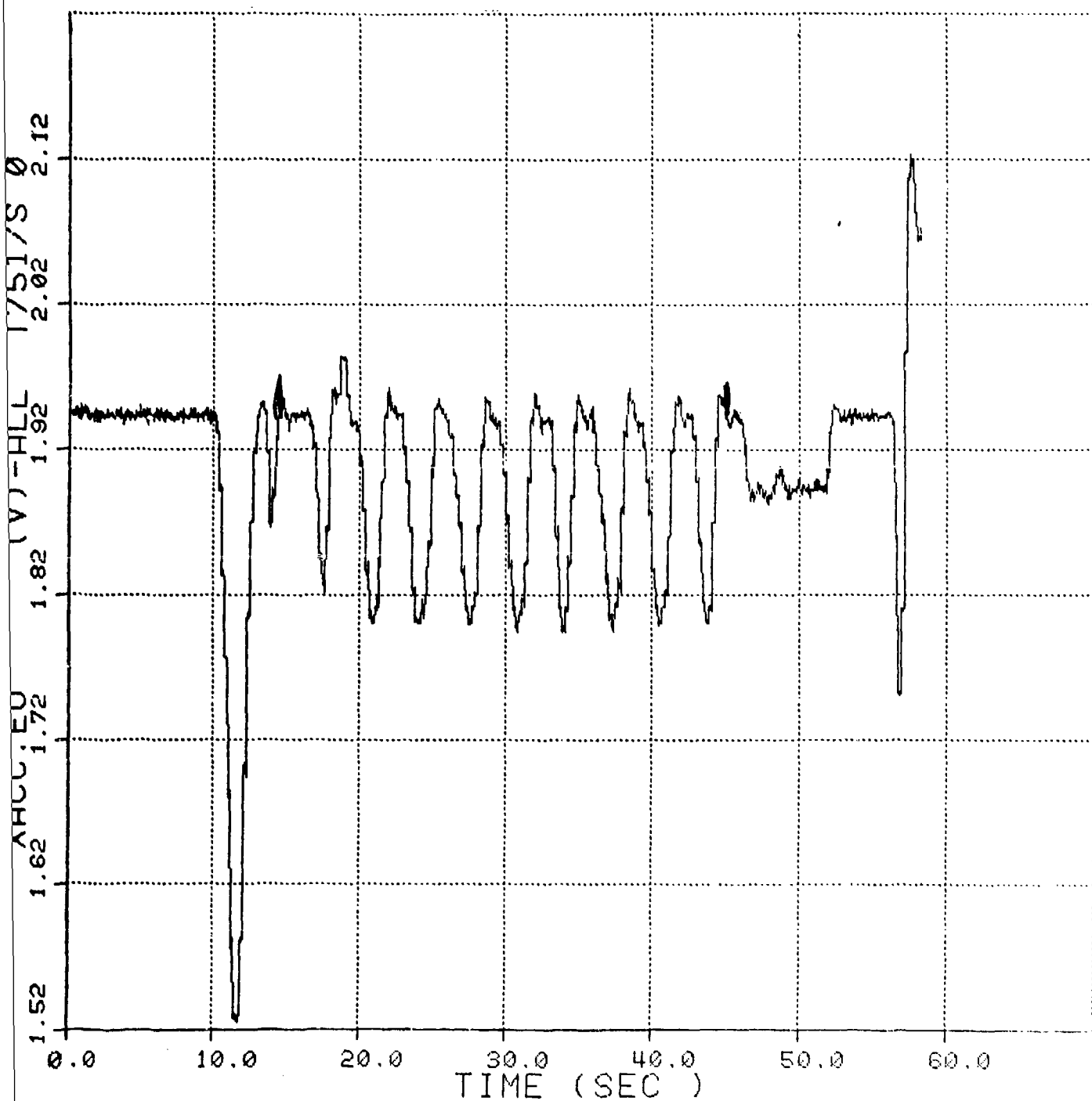


Figure No. 145. Towed Submersible's Longitudinal Acceleration vs Time, Case 11



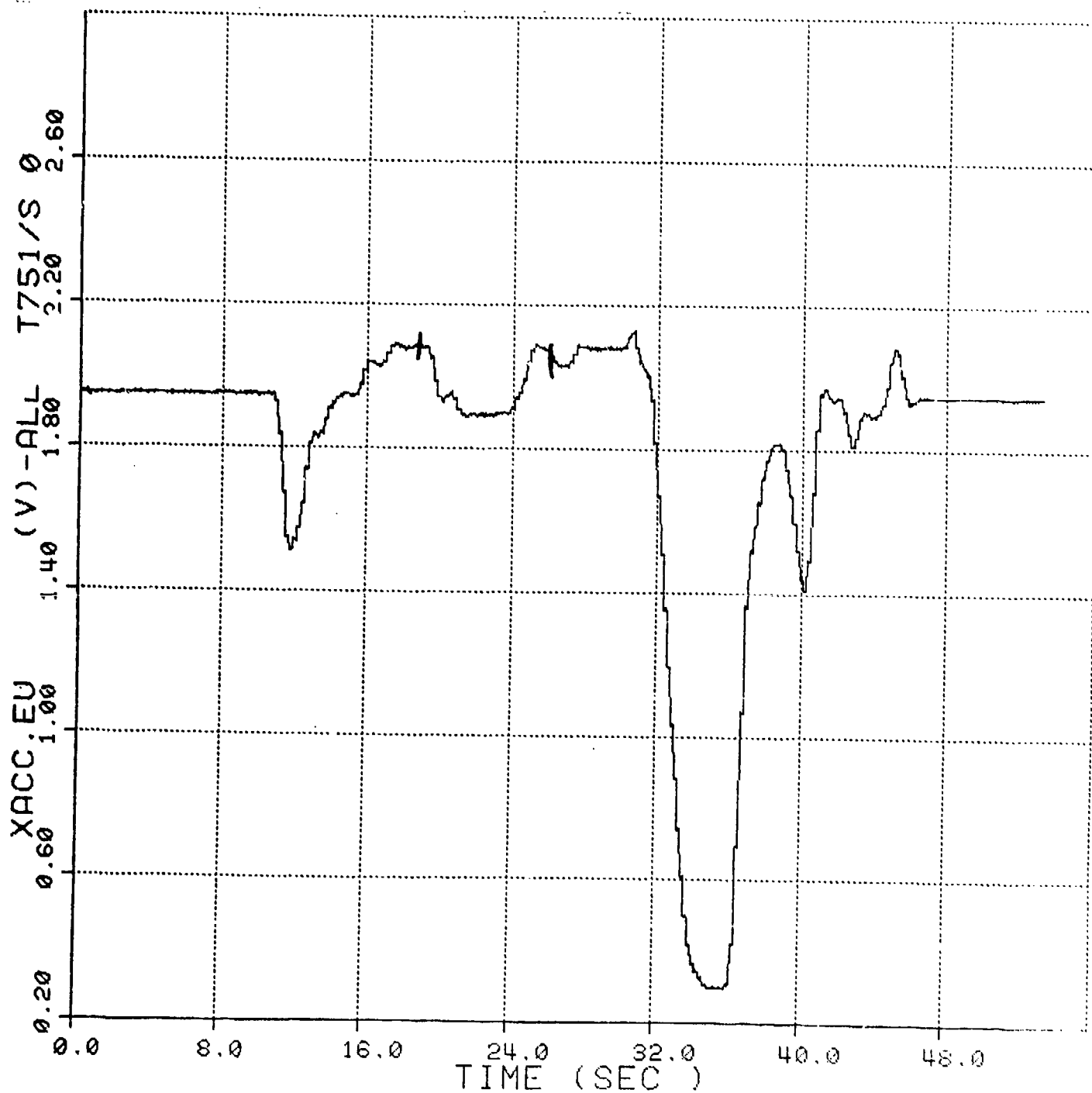


Figure No. 146. Towed Submersible's Longitudinal Acceleration vs Time, Case 13



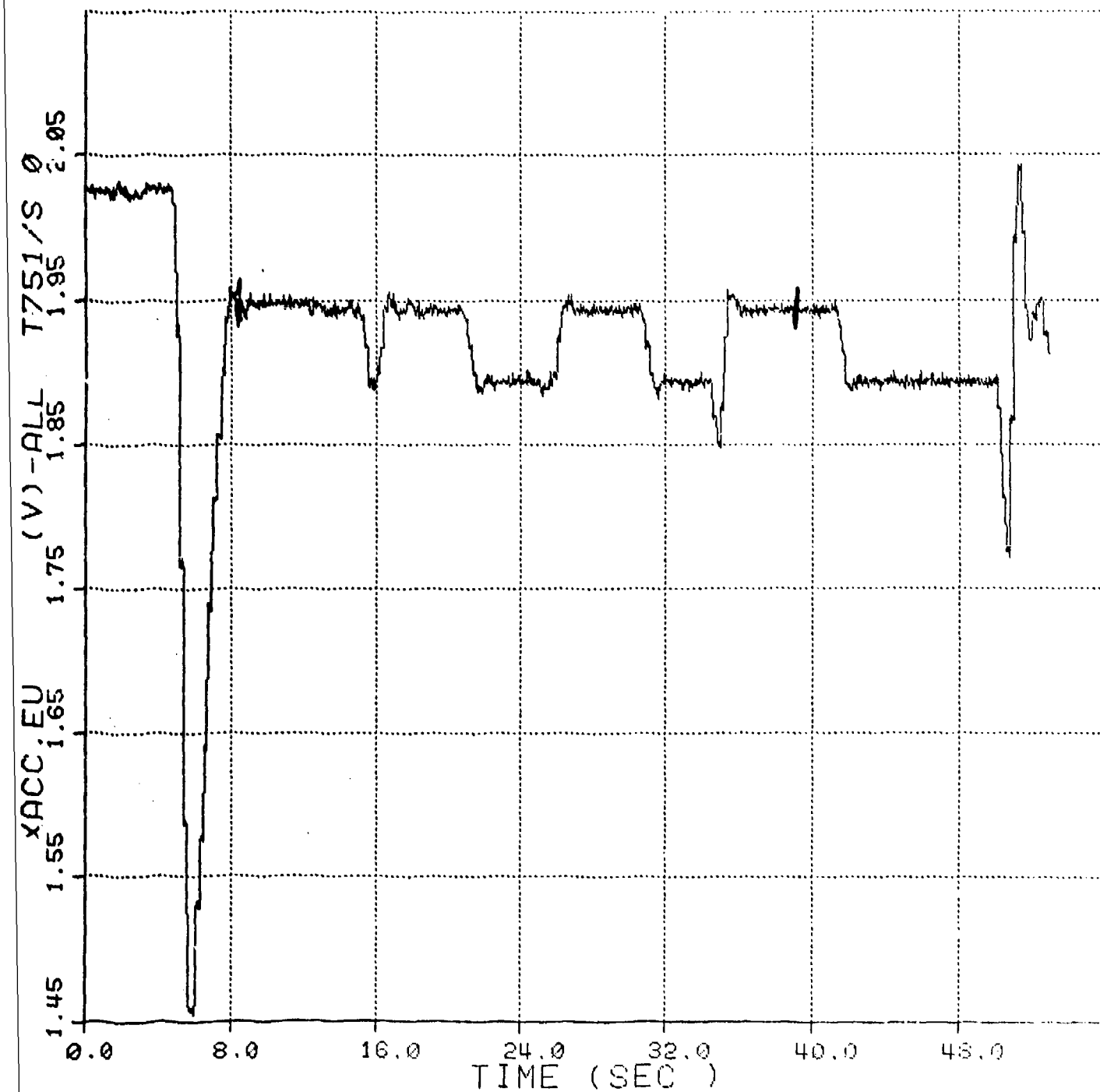


Figure No. 147. Towed Submersible's Longitudinal Acceleration vs Time, Case 14



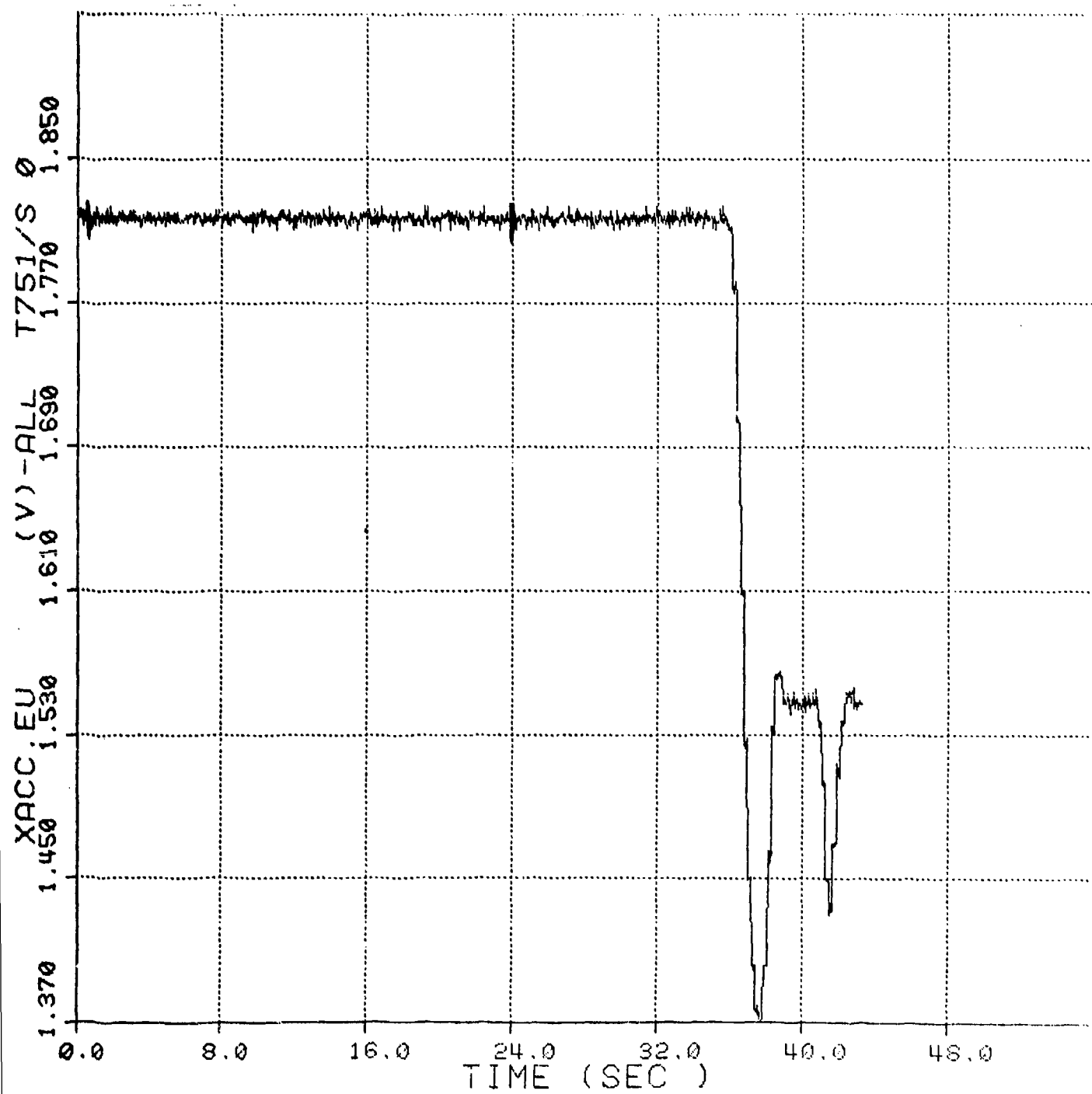


Figure No. 148. Towed Submersible's Longitudinal Acceleration vs Time, Case 15



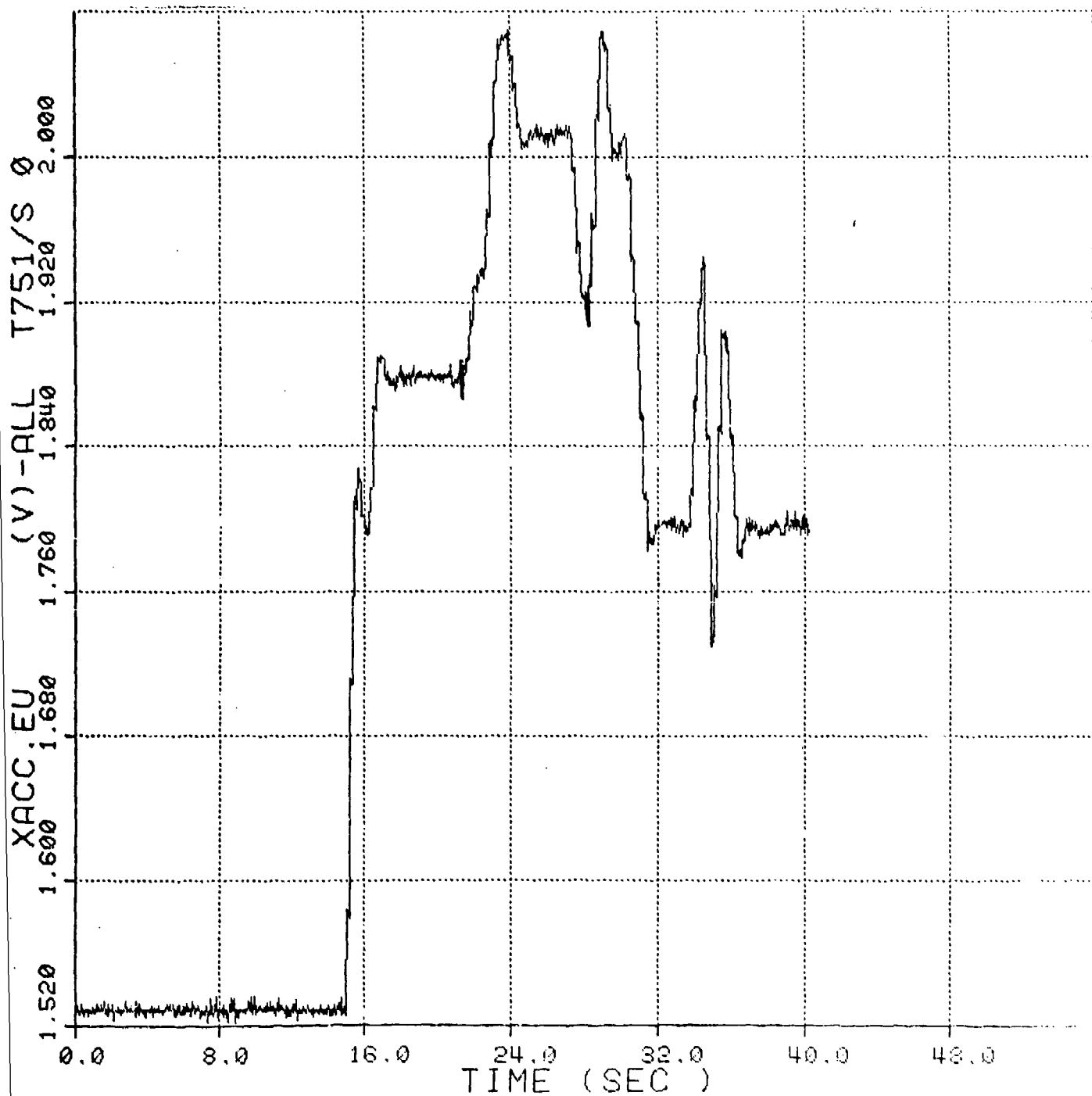


Figure No. 149. Towed Submersible's Longitudinal Acceleration vs Time, Case 16



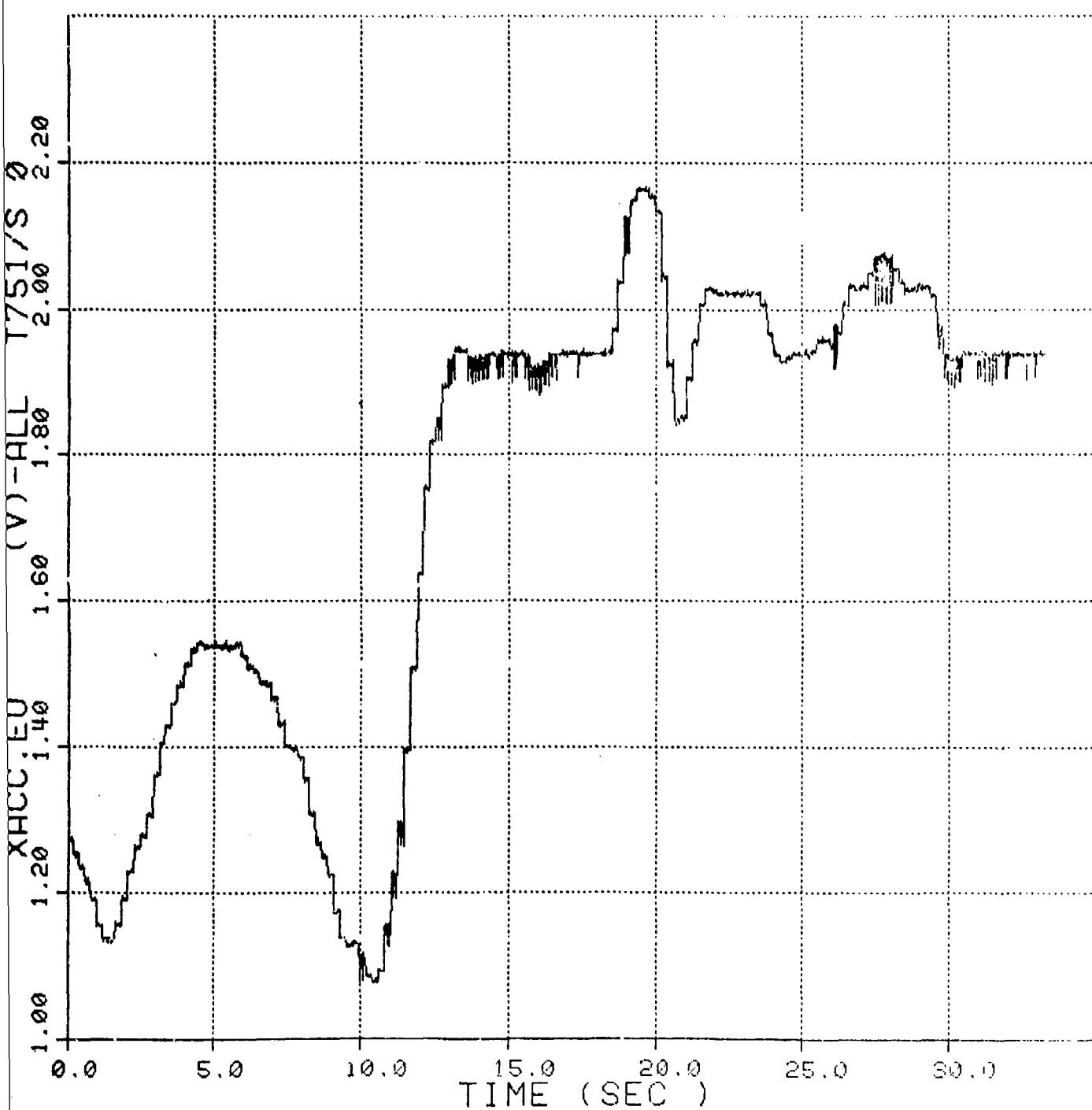


Figure No. 150. Towed Submersible's Longitudinal Acceleration vs Time, Case 17



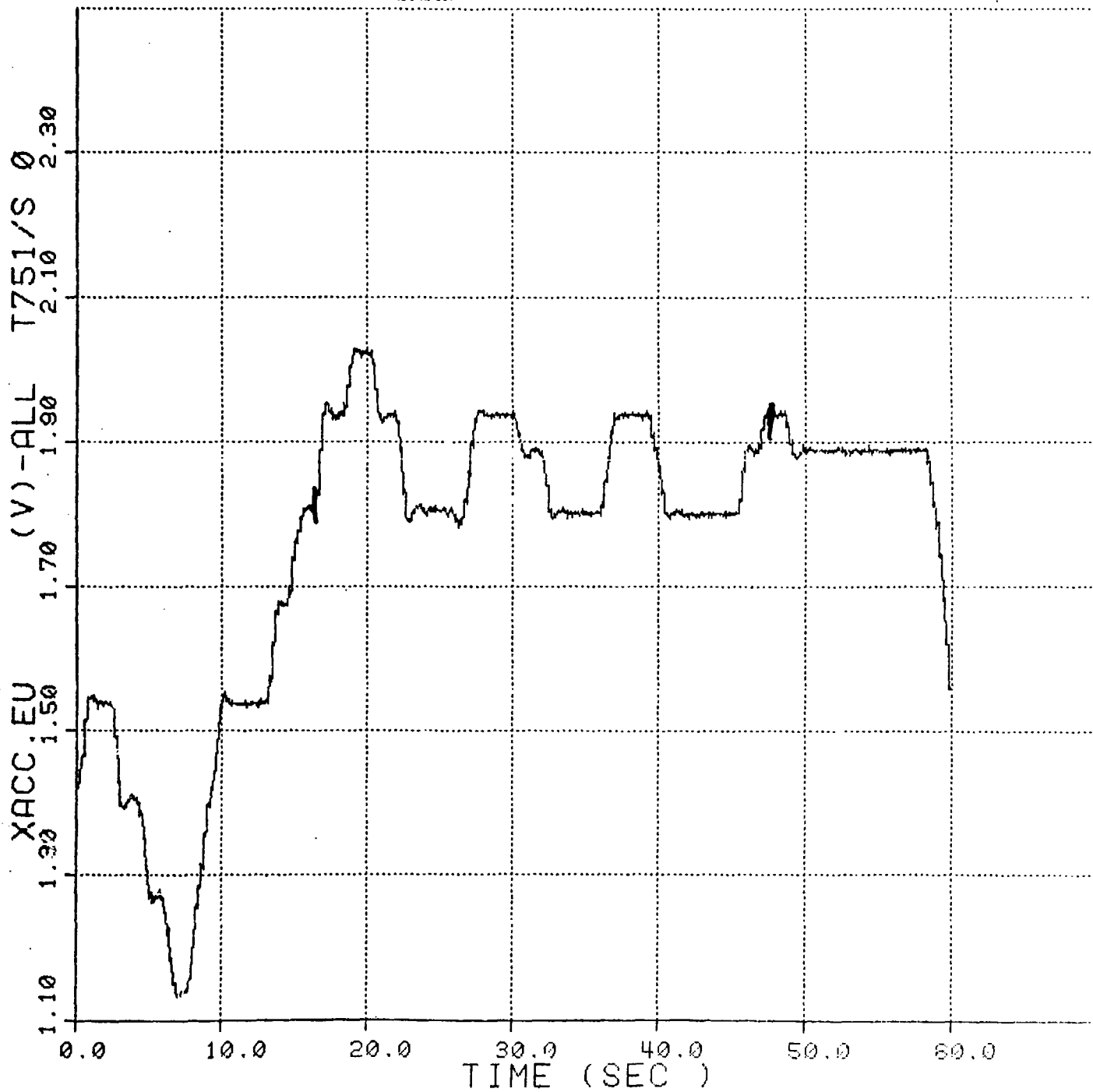


Figure No. 151. Towed Submersible's Longitudinal Acceleration vs Time, Case 18



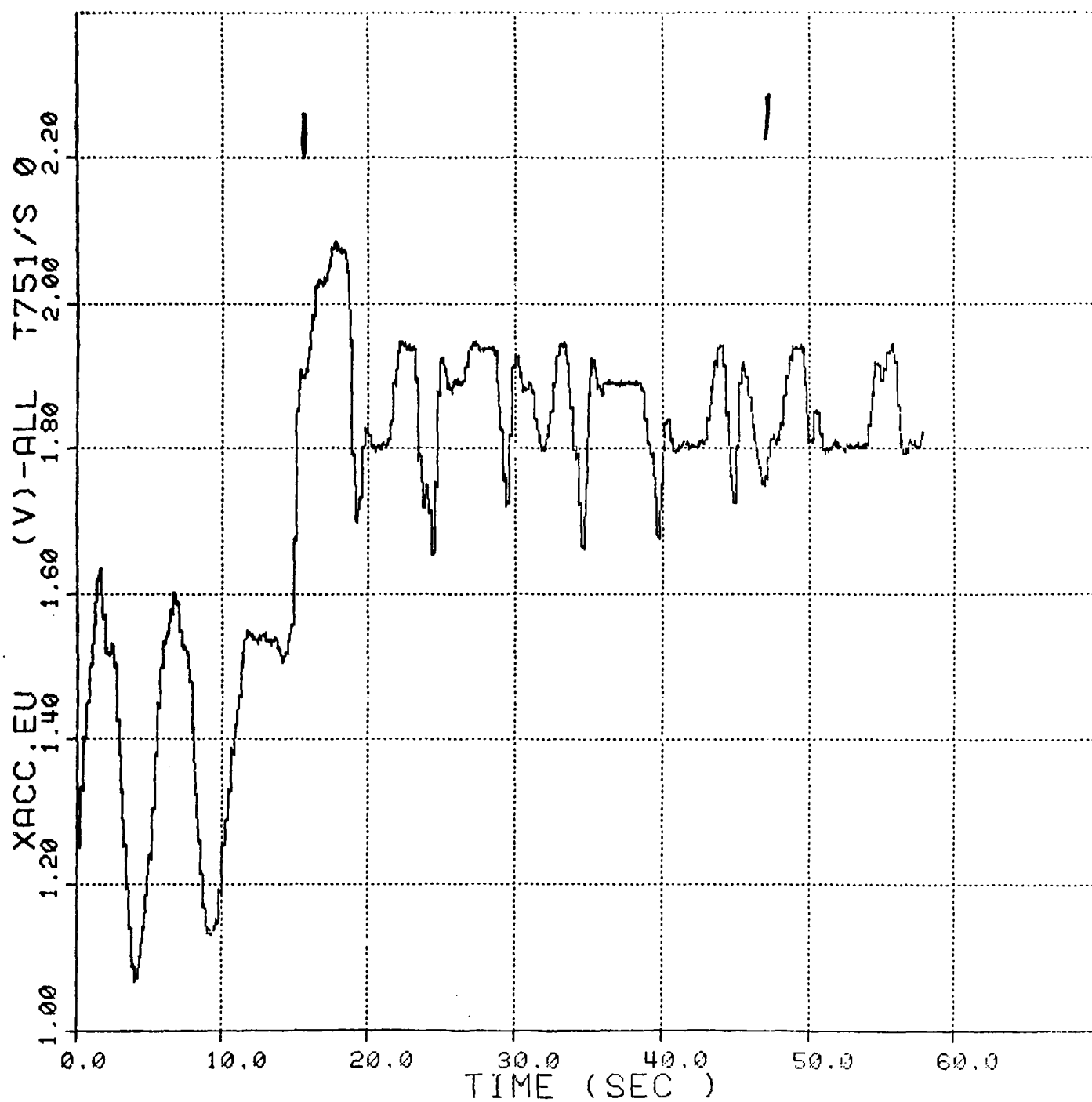


Figure No. 152. Towed Submersible's Longitudinal Acceleration vs Time, Case 19



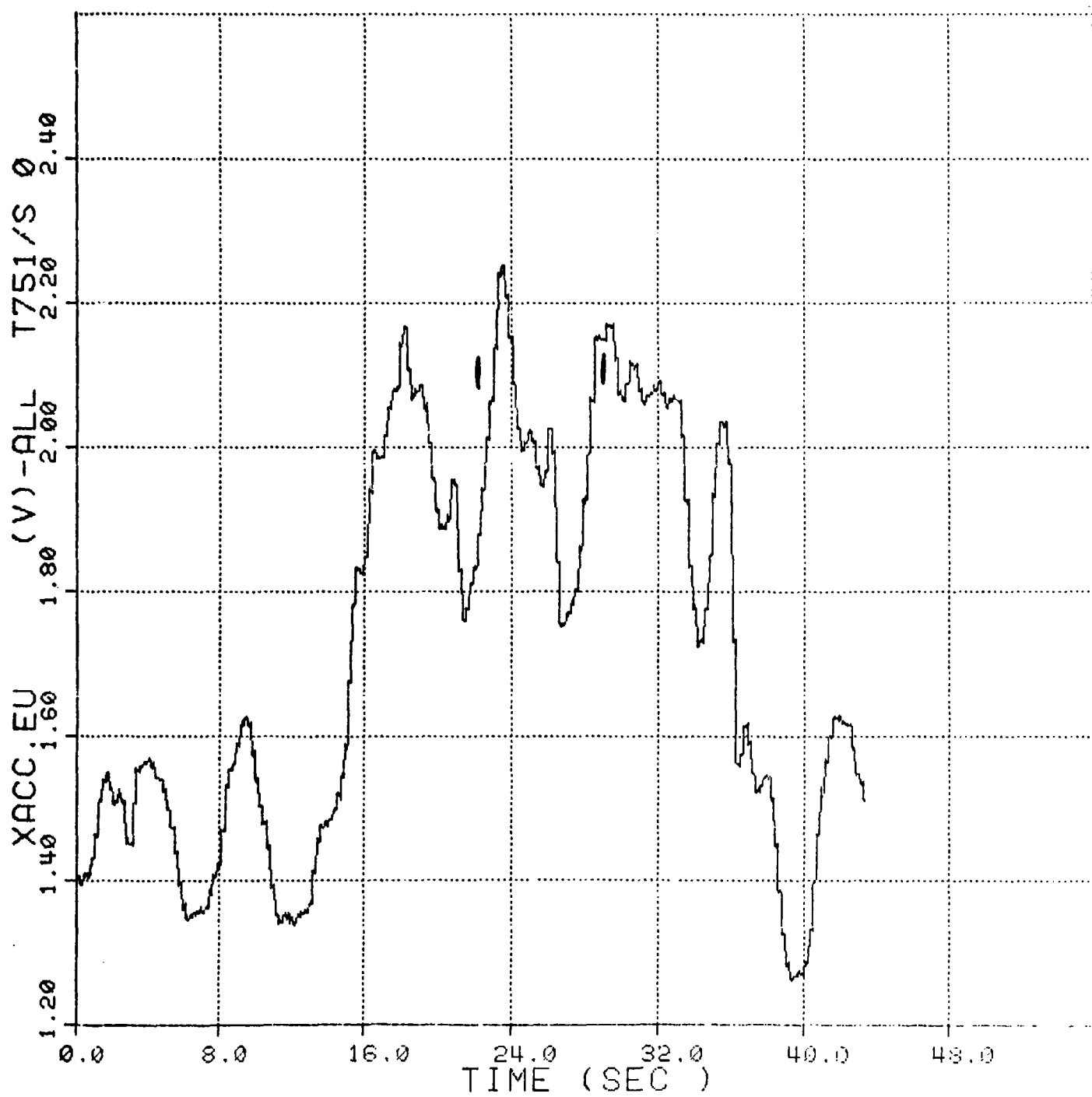


Figure No. 153. Towed Submersible's Longitudinal Acceleration vs Time, Case 20



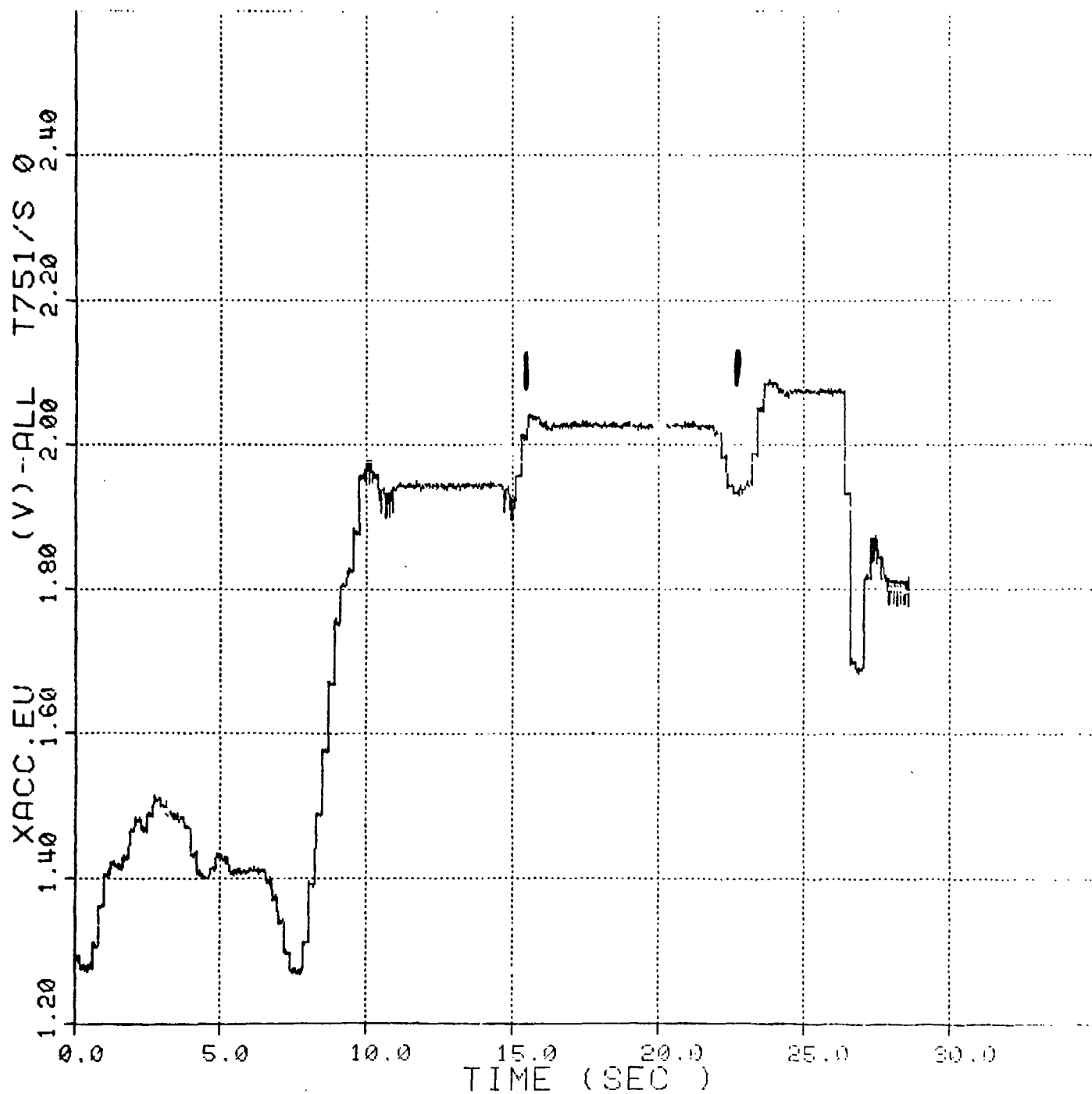


Figure No. 154. Towed Submersible's Longitudinal Acceleration vs Time, Case 21



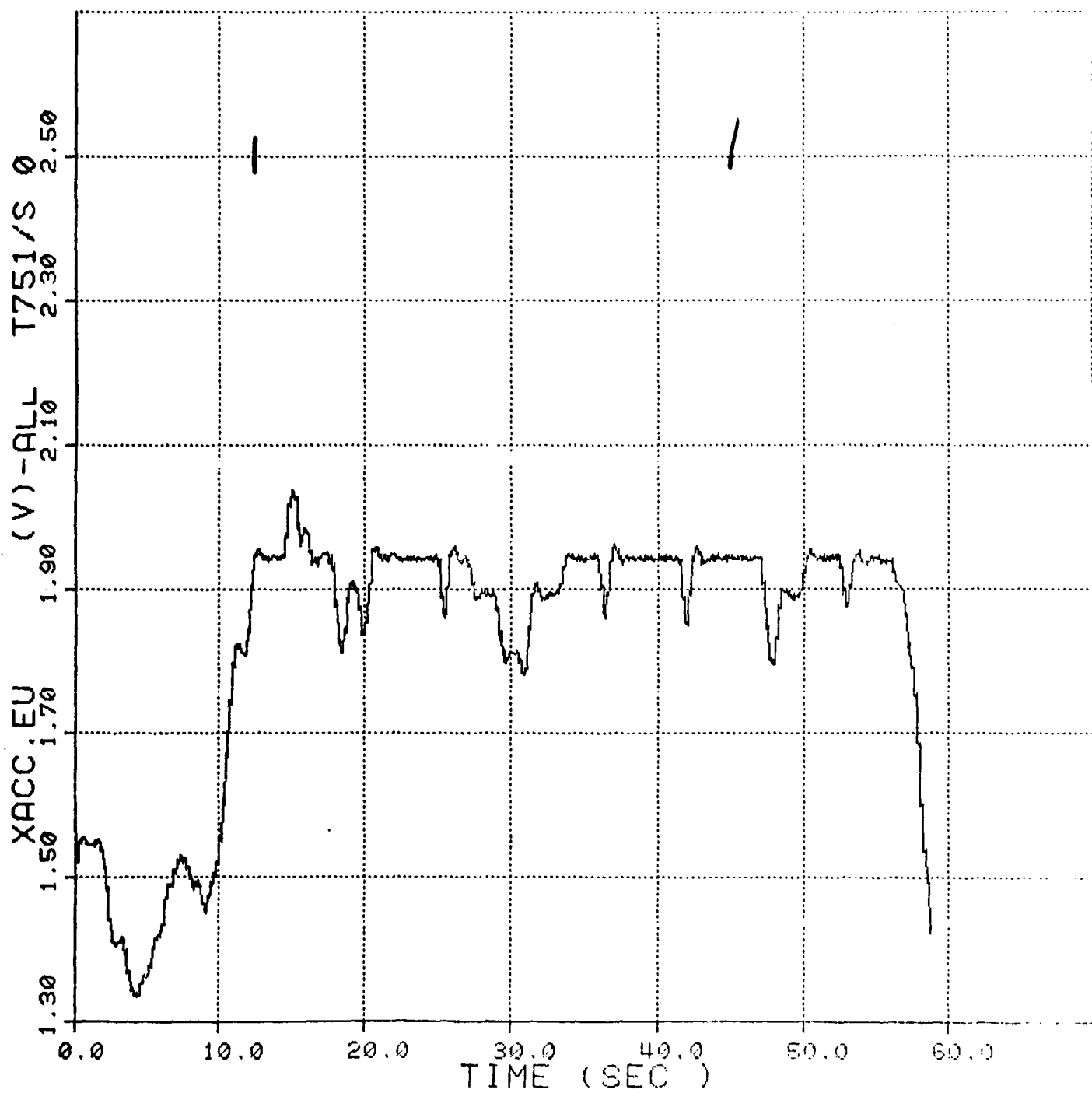


Figure No. 155. Towed Submersible's Longitudinal Acceleration vs Time, Case 22



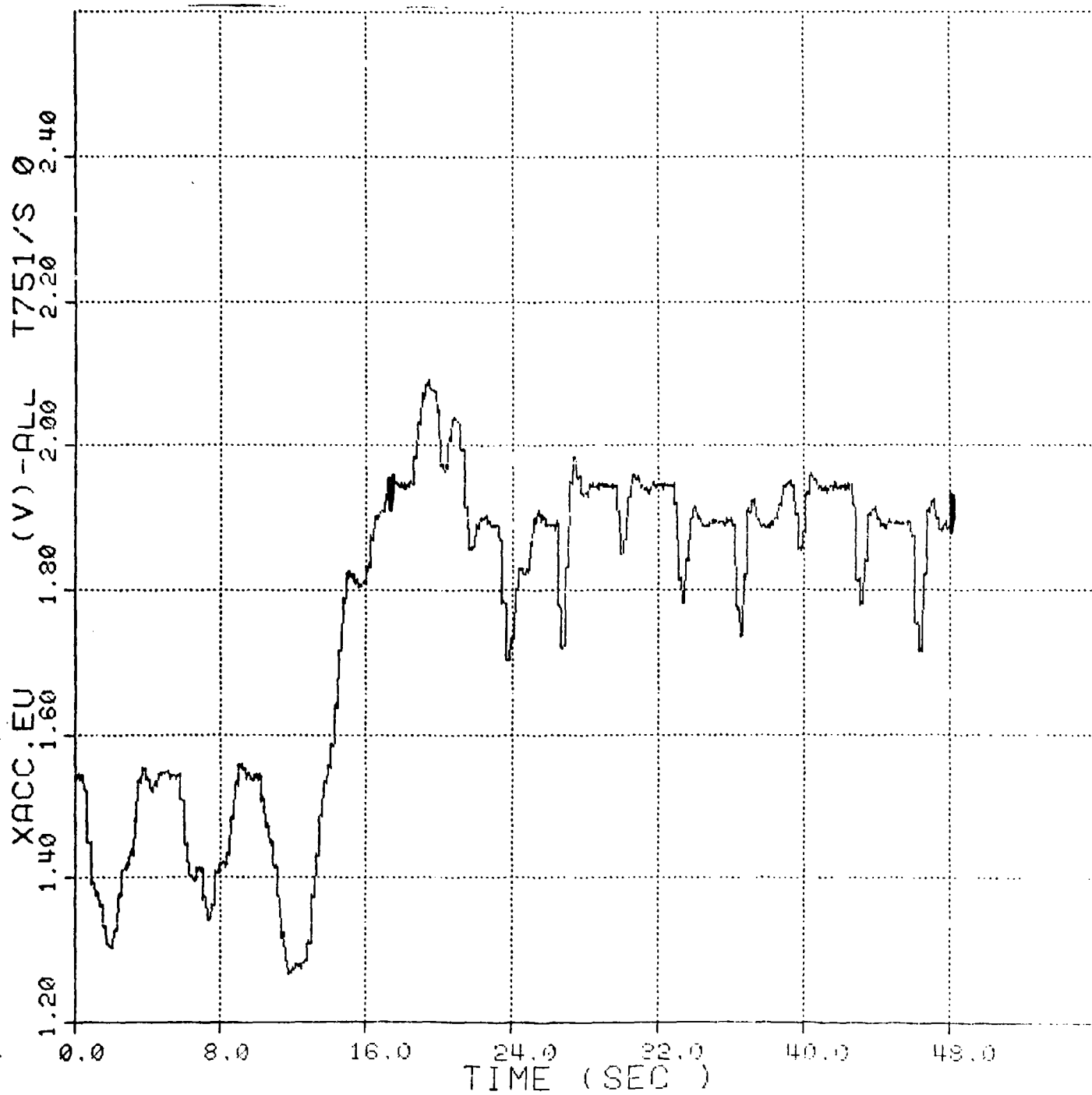


Figure No.156. Towed Submersible's Longitudinal Acceleration vs Time, Case 23



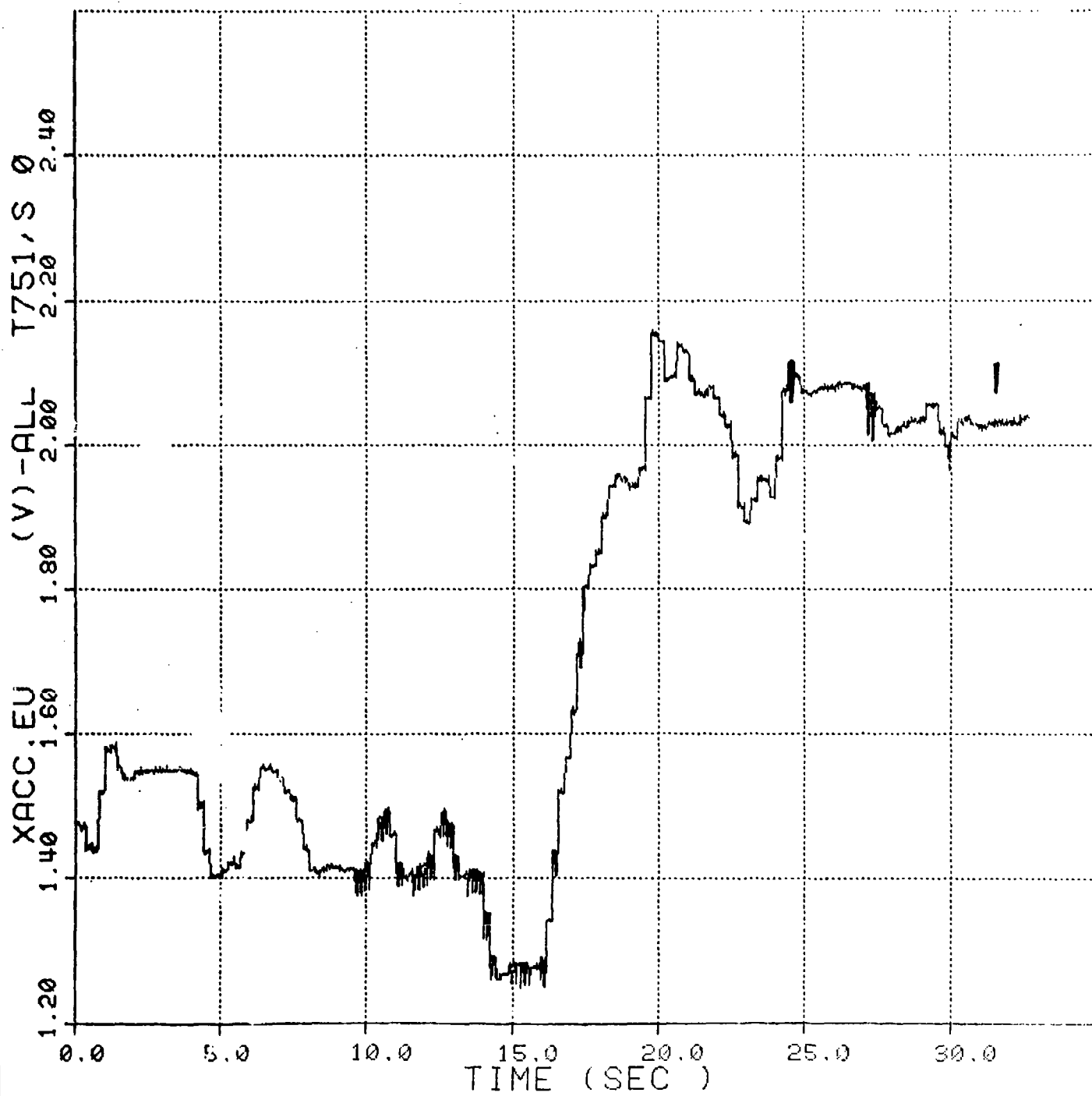


Figure No.157. Towed Submersible's Longitudinal Acceleration vs Time, Case 24



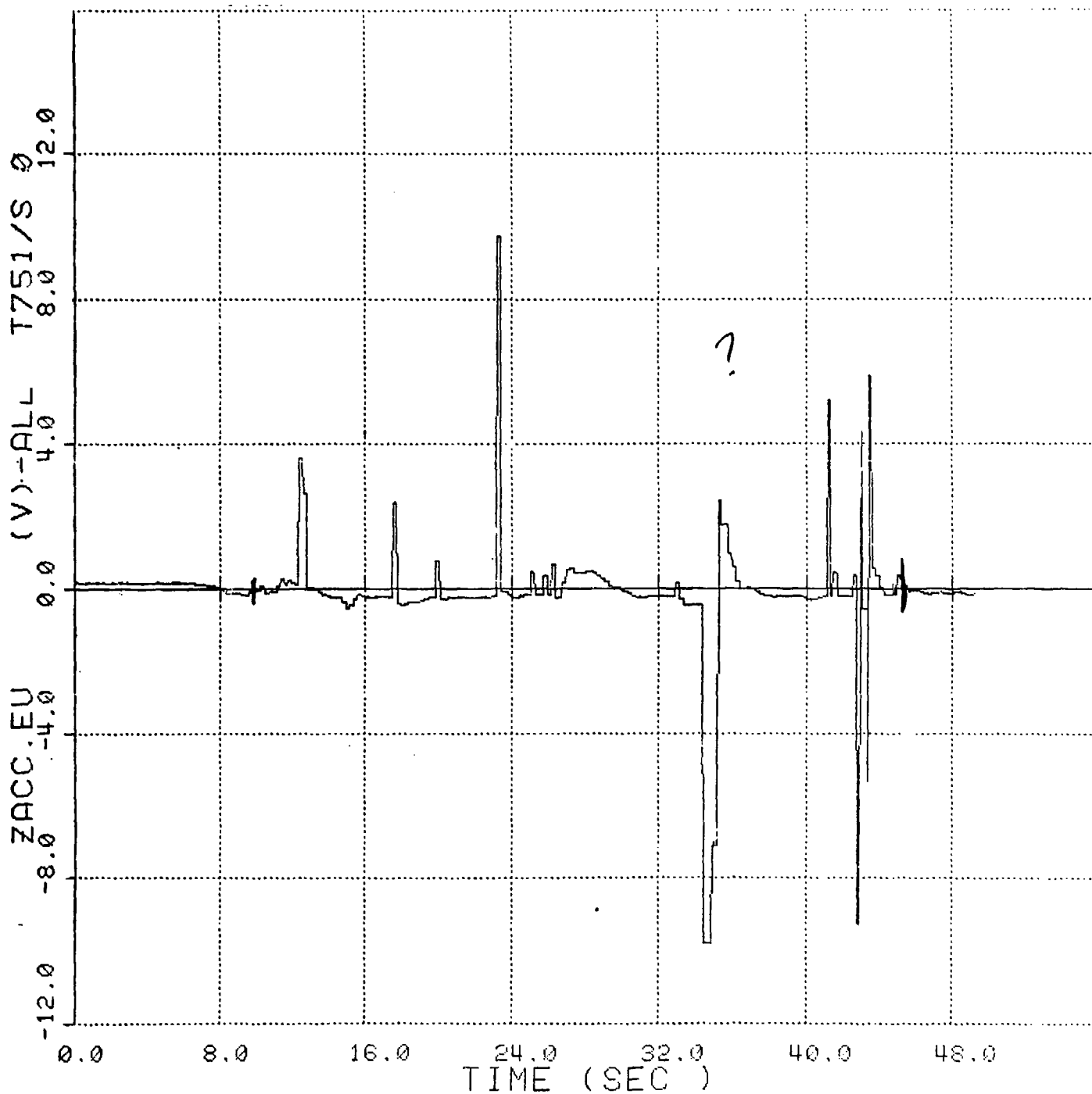


Figure No.158. Towed Submersible's Vertical Acceleration vs Time, Case 2



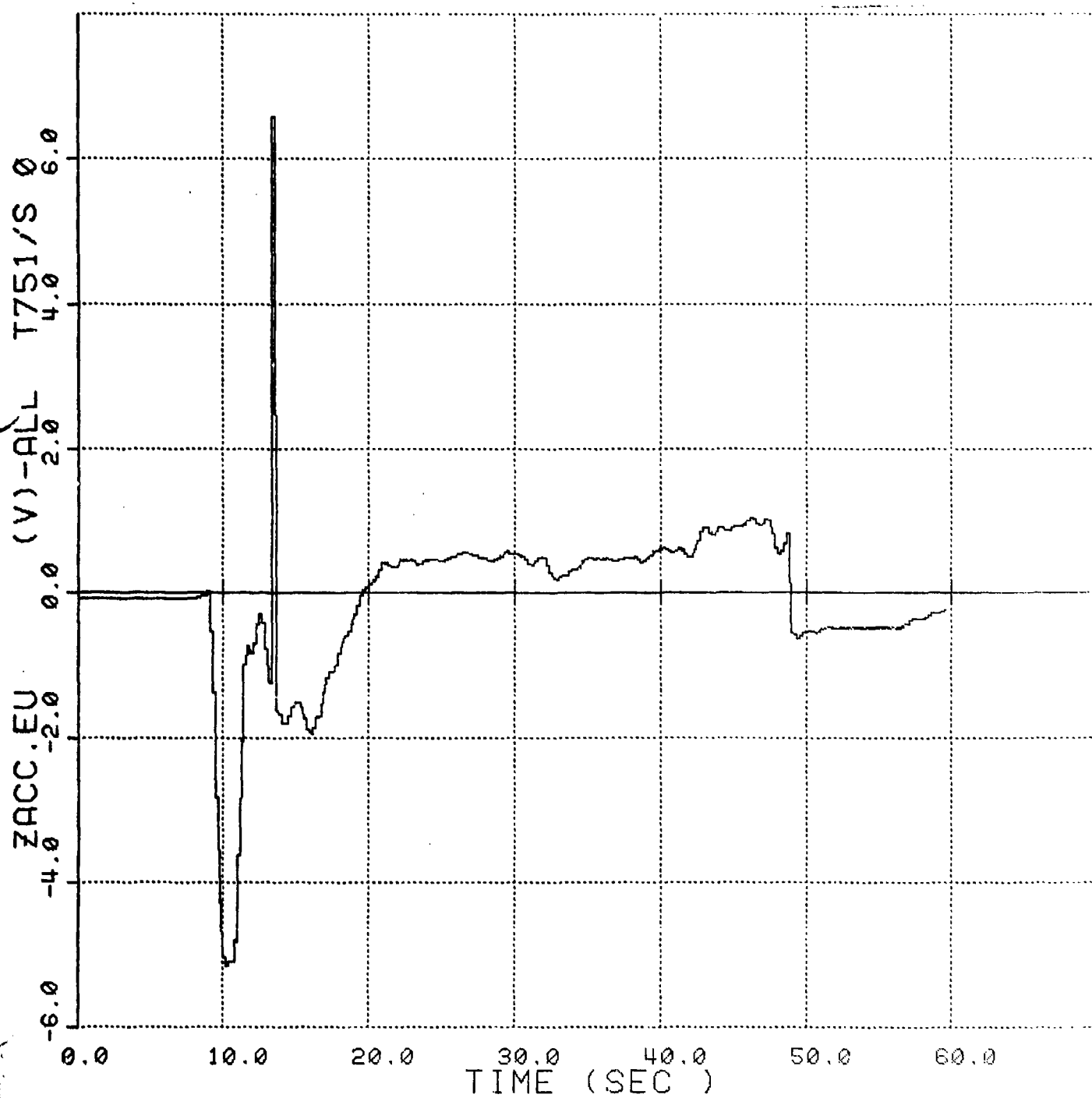


Figure No.159. Towed Submersible's Vertical Acceleration vs Time, Case 3



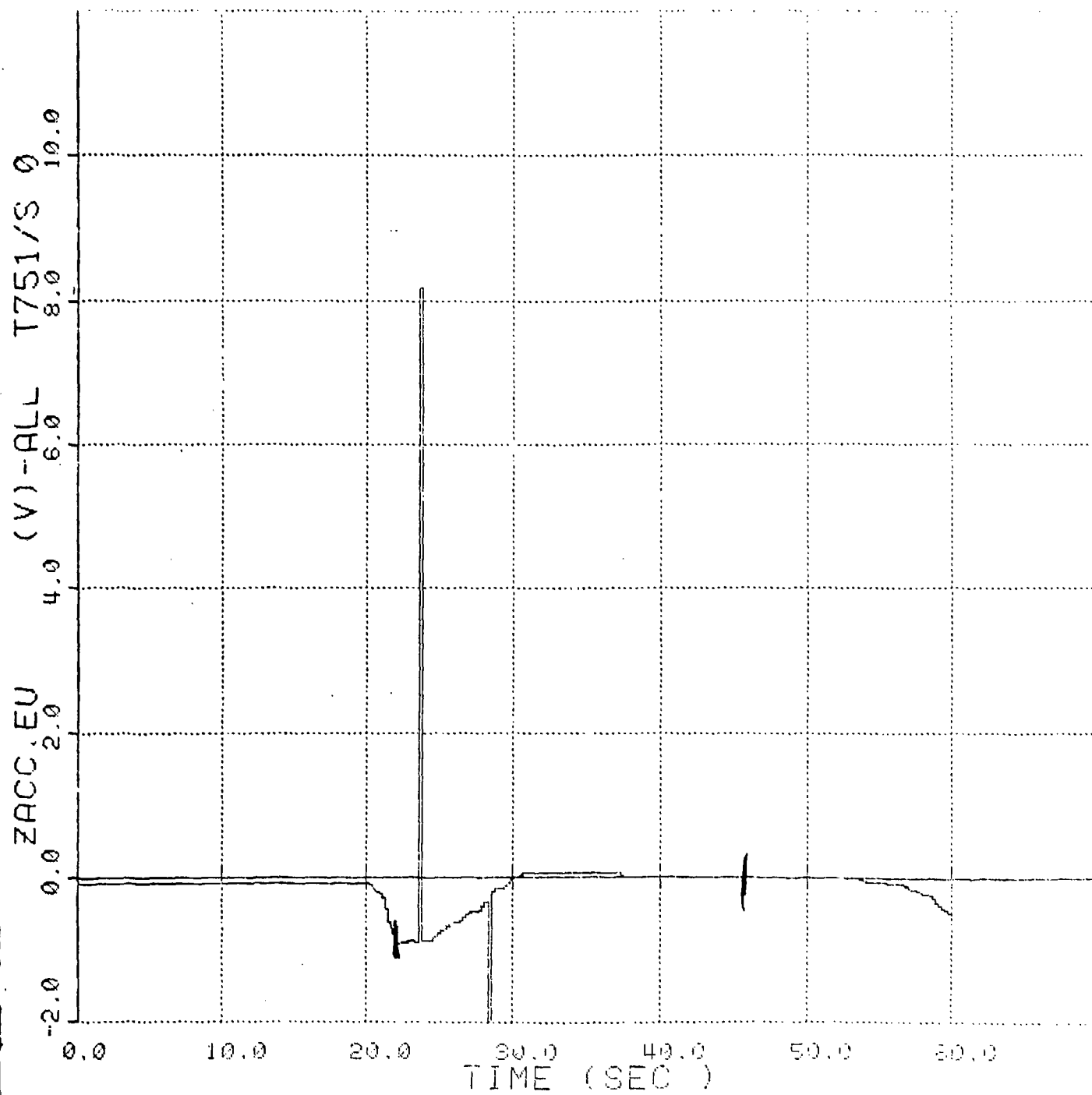


Figure No.160. Towed Submersible's Vertical Acceleration vs Time, Case 4.



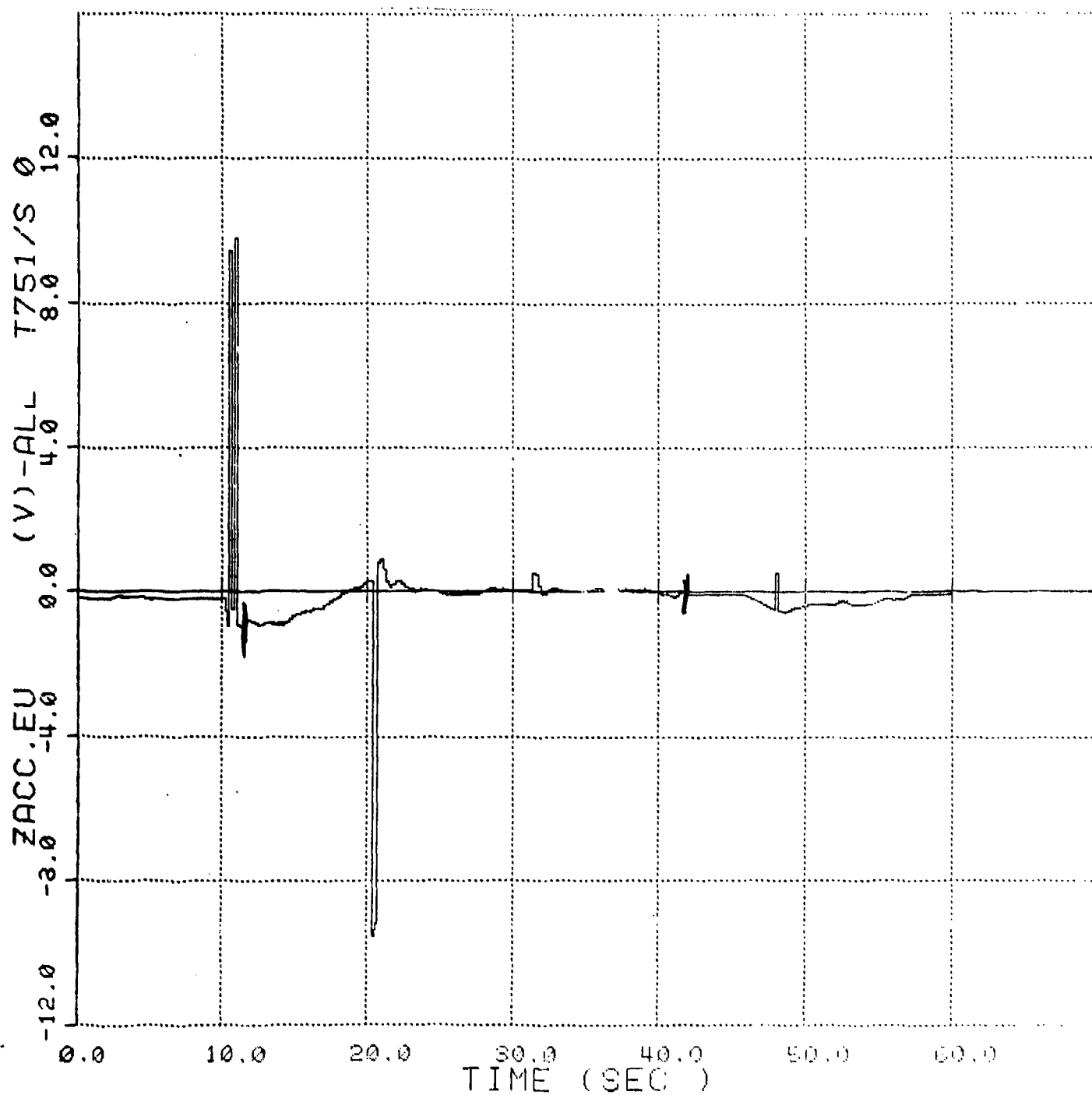


Figure No.161. Towed Submersible's Vertical Acceleration vs Time, Case 5



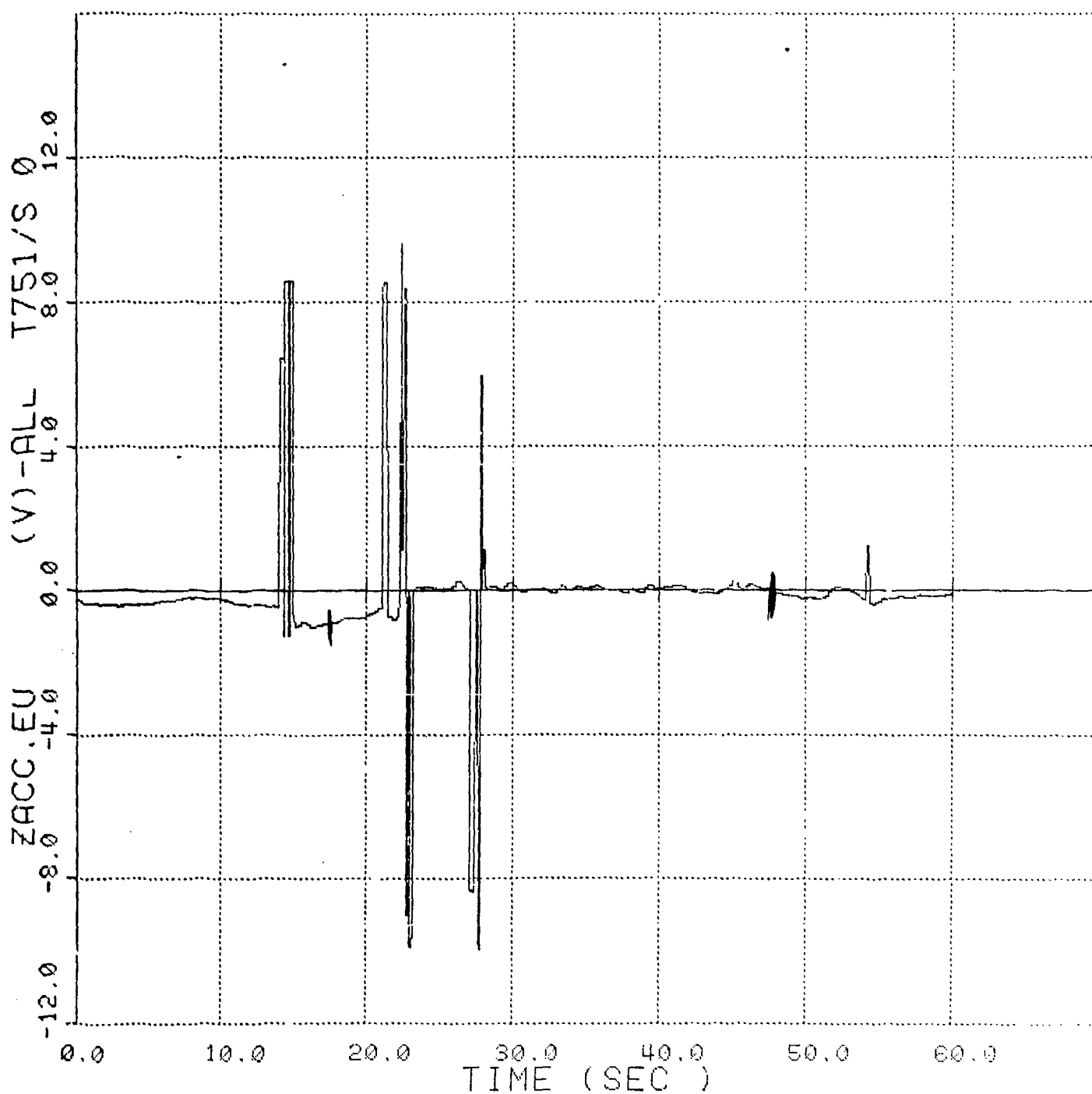


Figure No.162. Towed Submersible's Vertical Acceleration vs Time, Case 6



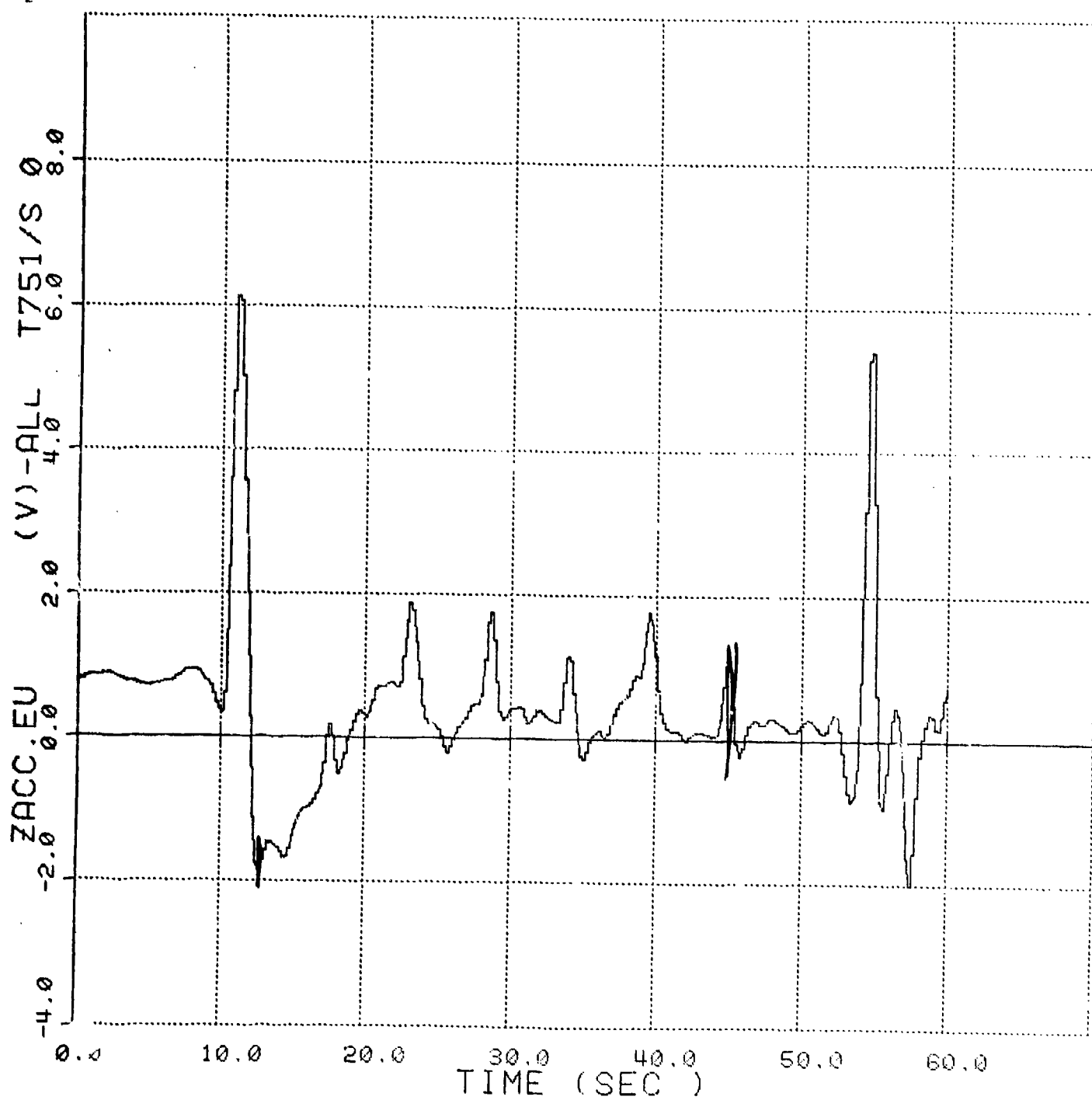


Figure No.163. Towed Submersible's Vertical Acceleration vs Time, Case 7



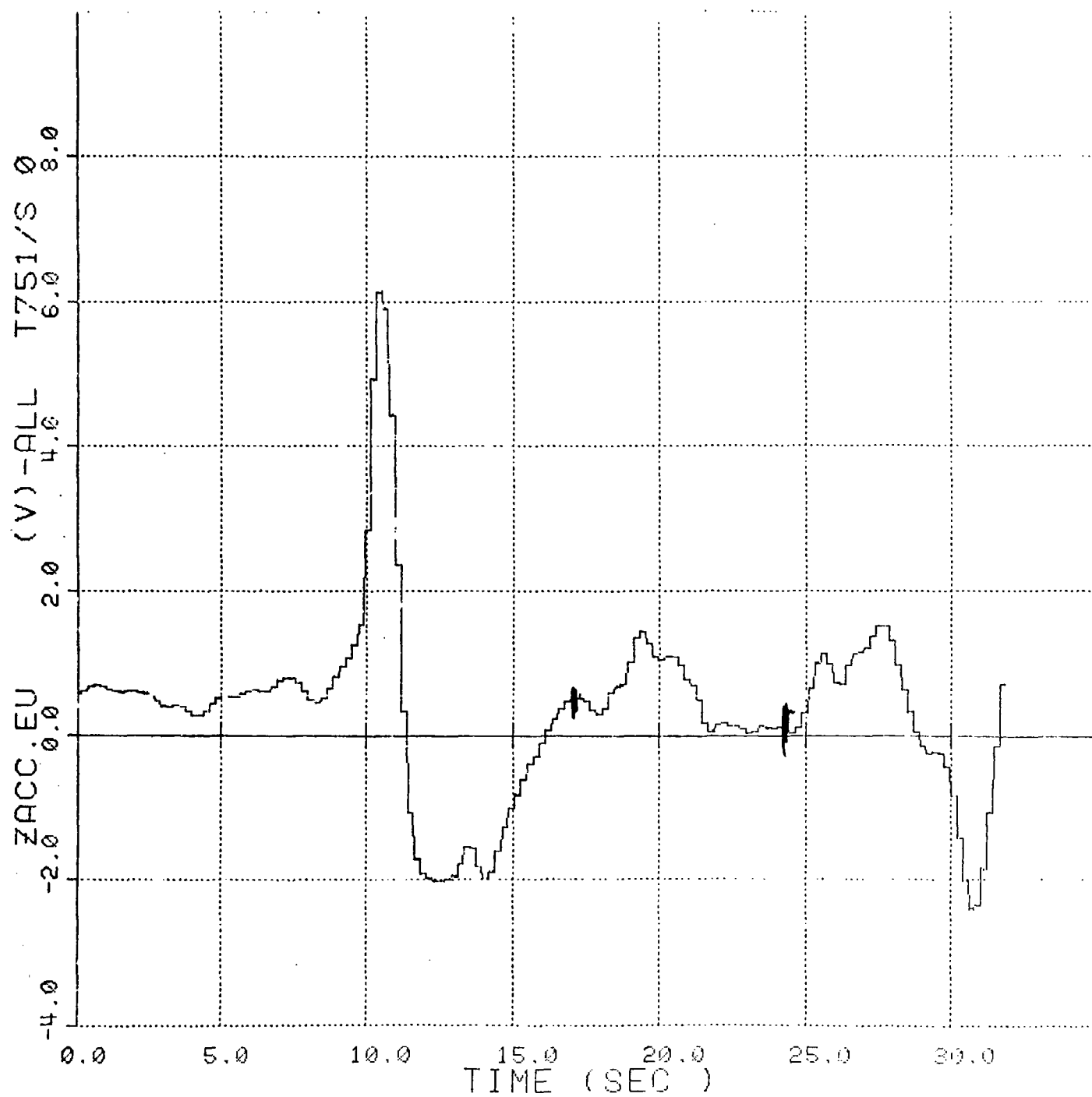


Figure No.164. Towed Submersible's Vertical Acceleration vs Time, Case 9



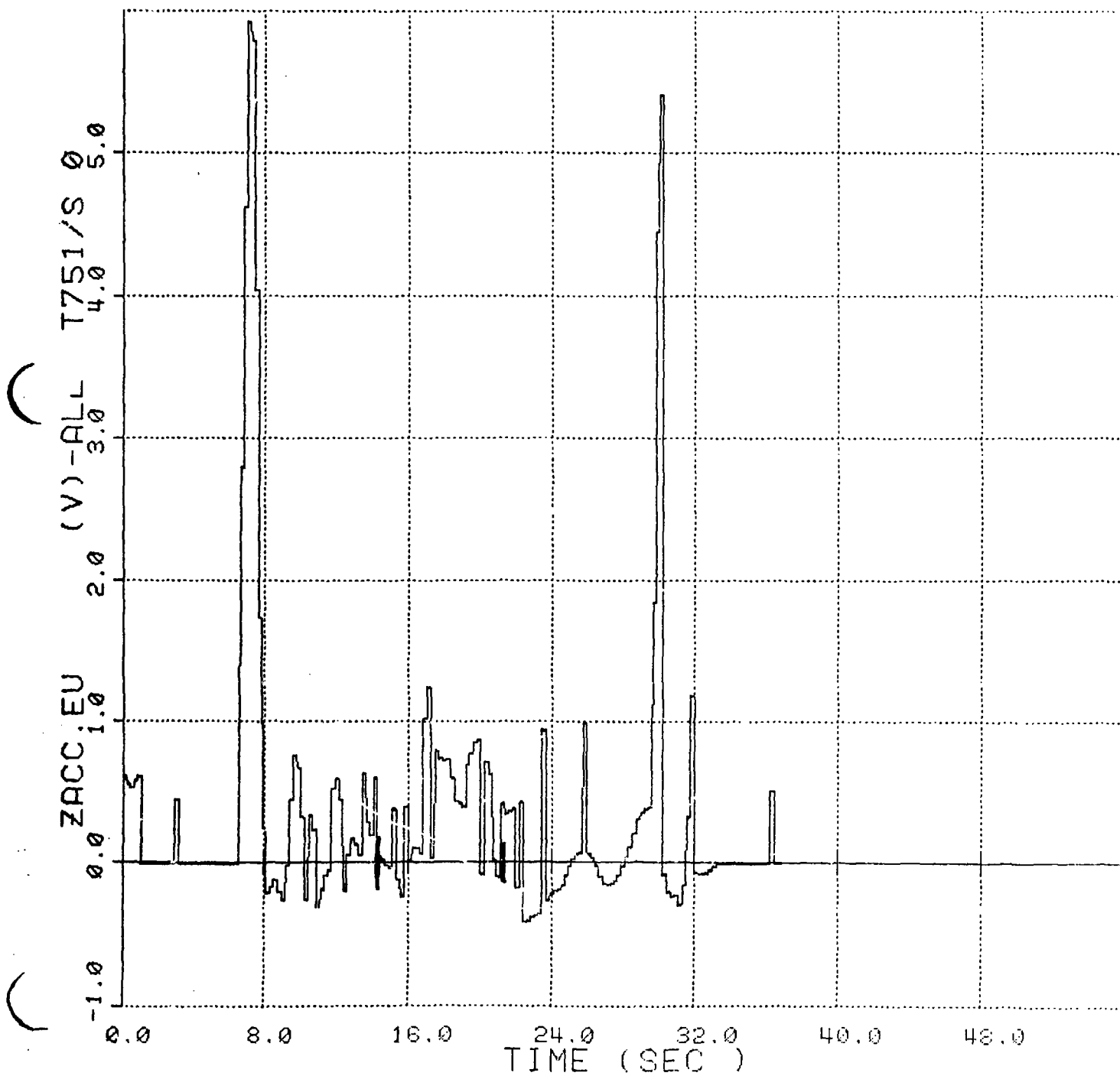


Figure No.165. Towed Submersible's Vertical Acceleration vs Time, Case 10 Page No.



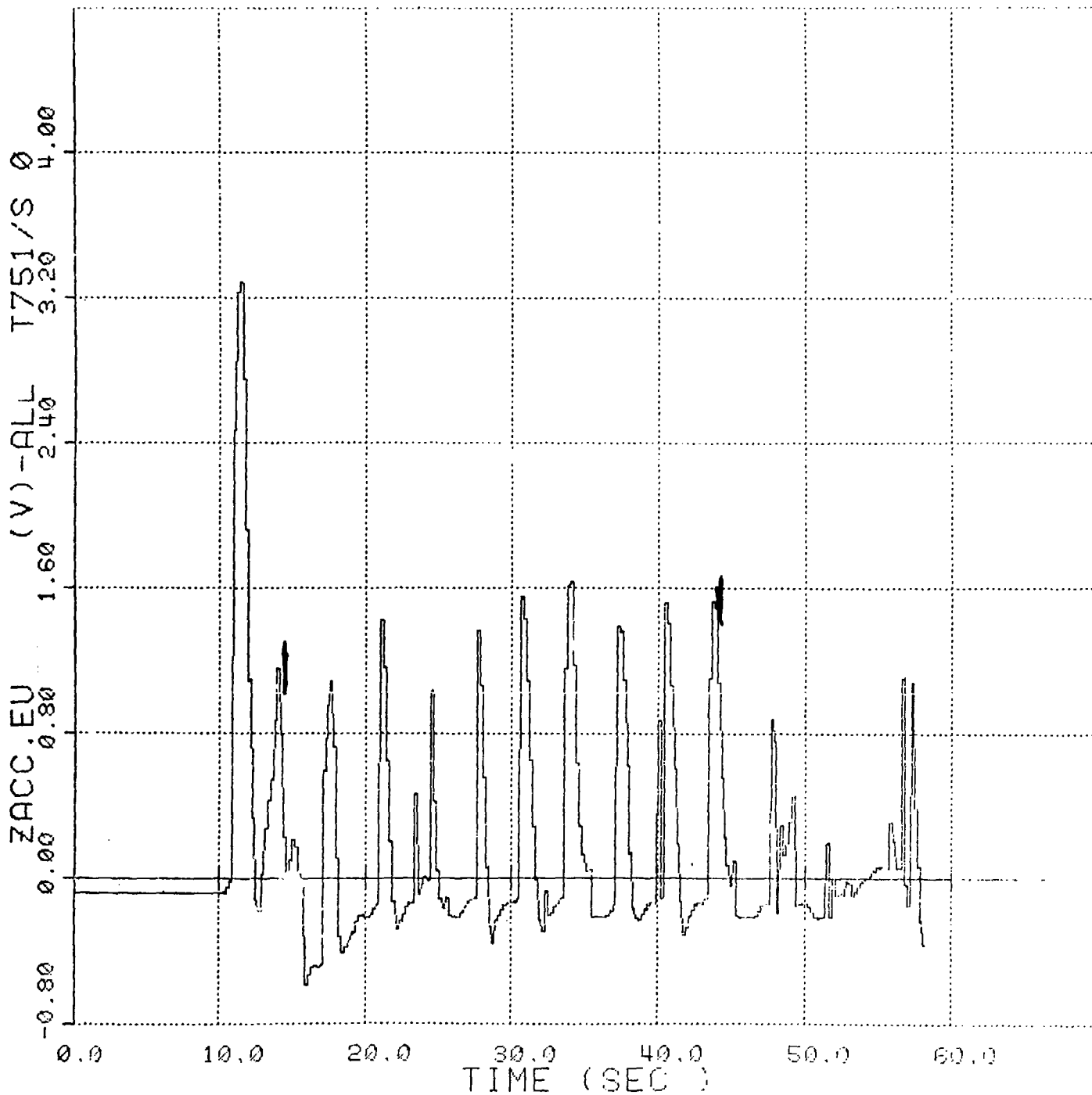


Figure No.166. Towed Submersible's Vertical Acceleration vs Time, Case 11



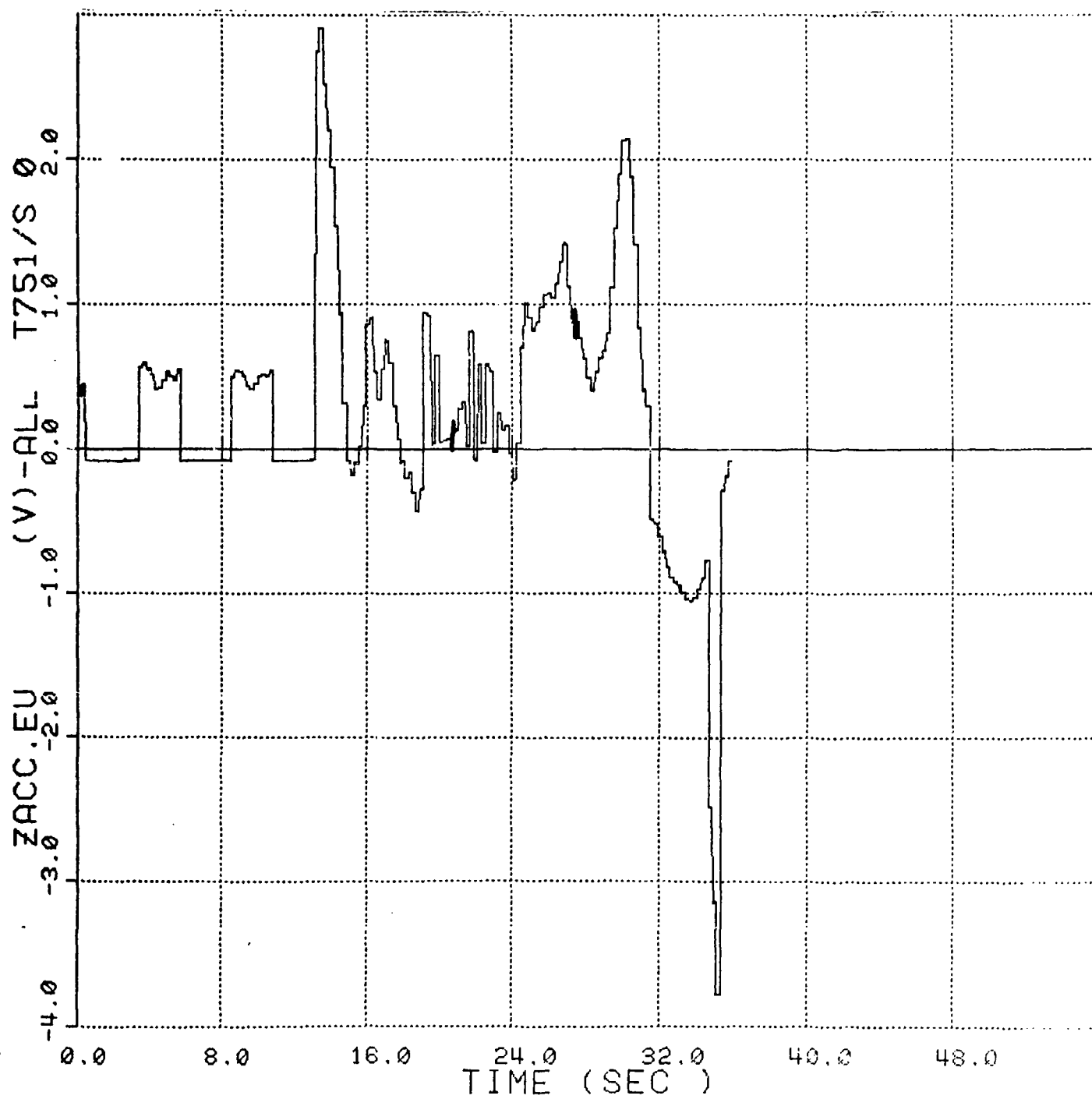
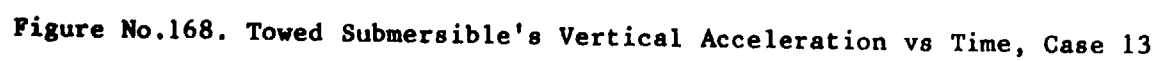


Figure No.167. Towed Submersible's Vertical Acceleration vs Time, Case 12







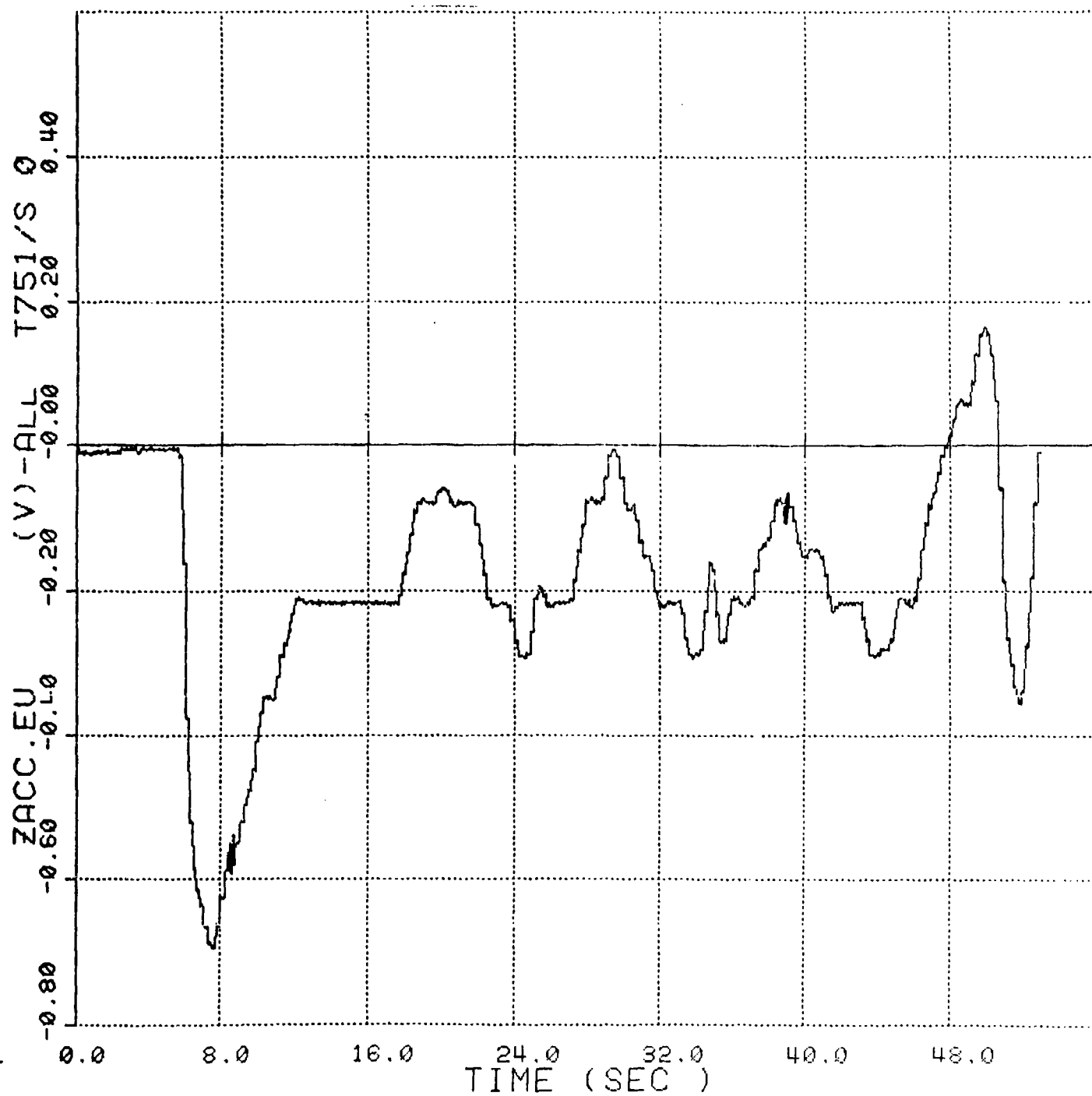


Figure No.169. Towed Submersible's Vertical Acceleration vs Time, Case 14



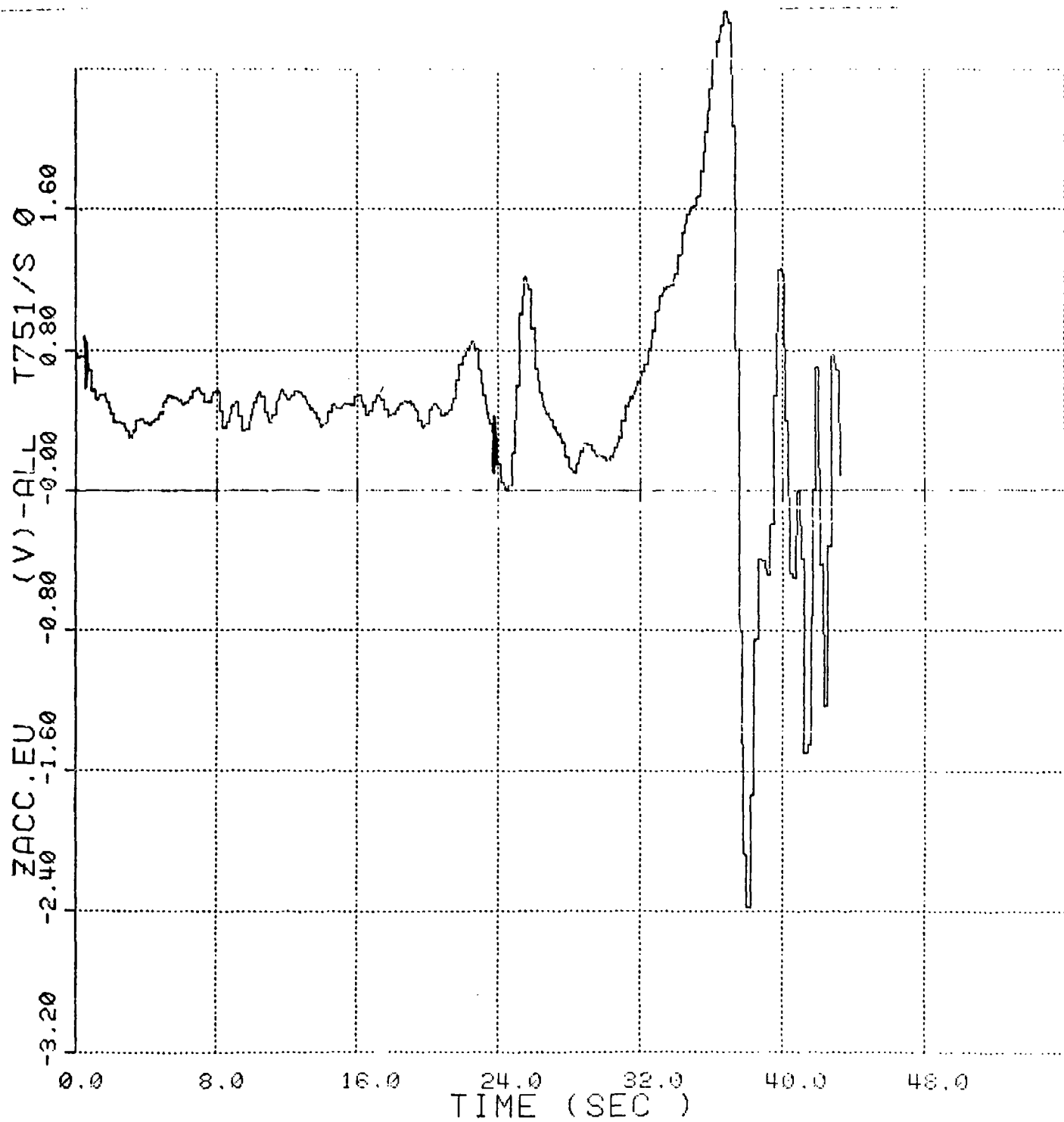


Figure No.170. Towed Submersible's Vertical Acceleration vs Time, Case 15



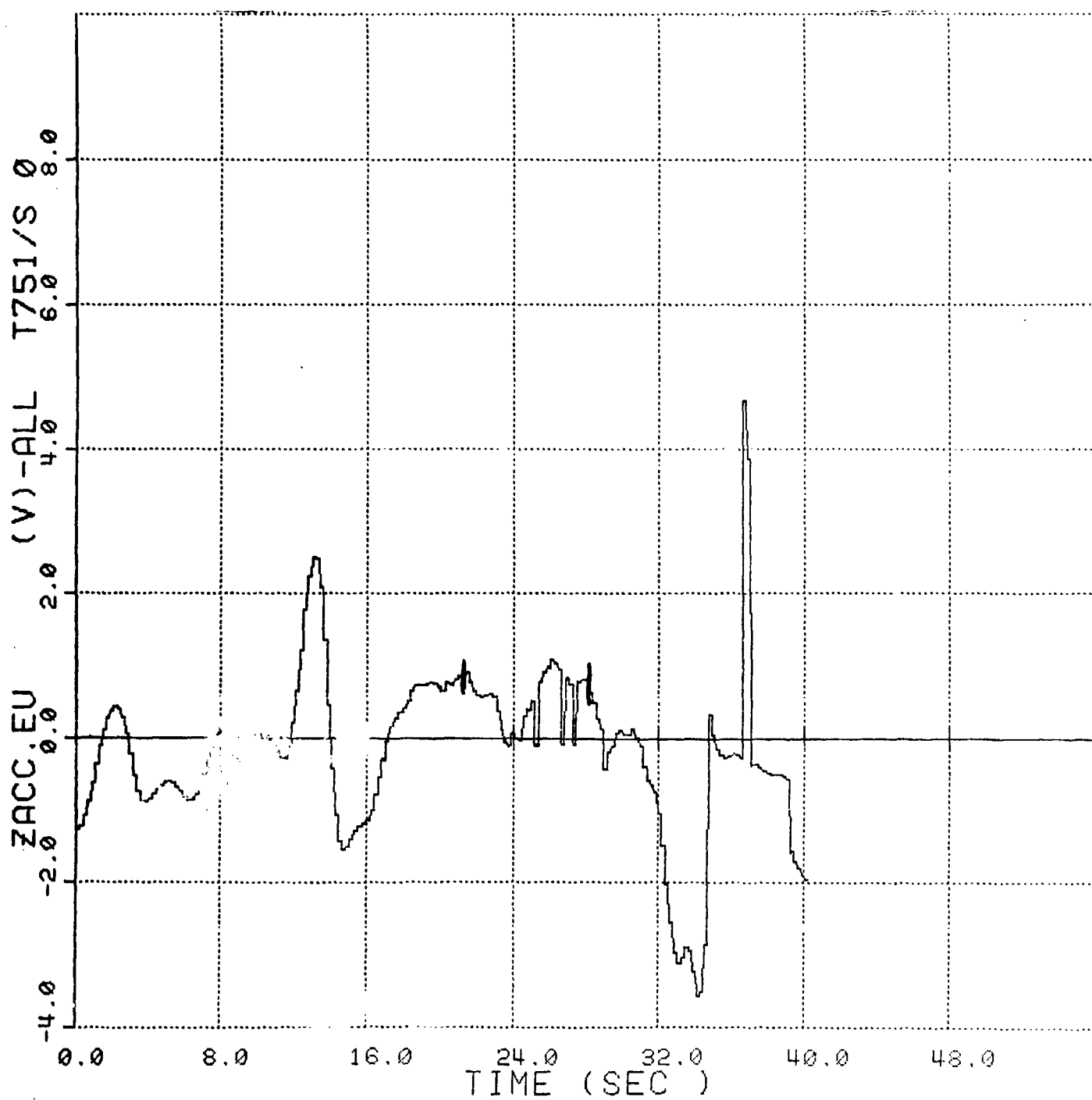


Figure No.171. Towed Submersible's Vertical Acceleration vs Time, Case 16



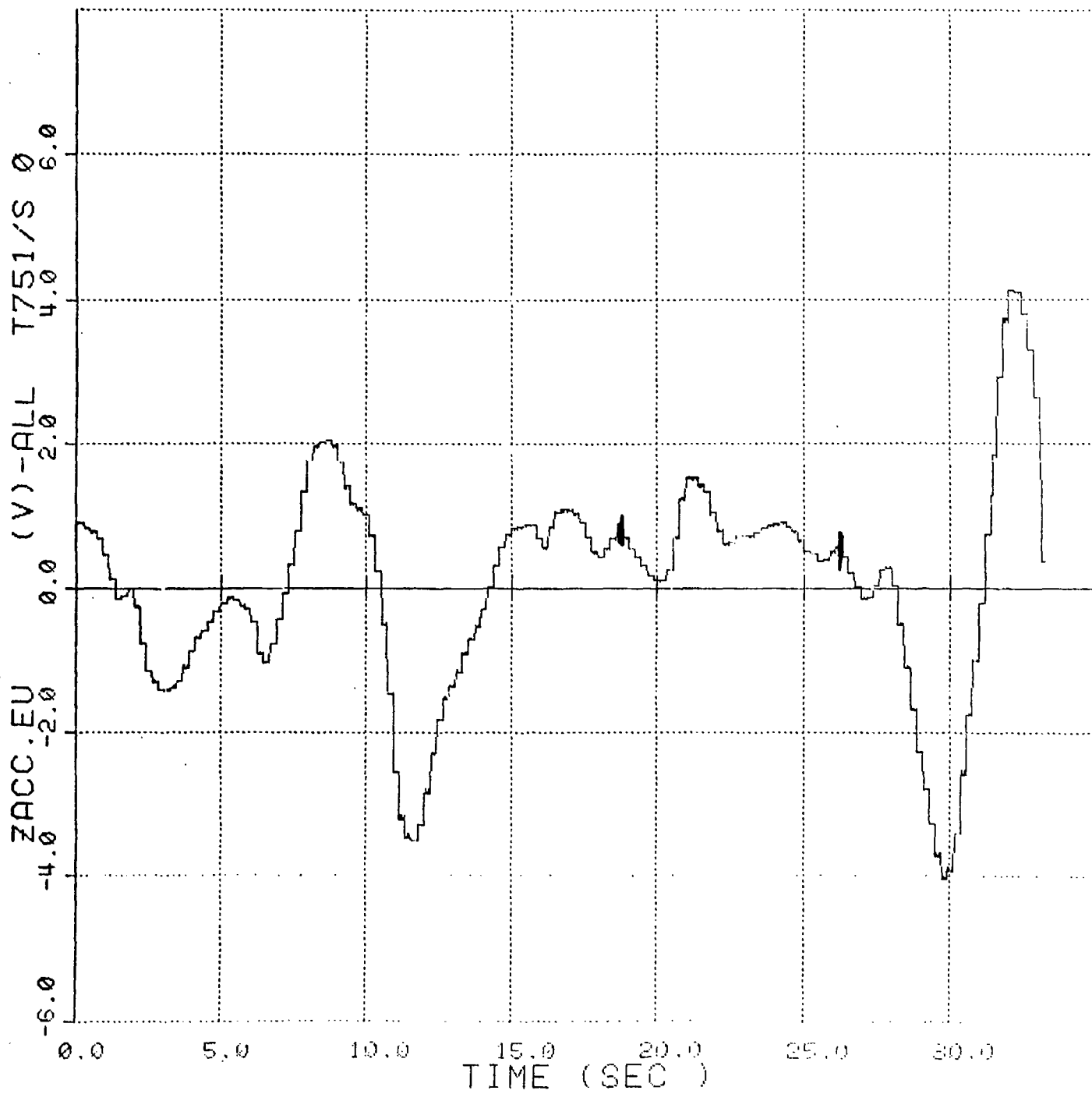


Figure No.172. Towed Submersible's Vertical Acceleration vs Time, Case 17



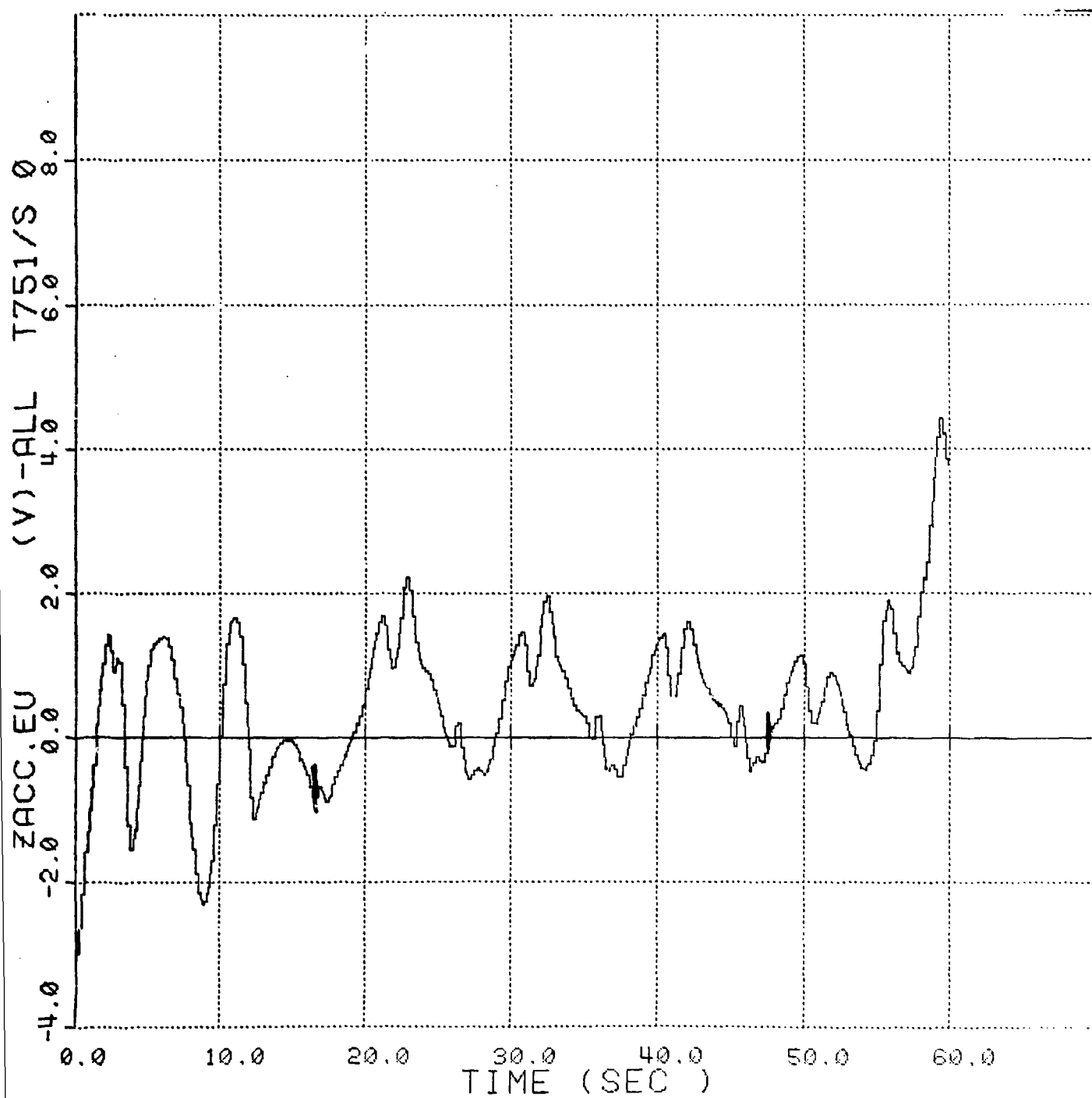


Figure No.173. Towed Submersible's Vertical Acceleration vs Time, Case 18



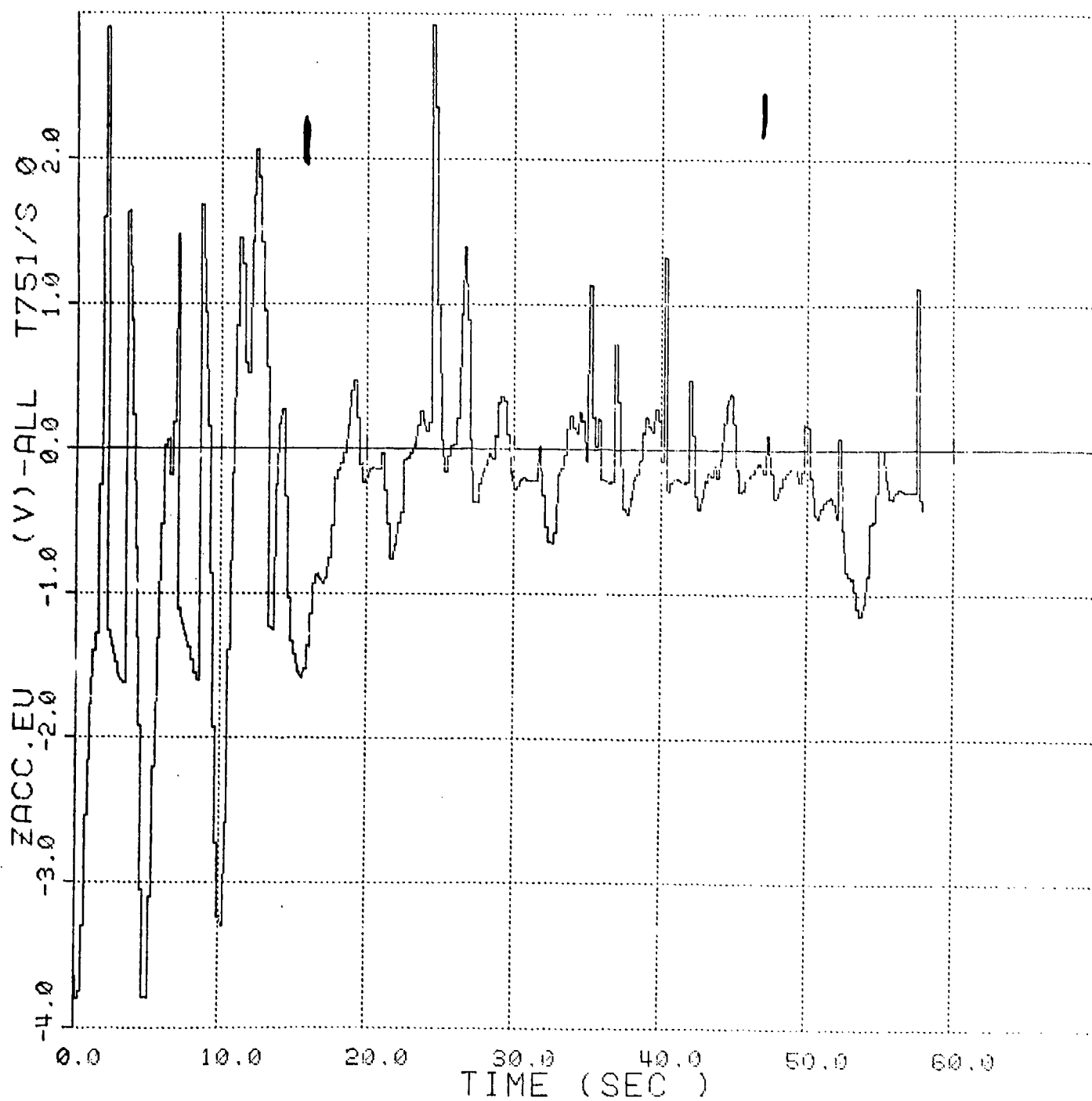


Figure No.174. Towed Submersible's Vertical Acceleration vs Time, Case 19



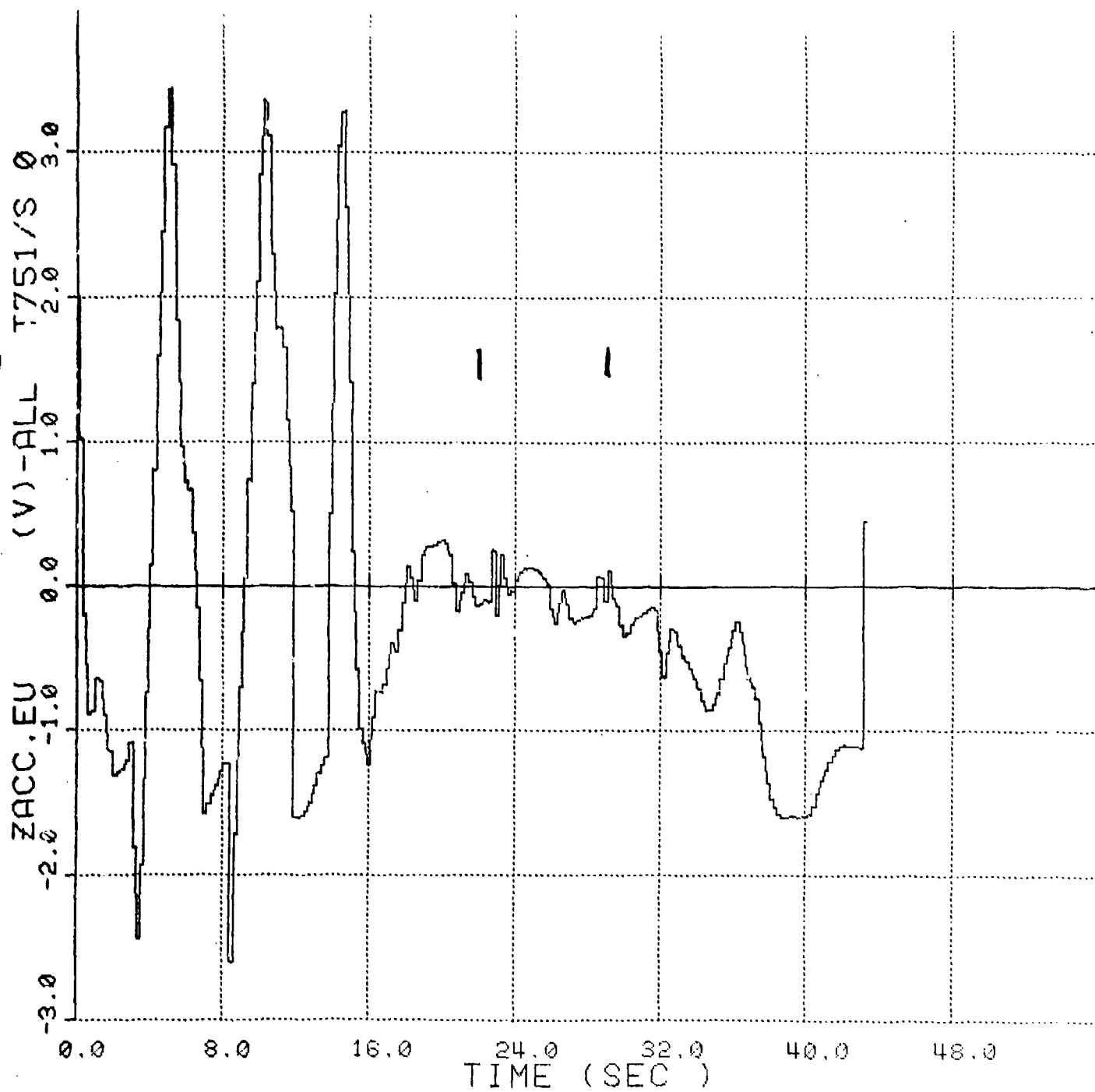


Figure No.175. Towed Submersible's Vertical Acceleration vs Time, Case 20



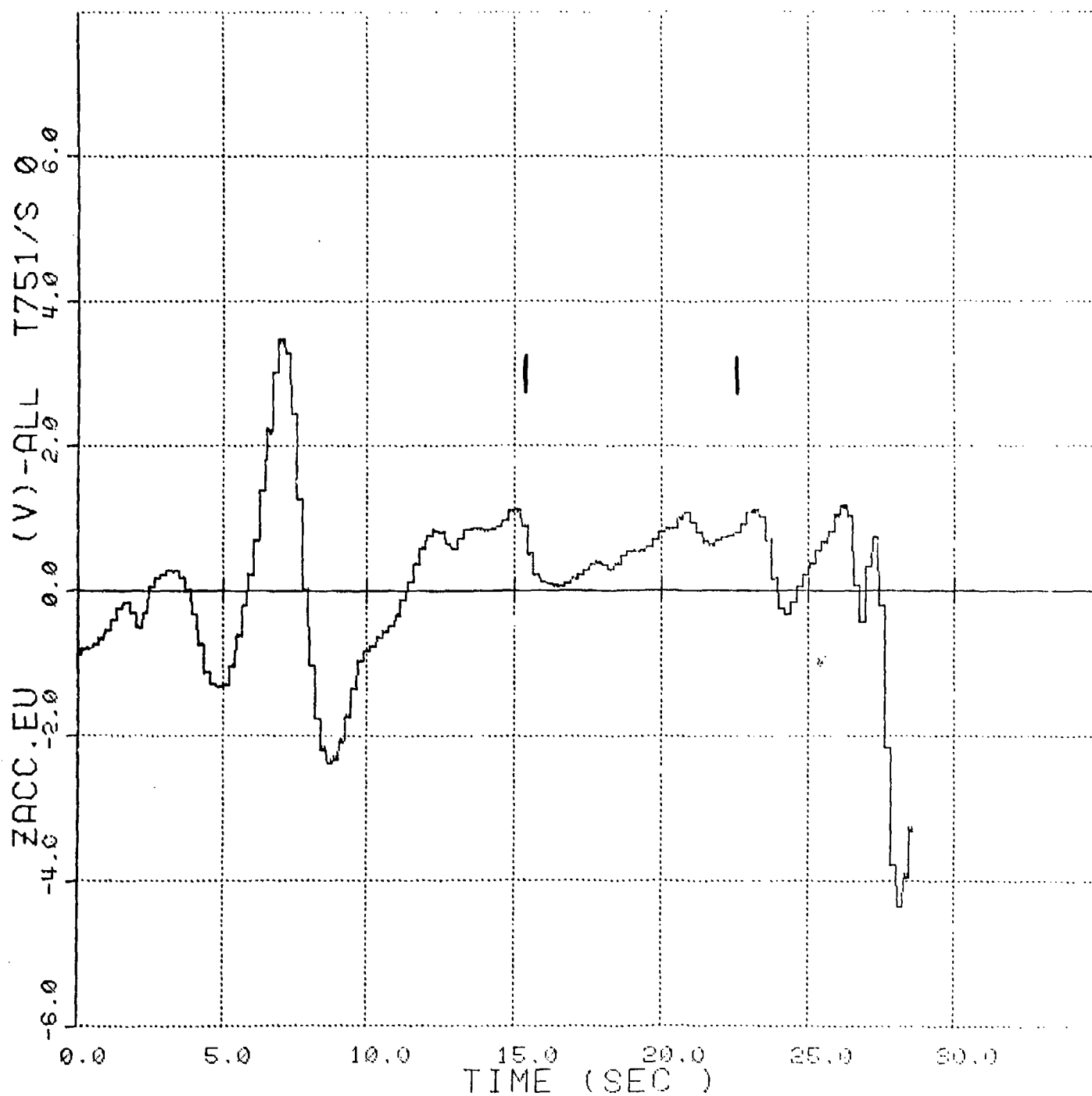


Figure No.176. Towed Submersible's Vertical Acceleration vs Time, Case 21



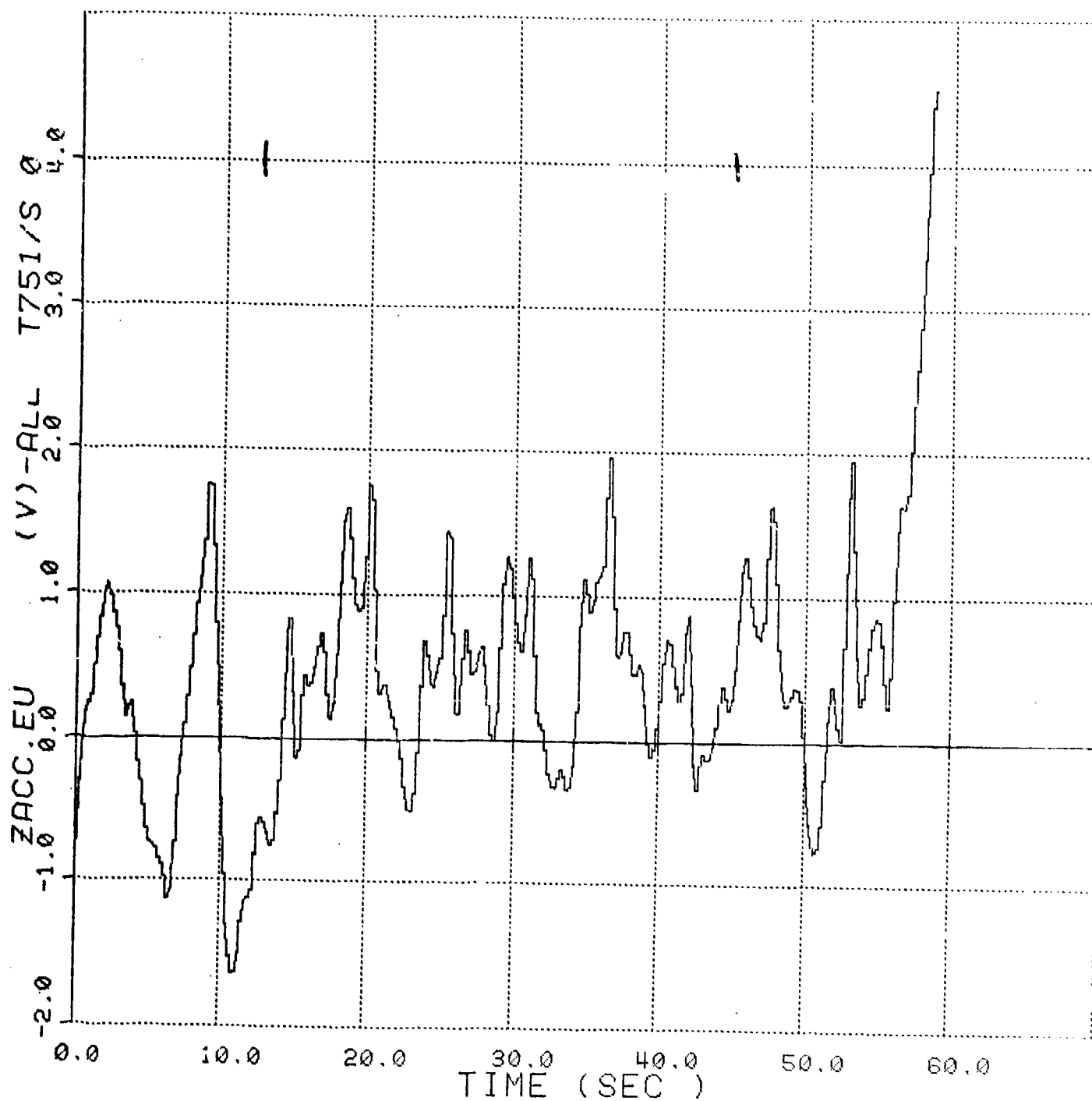


Figure No.177. Towed Submersible's Vertical Acceleration vs Time, Case 22



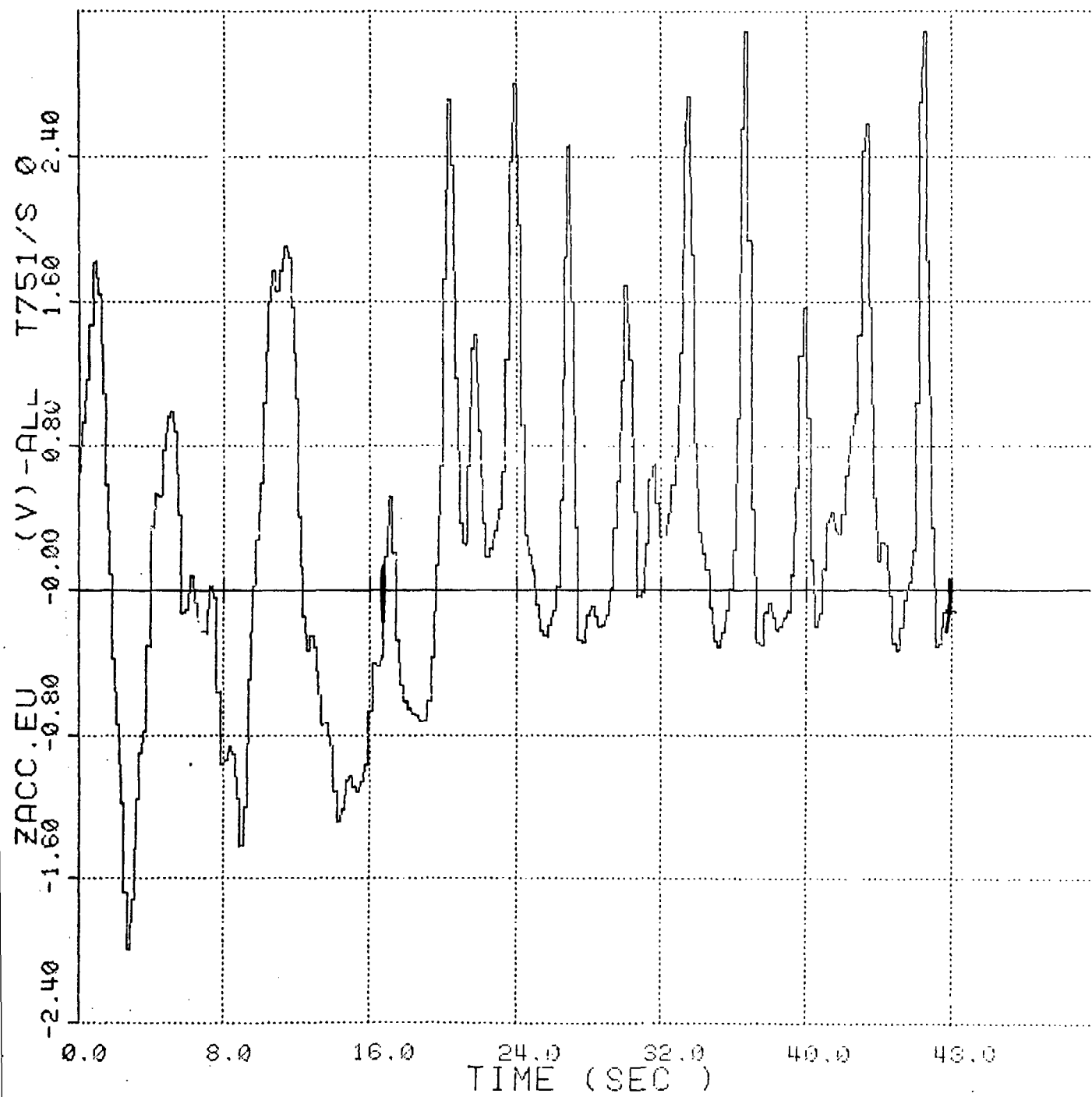


Figure No.178. Towed Submersible's Vertical Acceleration vs Time, Case 23



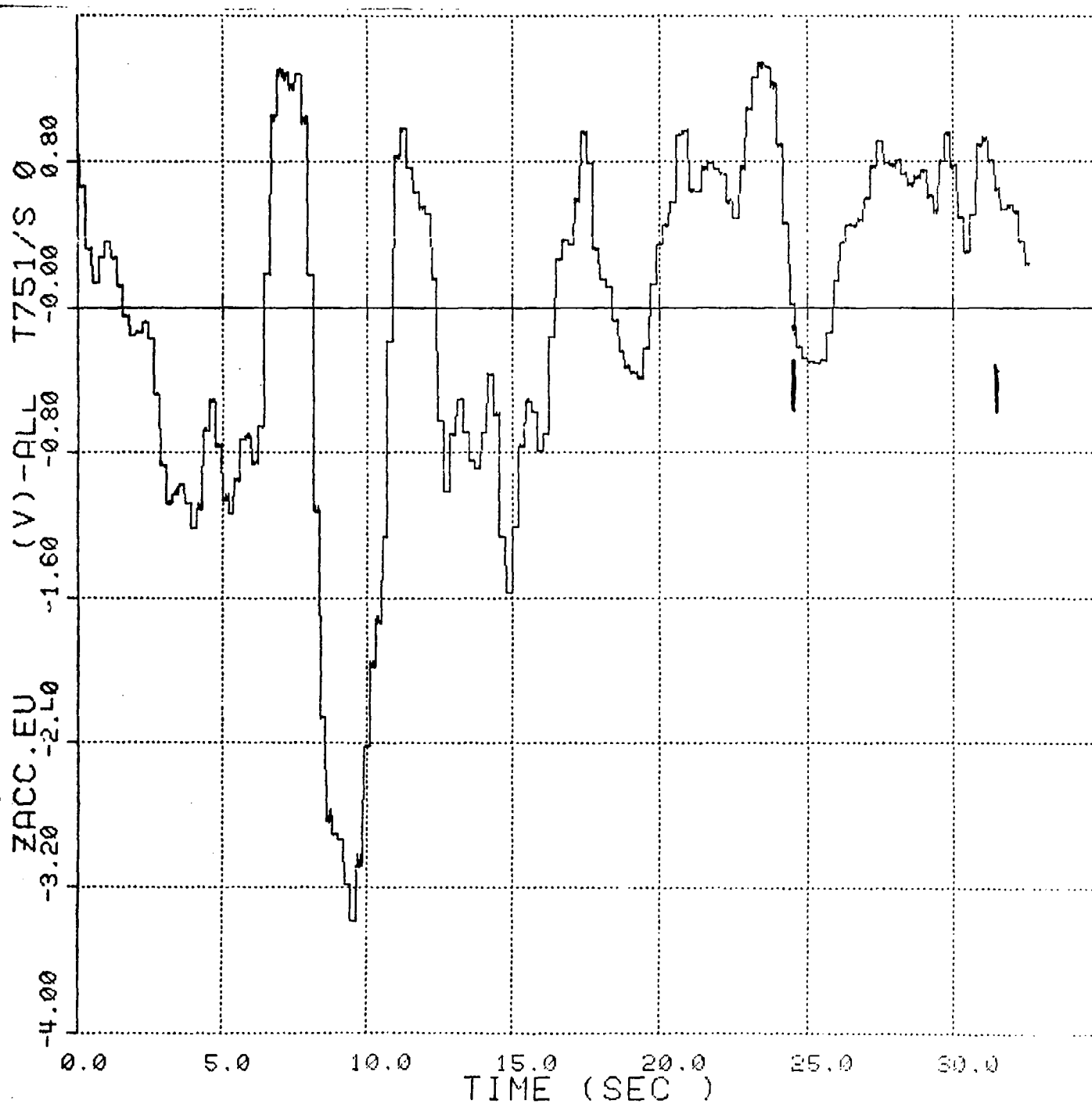


Figure No.179. Towed Submersible's Vertical Acceleration vs Time, Case 24



AD-A133 379

①

FINAL REPORT  
TRADOC RAM DATA EVALUATION SYSTEM (TRADES)  
(ACN 51235)

PART V: SYSTEM TECHNICAL PAPER

APJ 892-5

APJ



DTIC  
ELECTE  
S OCT 11 1983  
D

AMERICAN POWER & LIGHT CO. RIDGEFIELD N.J.

FILE COPY

83 : 10 06 033

DISTRIBUTION STATEMENT A  
Approved for public release  
Distribution Unlimited